

Probing the nature of electroweak symmetry breaking with Higgs boson pair-production at ATLAS

Alessandra Betti

on behalf of the ATLAS Collaboration

XI International Conference on New Frontiers in Physics (ICNFP 2022)

OAC conference center, Kolymbari, Crete, Greece

06/09/2022

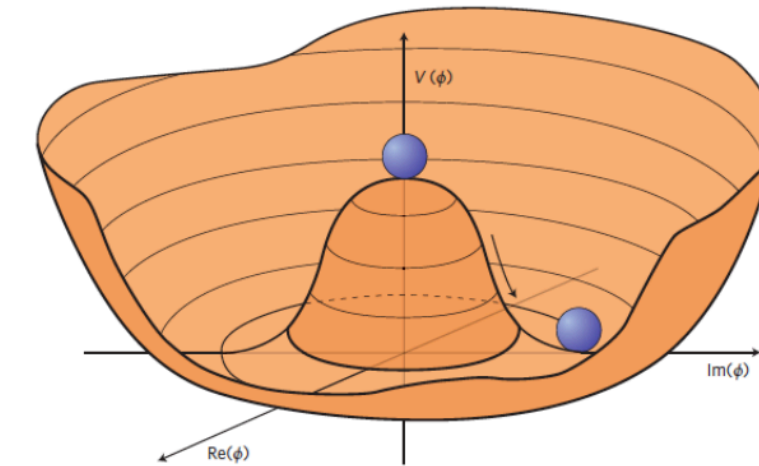


SAPIENZA
UNIVERSITÀ DI ROMA



Measuring the Higgs self-coupling at the LHC

di-Higgs production provides a direct probe of the triple Higgs coupling (κ_λ), one of the couplings defining the shape of the Higgs potential around the minimum, and thus provides a probe of the electroweak symmetry breaking mechanism

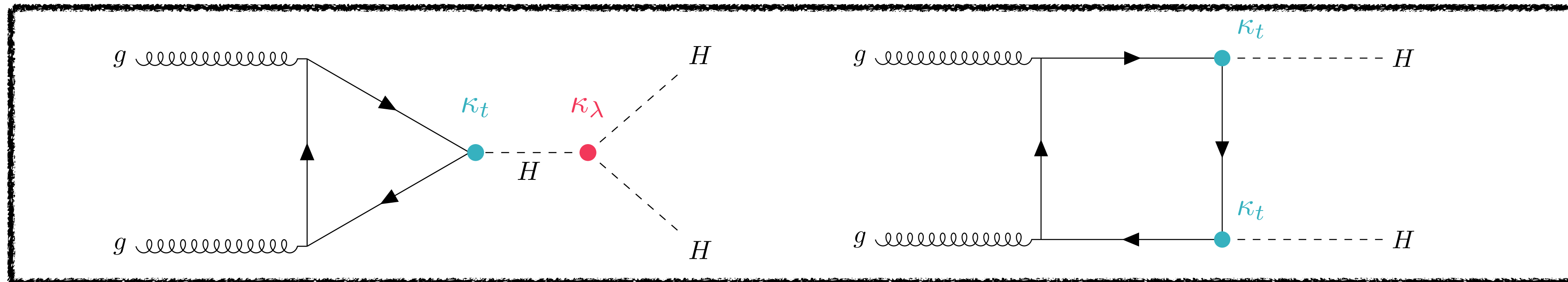


$$V(\Phi) = \mu^2\Phi^2 + \lambda\Phi^4$$

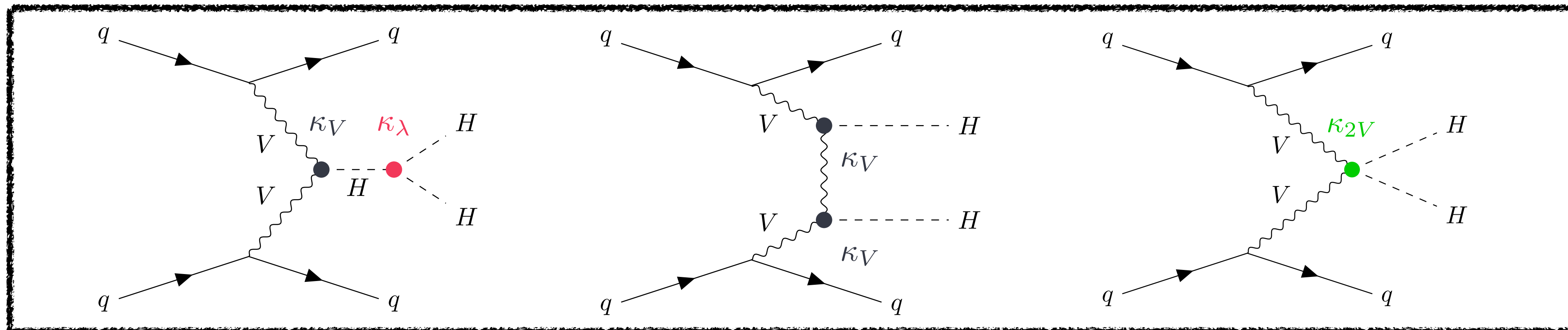
triple Higgs coupling

$$\lambda_3 = \lambda\nu = \frac{m_h^2}{2\nu}$$

At the LHC, the leading HH production mode is gluon-gluon Fusion (ggF): $\sigma_{ggF}^{SM} = 31.05 \text{ fb}$



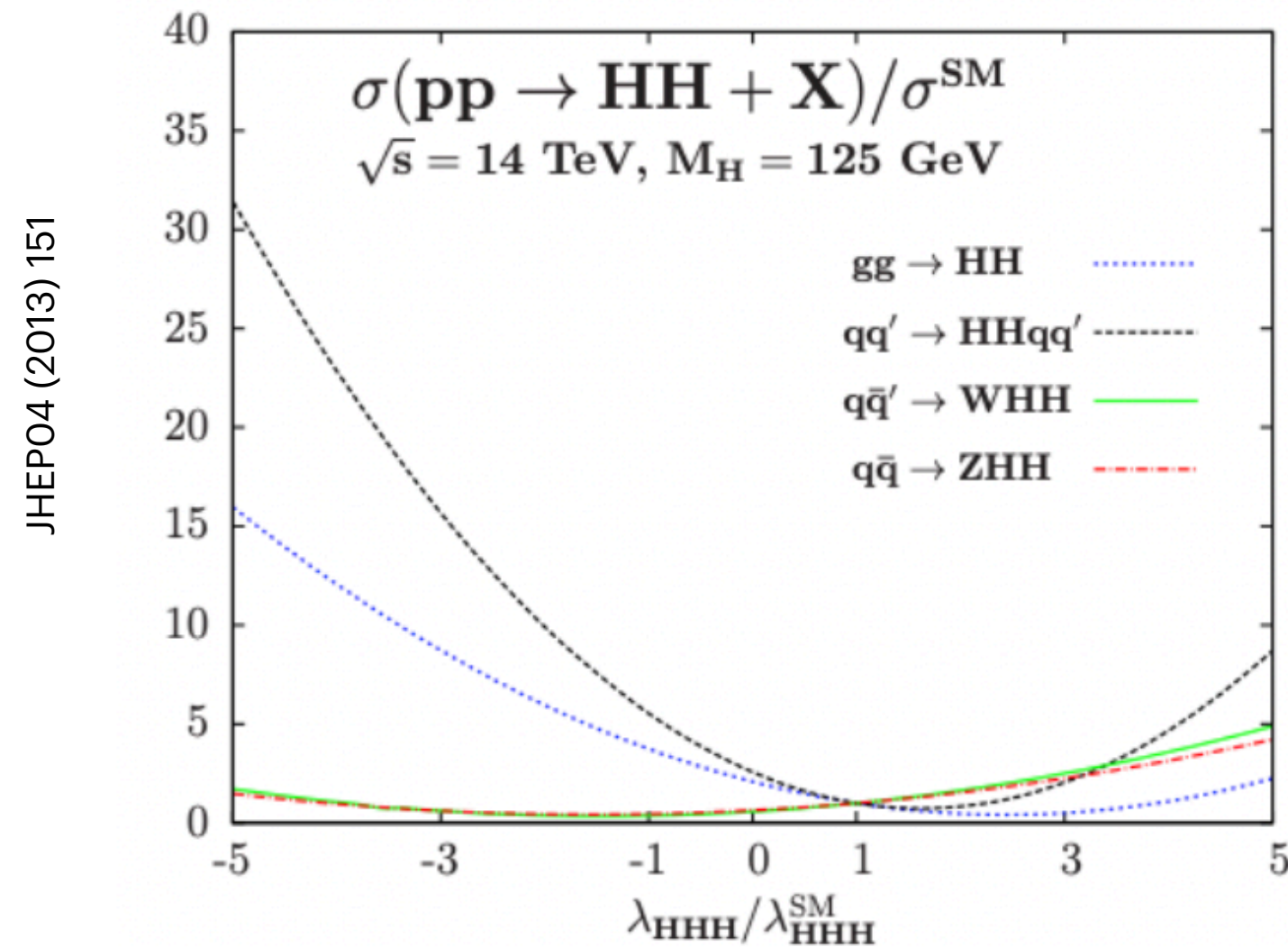
Second leading HH production mode is vector-boson-fusion (VBF): $\sigma_{VBF}^{SM} = 1.73 \text{ fb}$



Beyond Standard Model physics in di-Higgs production

SM HH production cross section very small (more than 1000 times smaller than single-Higgs production!)

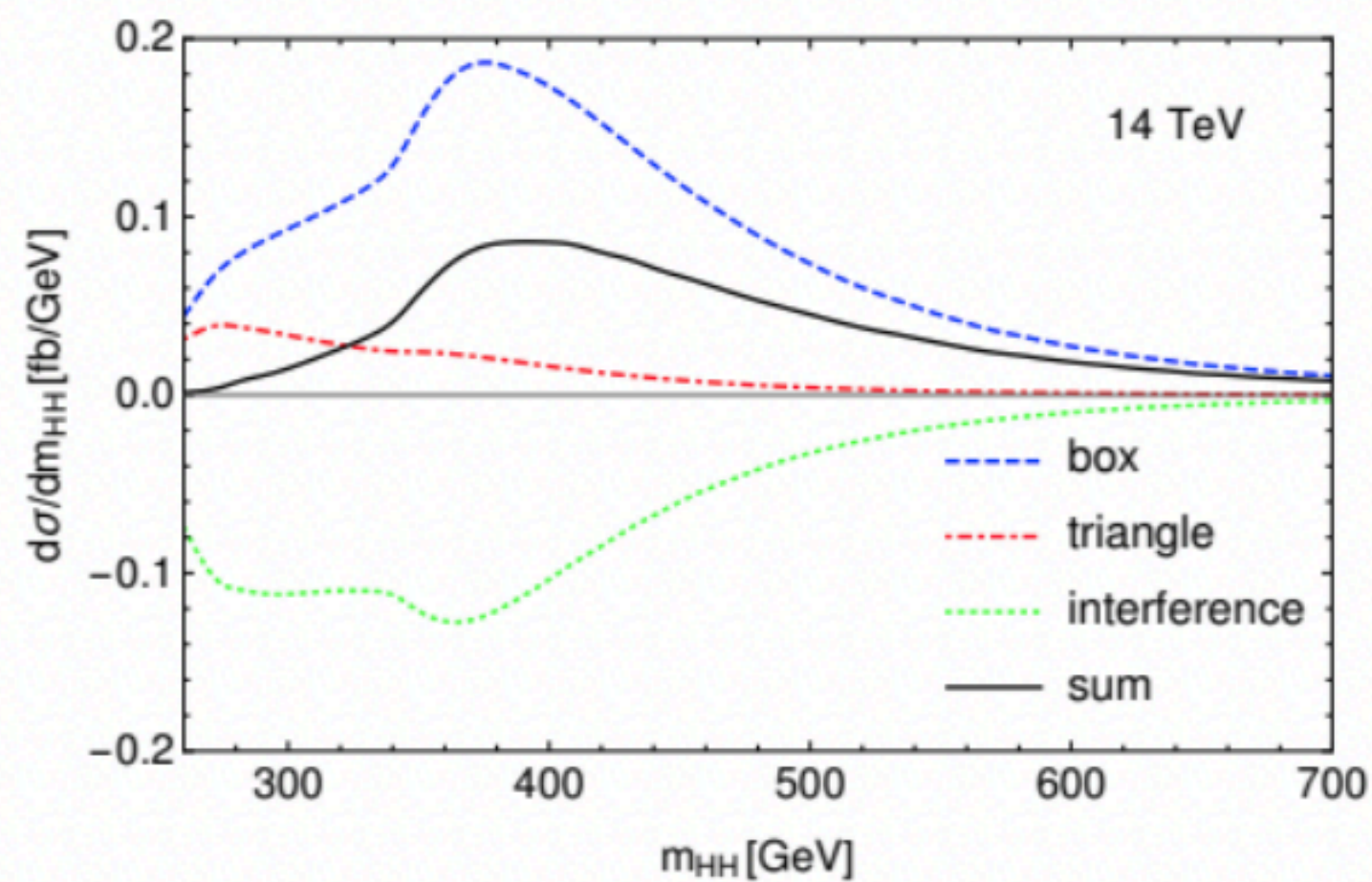
→ Needs very high statistics to be observed but still very interesting to study now as beyond the SM physics could lead to modified Higgs Boson self-coupling resulting in enhanced HH production rate and modified kinematics of the process



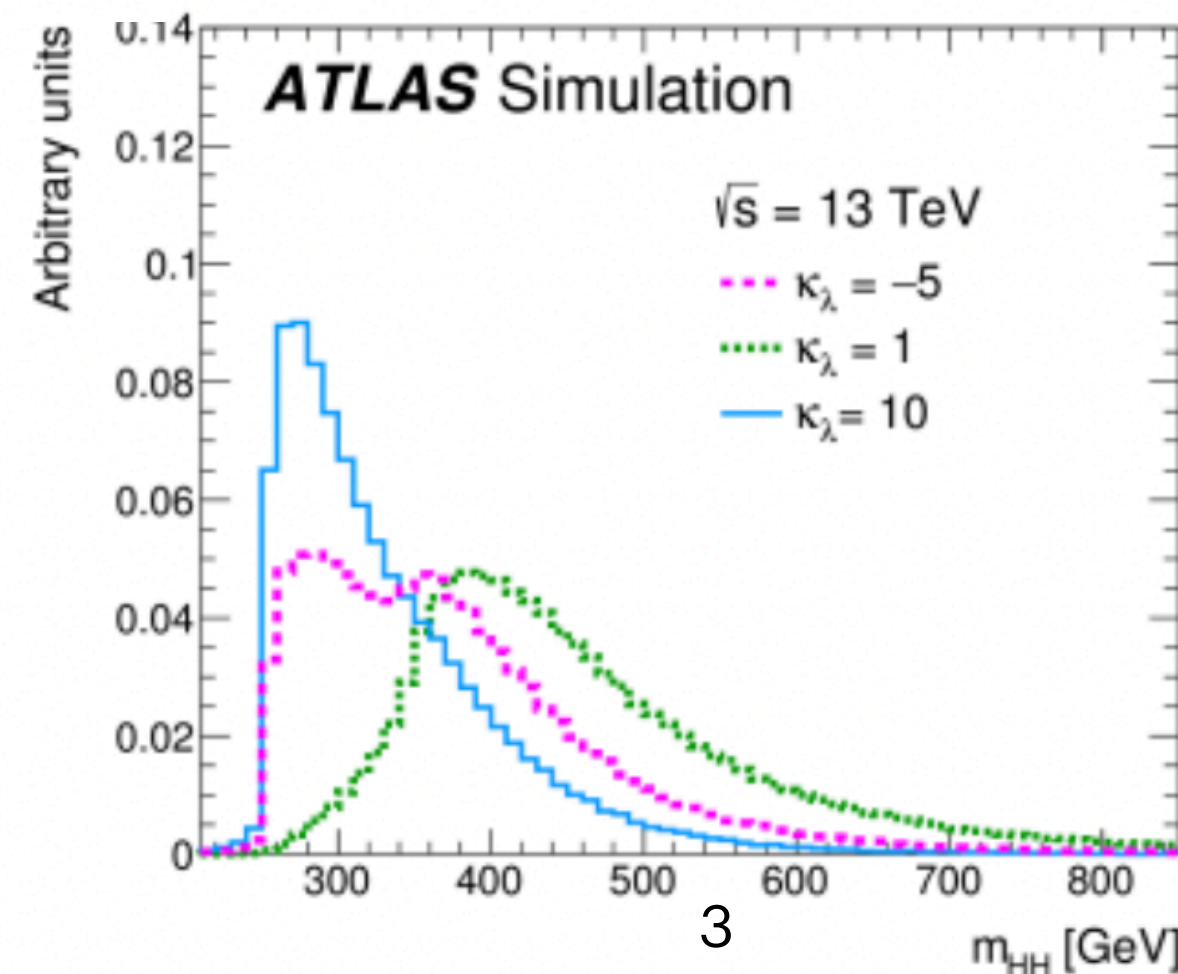
Large variations of non-resonant cross section with modifications of κ_λ for ggF and VBF:

- More than a factor of 2 increase at $\kappa_\lambda = 0$
- More than a factor of 4 increase at $\kappa_\lambda = -1$

Rev. Phys. 5, 100045 (2020)



Phys. Lett. B 800 (2020) 135103



Modifications of the kinematics of the process with variations of κ_λ due to different contributions and interference of the Feynman diagrams

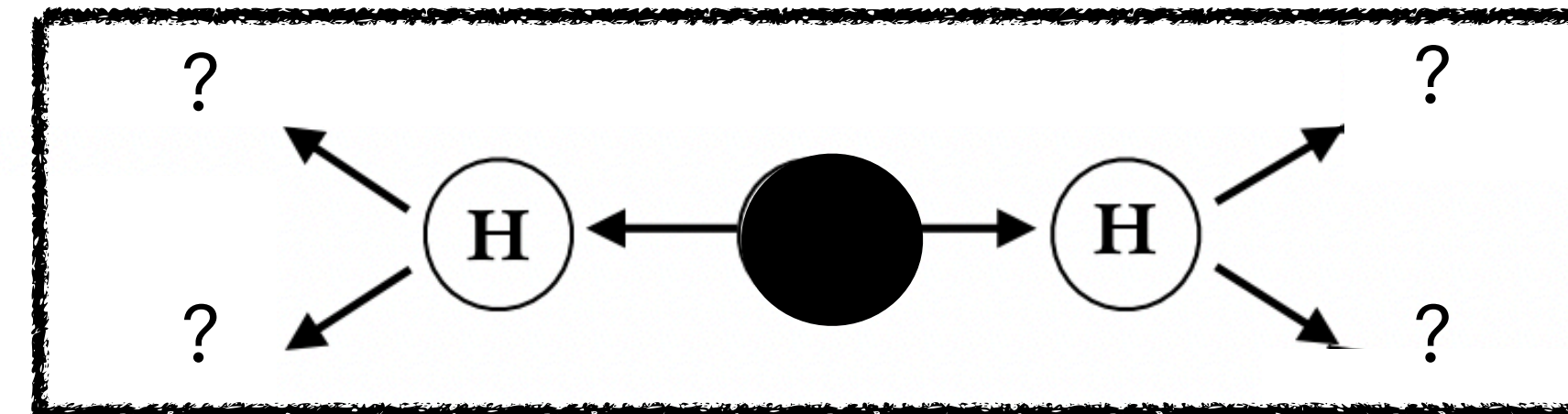
di-Higgs decay channels and ATLAS di-Higgs searches

Many different final states in the Higgs pair decay given by all possible combinations of Higgs Boson decays

ATLAS di-Higgs searches covering large part of possible decays with results on **partial** (36 fb^{-1}) and **full** (139 fb^{-1}) LHC Run 2 datasets

	bb	WW	$\tau\tau$	ZZ	$\gamma\gamma$
bb	34%				
WW	25%	4.6%			
$\tau\tau$	7.3%	2.7%	0.39%		
ZZ	3.1%	1.1%	0.33%	0.069%	
$\gamma\gamma$	0.26%	0.10%	0.028%	0.012%	0.0005%

Most HH searches exploit decay channels with one $H \rightarrow bb$ for the high BR



Analyses in different decay channels have very different characteristics given the different signal decay BRs, different objects in the final state and different backgrounds
 → No single golden channel for HH searches, combination of several decay channels very important!

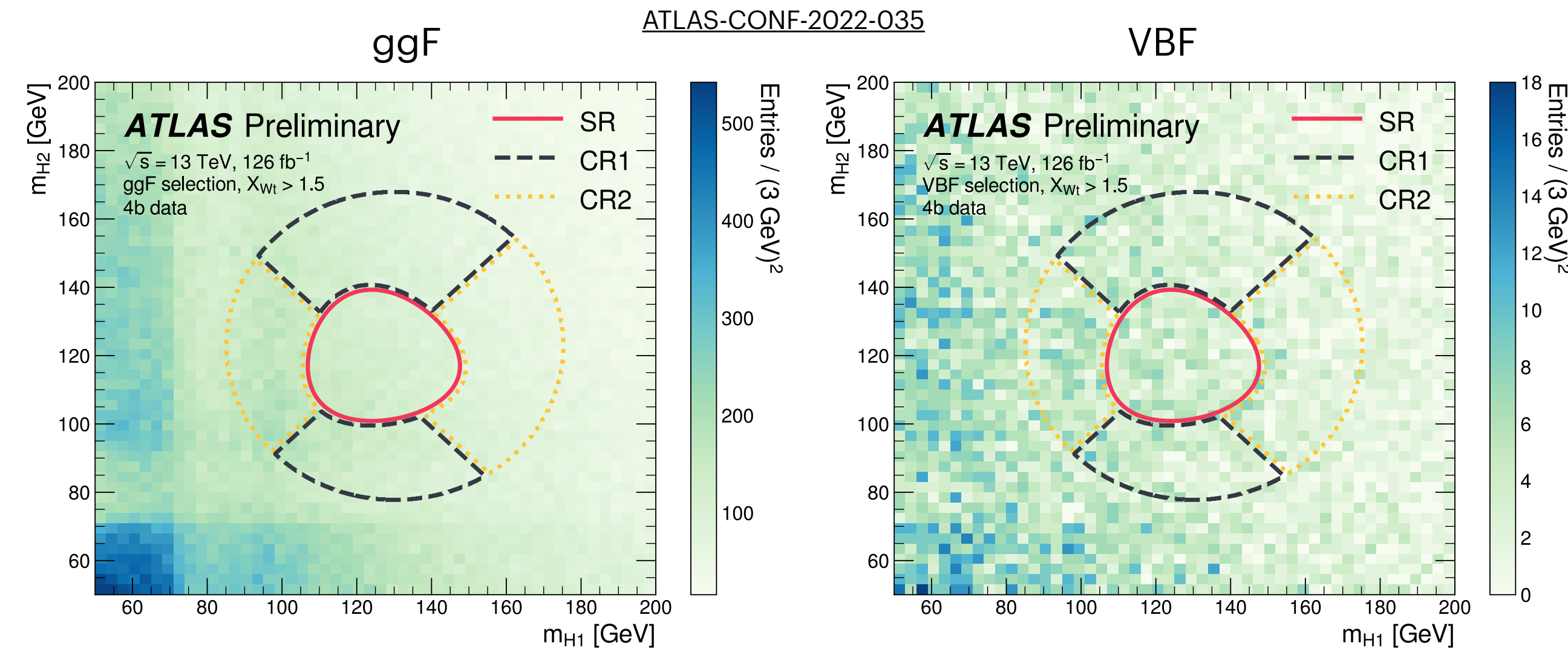
→ Presenting here the latest ATLAS non-resonant HH searches in the three most sensitive channels using full LHC Run 2 dataset: $bbbb$, $bb\tau\tau$ and $bb\gamma\gamma$

Non-resonant HH→bbbb with full Run 2 data

bbbb decay channel has the largest BR (34%), but large QCD multi-jet events background difficult to model and challenging combinatorial problem for building the Higgs candidates

- Search for SM and BSM non-resonant HH production
- ggF and VBF HH production
- **HH→bbbb**
- At least 4 b-tagged central jets
- Targeting ggF and VBF production modes with dedicated categories based on the presence of additional jets
- b-tagged jets paired to form the 2 Higgs candidates based on minimum dR requirement on the leading Higgs candidate
- Signal regions defined by selections in the 2D m_{H1} - m_{H2} plane

$$X_{HH} = \sqrt{\left(\frac{m_{H1} - 124 \text{ GeV}}{0.1 m_{H1}}\right)^2 + \left(\frac{m_{H2} - 117 \text{ GeV}}{0.1 m_{H2}}\right)^2}$$



- **Main backgrounds:** QCD multi-jet background (~95%) and ttbar (~5%)
- **Total background estimated from data** using a neural network trained in control regions to reweight 2b data to look like 4b data

Non-resonant $HH \rightarrow b\bar{b}b\bar{b}$ with full Run 2 data

ggF and VBF categories further split to enhance sensitivity to SM signal and to signals with BSM couplings

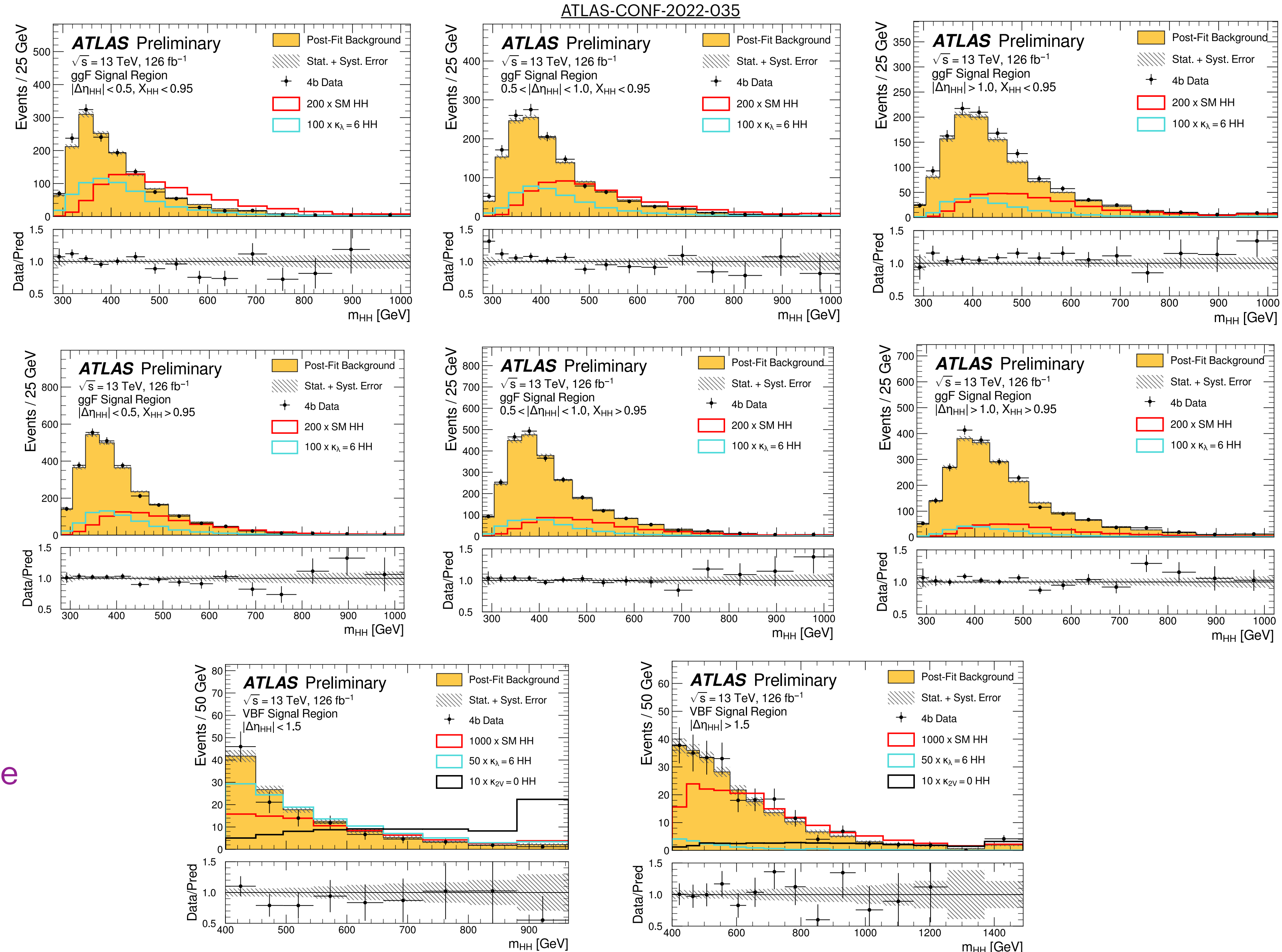
- **ggF categories:**
3x2 categories in bins of

$$|\Delta\eta_{HH}| \times X_{HH}$$

- **VBF categories:**
2 categories in bins of

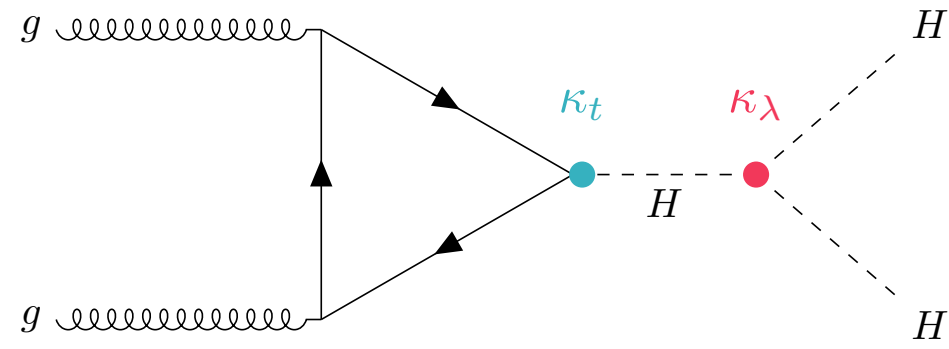
$$|\Delta\eta_{HH}|$$

m_{HH} used as final discriminant variable in the 8 signal regions, searching for an excess of events in the di-Higgs mass spectrum

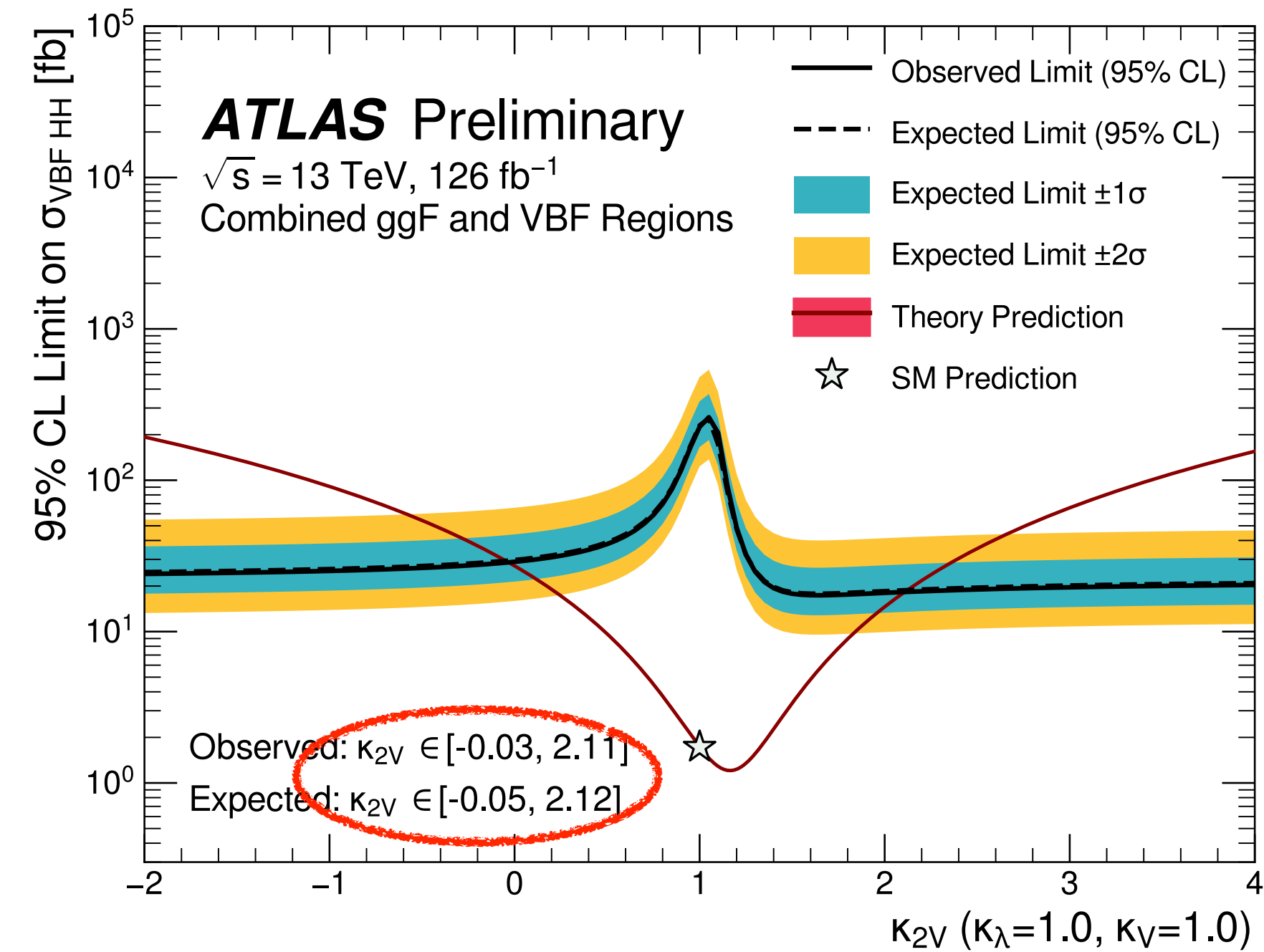
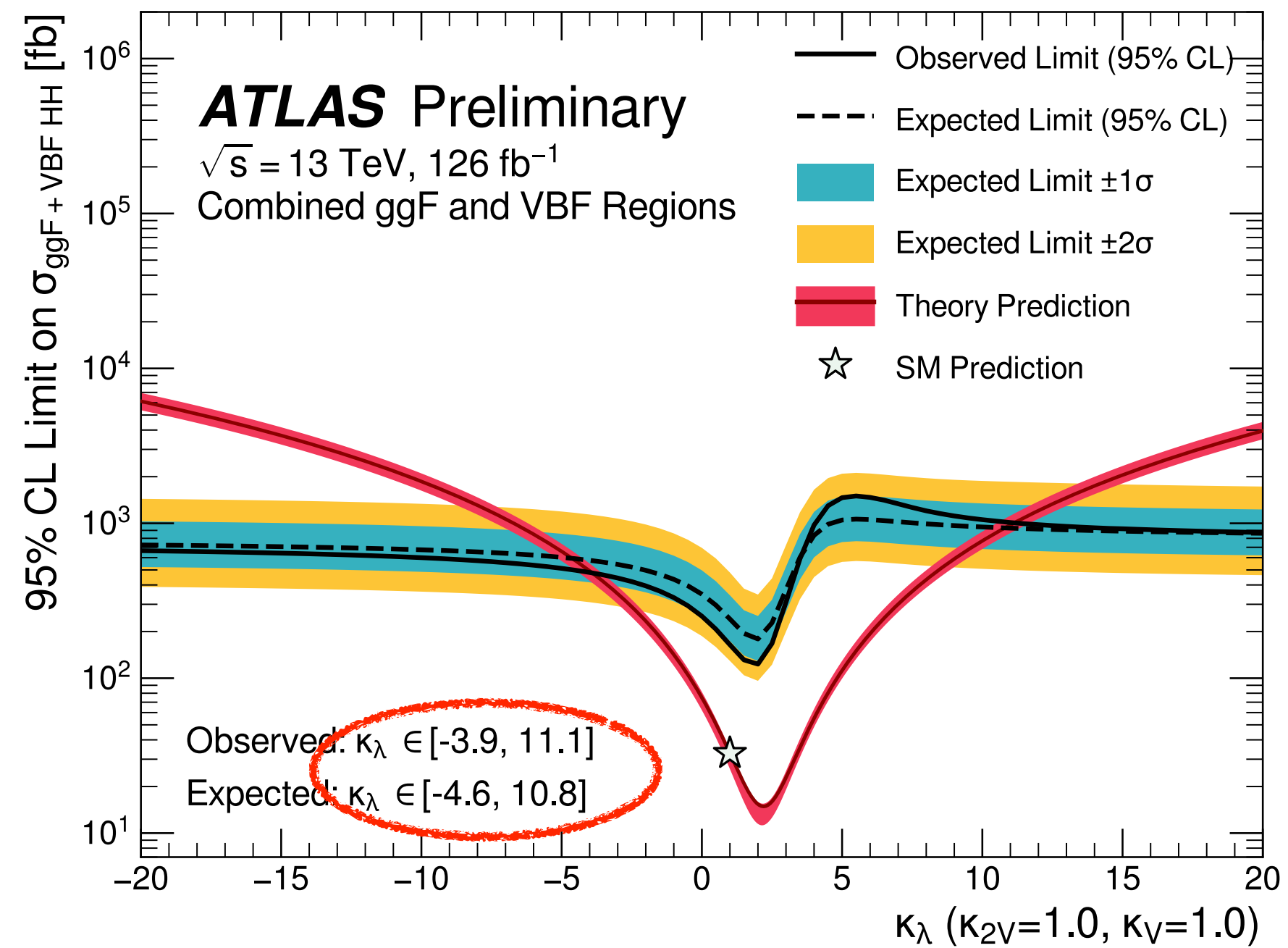
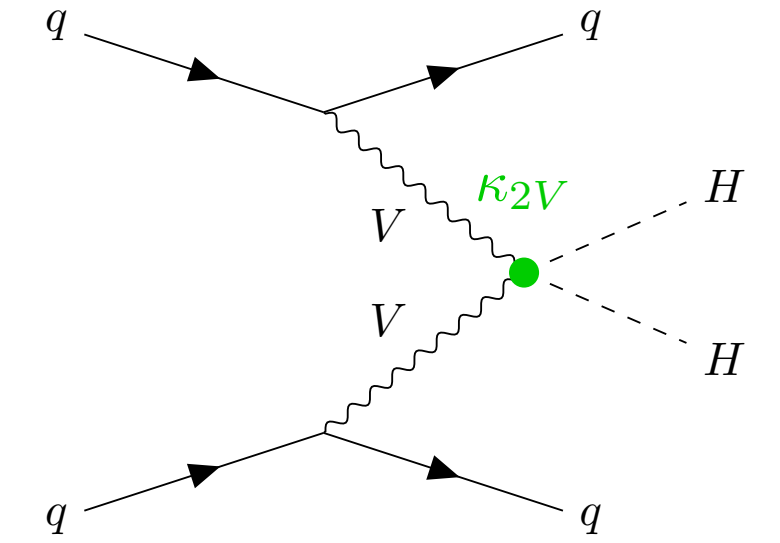


Non-resonant $HH \rightarrow bbbb$ with full Run 2 data

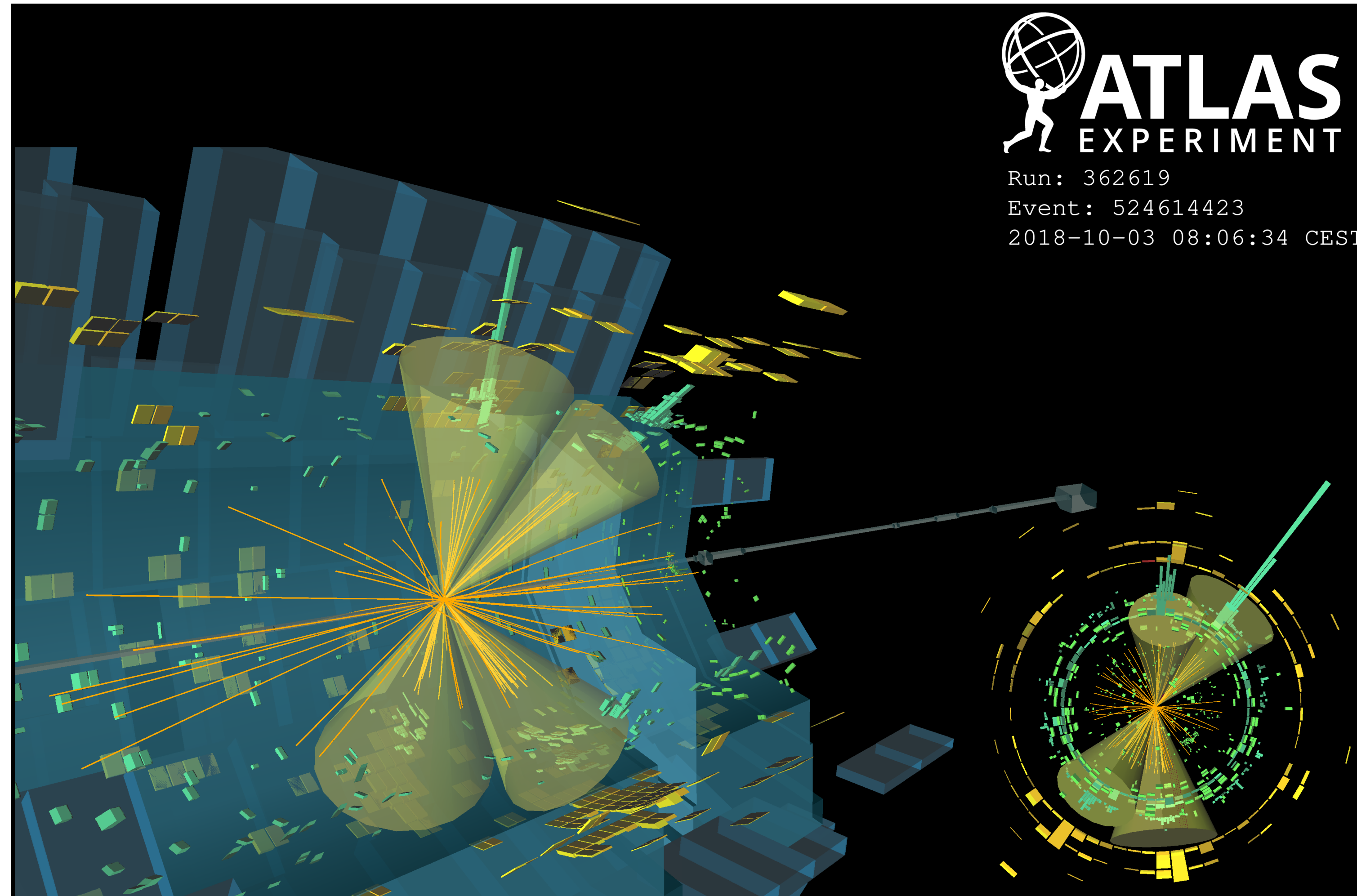
ATLAS-CONF-2022-035



	Observed Limit	-2σ	-1σ	Expected Limit	$+1\sigma$	$+2\sigma$
$\sigma_{\text{ggF}}/\sigma_{\text{ggF}}^{\text{SM}}$	5.5	4.4	5.9	8.2	12.4	19.6
$\sigma_{\text{VBF}}/\sigma_{\text{VBF}}^{\text{SM}}$	130.5	71.6	96.1	133.4	192.9	279.3
$\sigma_{\text{ggF+VBF}}/\sigma_{\text{ggF+VBF}}^{\text{SM}}$	5.4	4.3	5.8	8.1	12.2	19.1



Non-resonant HH → bbbb with full Run 2 data



Candidate HH data event in the ggF category

$$m_{HH} = 588 \text{ GeV}, m_{bb} = 126 \text{ GeV} \text{ and } m_{bb} = 114 \text{ GeV}$$

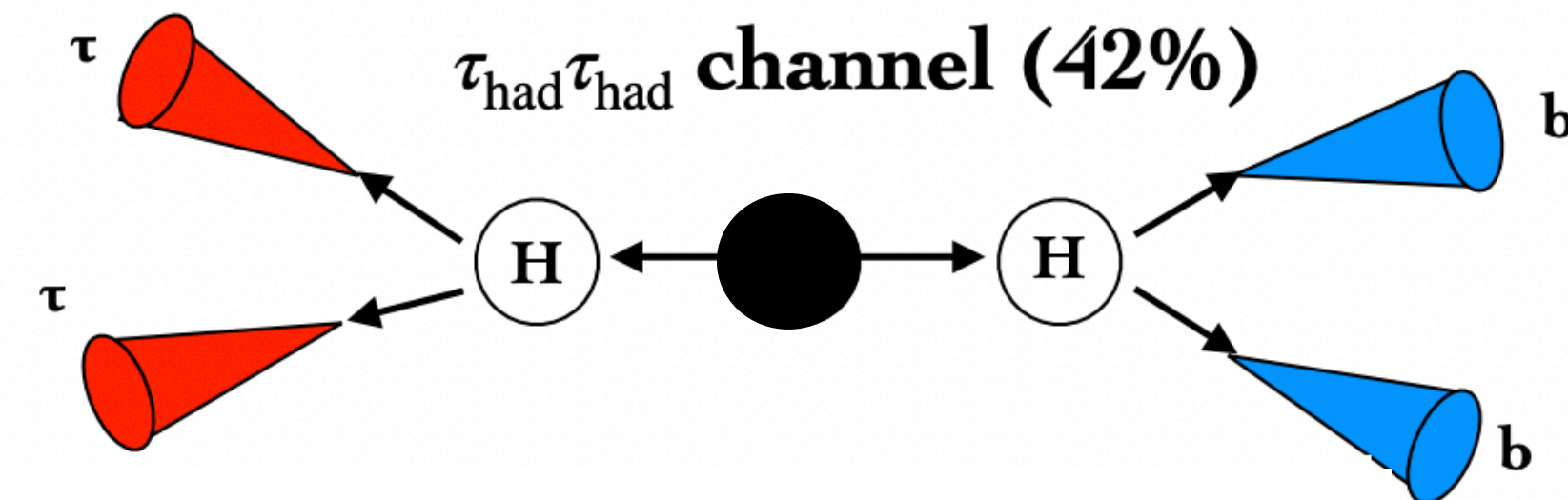
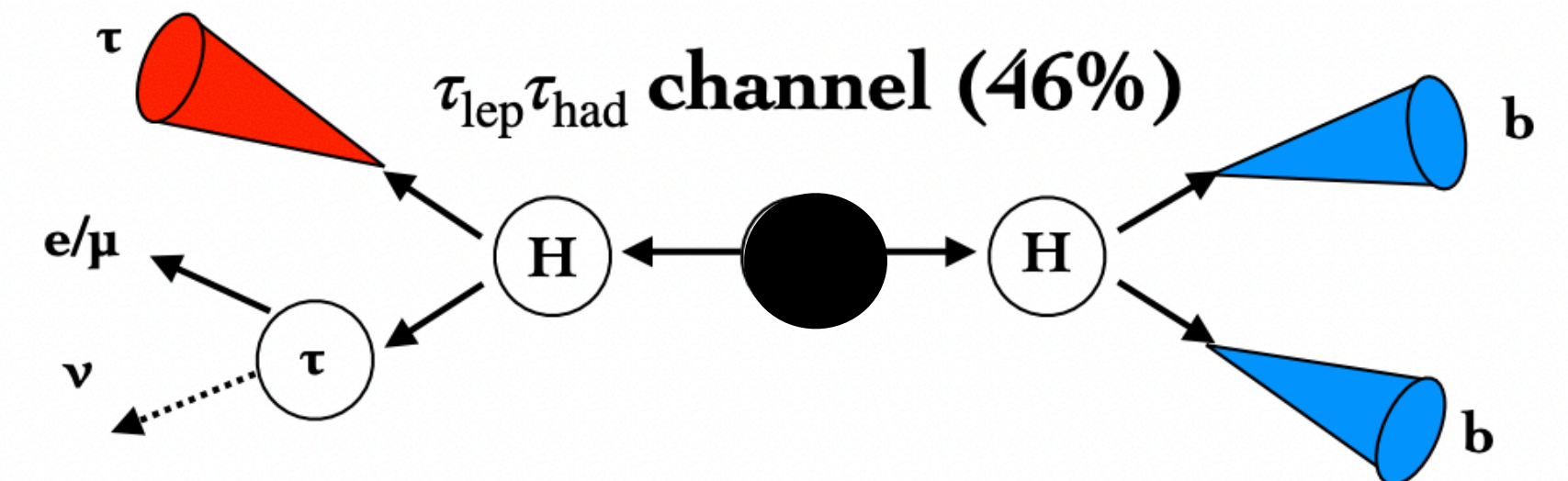
Non-resonant $HH \rightarrow bb\tau\tau$ with full Run 2 data

$bb\tau\tau$ decay channel has relatively high BR (7.3%) and relatively clean signature, but background with jets faking hadronically decaying τ -leptons difficult to model

- Search for SM and BSM non-resonant HH production
- ggF and VBF HH production
- $H \rightarrow bb$ and $H \rightarrow \tau\tau$
- Semi-leptonic (LepHad) and fully hadronic (HadHad) decays of the di- τ system
- 1 lepton (e/ μ) and 1 τ in LepHad, 2 τ in HadHad
- 2 b-tagged jets
- 3 signal regions defined depending on the di- τ system decay mode and trigger decision

Main backgrounds:

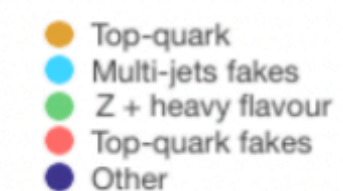
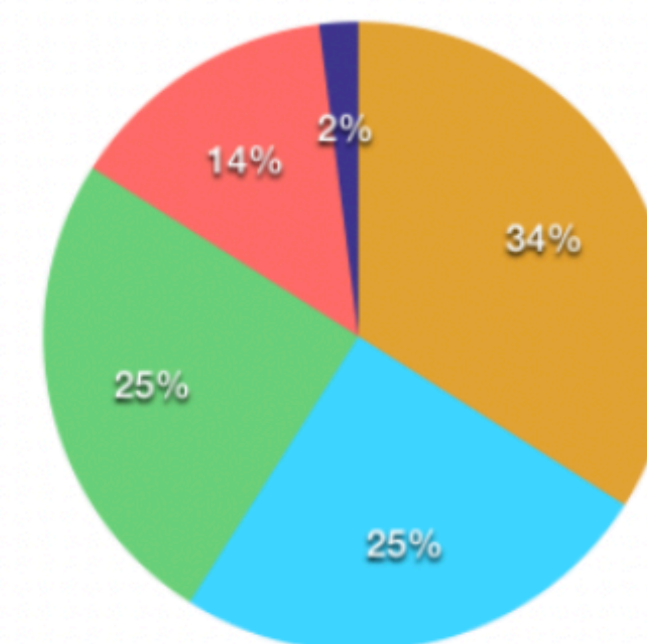
- $t\bar{t}$ and Z+heavy flavour jets (with real τ), modelled with Monte Carlo simulations
- Events with jets faking hadronically decaying τ from $t\bar{t}$ and QCD multi-jet data-driven (fake-factor and scale factor methods)



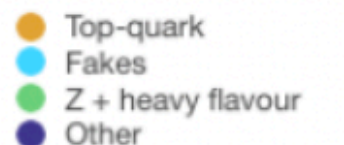
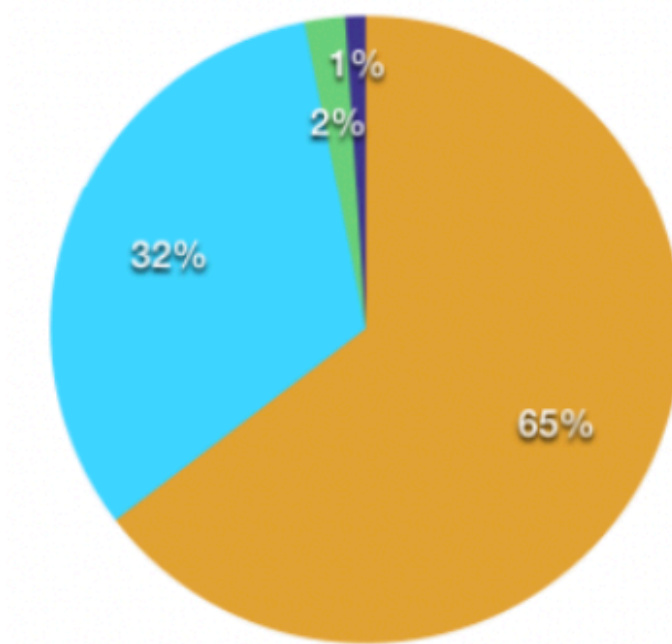
HadHad

LepHad

SR background composition



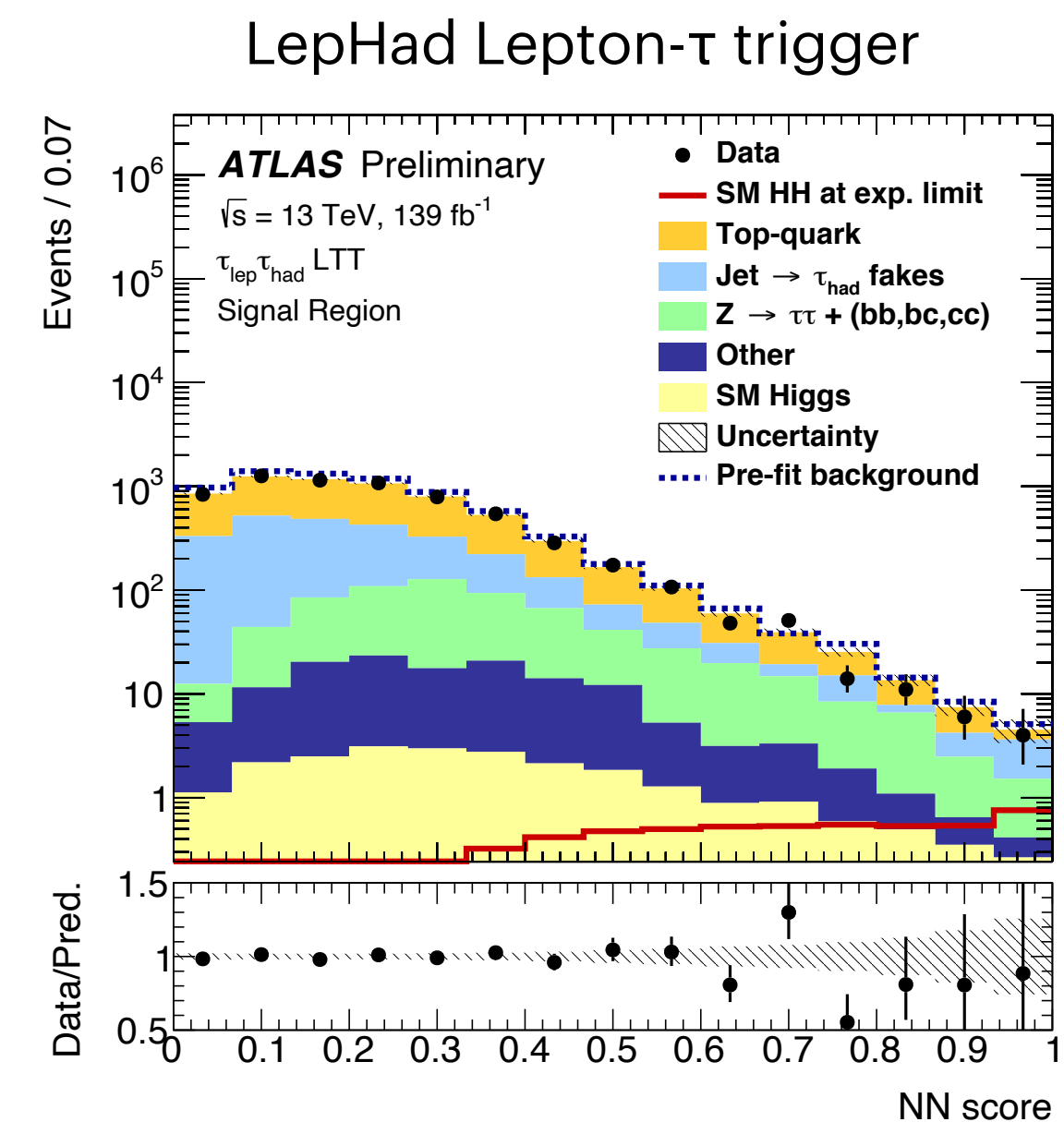
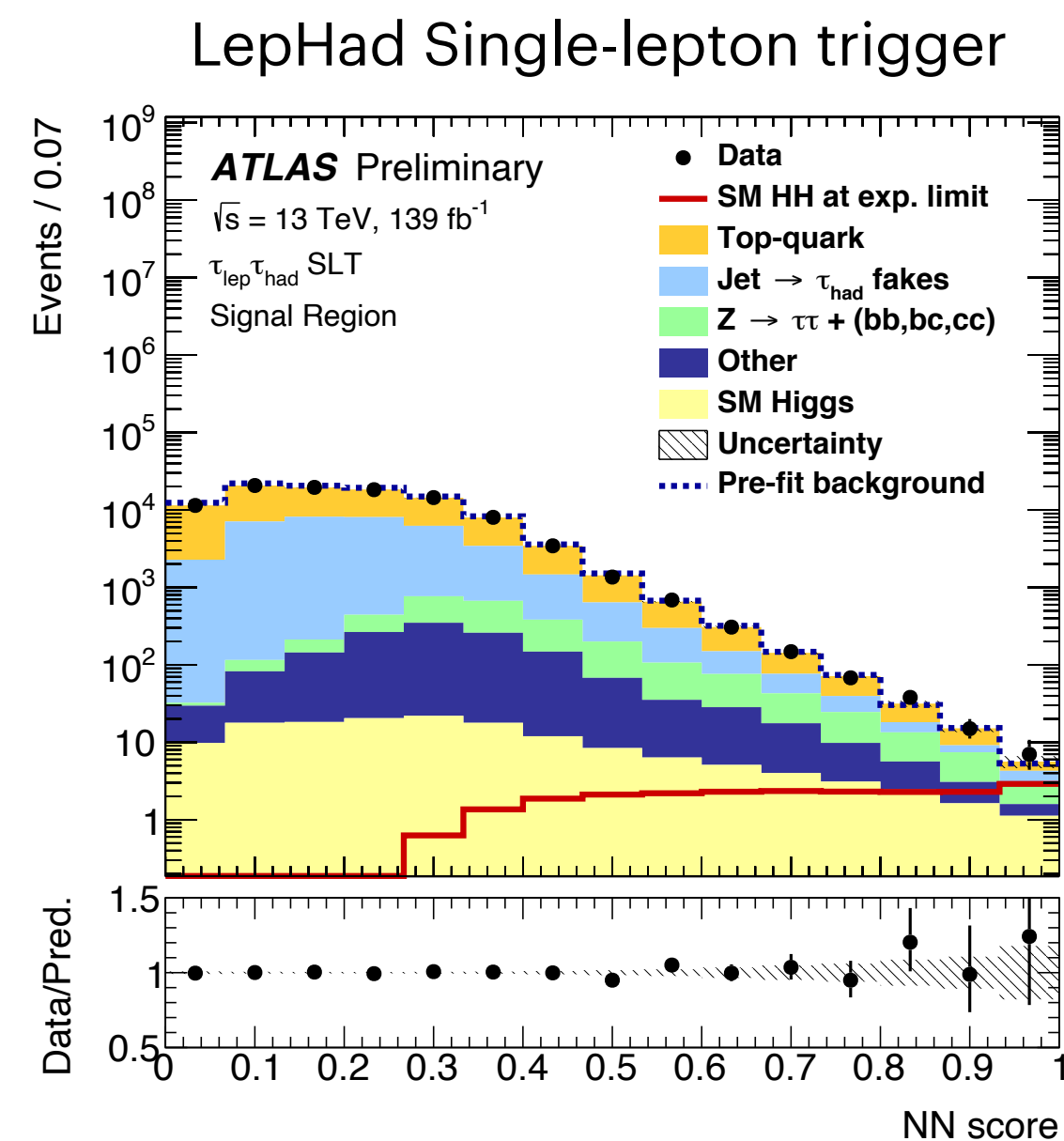
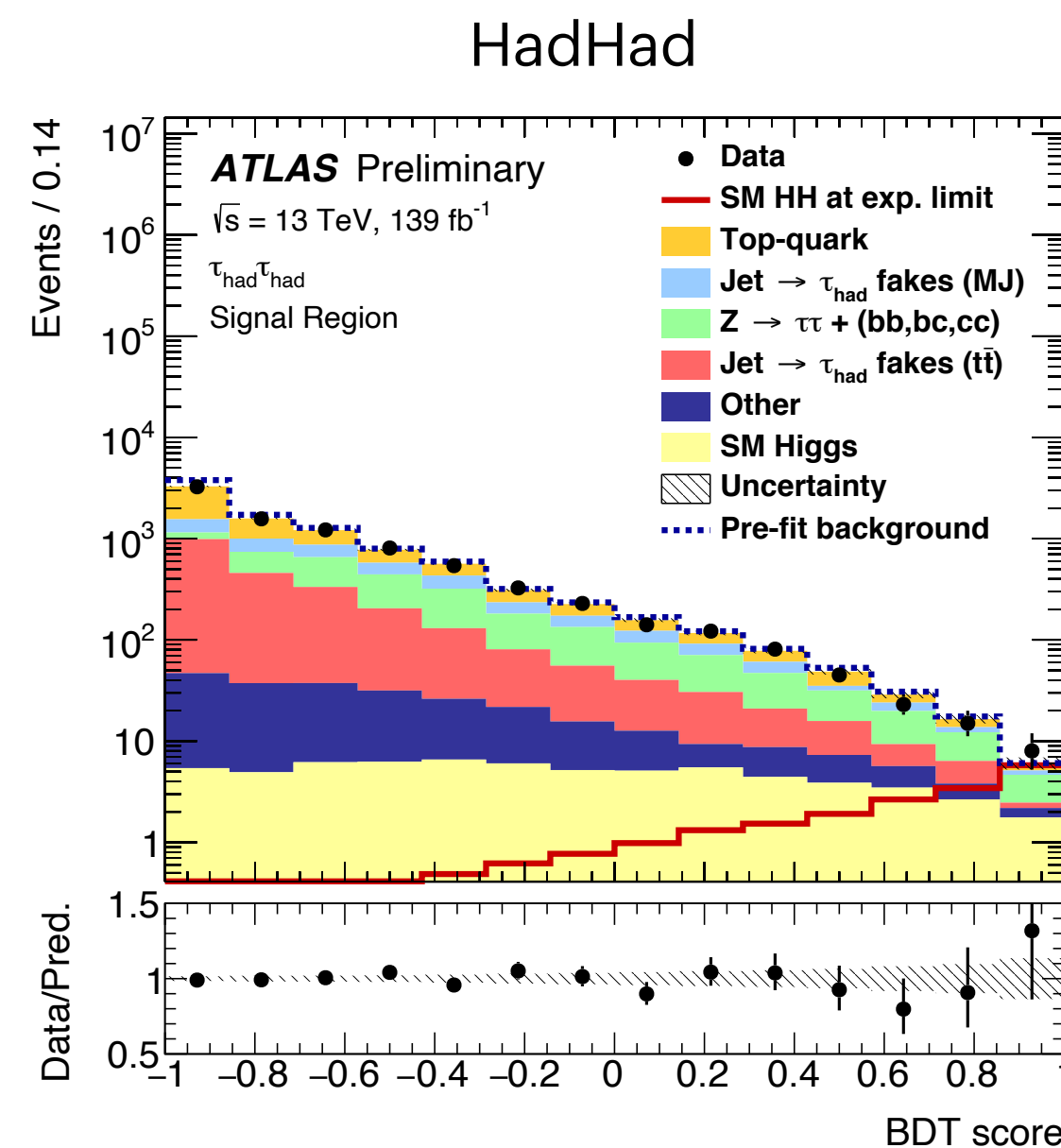
SR background composition



Non-resonant HH → bbττ with full Run 2 data

- Multi-variate analysis (MVA) discriminants (Boosted Decision Trees and Neural Networks) used to separate signal from background
- Important input variables: reconstructed di-Higgs invariant mass m_{HH} , reconstructed invariant masses of the two Higgs boson candidates m_{bb} and $m_{\tau\tau}$
- MVA outputs used as final discriminants searching for an excess of events in the most signal-like bins of the MVAs

ATLAS-CONF-2021-030

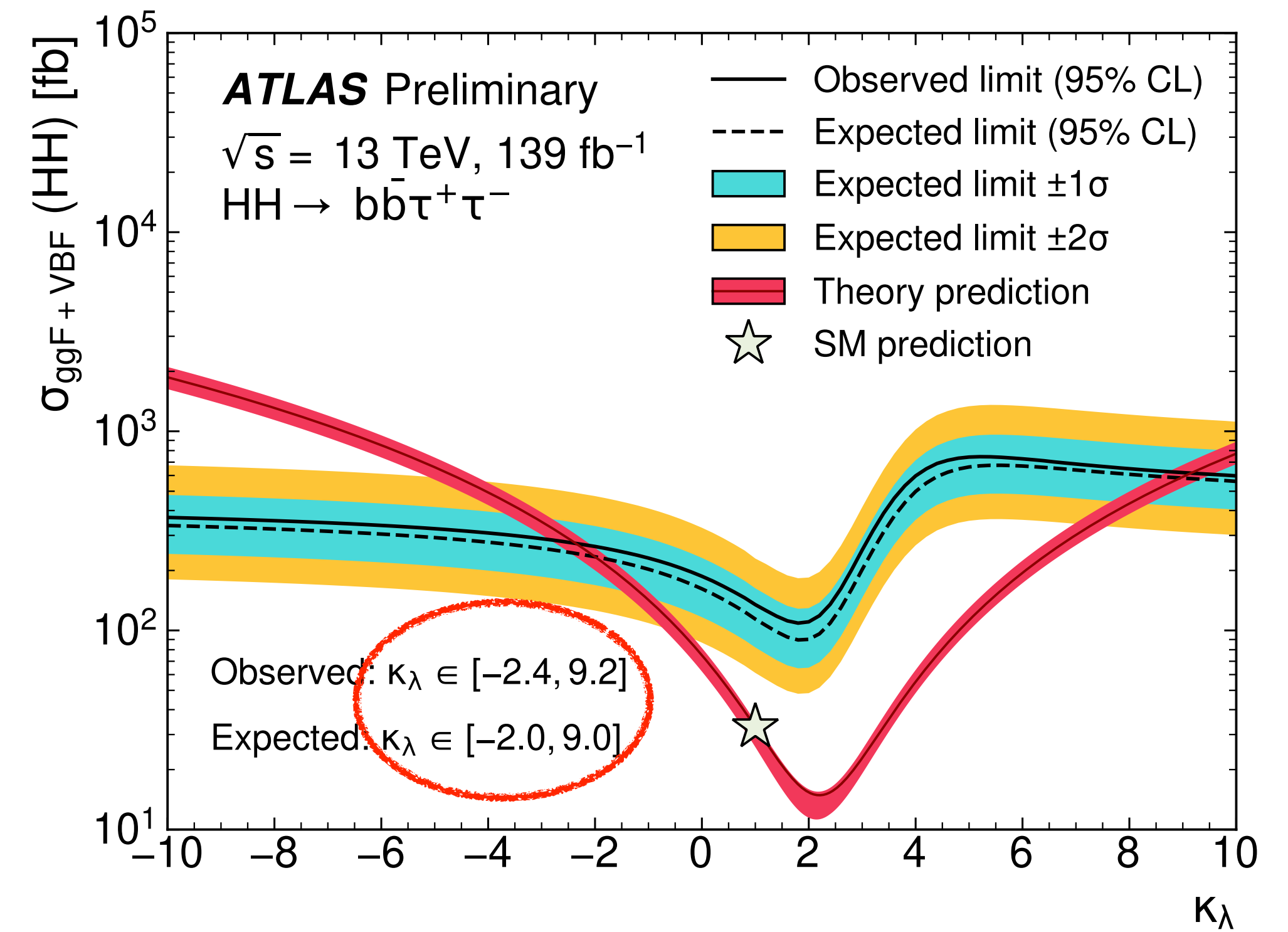


Non-resonant HH → bbττ with full Run 2 data

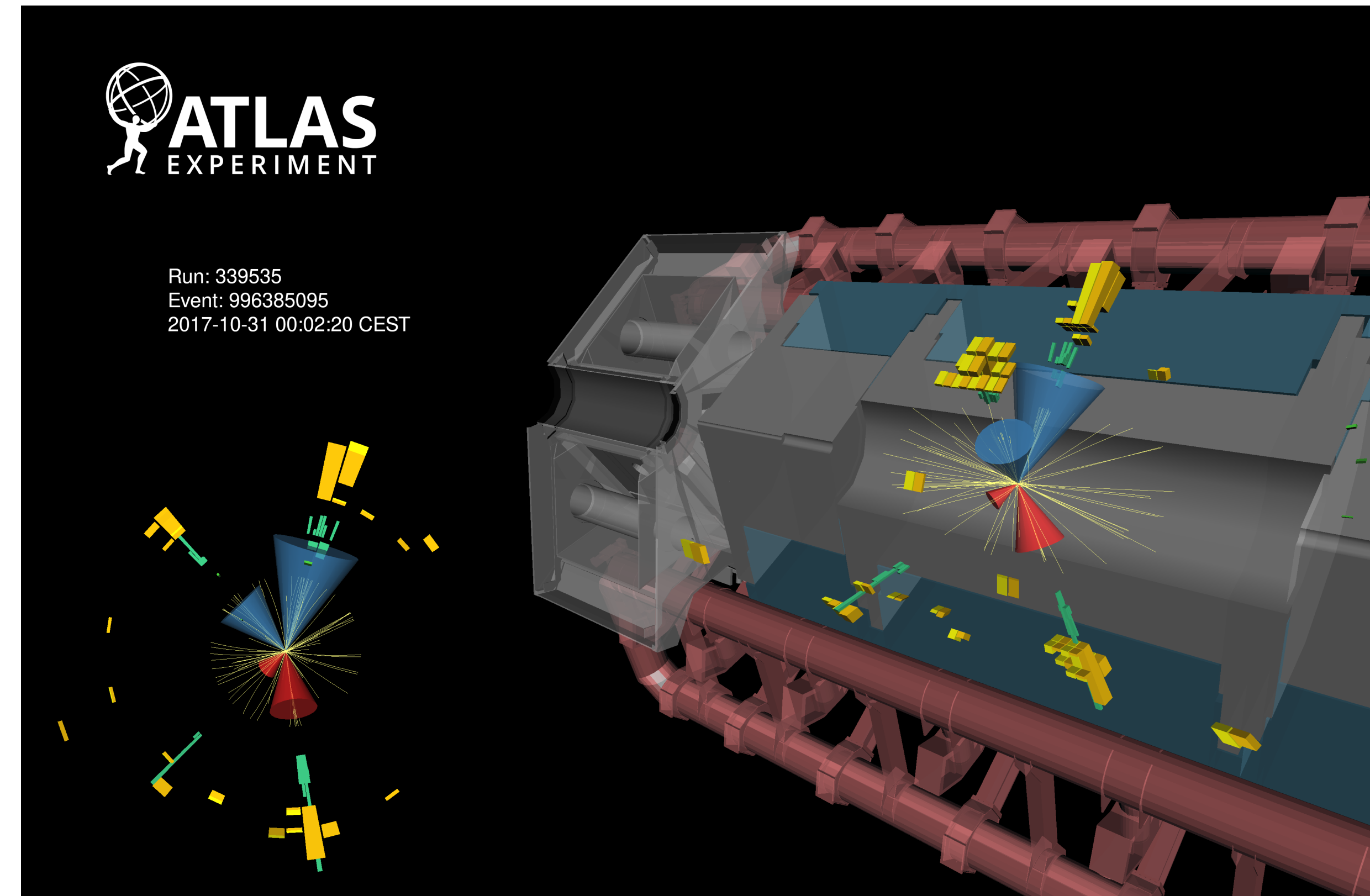
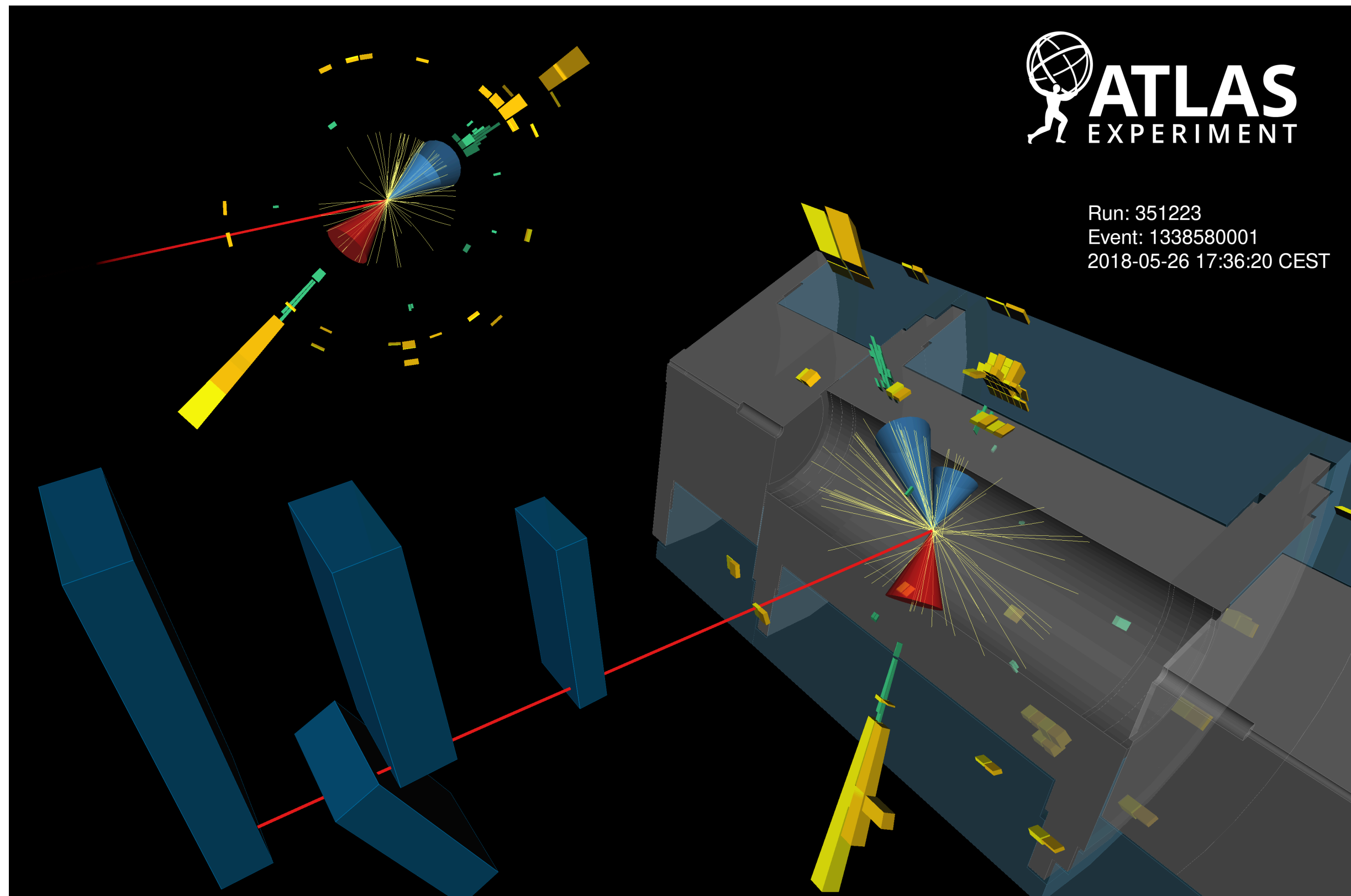
ATLAS-CONF-2021-030

		Observed	-2 σ	-1 σ	Expected	+1 σ	+2 σ
$\tau_{\text{had}}\tau_{\text{had}}$	$\sigma_{\text{ggF+VBF}}$ [fb]	145	70.5	94.6	131	183	245
	$\sigma_{\text{ggF+VBF}}/\sigma_{\text{ggF+VBF}}^{\text{SM}}$	4.95	2.38	3.19	4.43	6.17	8.27
$\tau_{\text{lep}}\tau_{\text{had}}$	$\sigma_{\text{ggF+VBF}}$ [fb]	265	124	167	231	322	432
	$\sigma_{\text{ggF+VBF}}/\sigma_{\text{ggF+VBF}}^{\text{SM}}$	9.16	4.22	5.66	7.86	10.9	14.7
Combined	$\sigma_{\text{ggF+VBF}}$ [fb]	135	61.3	82.3	114	159	213
	$\sigma_{\text{ggF+VBF}}/\sigma_{\text{ggF+VBF}}^{\text{SM}}$	4.65	2.08	2.79	3.87	5.39	7.22

ATLAS-CONF-2021-052



Non-resonant HH → bbττ with full Run 2 data



Candidate HH data event in the $\tau_{\text{lep}}\tau_{\text{had}}$ channel signal region

$$m_{HH} = 680 \text{ GeV}, m_{bb} = 120 \text{ GeV} \text{ and } m_{\tau\tau}^{\text{MMC}} = 120 \text{ GeV}$$

Candidate HH data event in the $\tau_{\text{had}}\tau_{\text{had}}$ channel signal region

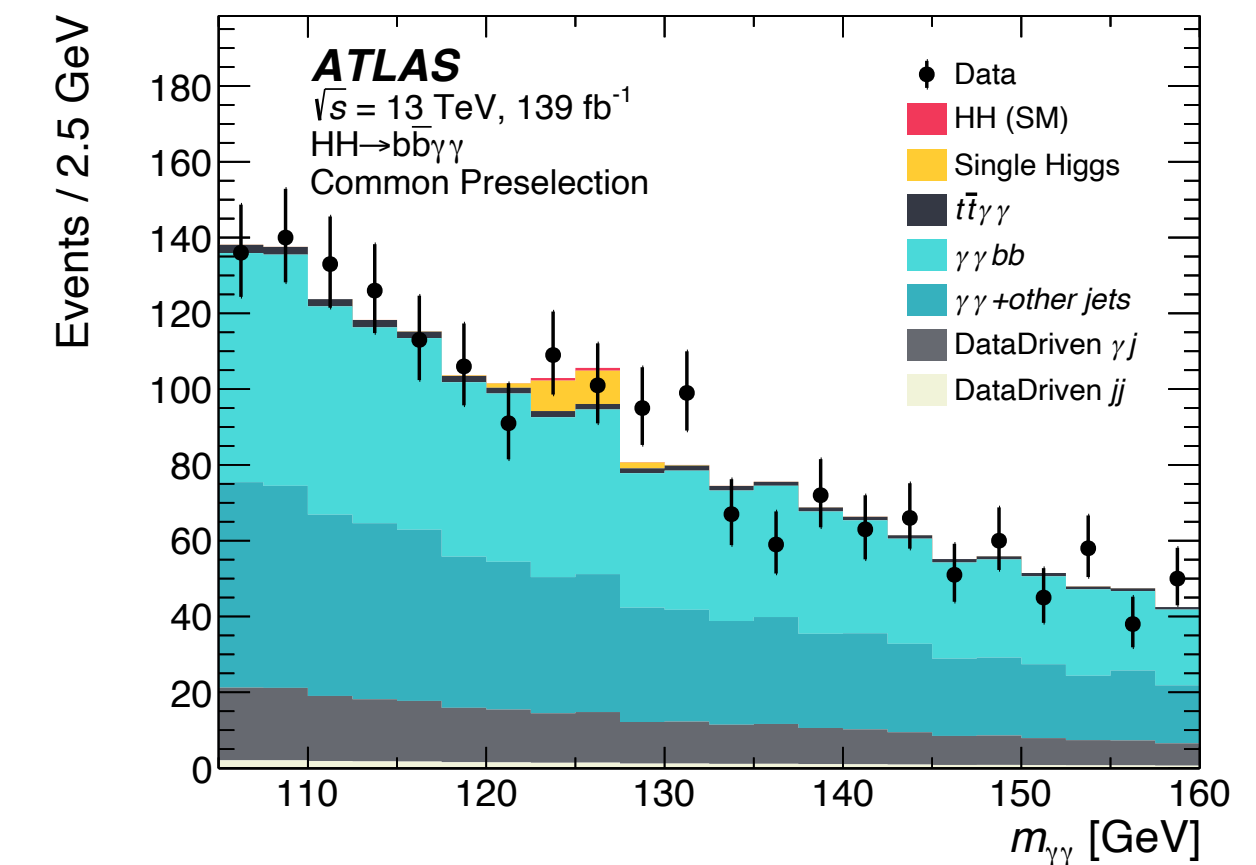
$$m_{HH} = 510 \text{ GeV}, m_{bb} = 130 \text{ GeV} \text{ and } m_{\tau\tau}^{\text{MMC}} = 130 \text{ GeV}$$

Non-resonant HH→bbγγ with full Run 2 data

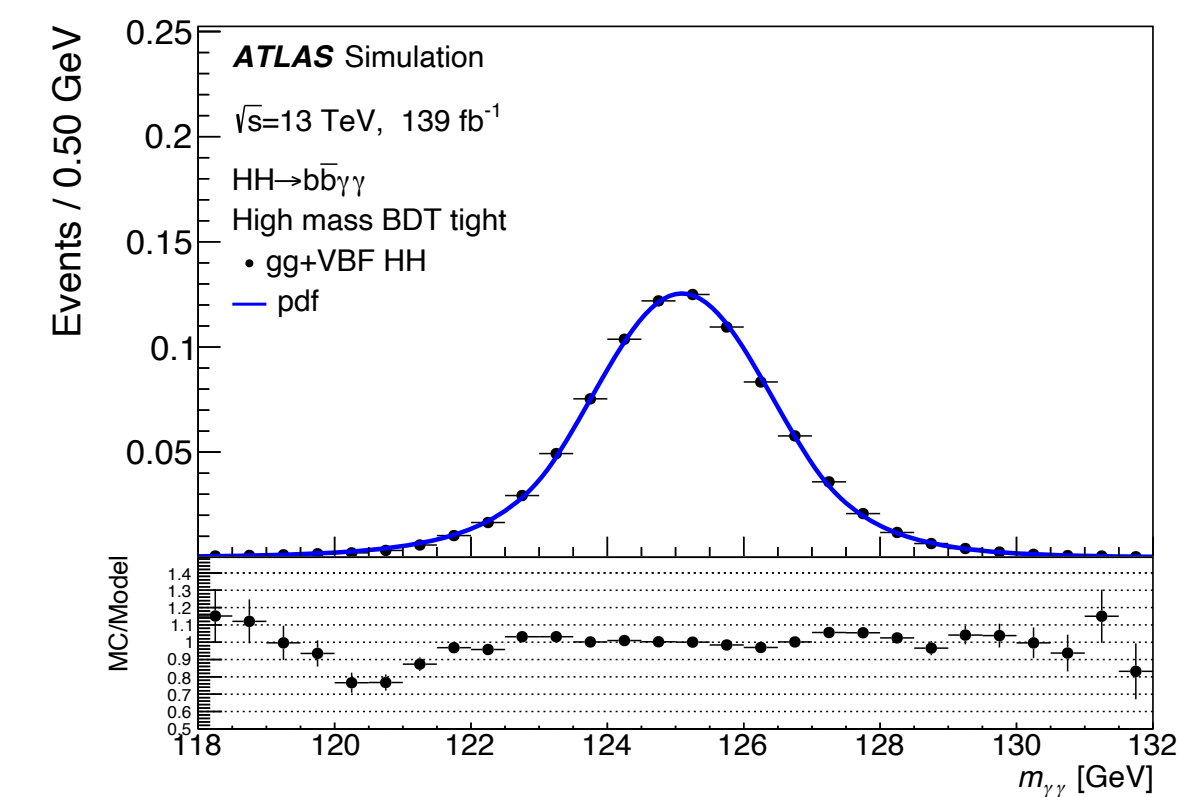
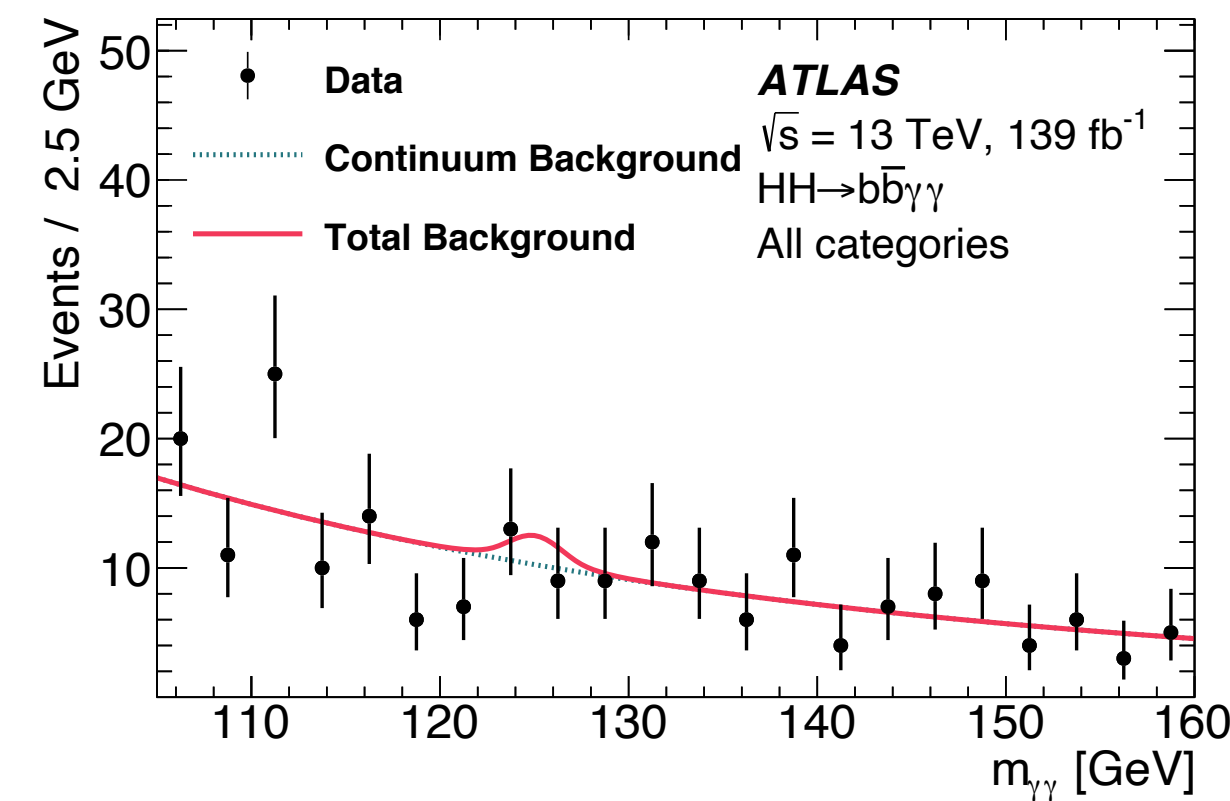
bbγγ decay channel has very small BR (0.26%) but very clean signature from the photons and clean smoothly falling di-photon background

arXiv:2112.11876

- Search for SM and BSM non-resonant HH production
- ggF and VBF HH production
- H→bb and H→γγ
- 2 photons and 2 b-tagged jets
- $105 \text{ GeV} < m_{\gamma\gamma} < 160 \text{ GeV}$



- Major backgrounds: γγ+jets modelled with exponential function derived from data in CRs and single-Higgs modelled with double-sided Crystal-Ball function derived from Monte Carlo simulations
- Signal shape also modelled with double-sided Crystal-ball function derived from Monte Carlo simulations



- Boosted Decision Trees used to discriminate signal and background
- Important input variable: reconstructed invariant mass of the Higgs boson candidate m_{bb}

Non-resonant $HH \rightarrow b\bar{b}\gamma\gamma$ with full Run 2 data

4 signal region categories

defined by selections on $m_{b\bar{b}\gamma\gamma}$ and on BDT outputs,

targeting the SM HH signal and BSM signals with varied κ_λ

- Two HH mass categories:

low mass and high mass

- One BDT trained in each mass region,

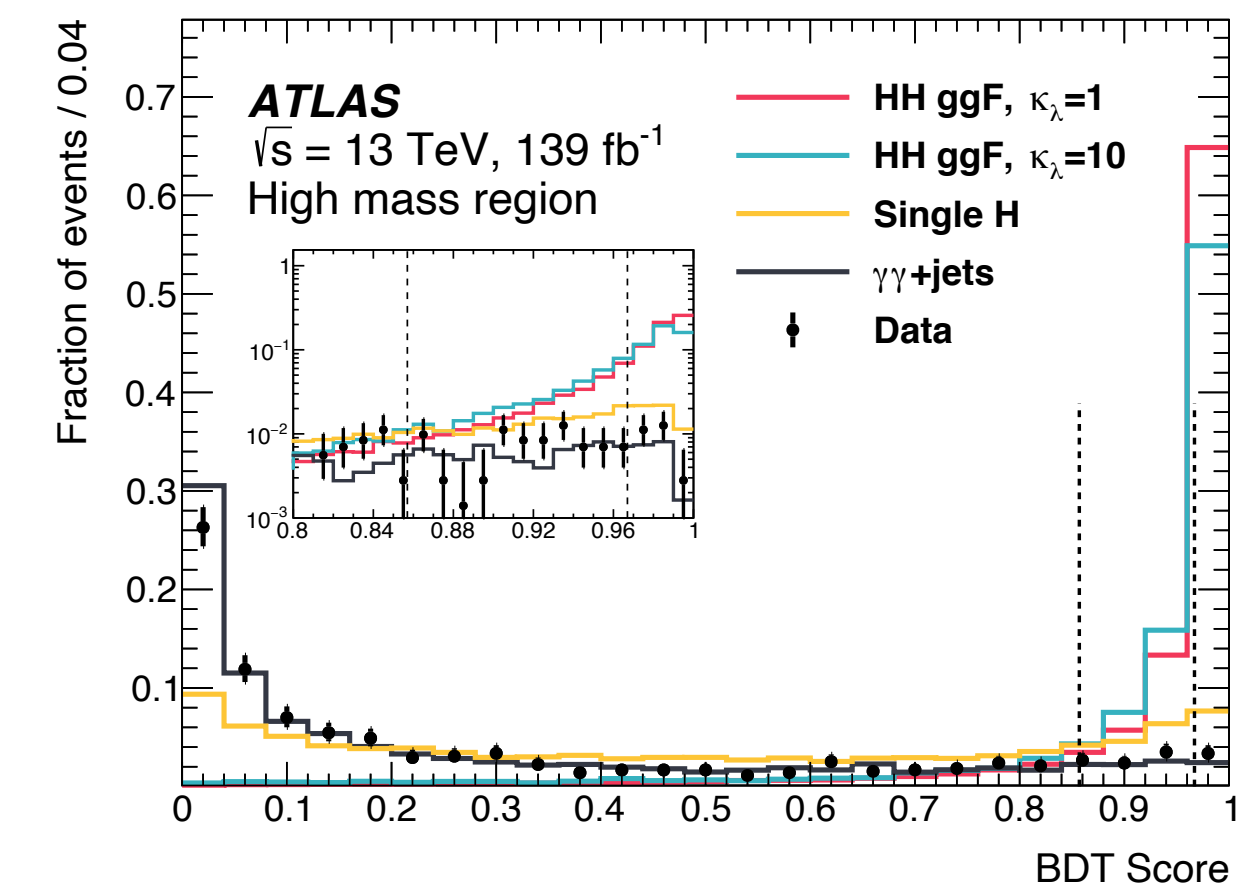
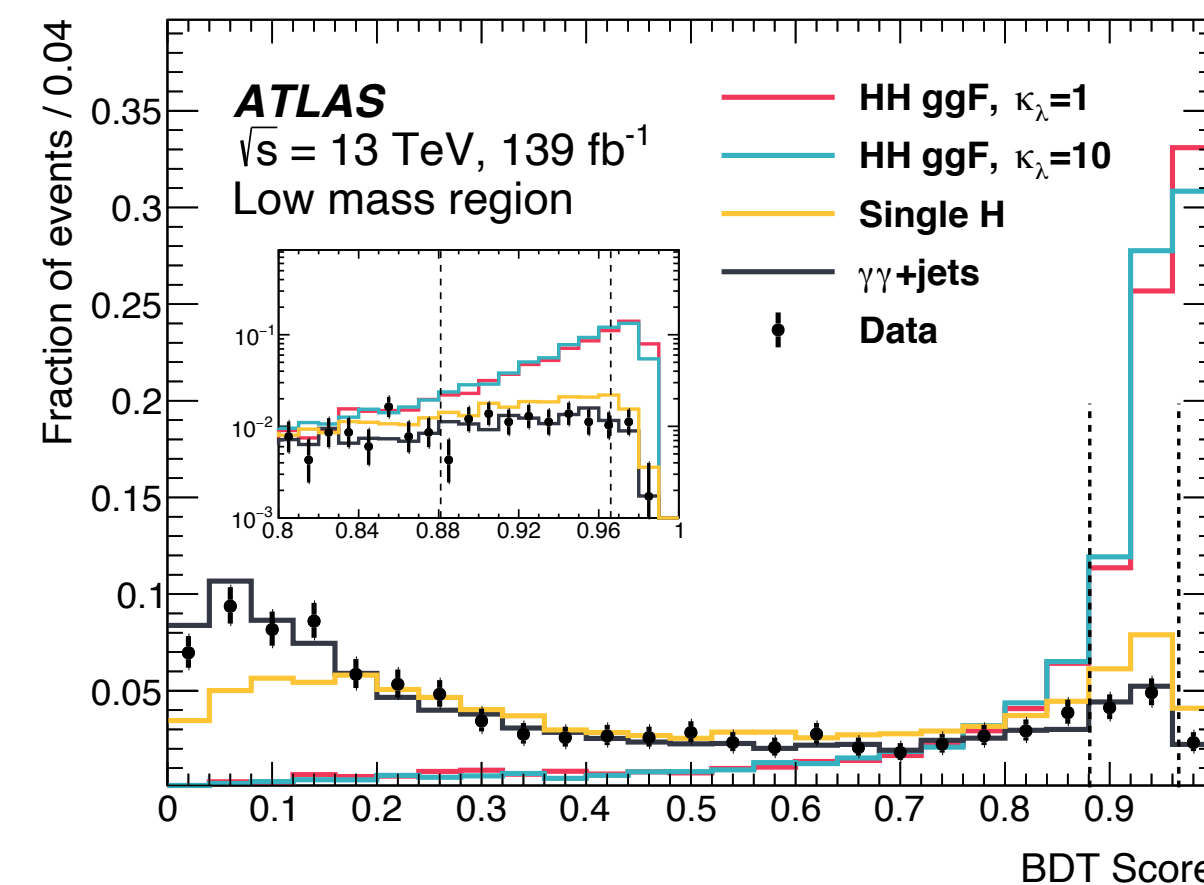
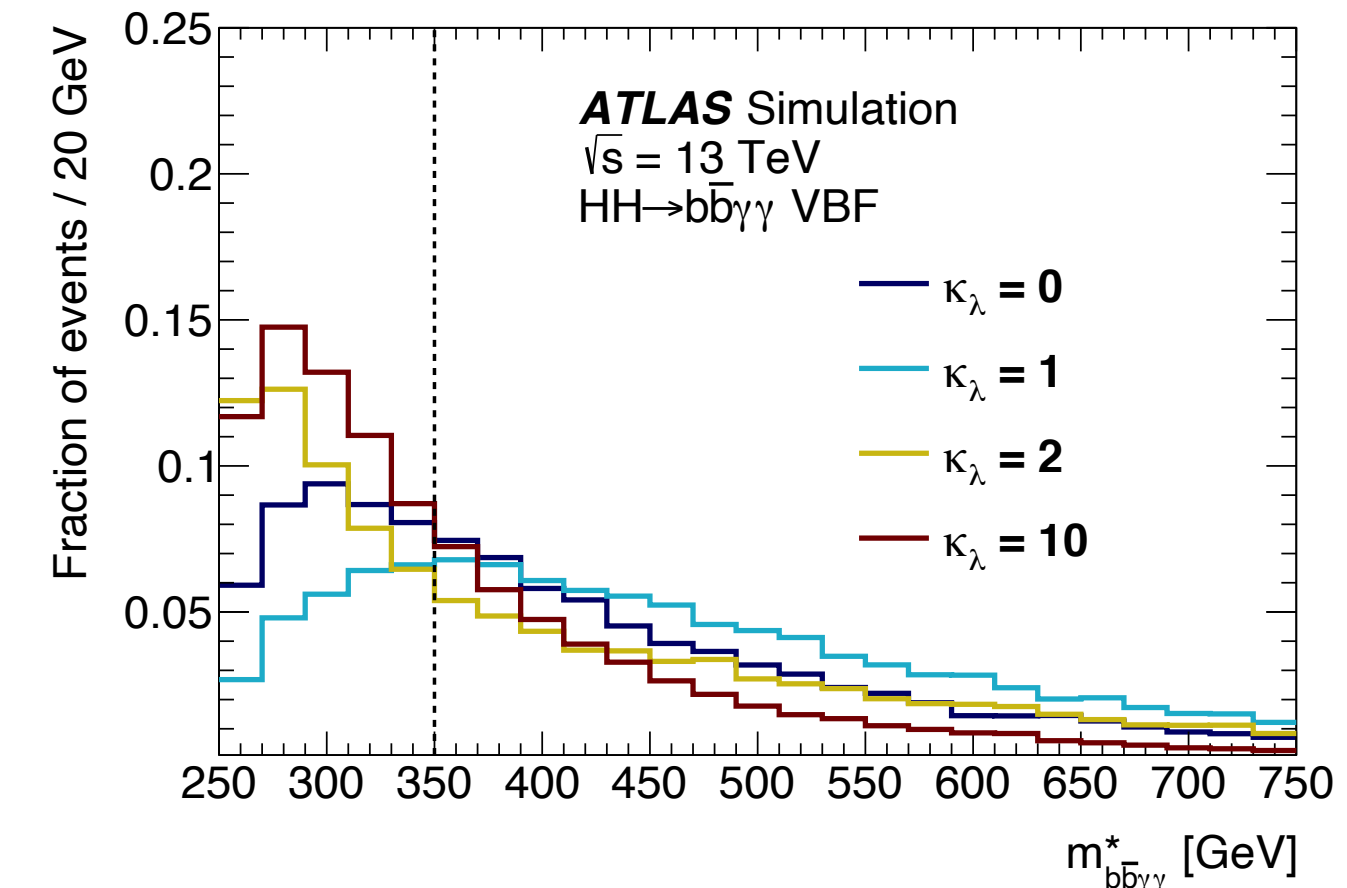
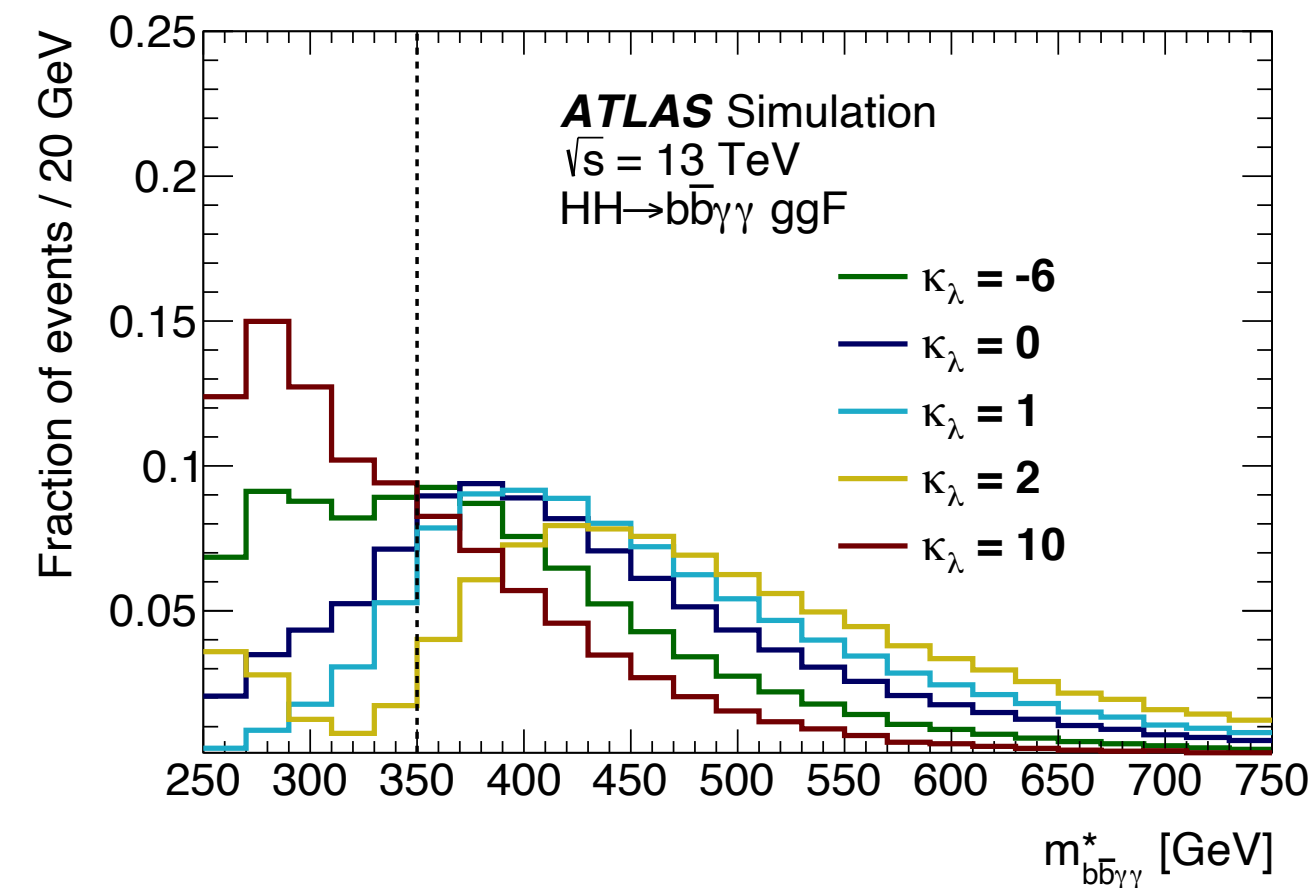
on BSM signal with $\kappa_\lambda = 10$ for low mass

and on SM signal with $\kappa_\lambda = 1$ for high mass

- Two BDT categories in each of the two mass categories:

BDT-tight and BDT-loose

arXiv:2112.11876

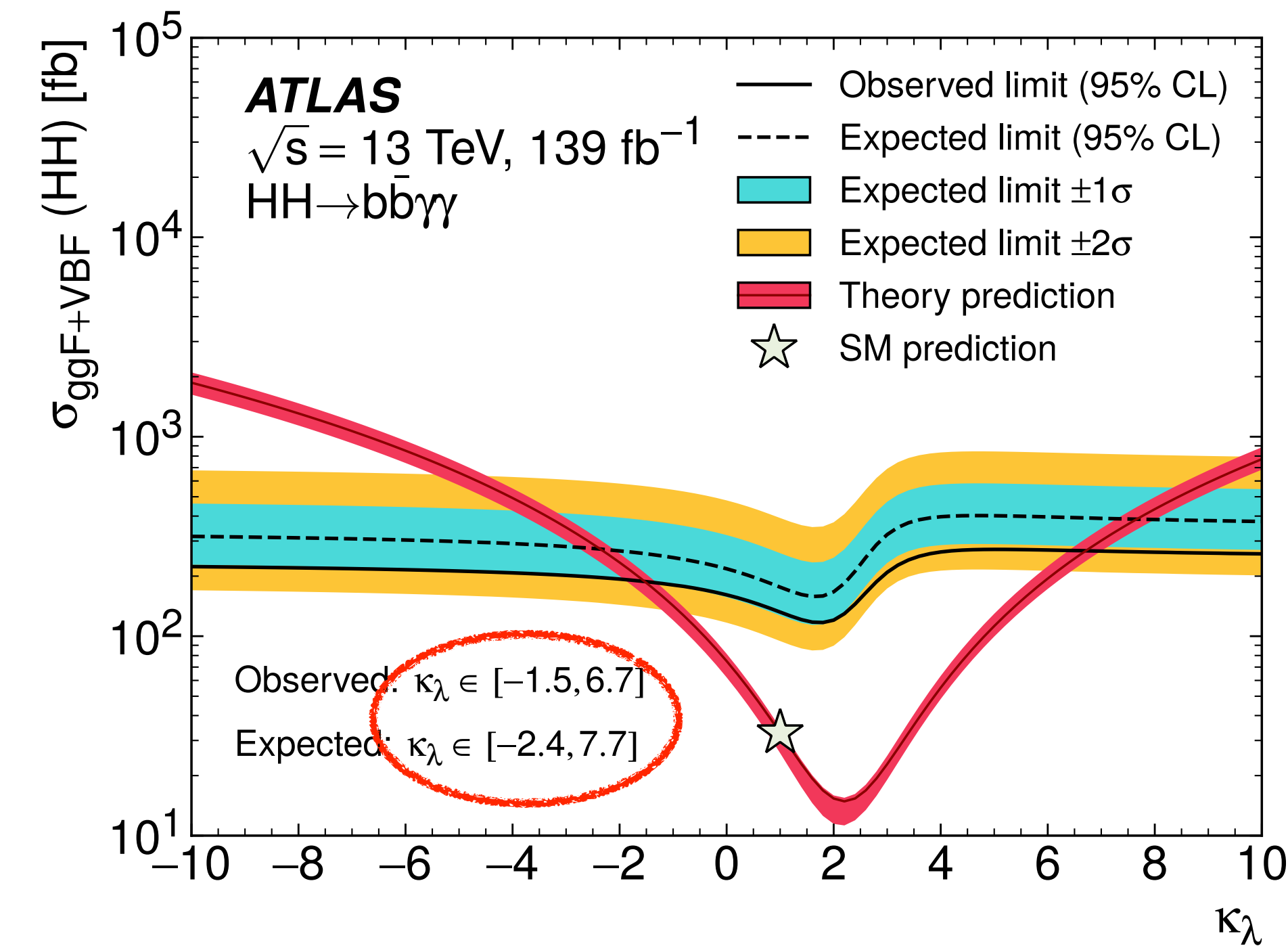
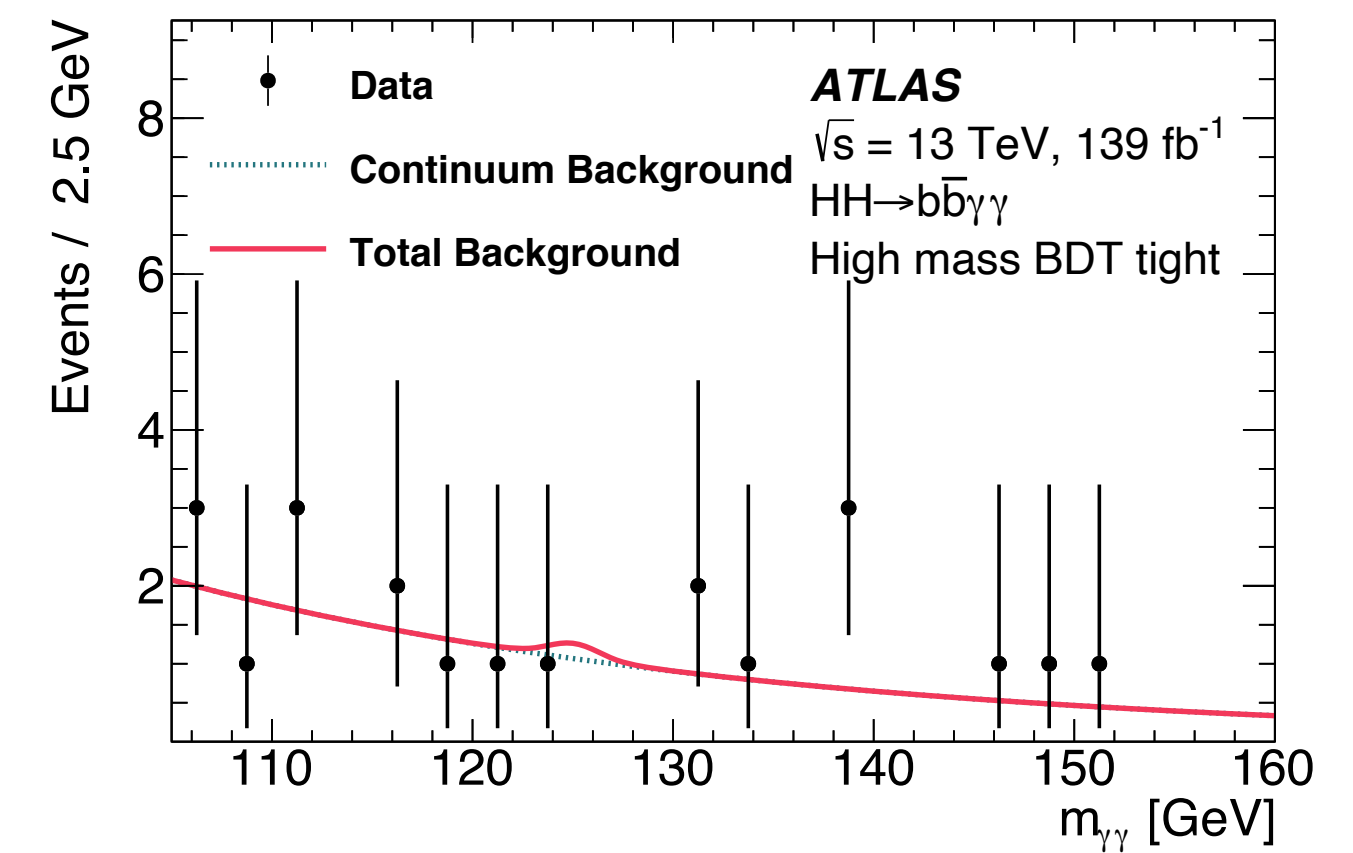
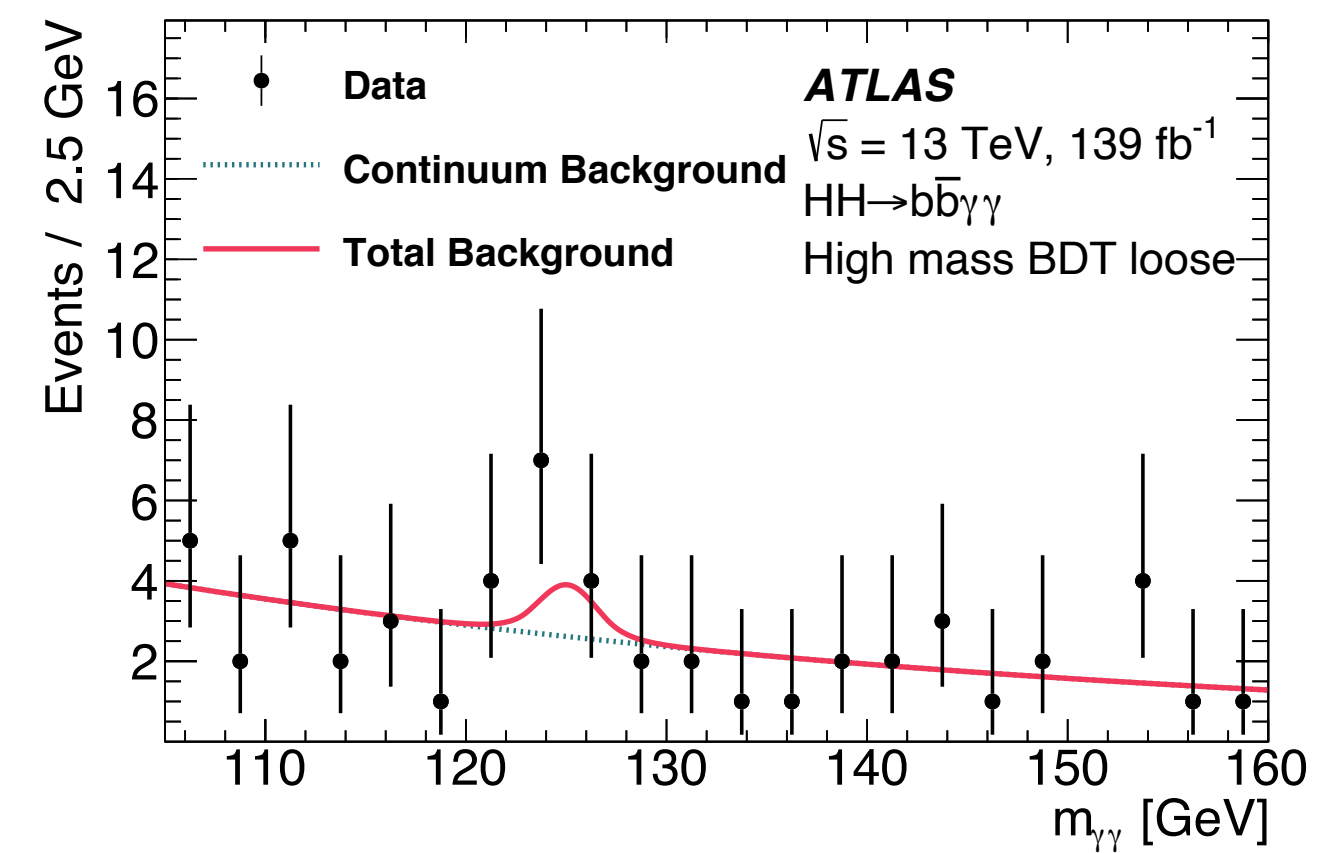
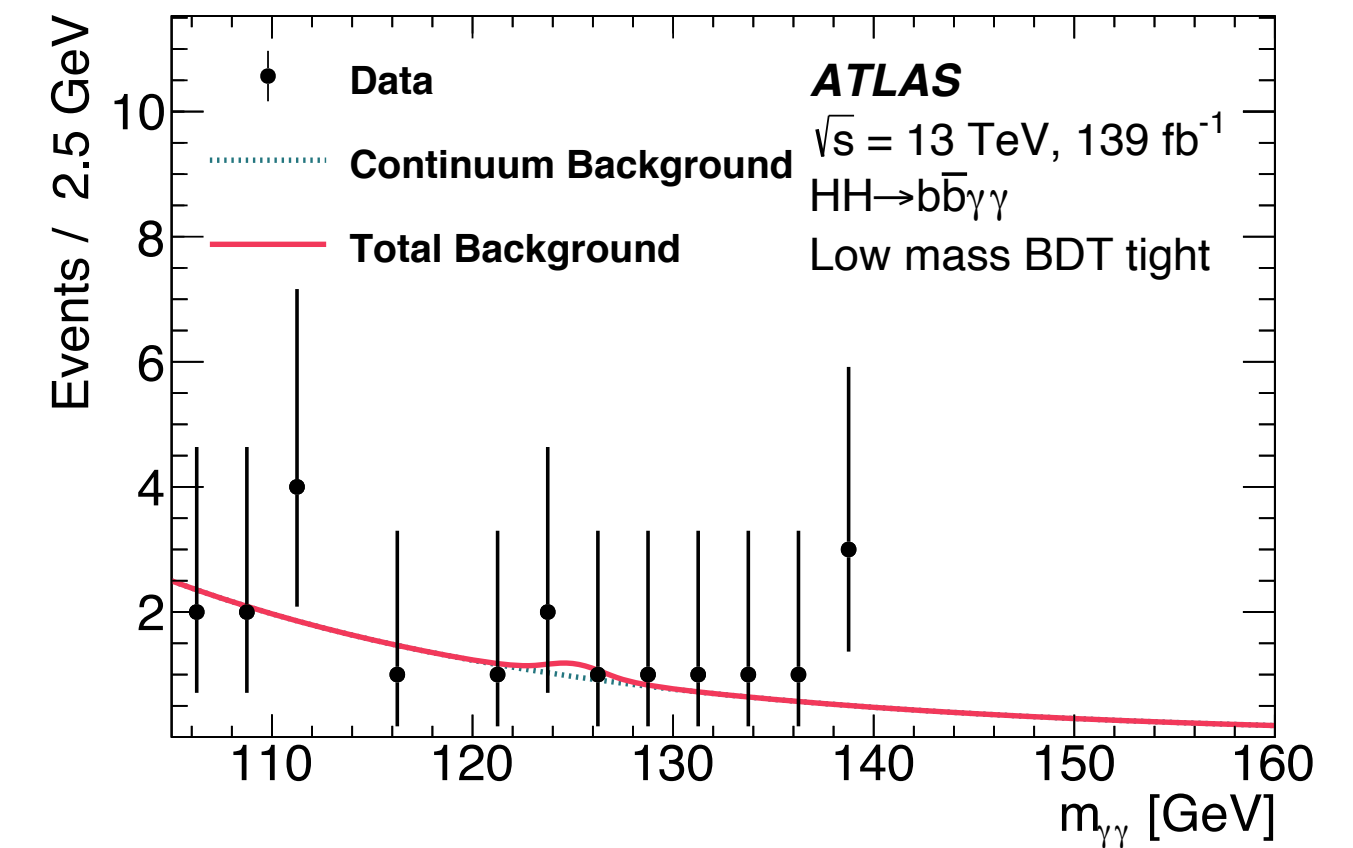
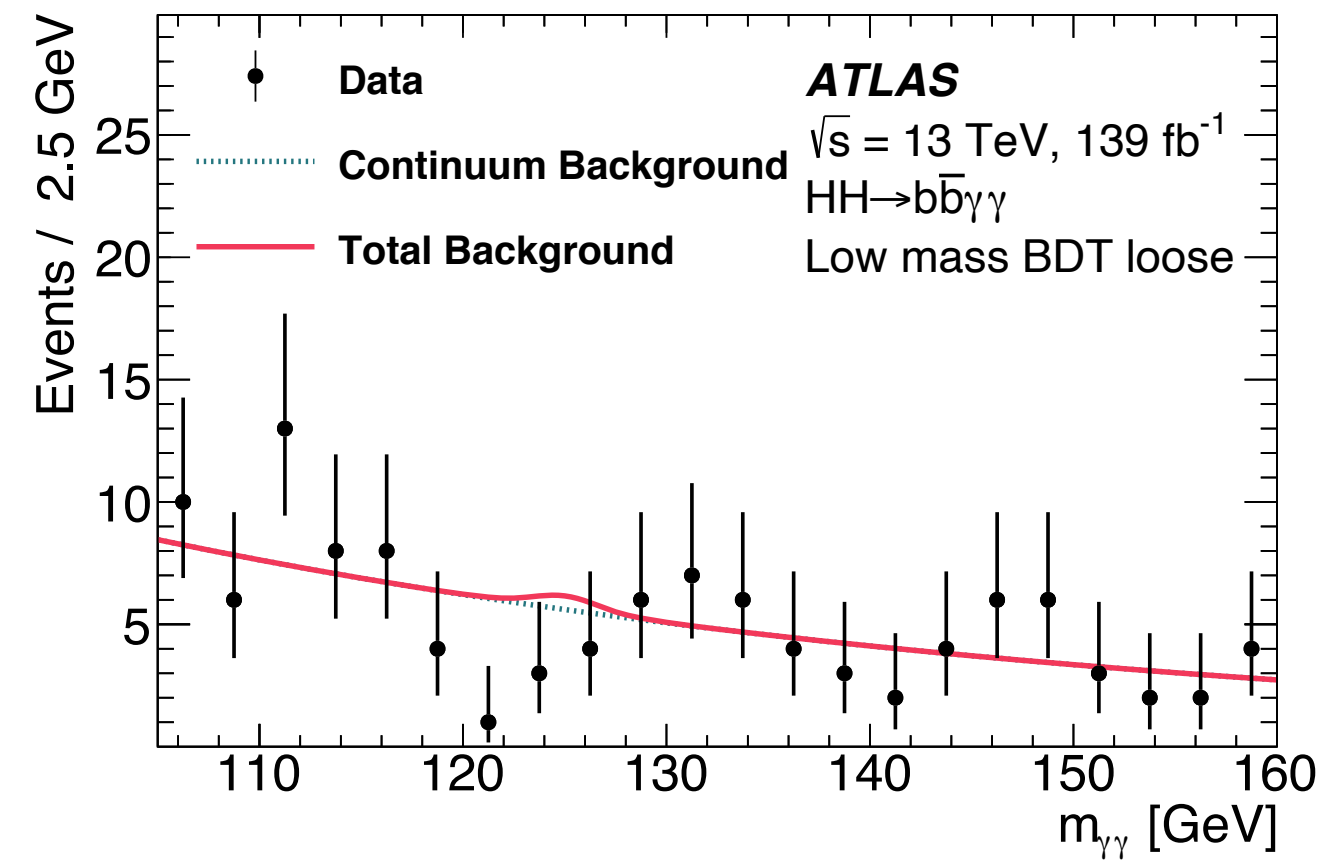


Non-resonant $HH \rightarrow b\bar{b}\gamma\gamma$ with full Run 2 data

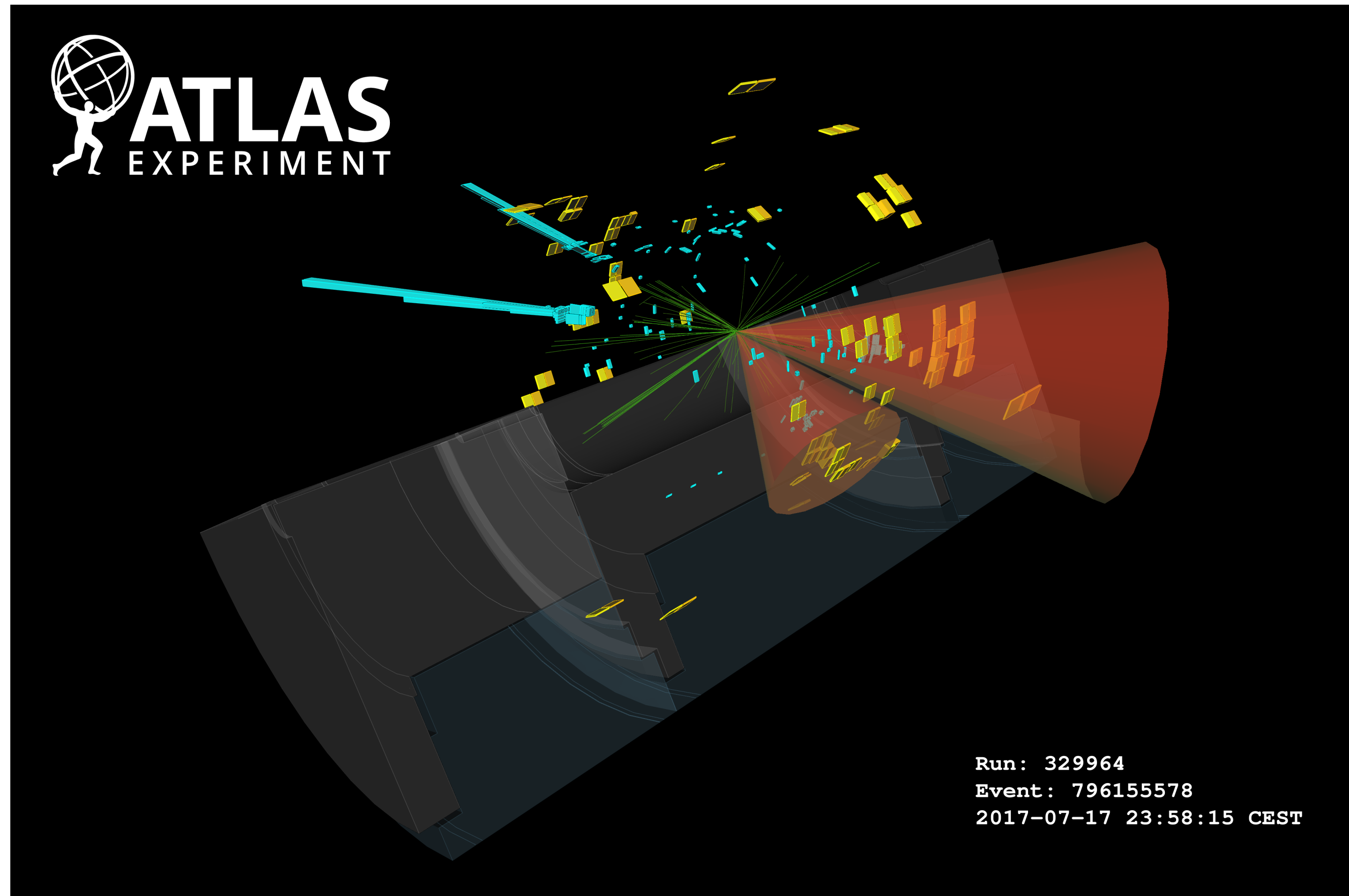
$m_{\gamma\gamma}$ used as final discriminant variable
 in the 4 signal regions,
 searching for an excess of events
 in the Higgs mass peak

arXiv:2112.11876

Upper limit on the non-resonant
 ggF+VBF HH cross section of 4.2
 x SM observed (5.7 x SM
 expected)



Non-resonant $HH \rightarrow b\bar{b}\gamma\gamma$ with full Run 2 data



Candidate HH data event of the non-resonant high mass BDT tight signal region

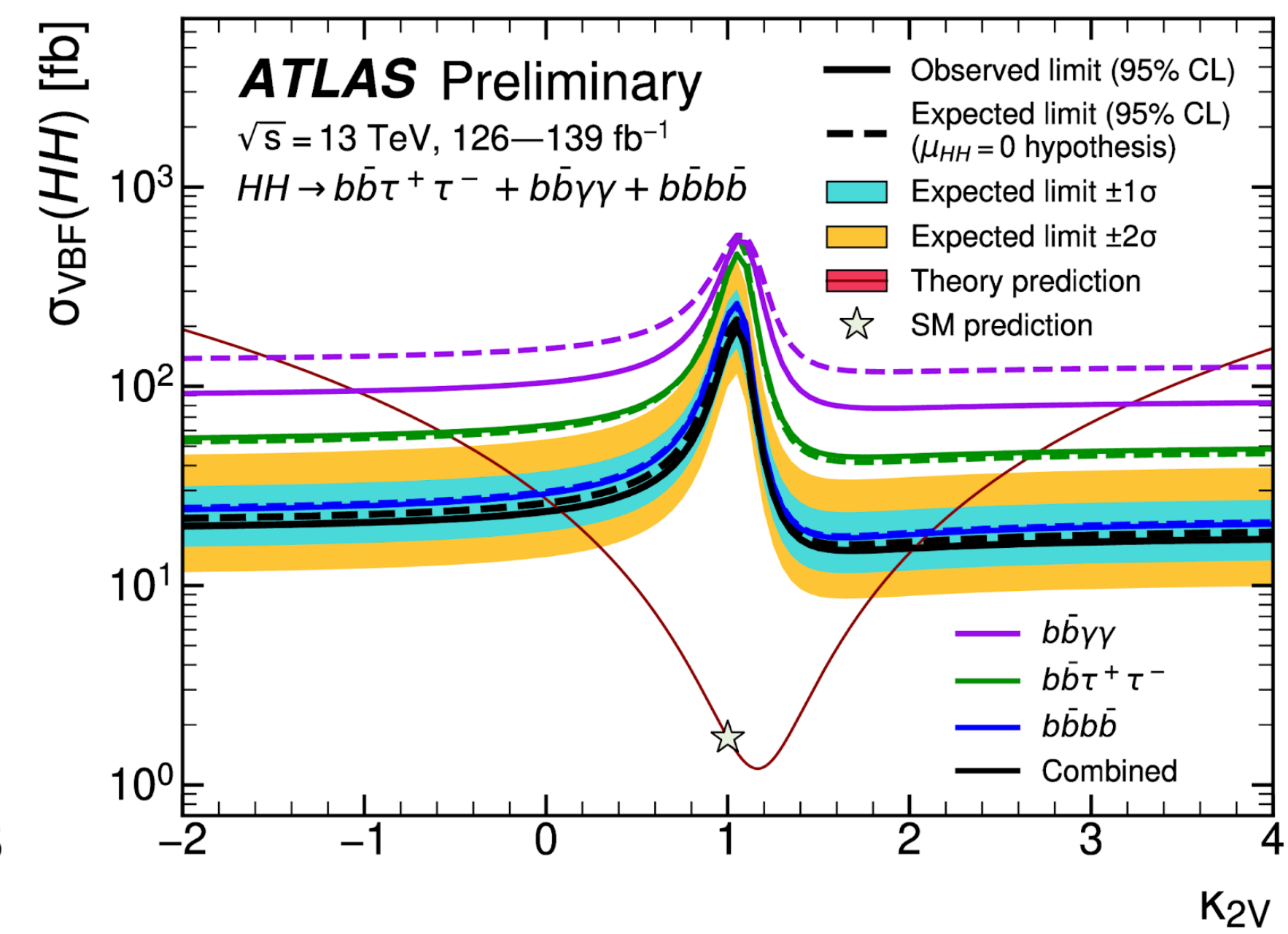
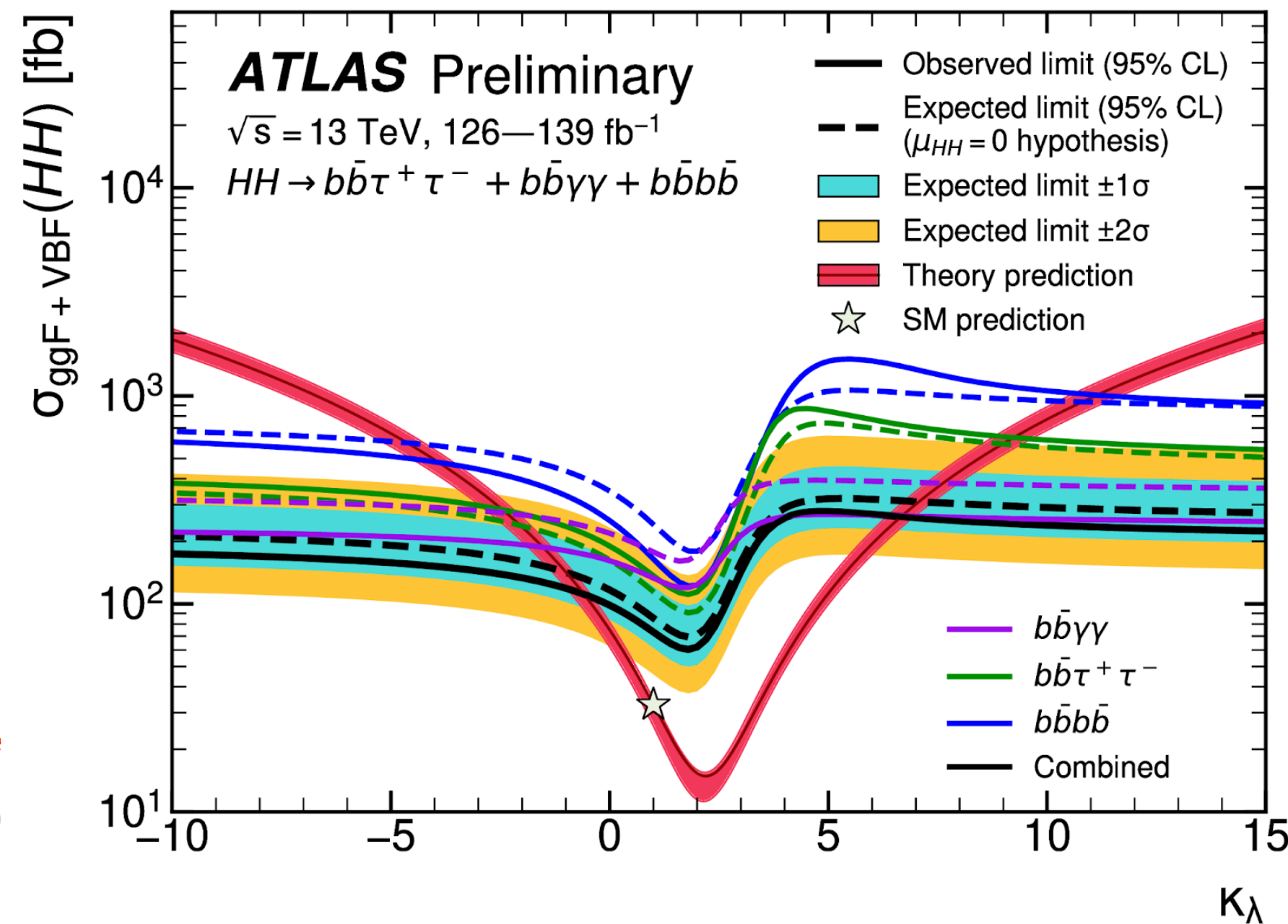
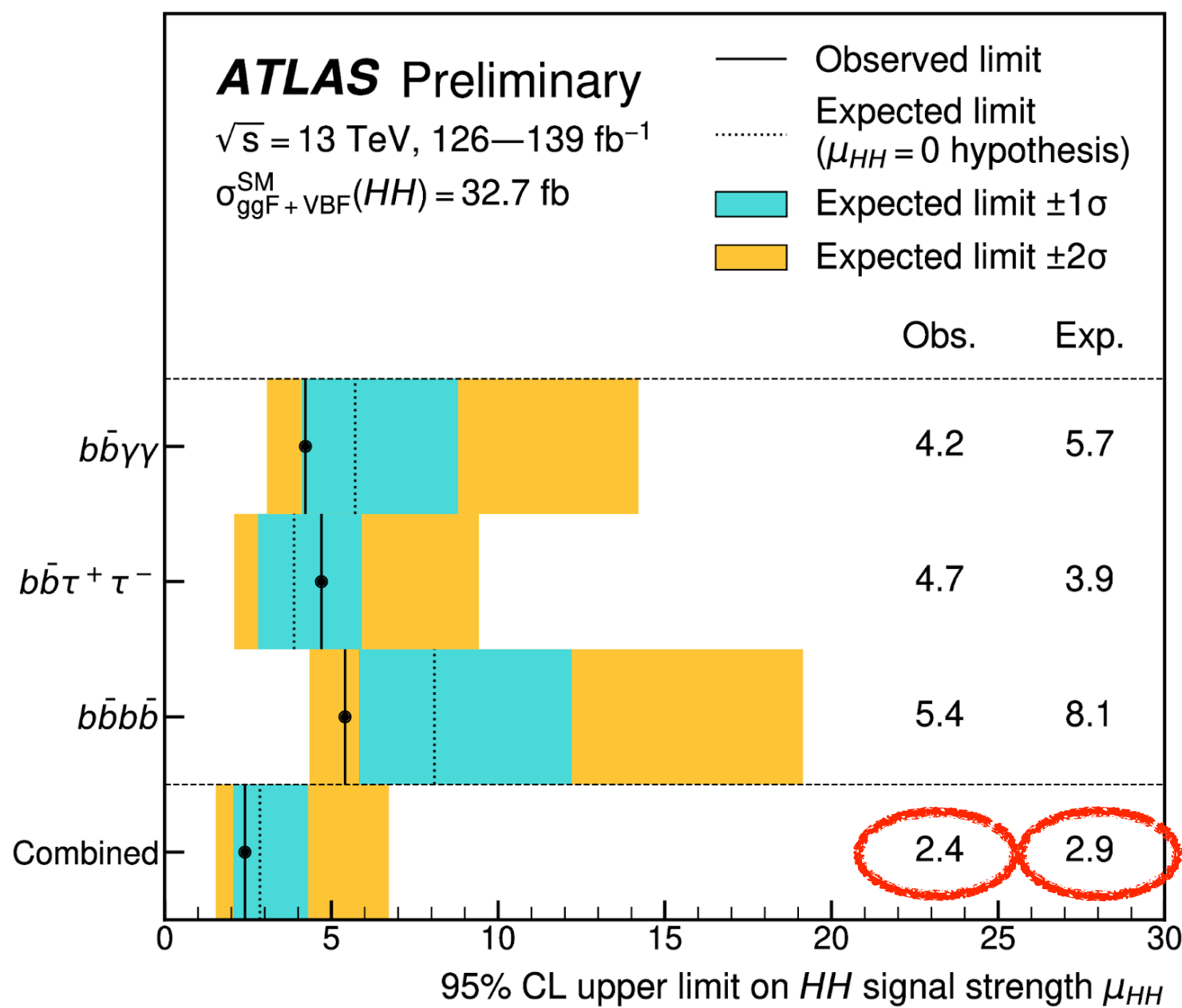
$$m_{HH} = 625 \text{ GeV}, m_{bb} = 113 \text{ GeV} \text{ and } m_{\gamma\gamma} = 123 \text{ GeV}$$

Non-resonant HH combination with full Run 2 data

Combination of HH analyses performed in 3 decay channels using full LHC Run 2 data corresponding to 139 fb^{-1} :

- $bbbb$, $bb\tau\tau$ and $bb\gamma\gamma$ channels for the search of non-resonant HH production

ATLAS-CONF-2022-050



Improvement of more than a factor 3 compared to partial Run 2 dataset combination (even including less decay channels),
 Most stringent upper limit on HH production to date

Complementarity of searches in different decay channels:

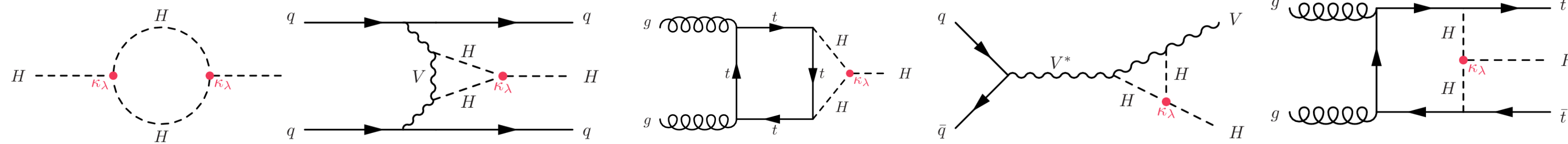
- $bb\gamma\gamma$ most sensitive for large variations of κ_λ
- $bb\tau\tau$ most sensitive for κ_λ values close to the SM
- $bbbb$ most sensitive to VBF production and variations of κ_{2V}

Combination of HH and H analyses with full Run 2 data

Combination of HH and single-H analyses using full LHC Run 2 data corresponding to 139 fb^{-1} :

Channel
$HH \rightarrow b\bar{b}\gamma\gamma$
$HH \rightarrow b\bar{b}\tau\bar{\tau}$
$HH \rightarrow b\bar{b}b\bar{b}$
$H \rightarrow \gamma\gamma$
$H \rightarrow ZZ^* \rightarrow 4\ell$
$H \rightarrow \tau^+\tau^-$
$H \rightarrow WW^* \rightarrow e\nu\mu\nu$ (ggF,VBF)
$H \rightarrow b\bar{b}$ (VH)
$H \rightarrow b\bar{b}$ (VBF)
$H \rightarrow b\bar{b}$ ($t\bar{t}H$)

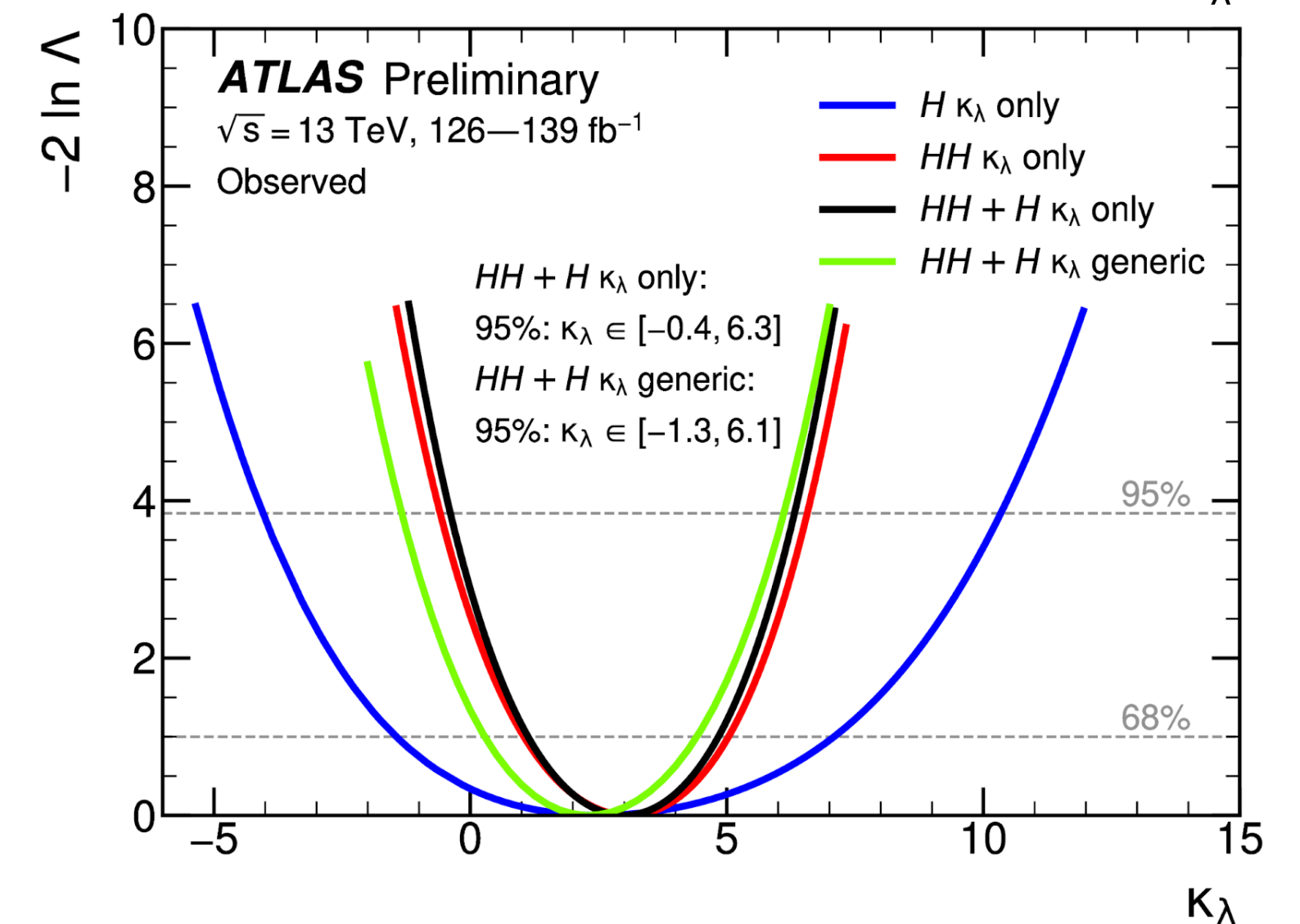
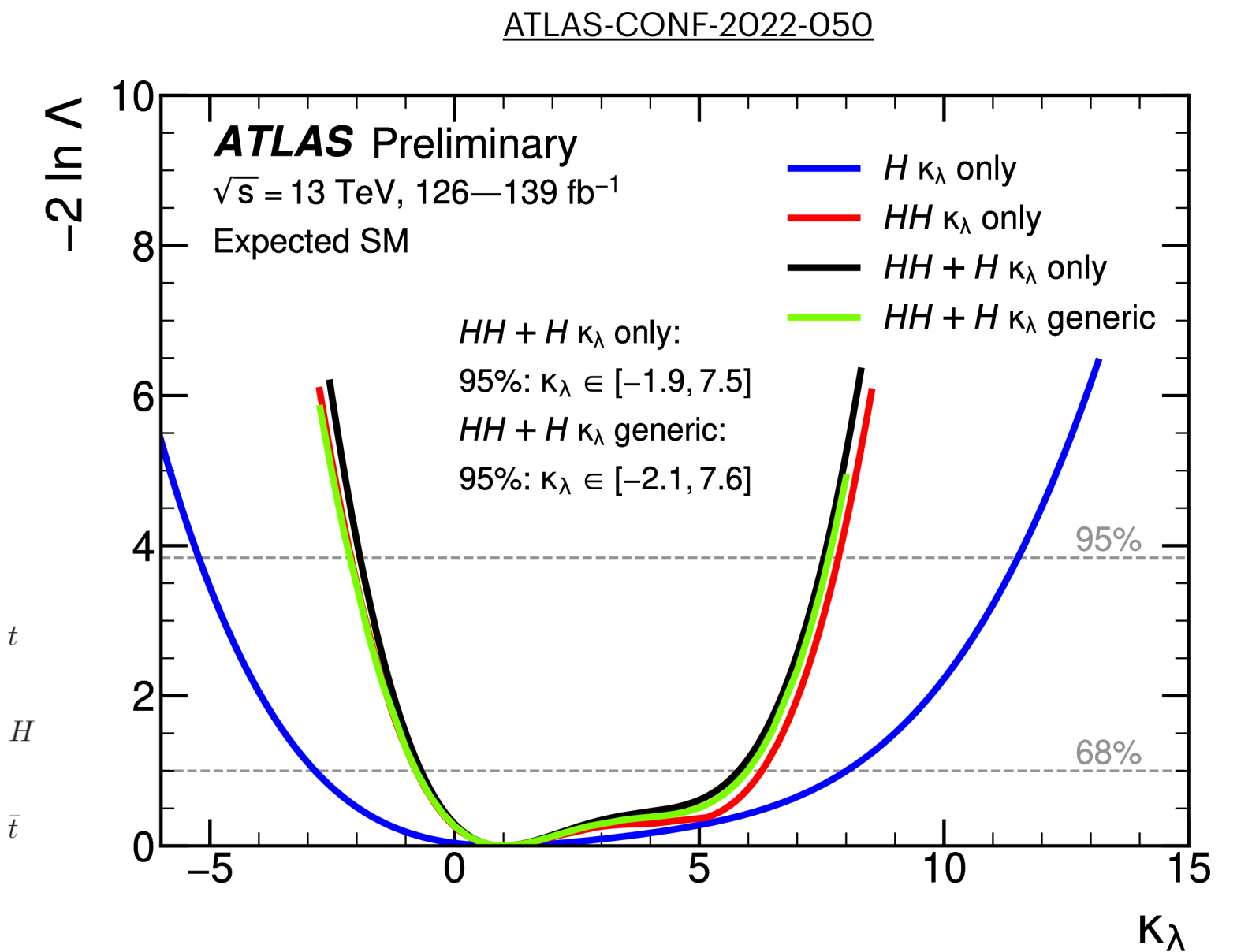
Exploits direct sensitivity to κ_λ of HH and indirect sensitivity to κ_λ of single-H through NLO EW corrections affecting single-Higgs production and decay



Combination assumption	Obs. 95% CL	Exp. 95% CL	Obs. value $^{+1\sigma}_{-1\sigma}$
HH combination	$-0.6 < \kappa_\lambda < 6.6$	$-2.1 < \kappa_\lambda < 7.8$	$\kappa_\lambda = 3.1^{+1.9}_{-2.0}$
Single-H combination	$-4.0 < \kappa_\lambda < 10.3$	$-5.2 < \kappa_\lambda < 11.5$	$\kappa_\lambda = 2.5^{+4.6}_{-3.9}$
HH+H combination	$-0.4 < \kappa_\lambda < 6.3$	$-1.9 < \kappa_\lambda < 7.5$	$\kappa_\lambda = 3.0^{+1.8}_{-1.9}$
HH+H combination, κ_t floating	$-0.4 < \kappa_\lambda < 6.3$	$-1.9 < \kappa_\lambda < 7.6$	$\kappa_\lambda = 3.0^{+1.8}_{-1.9}$
HH+H combination, $\kappa_t, \kappa_V, \kappa_b, \kappa_\tau$ floating	$-1.3 < \kappa_\lambda < 6.1$	$-2.1 < \kappa_\lambda < 7.6$	$\kappa_\lambda = 2.3^{+2.1}_{-2.0}$

Combination of HH and single-H analyses:

- Improves sensitivity to κ_λ , providing the **most stringent constraints on κ_λ to date**
- Allows setting constraints on κ_λ in a more generic model with fewer assumptions on the other Higgs boson couplings



Summary and outlook

di-Higgs searches allow to directly probe the triple Higgs boson coupling

Latest ATLAS di-Higgs searches with full LHC Run 2 dataset in the $b\bar{b}b\bar{b}$, $b\bar{b}\tau\tau$ and $b\bar{b}\gamma\gamma$ channels have significantly improved the results beyond luminosity increase compared to previous partial Run 2 dataset results, providing the most stringent upper limit on the HH production up to now:

$$\mu_{HH} < 2.4 \text{ at } 95\% \text{ CL}$$

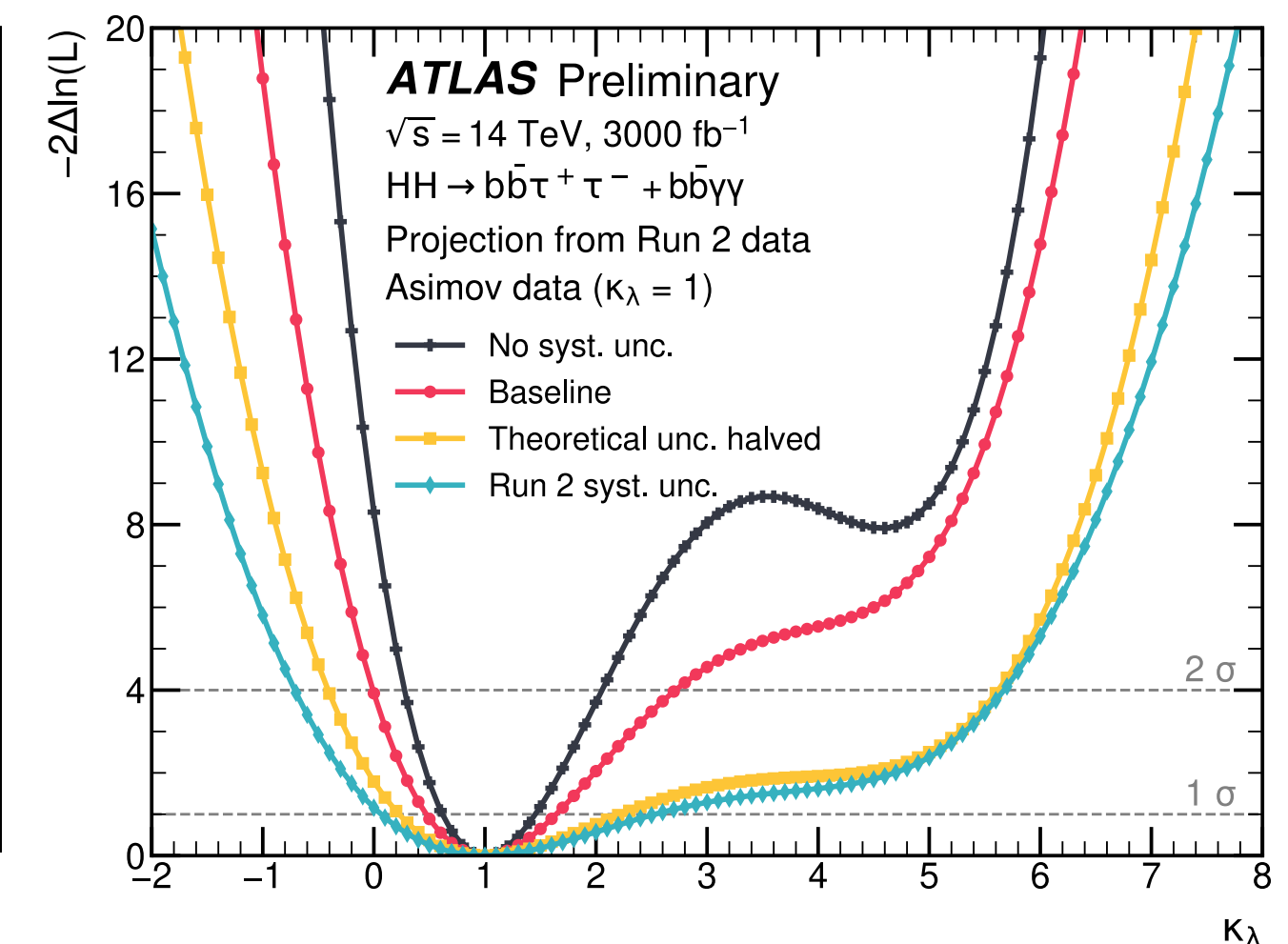
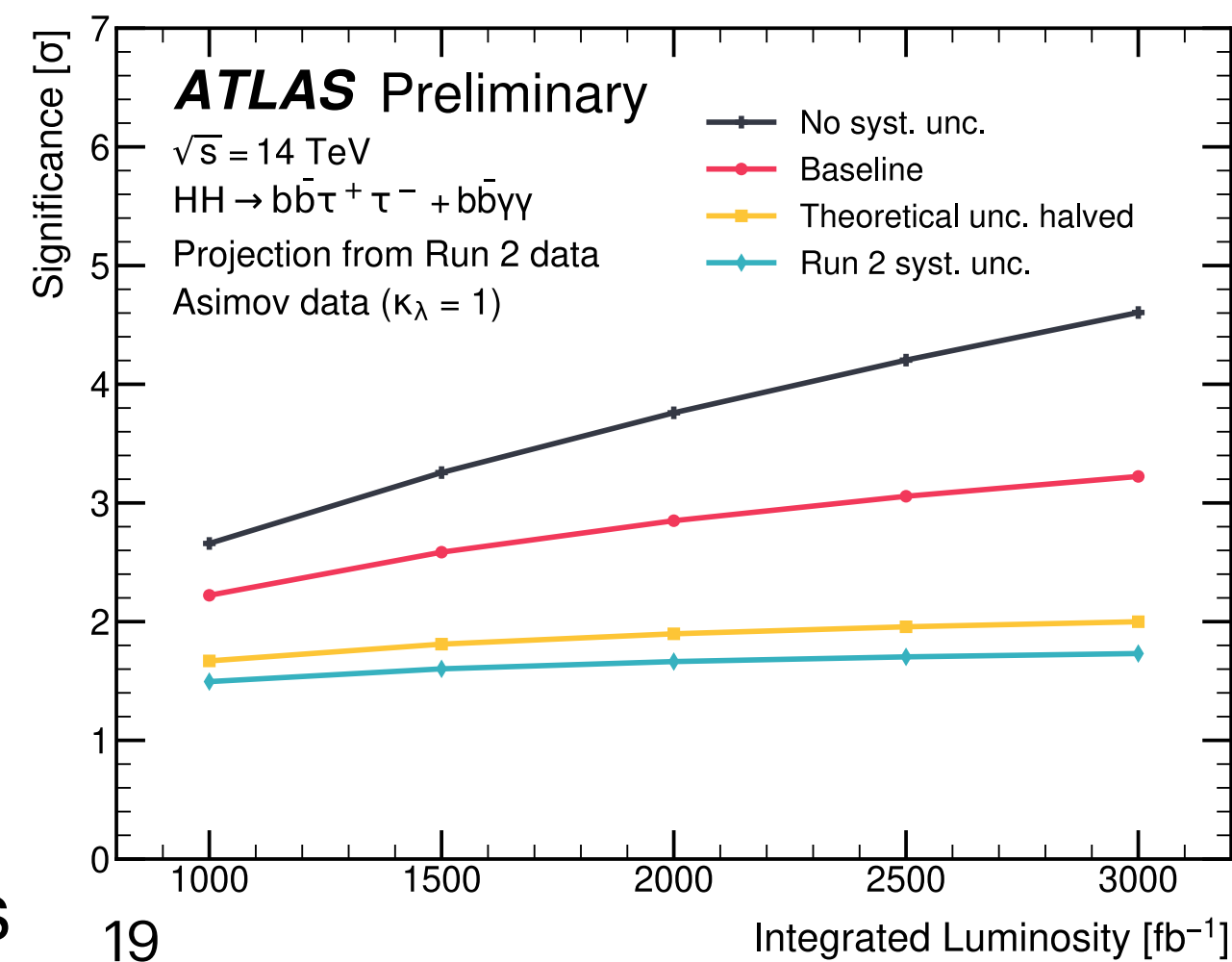
Recent ATLAS combination of HH and single-Higgs analyses with full LHC Run 2 dataset provides the most stringent constraints on κ_λ obtained up to now:

$$-0.4 < \kappa_\lambda < 6.3 \text{ at } 95\% \text{ CL}$$

→ Now preparing for the new ATLAS HH analyses with LHC Run 3 data, exploiting increased statistics and exploring new analysis techniques!

→ Preparation towards the HL-LHC, where we already expect to be able to achieve 3.2σ evidence for HH production and to measure κ_λ with a 50% uncertainty from extrapolations of ATLAS $b\bar{b}\tau\tau$ and $b\bar{b}\gamma\gamma$ Run 2 analyses

ATL-PHYS-PUB-2022-005



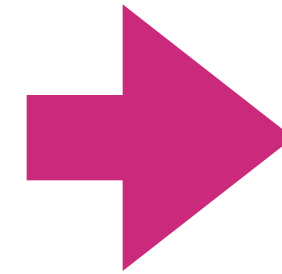
Thank you for your attention!

Back-up slides

Effective Field Theory (EFT) interpretations

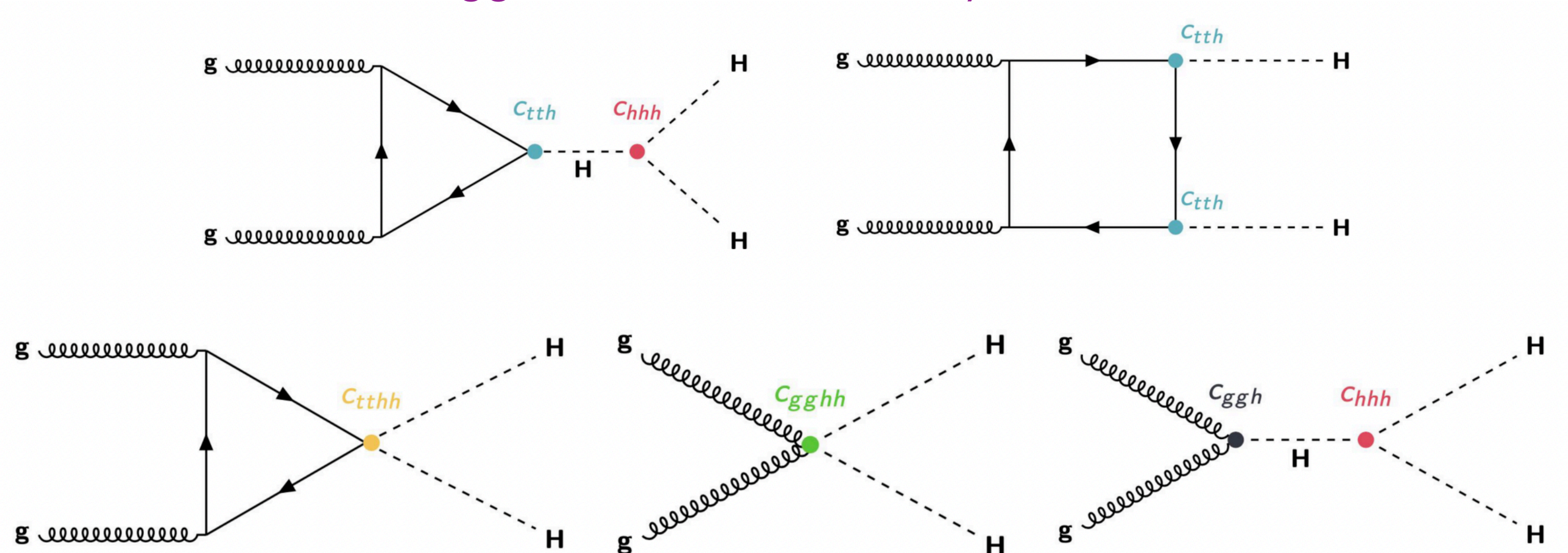
In addition to the interpretations of the results in the κ -framework, where the effect of the BSM physics is modelled simply through

$$\text{Higgs Boson coupling modifiers } \kappa = \frac{c}{c^{SM}}$$



Interpretations in the Effective Field Theory (EFT) framework, where the effect of BSM physics is parameterised through the addition of higher orders operators with effective couplings at the low-energy scale

Higgs Effective Field Theory (HEFT):



In HEFT for ggF HH production at LO there are 5 operators and their corresponding Wilson coefficients representing the Higgs Boson coupling modifiers affecting ggF HH production

→ HH production has unique access to c_{hhh} , c_{tthh} and $c_{gg hh}$

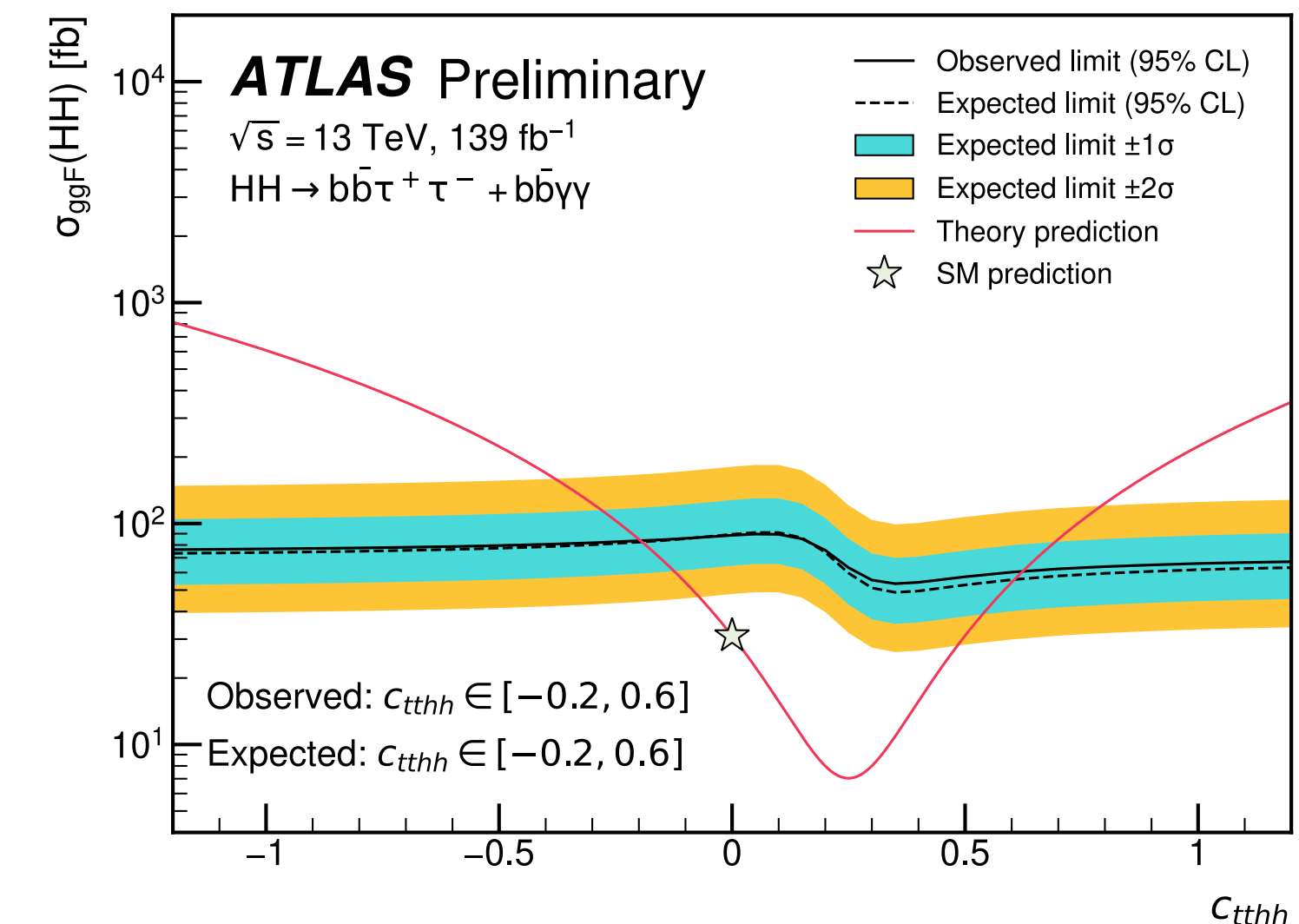
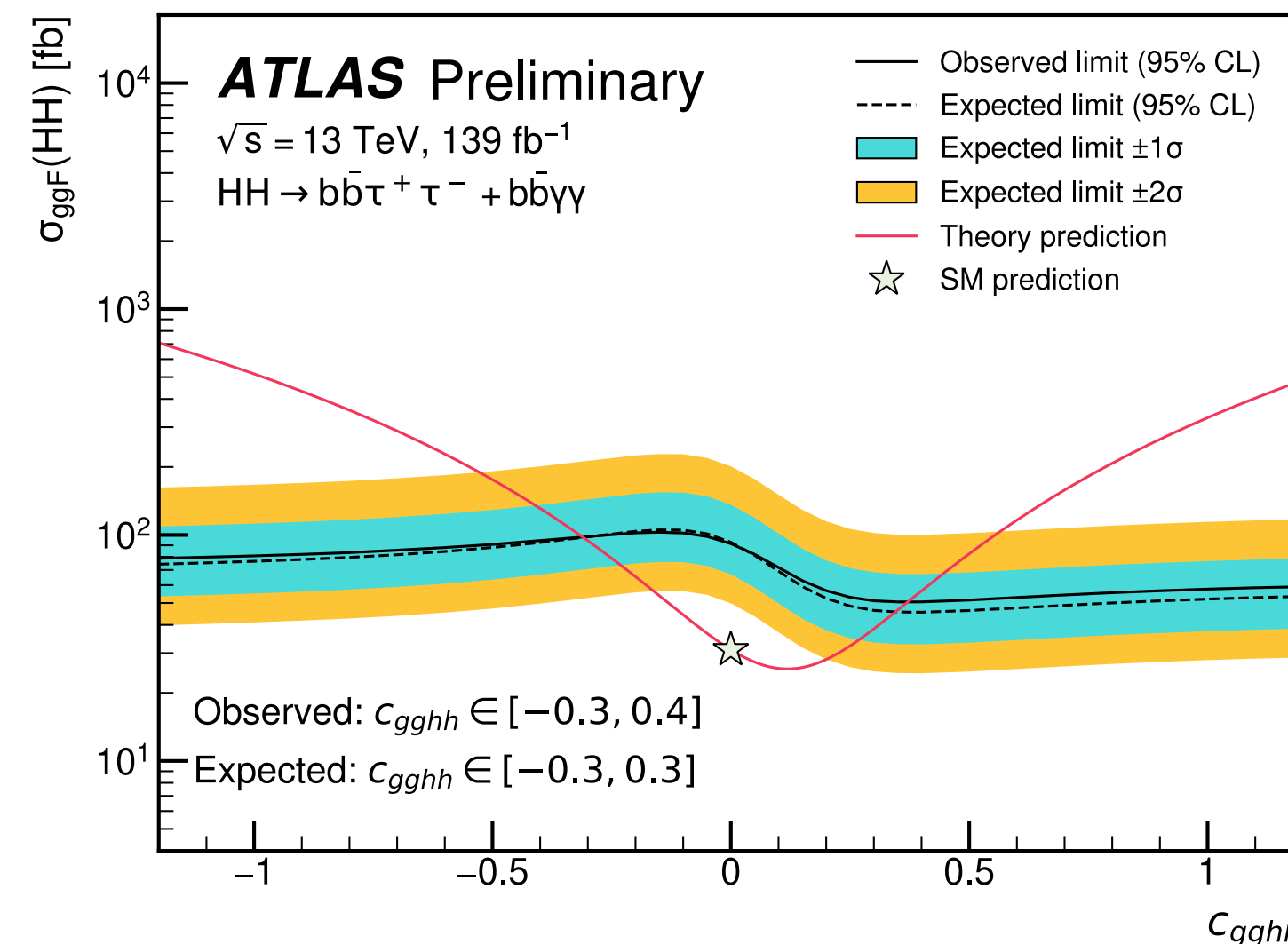
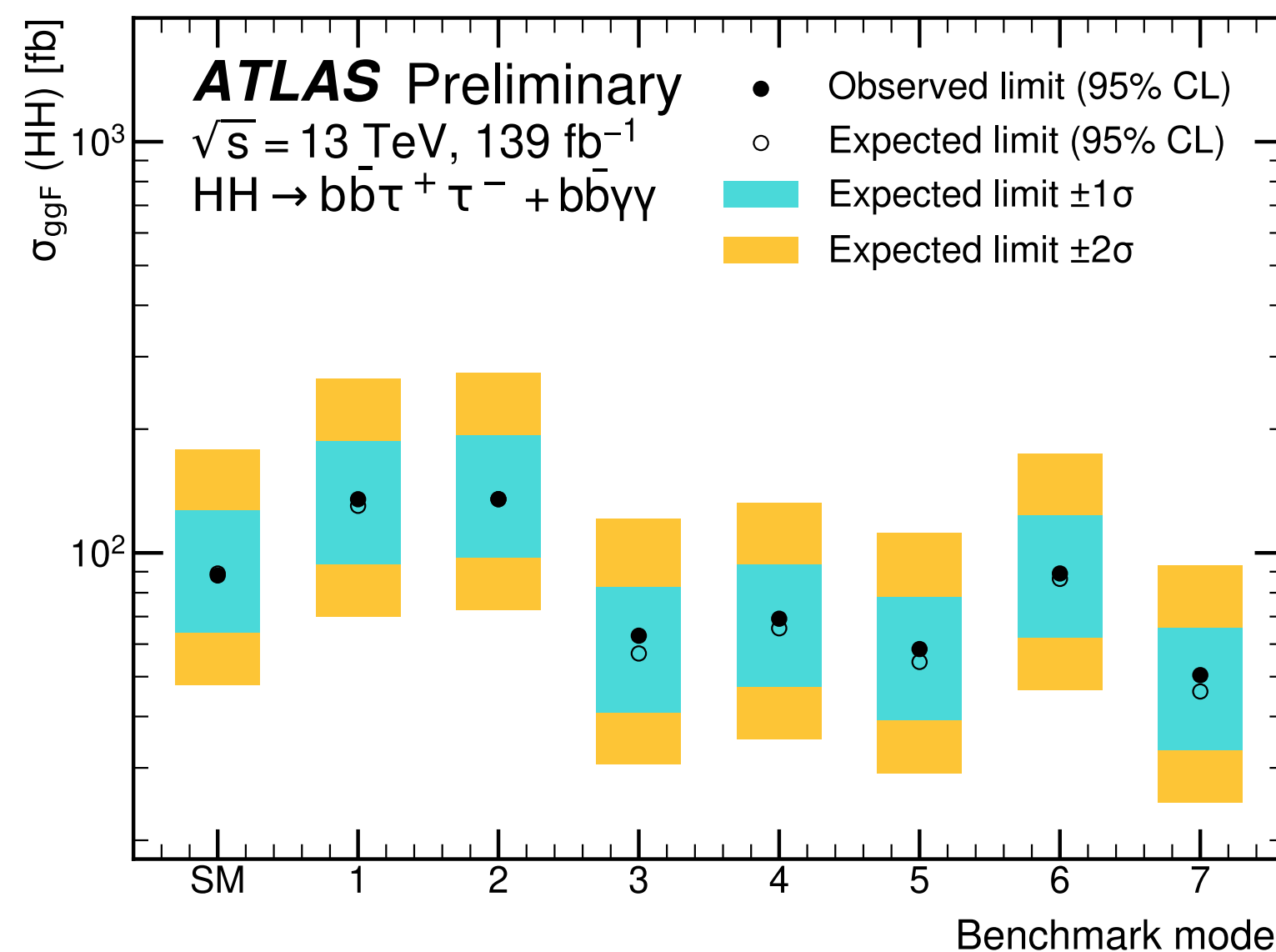
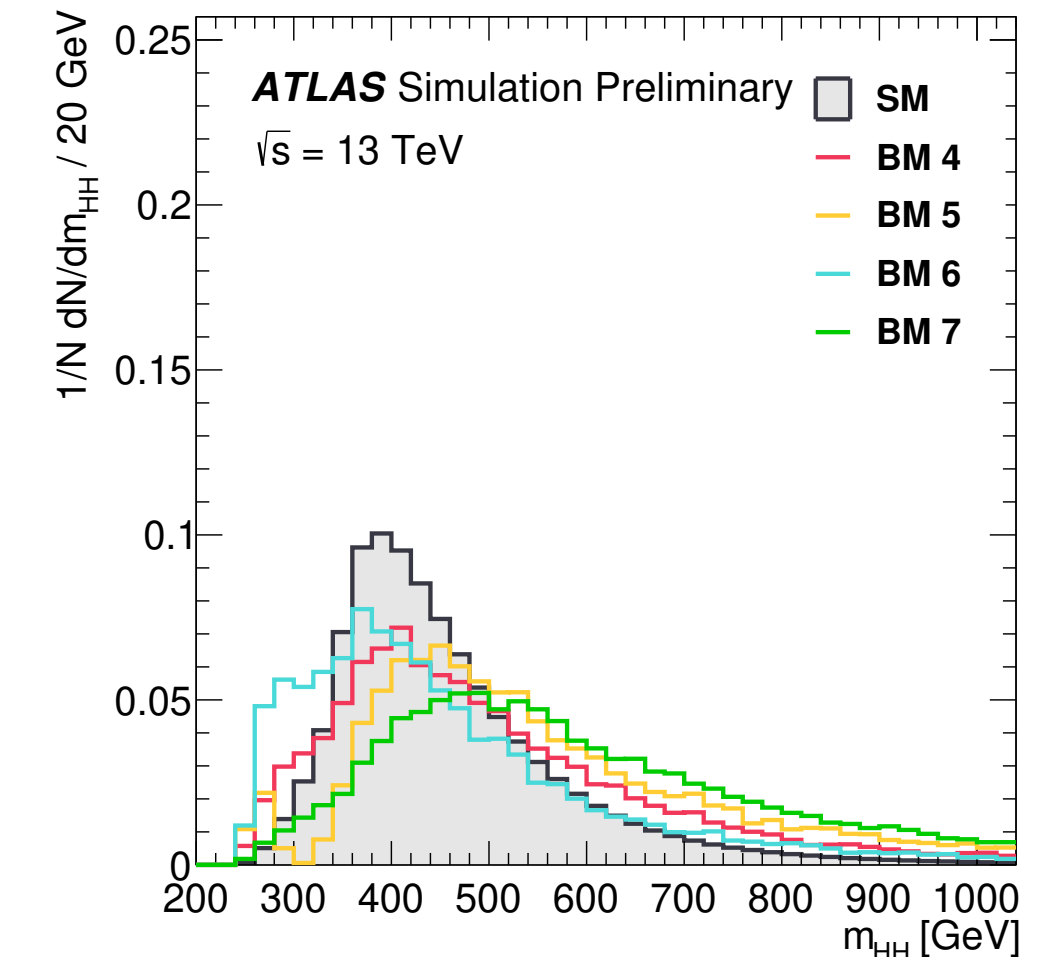
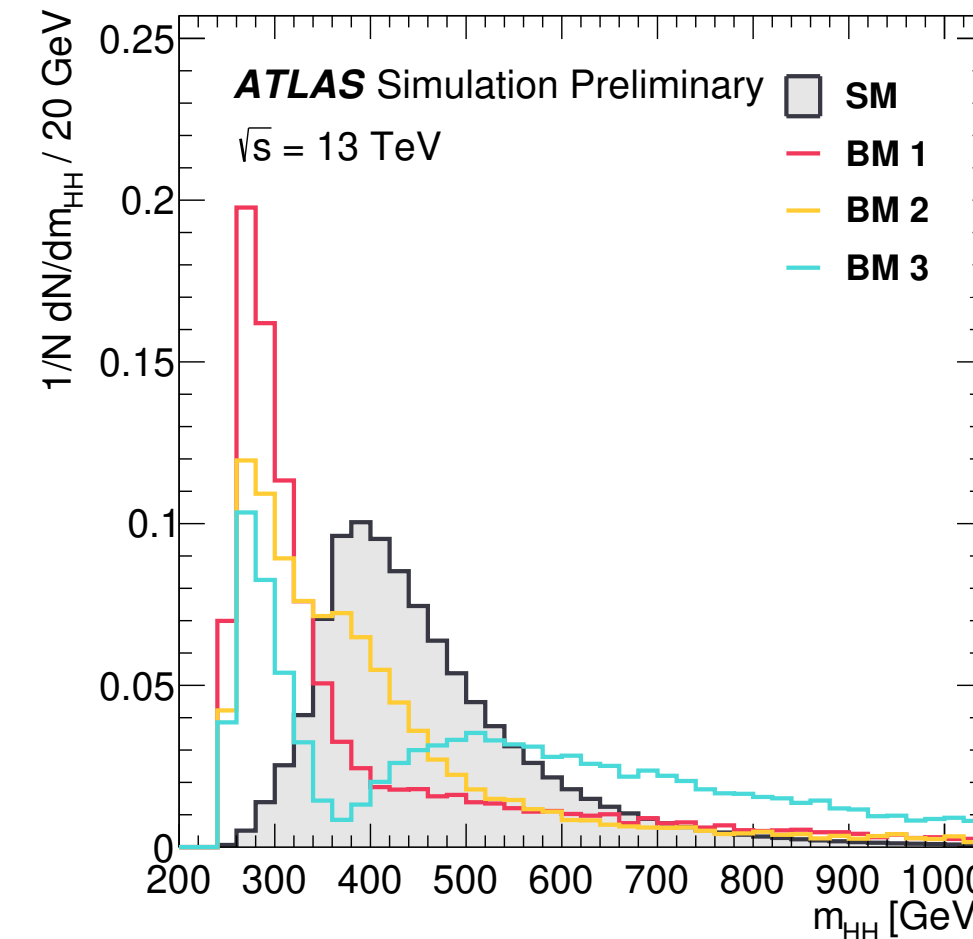
Effective Field Theory (EFT) interpretations

Using 7 HEFT m_{HH} shape benchmarks identified with a cluster analysis on the modified m_{HH} shape obtained with different values of the HEFT Higgs coupling parameters

ATL-PHYS-PUB-2022-019

JHEP03(2020)091

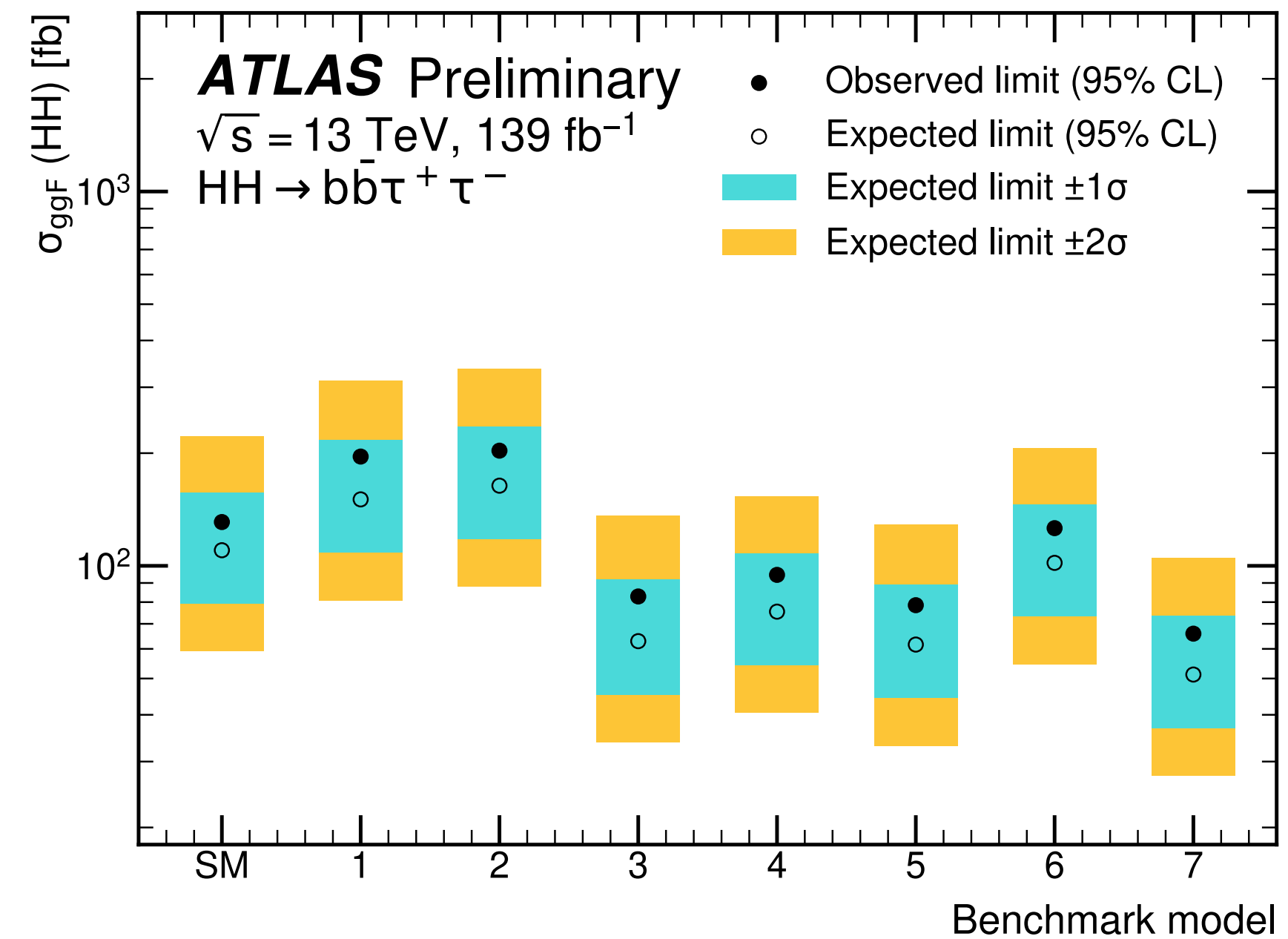
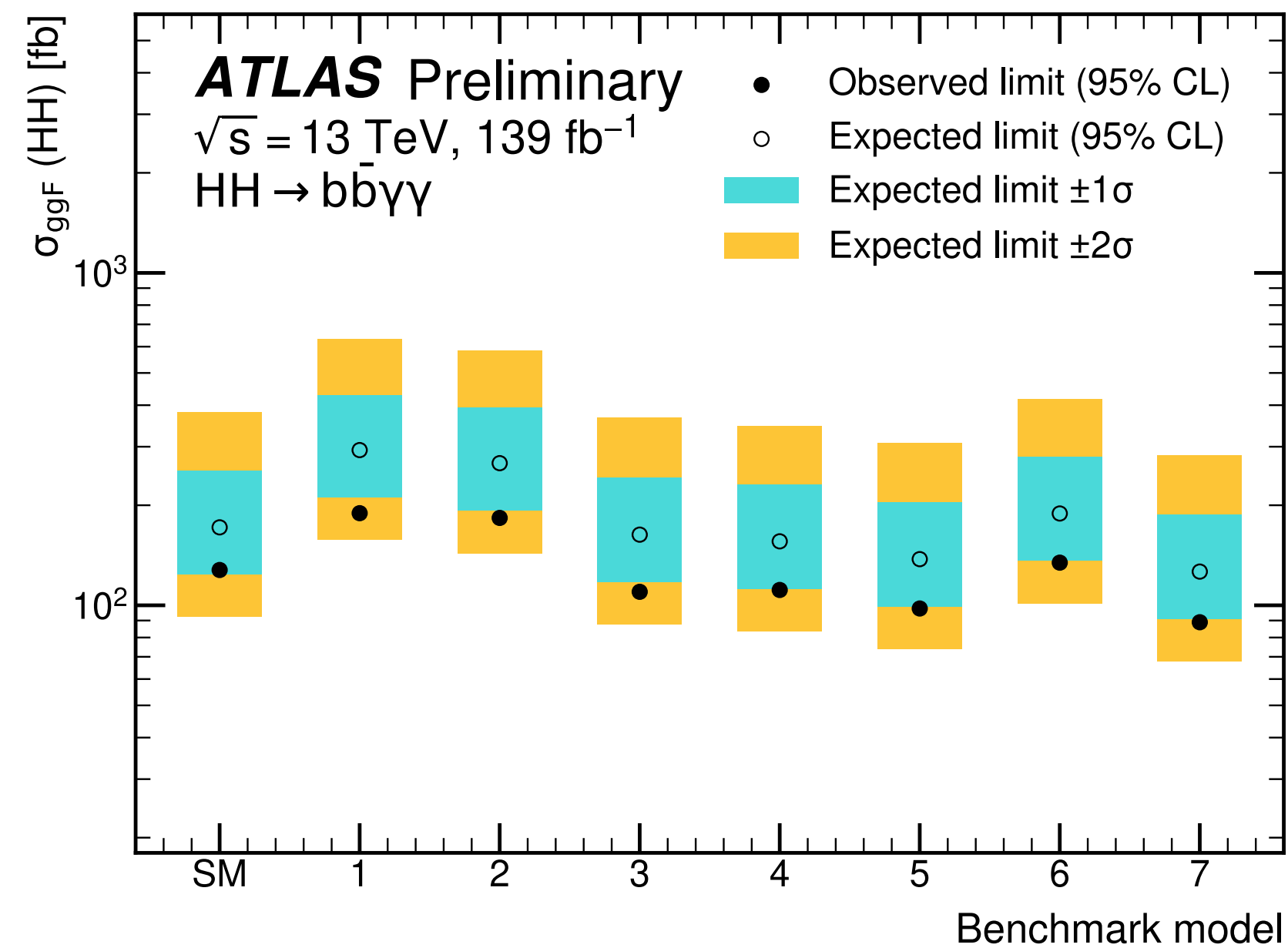
Benchmark model	c_{hhh}	c_{tth}	c_{ggh}	c_{gghh}	c_{tthh}
SM	1	1	0	0	0
BM 1	3.94	0.94	1/2	1/3	-1/3
BM 2	6.84	0.61	0.0	-1/3	1/3
BM 3	2.21	1.05	1/2	1/2	-1/3
BM 4	2.79	0.61	-1/2	1/6	1/3
BM 5	3.95	1.17	1/6	-1/2	-1/3
BM 6	5.68	0.83	-1/2	1/3	1/3
BM 7	-0.10	0.94	1/6	-1/6	1



Unique access to c_{tthh} and c_{gghh} from HH production in HEFT

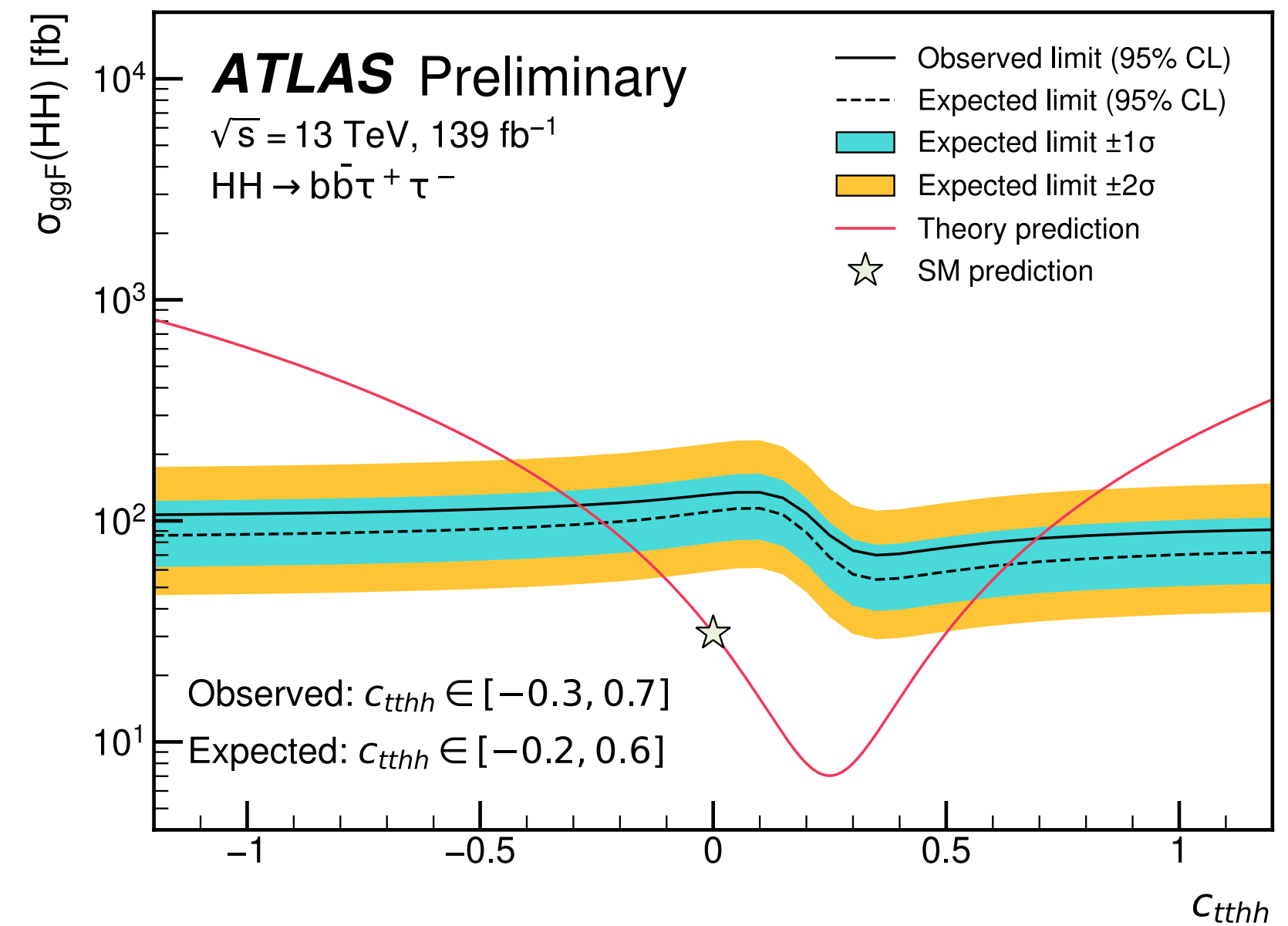
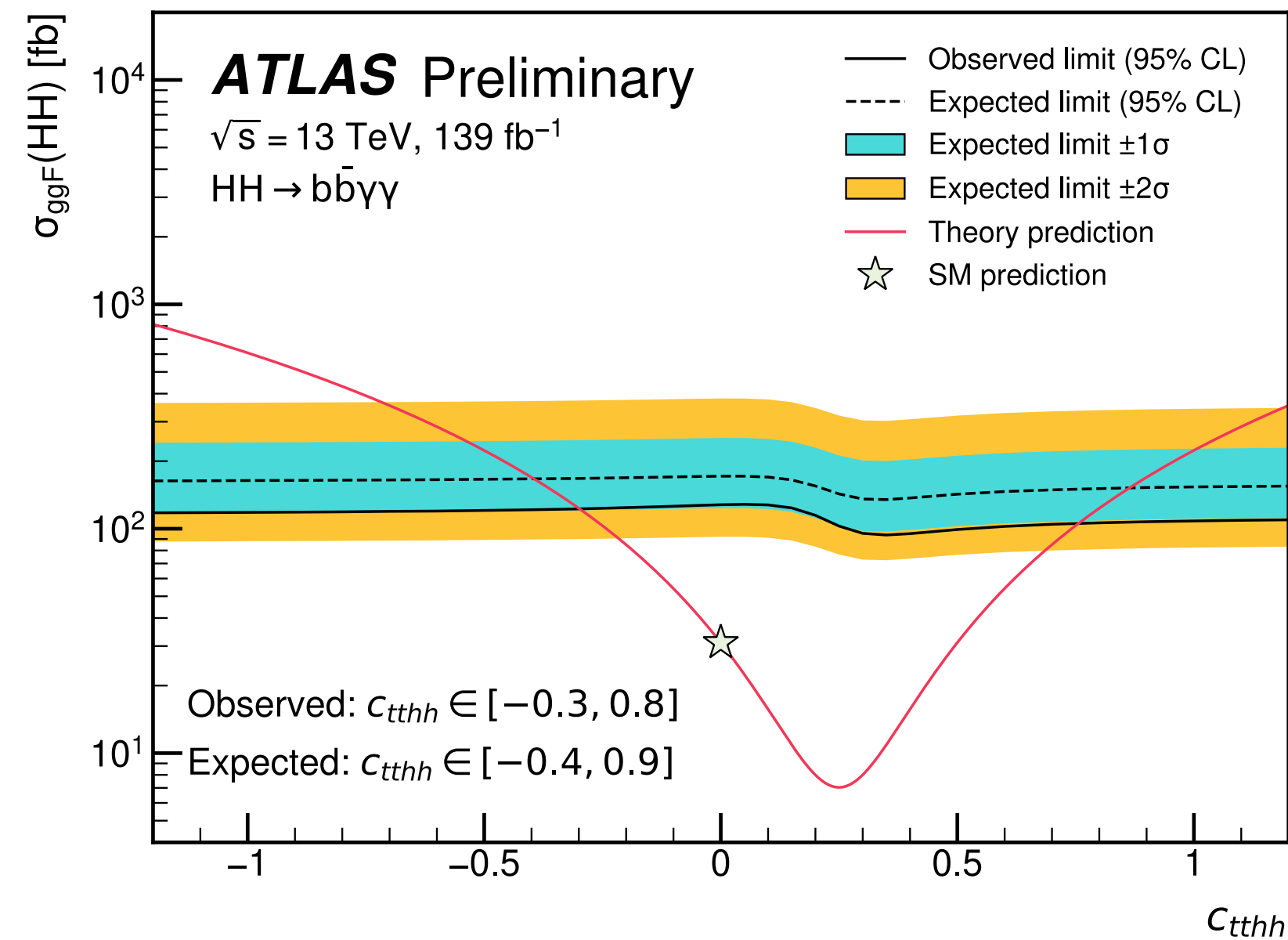
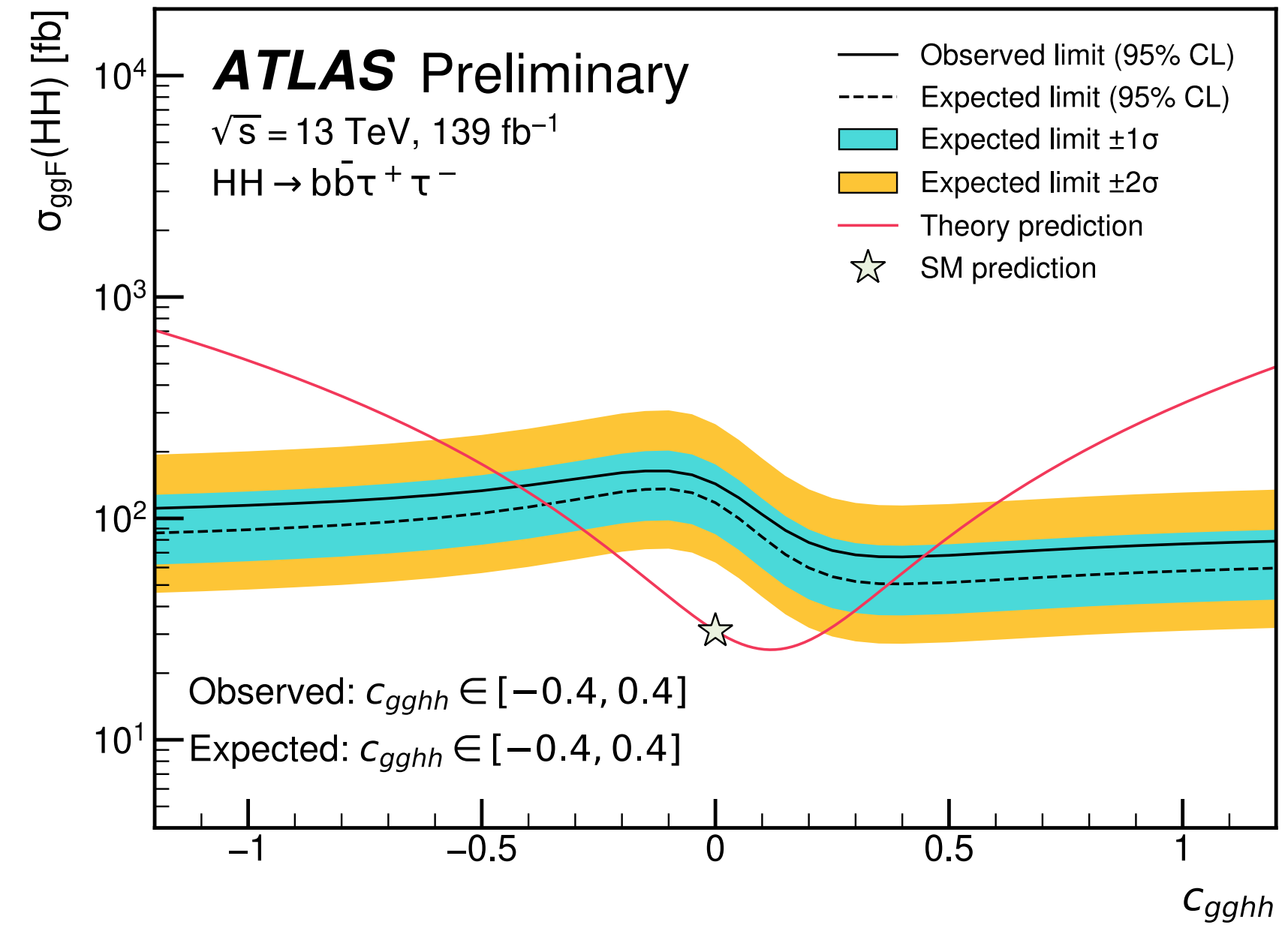
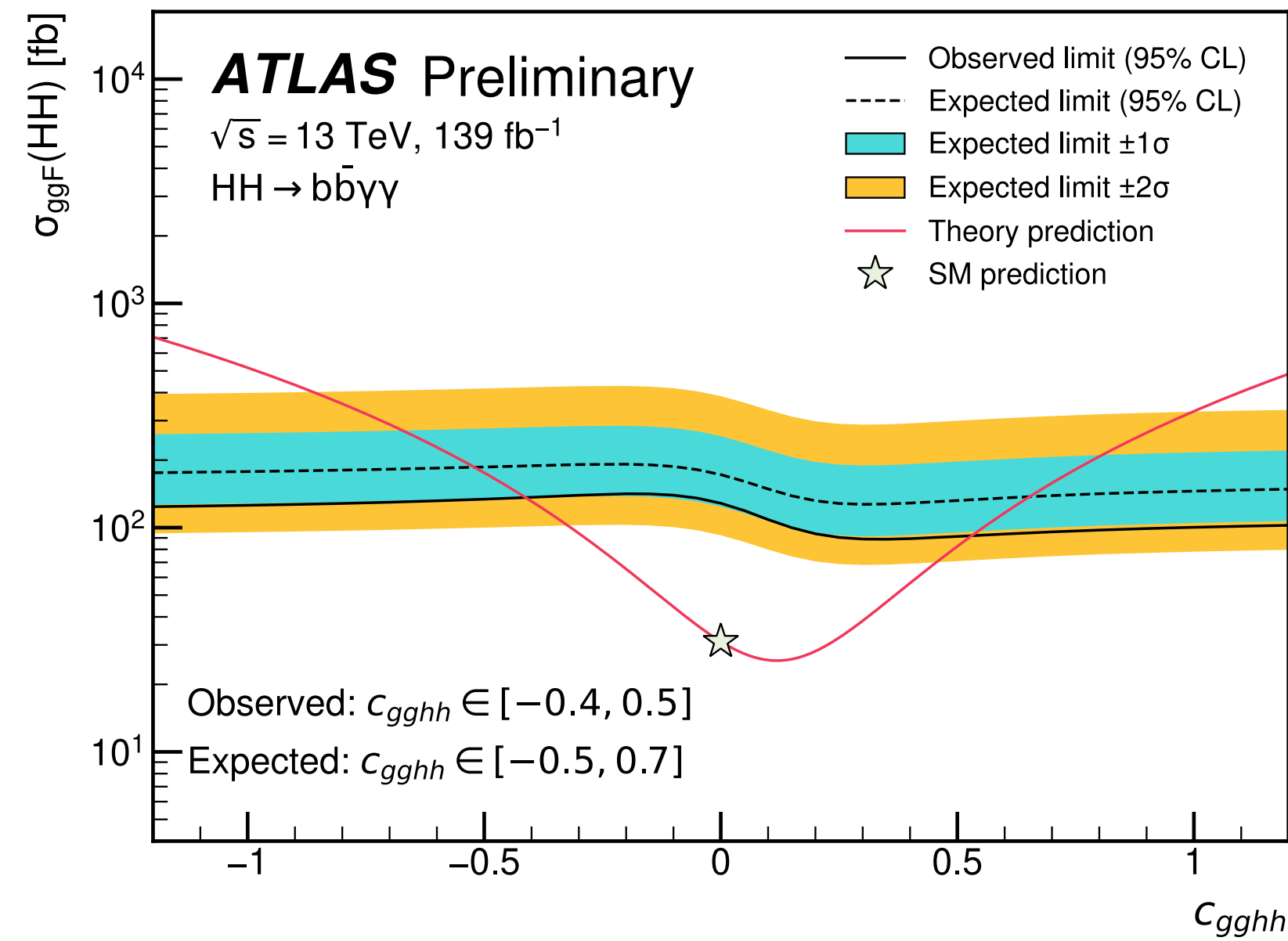
Effective Field Theory (EFT) interpretations

ATL-PHYS-PUB-2022-019



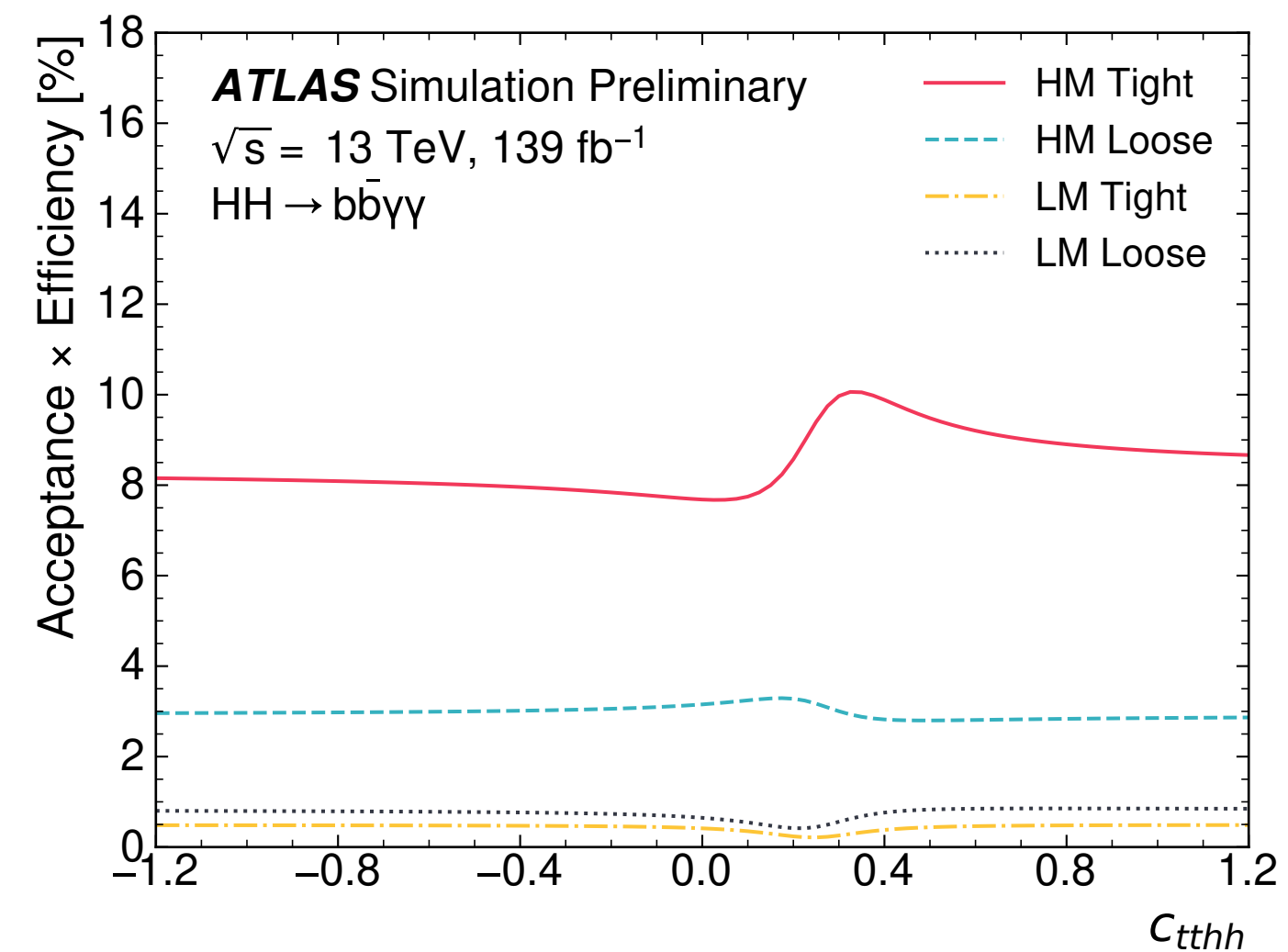
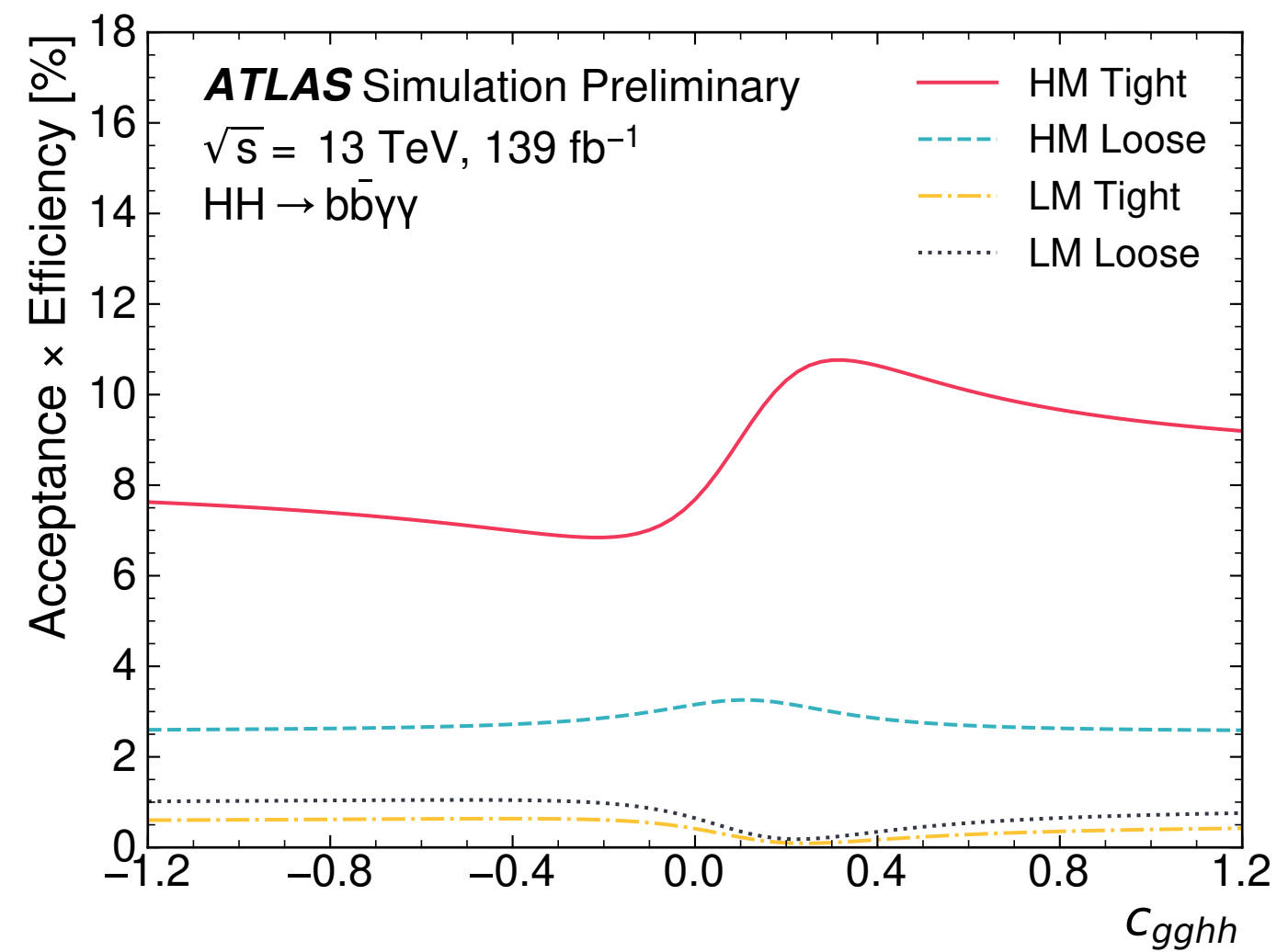
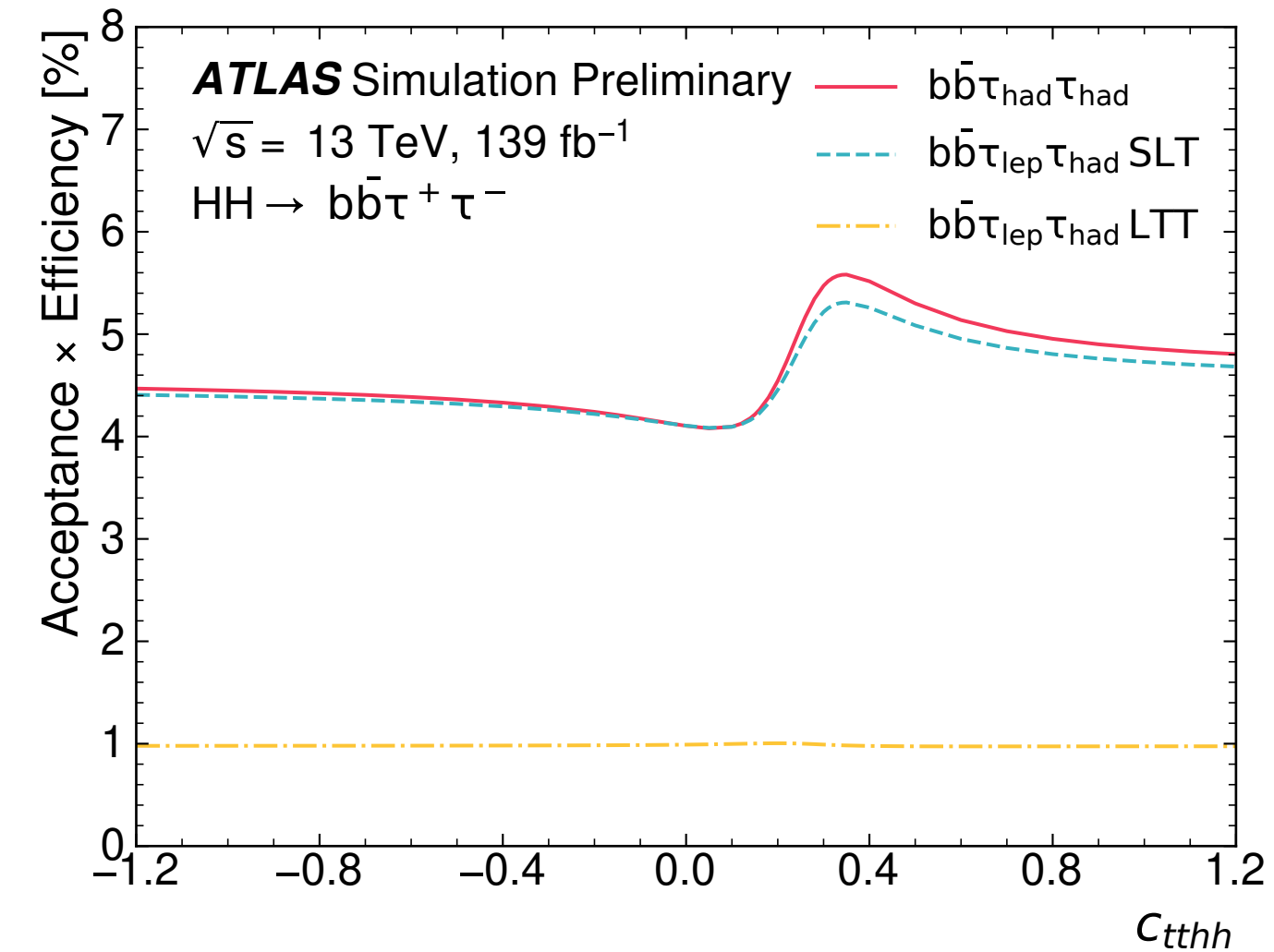
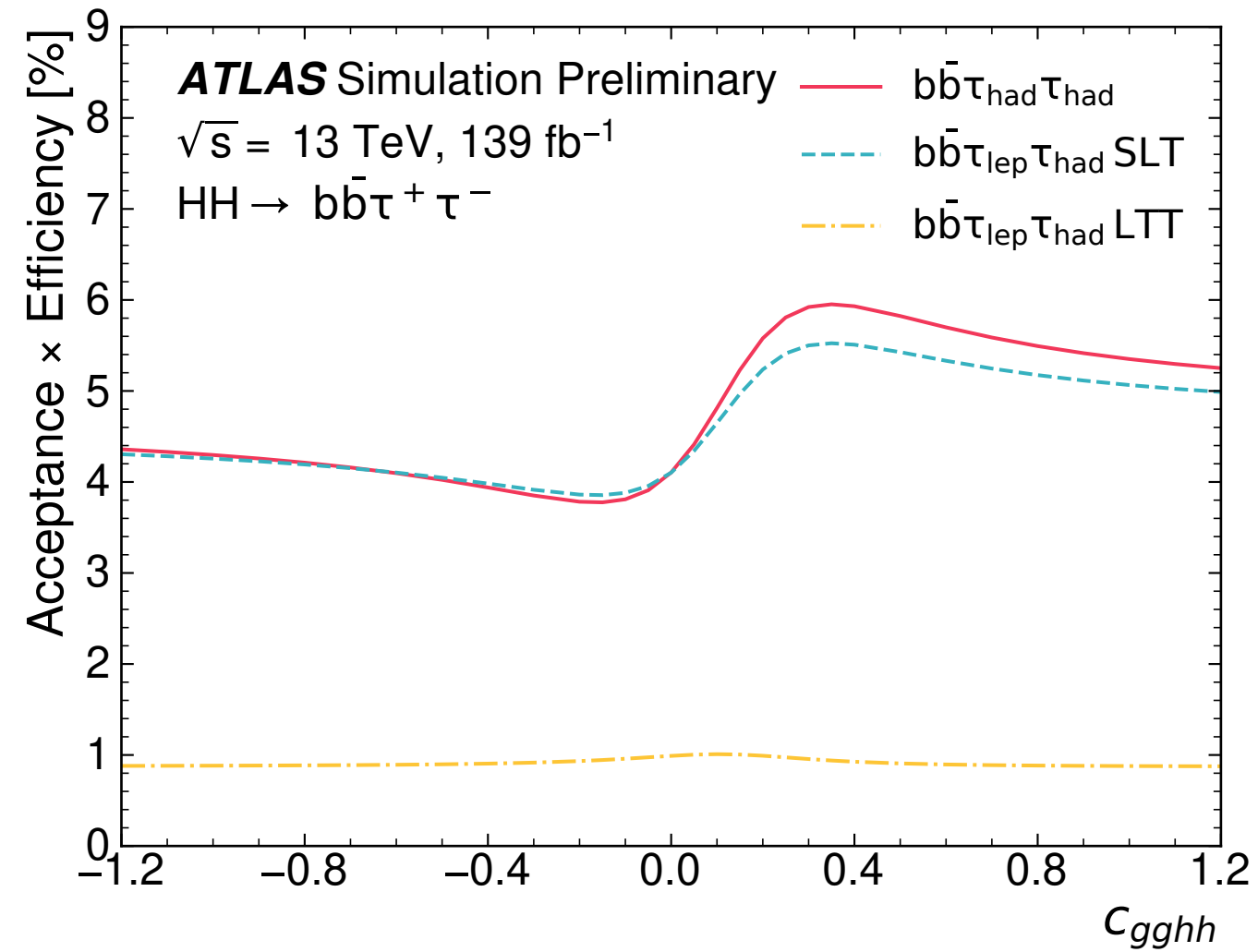
Effective Field Theory (EFT) interpretations

ATL-PHYS-PUB-2022-019



Effective Field Theory (EFT) interpretations

ATL-PHYS-PUB-2022-019



Prospects for HL-LHC

Extrapolations of ATLAS full Run 2 non-resonant HH searches in the $b\bar{b}\tau\tau$ and $b\bar{b}\gamma\gamma$ channels to HL-LHC with 3000 fb^{-1}

Extrapolations performed with different assumptions on the systematic uncertainties:

- **Run 2 systematics:** both the theoretical and experimental systematic uncertainties are assumed to keep their Run 2 values
- **Theoretical systematic uncertainties halved:** theoretical systematic uncertainties are reduced by a factor of 2, while experimental systematic uncertainties are assumed to keep their Run 2 values
- **Baseline:** both theoretical and experimental systematic uncertainties reduced
- **No systematic uncertainties**

ATL-PHYS-PUB-2022-005

Baseline scenario:

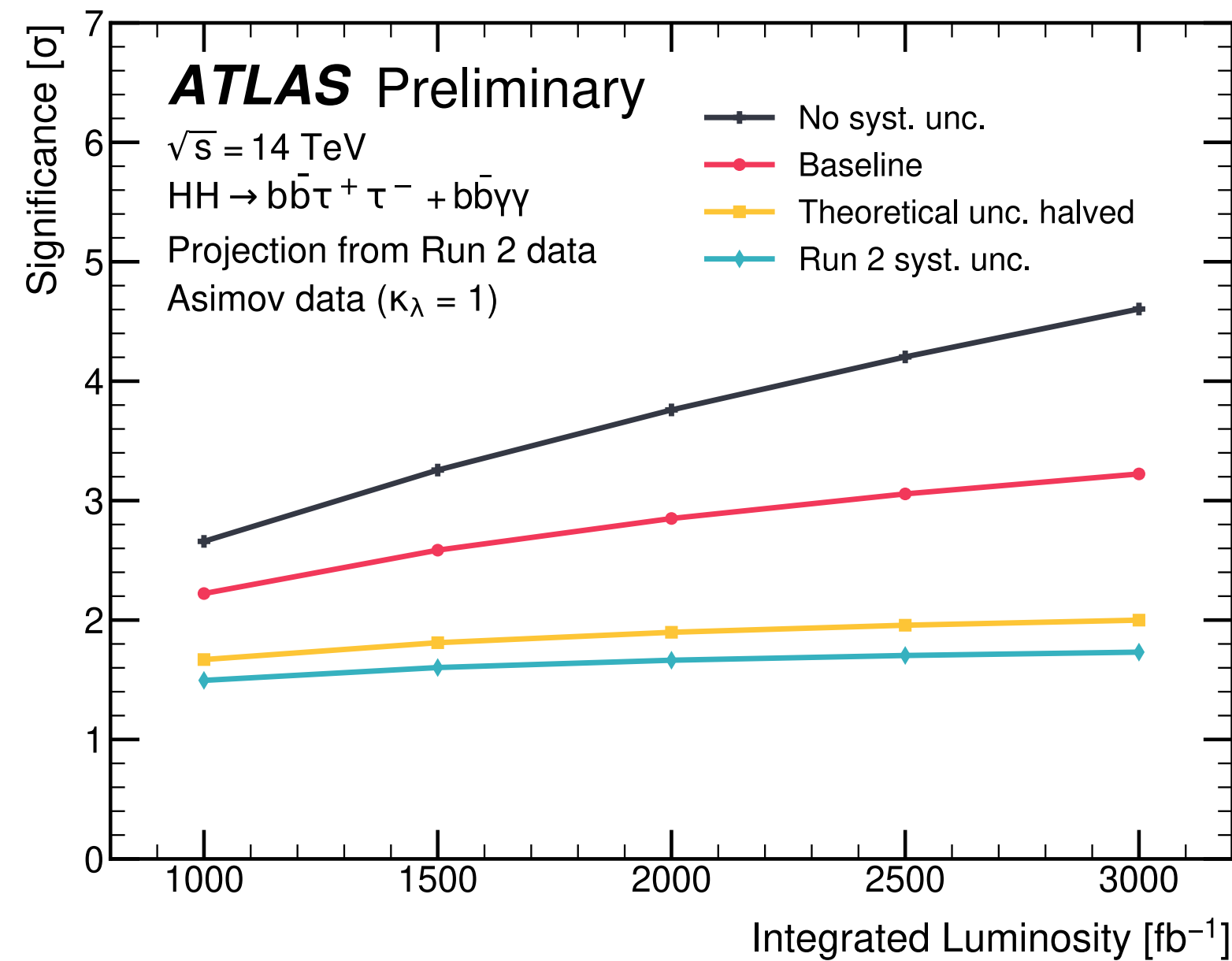
- Theoretical systematic uncertainties reduced by a factor of two
- Experimental systematic uncertainties are reduced taking into account the reduction of their statical component
- MC statistical uncertainties neglected (dominant systematic uncertainty for $b\bar{b}\tau\tau$)
- Spurious signal uncertainty neglected (dominant systematic uncertainty for $b\bar{b}\gamma\gamma$)

Source	Scale factor	$b\bar{b}\gamma\gamma$	$b\bar{b}\tau^+\tau^-$
Experimental Uncertainties			
Luminosity	0.6	*	*
b -jet tagging efficiency	0.5	*	*
c -jet tagging efficiency	0.5	*	*
Light-jet tagging efficiency	1.0	*	*
Jet energy scale and resolution, E_T^{miss}	1.0	*	*
κ_λ reweighting	0.0	*	*
Photon efficiency (ID, trigger, isolation efficiency)	0.8	*	
Photon energy scale and resolution	1.0	*	
Spurious signal	0.0	*	
Value of m_H	0.08	*	
τ_{had} efficiency (statistical)	0.0		*
τ_{had} efficiency (systematic)	1.0		*
τ_{had} energy scale	1.0		*
Fake- τ_{had} estimation	1.0		*
MC statistical uncertainties	0.0		*
Theoretical Uncertainties			
	0.5	*	*

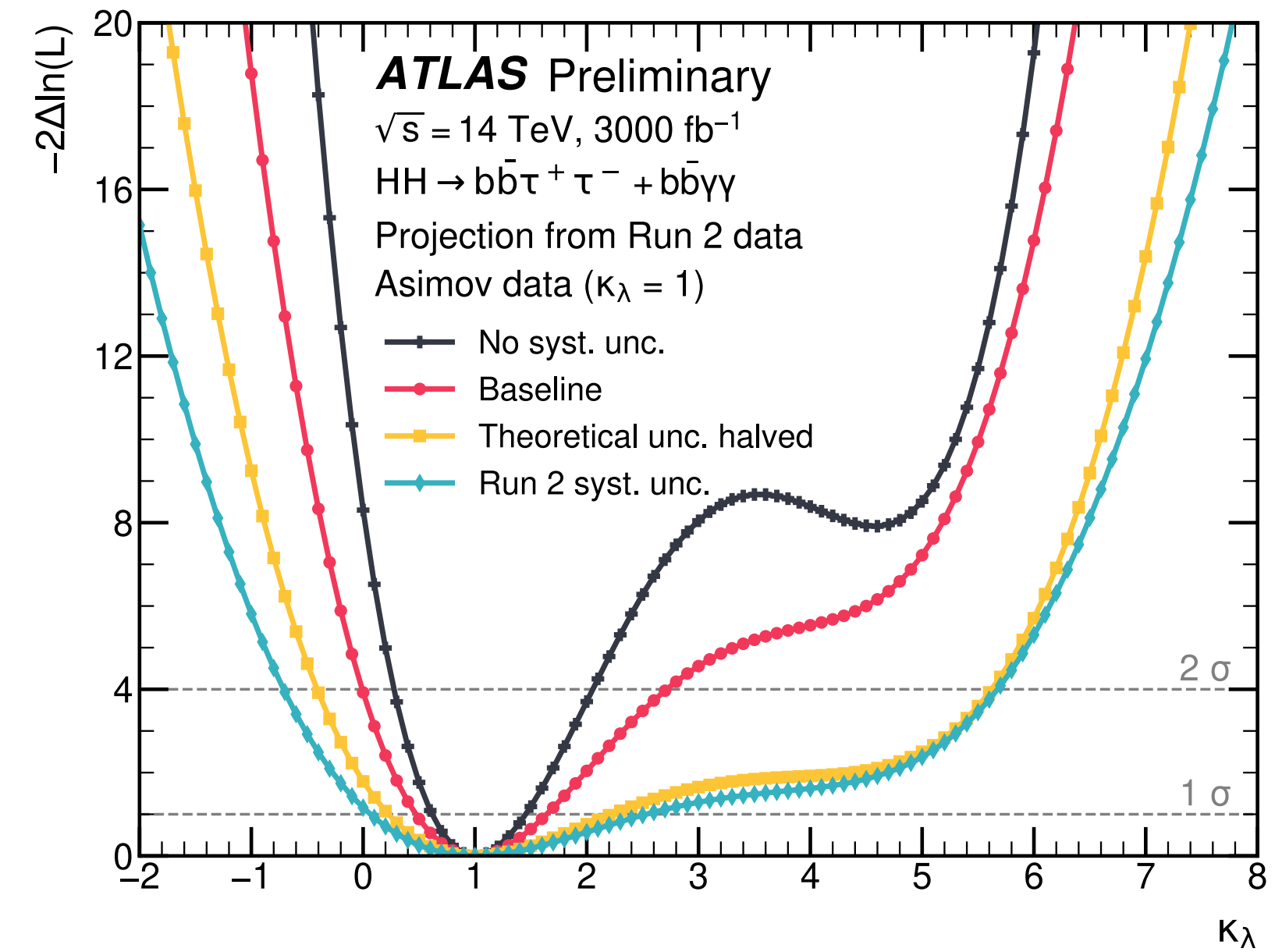
Detector performance assumed to be the same as Run 2 in the more challenging HL-LHC detector operation environment thanks to the program of upgrades of the detector, trigger and data acquisition systems

Prospects for HL-LHC

Extrapolations of NEW ATLAS full Run 2 non-resonant HH searches in the $bb\tau\tau$ and $bb\gamma\gamma$ channels to HL-LHC with 3000 fb^{-1}



ATL-PHYS-PUB-2022-005



Uncertainty scenario	Significance [σ]			Combined signal strength precision [%]
	$bb\gamma\gamma$	$bb\tau^+\tau^-$	Combination	
No syst. unc.	2.3	4.0	4.6	-23/ + 23
Baseline	2.2	2.8	3.2	-31/ + 34
Theoretical unc. halved	1.1	1.7	2.0	-49/ + 51
Run 2 syst. unc.	1.1	1.5	1.7	-57/ + 68

Uncertainty scenario	Likelihood scan 1σ CI	Likelihood scan 2σ CI
No syst. unc.	[0.6, 1.5]	[0.3, 2.1]
Baseline	[0.5, 1.6]	[0.0, 2.7]
Theoretical unc. halved	[0.2, 2.2]	[-0.4, 5.6]
Run 2 syst. unc.	[0.1, 2.5]	[-0.7, 5.7]

Baseline scenario: Expected significance of 3.2σ and 30% uncertainty on the signal strength for SM HH signal

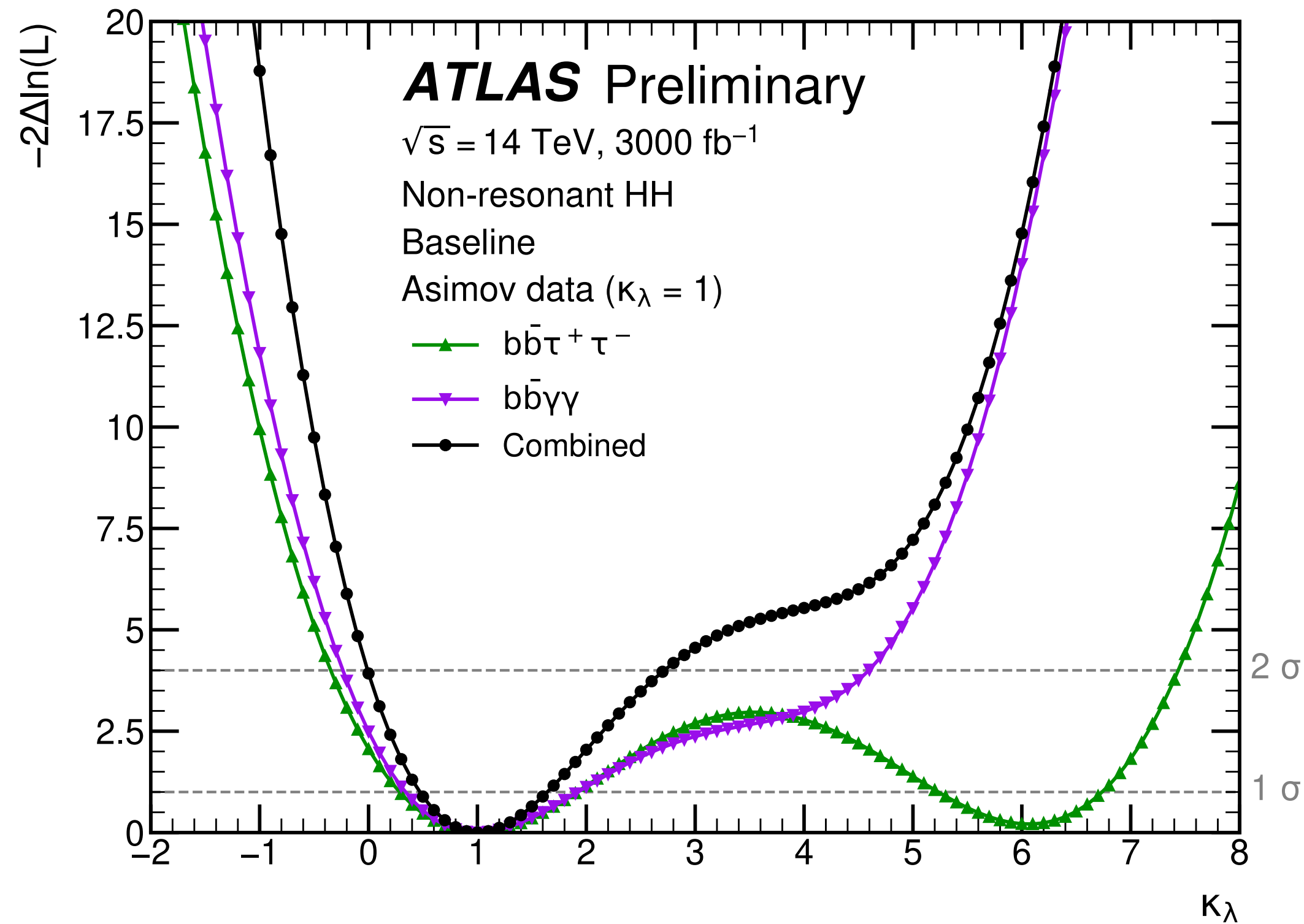
Baseline scenario: 50% uncertainty on κ_λ for SM HH signal

New projected precision from ATLAS alone is of the same order of the previous ATLAS+CMS projection!

Systematic uncertainties will become important at the HL-LHC

Prospects for HL-LHC

ATL-PHYS-PUB-2022-005



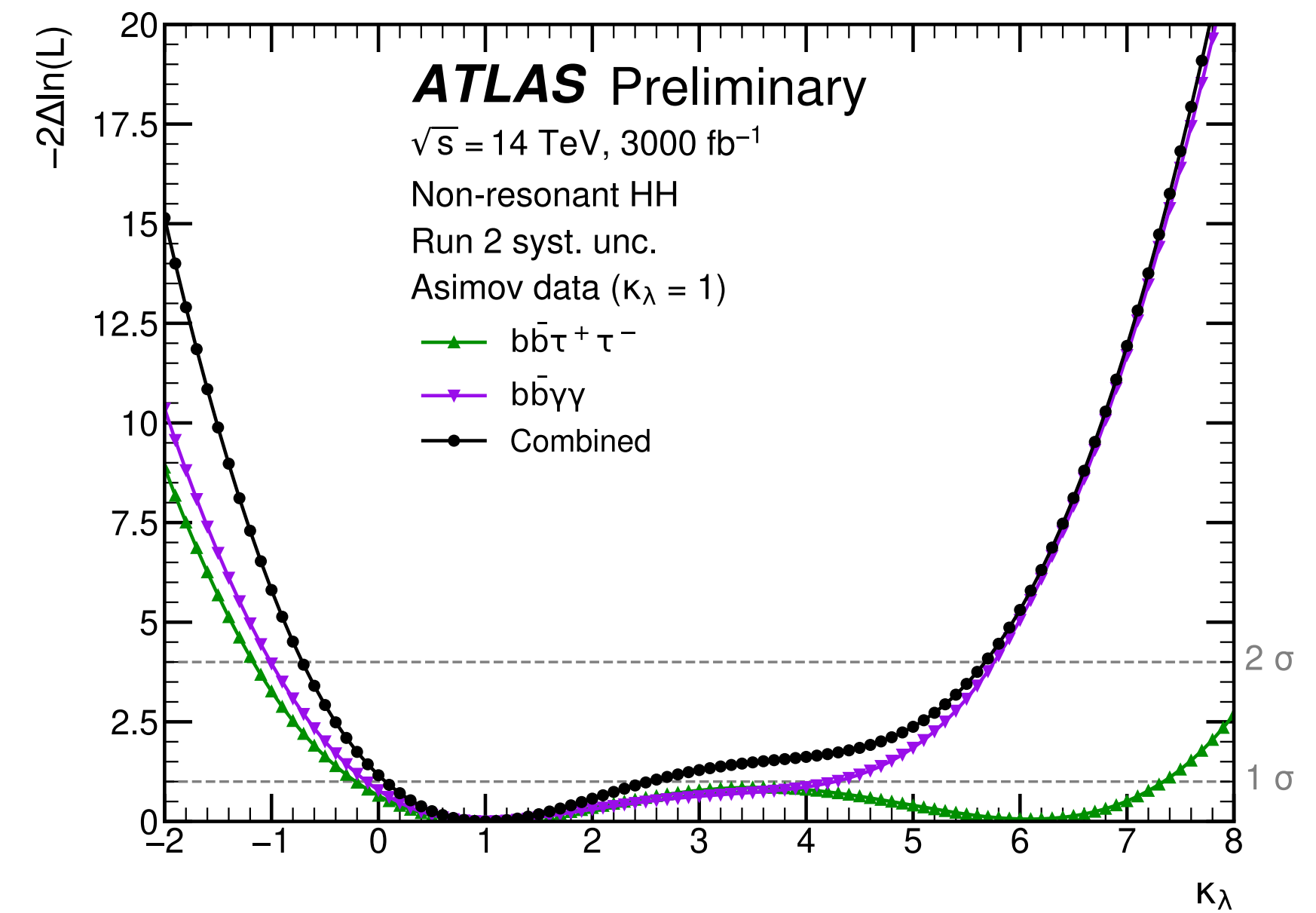
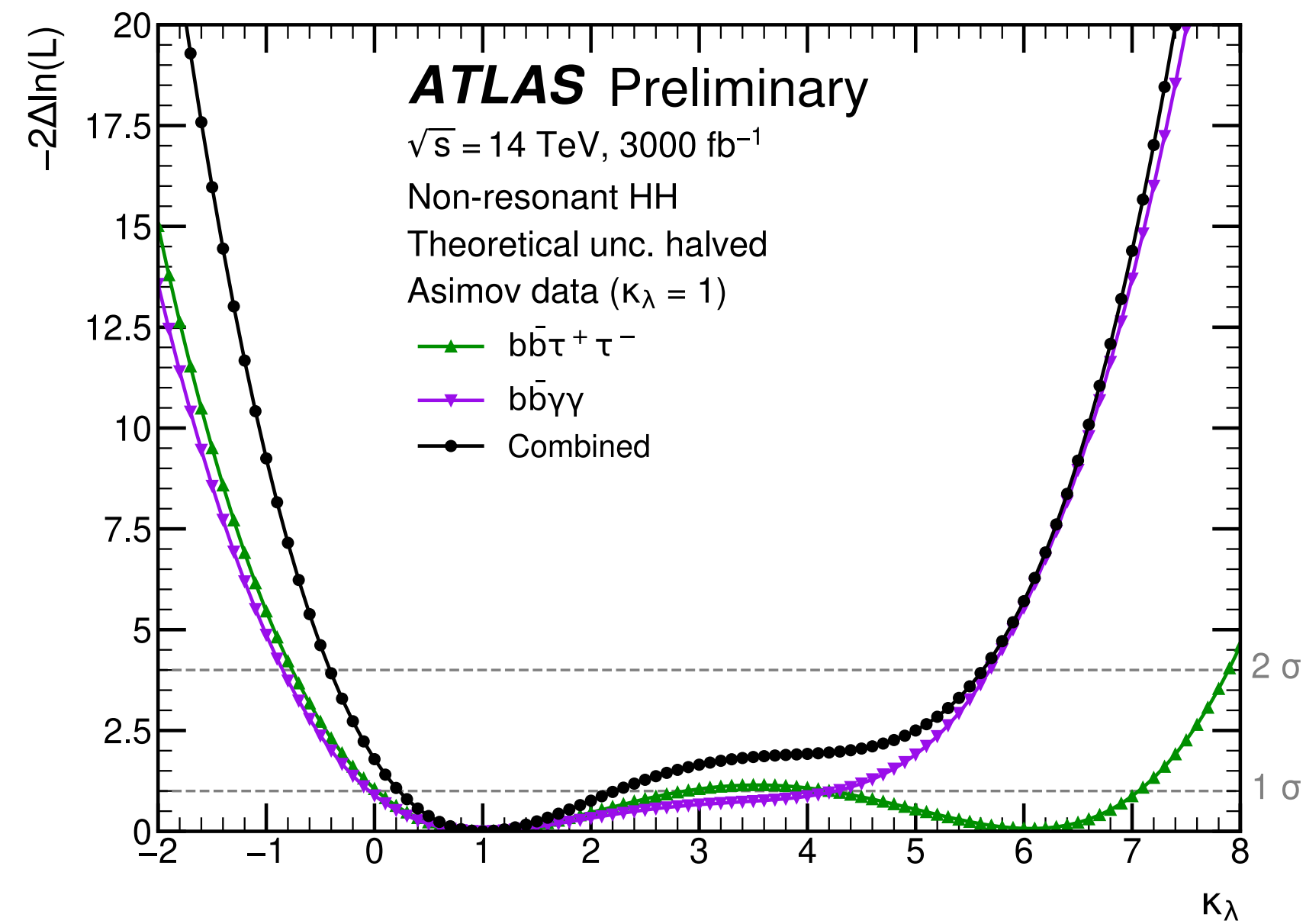
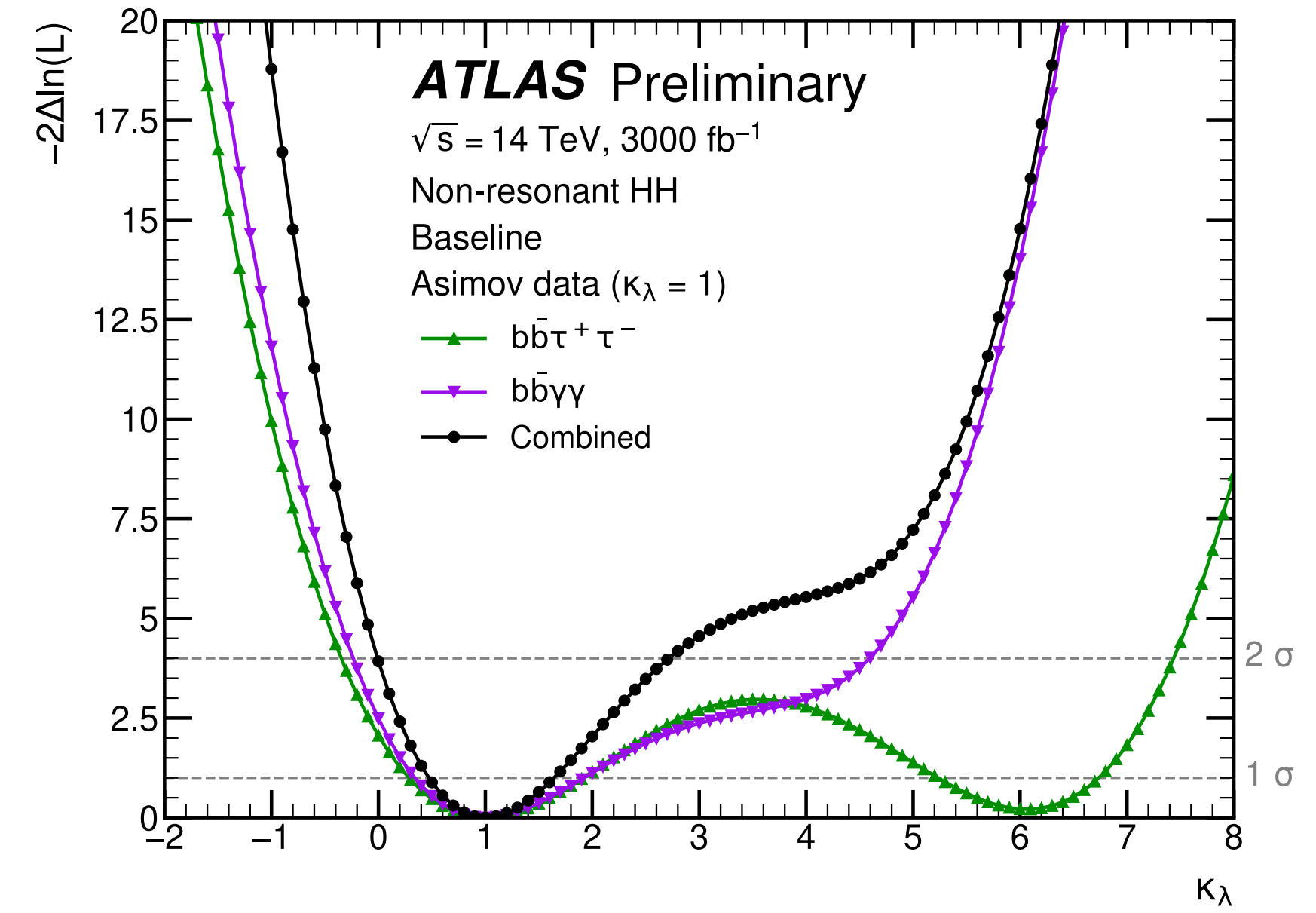
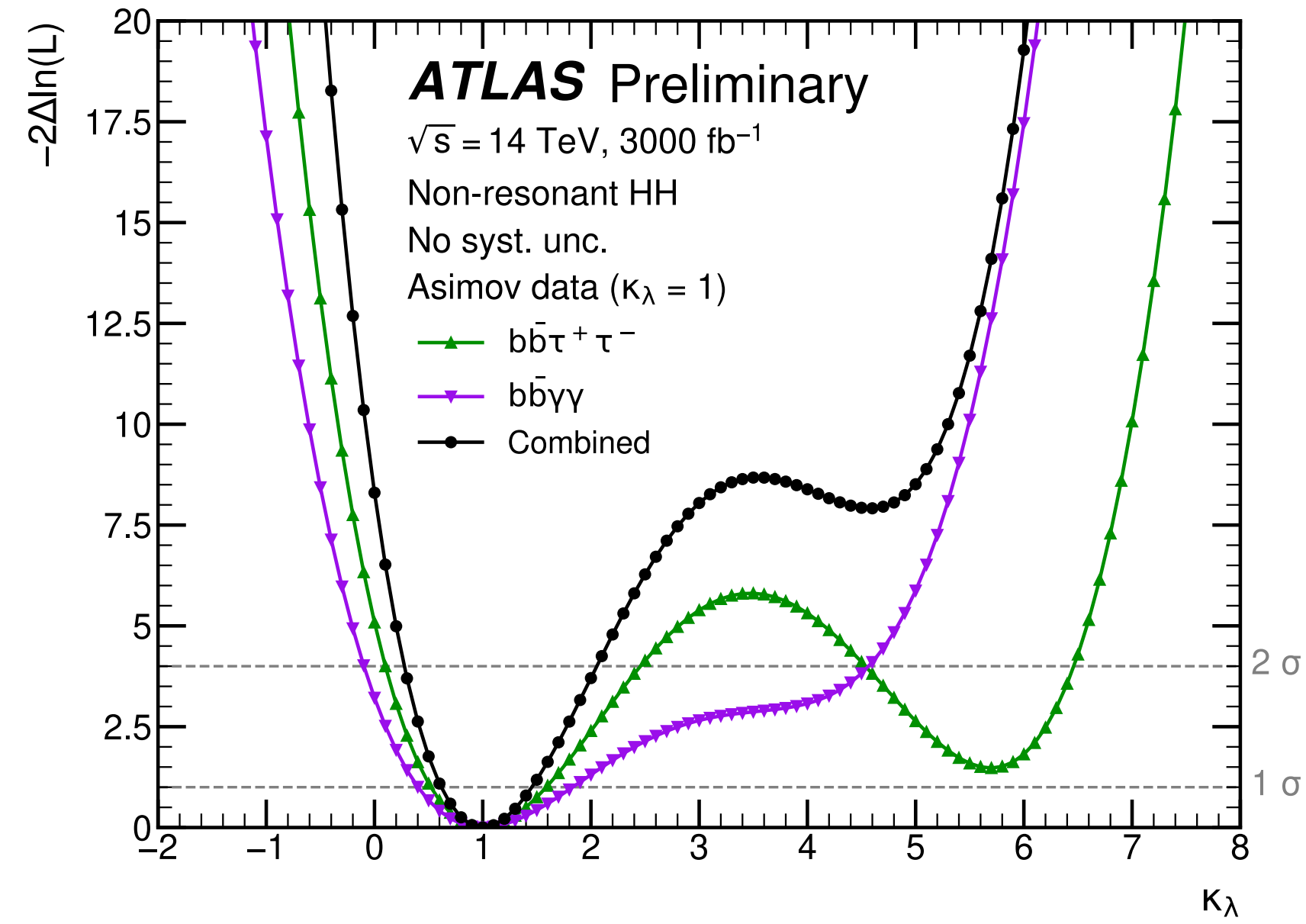
Uncertainty configuration	Likelihood scan 1σ CI for κ_λ		
	$b\bar{b}\gamma\gamma$	$b\bar{b}\tau^+\tau^-$	Combination
No syst. unc.	[0.4, 1.8]	[0.5, 1.6]	[0.6, 1.5]
Baseline	[0.3, 1.9]	[0.3, 1.9] \cup [5.2, 6.7]	[0.5, 1.6]
Theoretical unc. halved	[-0.1, 4.3]	[0.0, 2.9] \cup [4.2, 7.1]	[0.2, 2.2]
Run 2 syst. unc.	[-0.1, 4.3]	[-0.2, 7.3]	[0.1, 2.5]

Uncertainty configuration	Likelihood scan 2σ CI for κ_λ		
	$b\bar{b}\gamma\gamma$	$b\bar{b}\tau^+\tau^-$	Combination
No syst. unc.	[-0.1, 4.6]	[0.1, 2.5] \cup [4.5, 6.5]	[0.3, 2.1]
Baseline	[-0.2, 4.6]	[-0.3, 7.4]	[0.0, 2.7]
Theoretical unc. halved	[-0.8, 5.7]	[-0.8, 8.0]	[-0.4, 5.6]
Run 2 syst. unc.	[-1.0, 5.8]	[-1.2, 8.3]	[-0.7, 5.7]

- $b\bar{b}\gamma\gamma$ and $b\bar{b}\tau^+\tau^-$ have comparable contribution to the κ_λ constraint on the negative side
- $b\bar{b}\gamma\gamma$ κ_λ constraining power dominates on the positive side

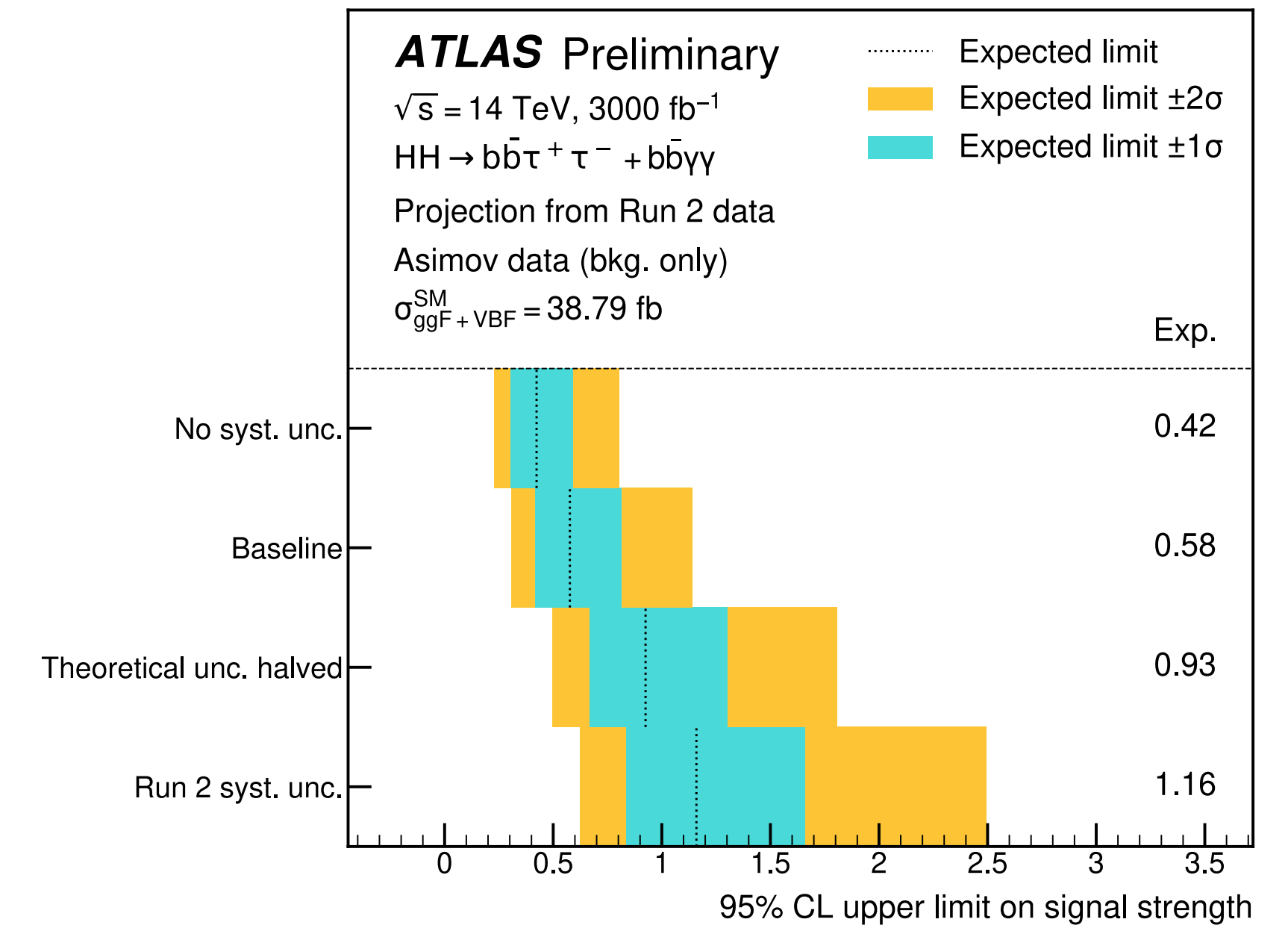
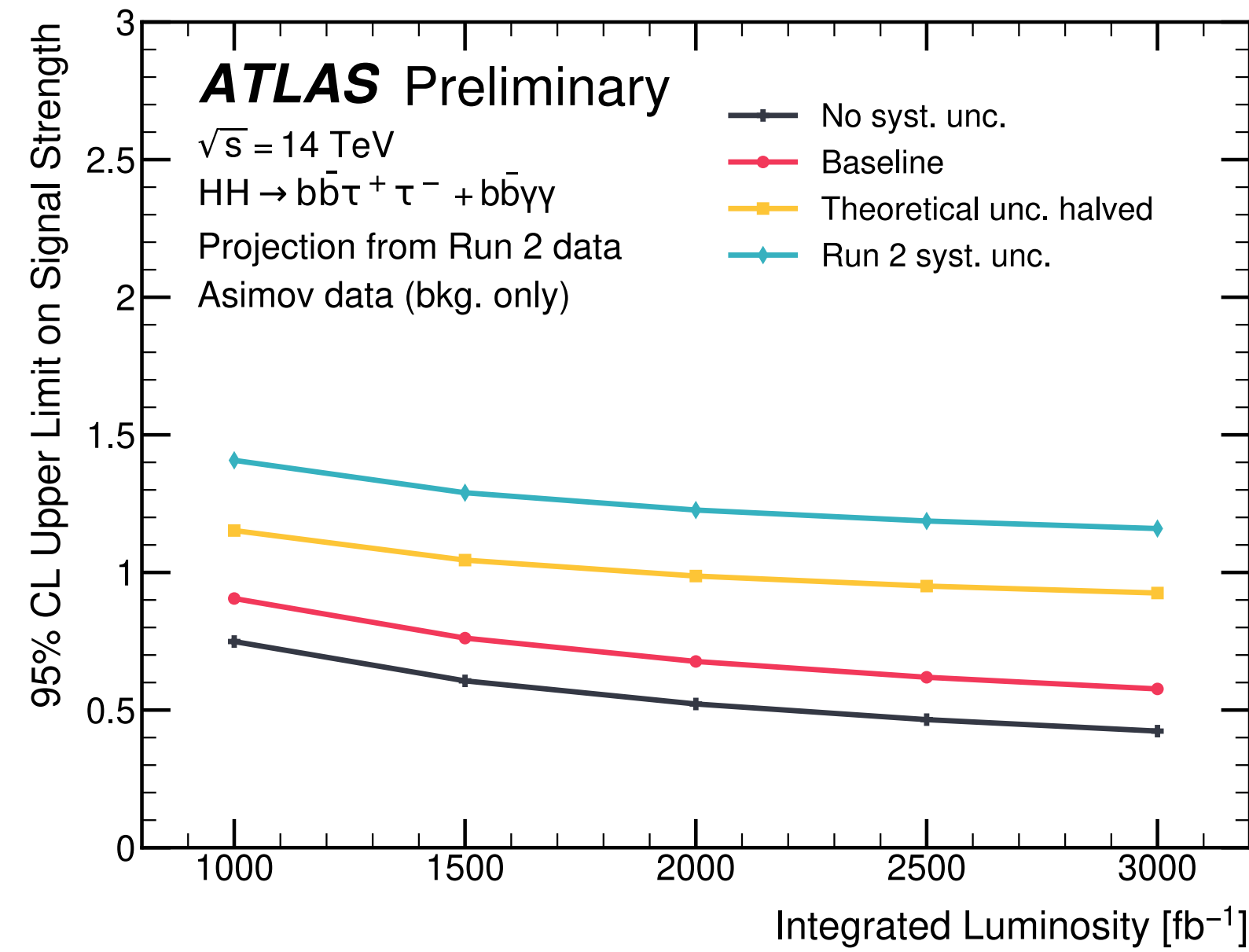
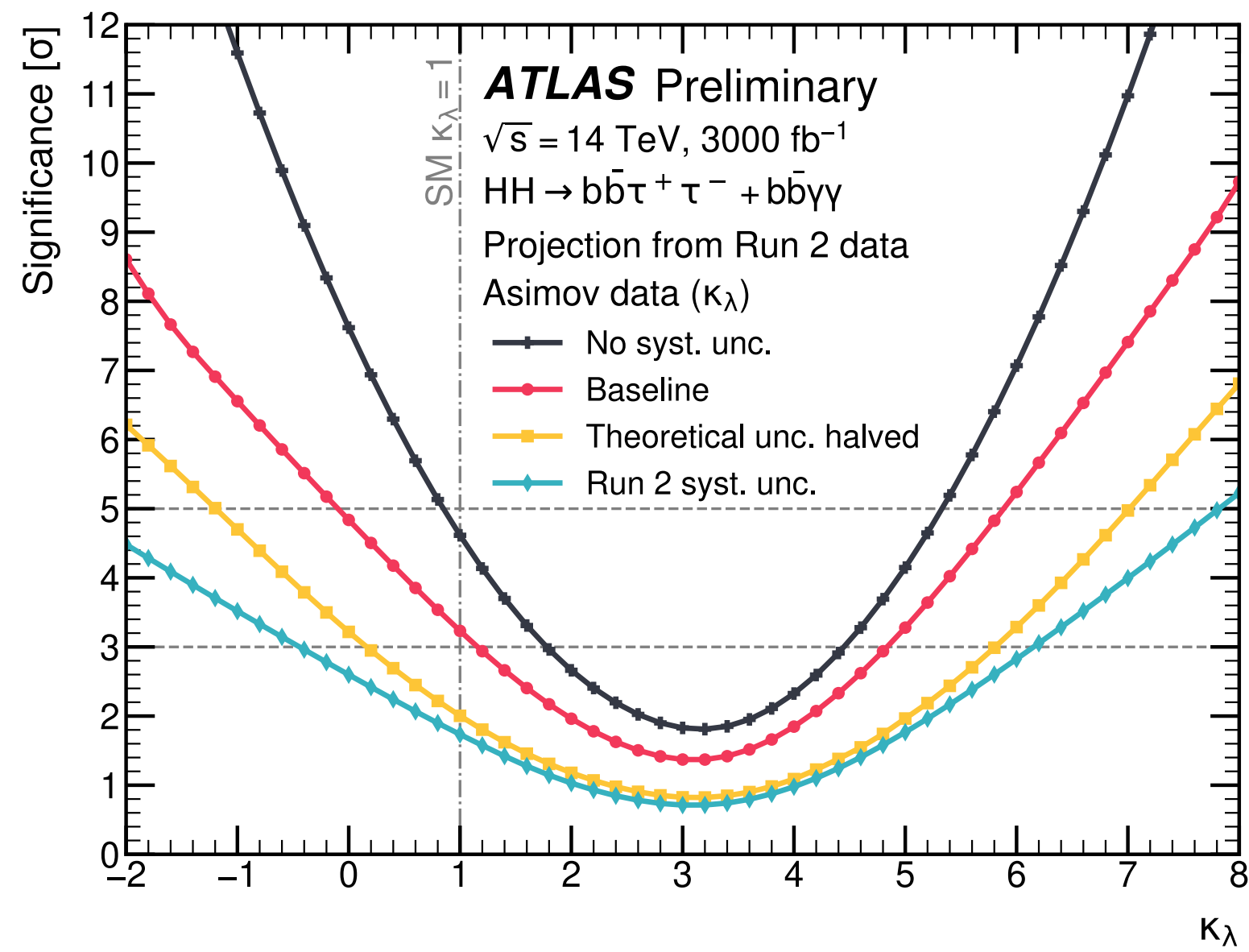
Prospects for HL-LHC

ATL-PHYS-PUB-2022-005



Prospects for HL-LHC

ATL-PHYS-PUB-2022-005



Resonant $HH \rightarrow bbbb$ with full Run 2 data

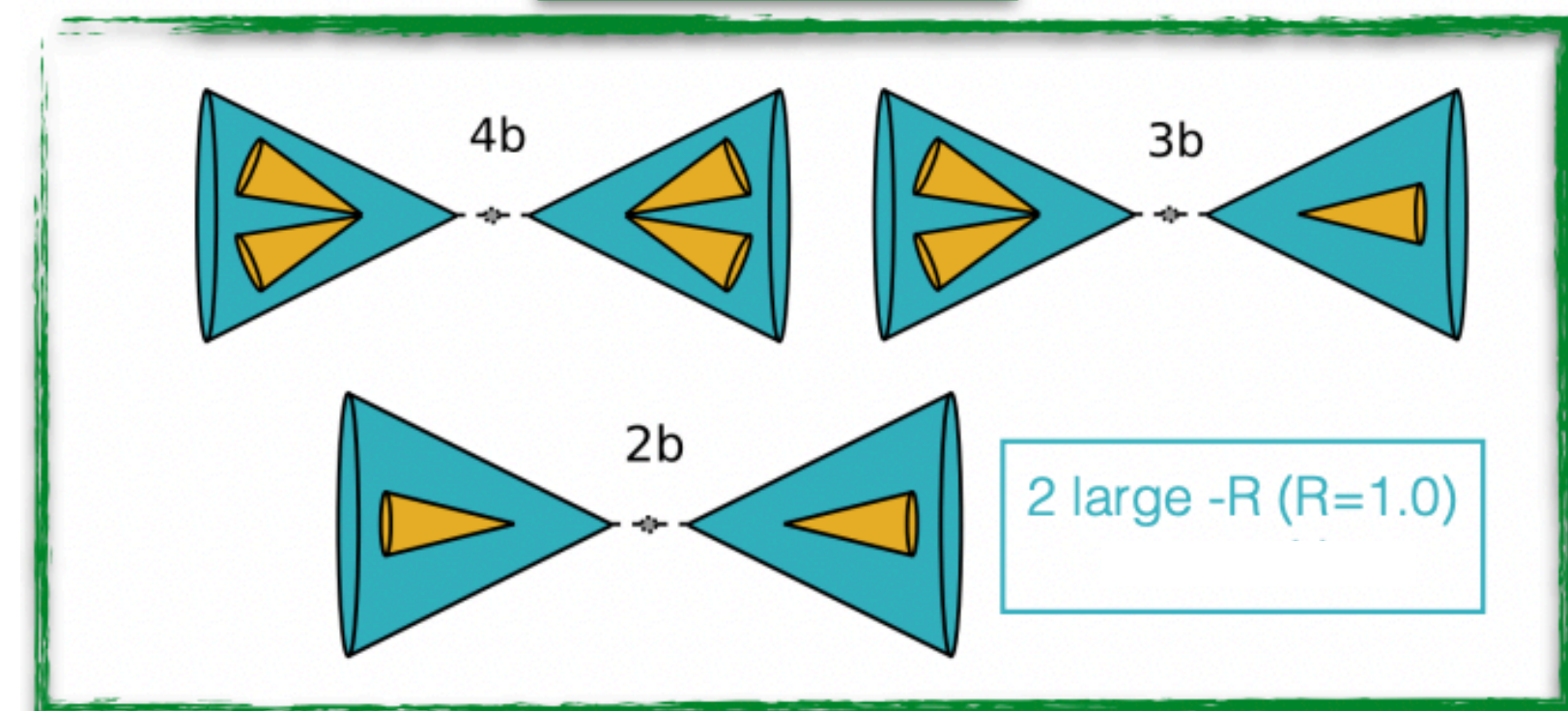
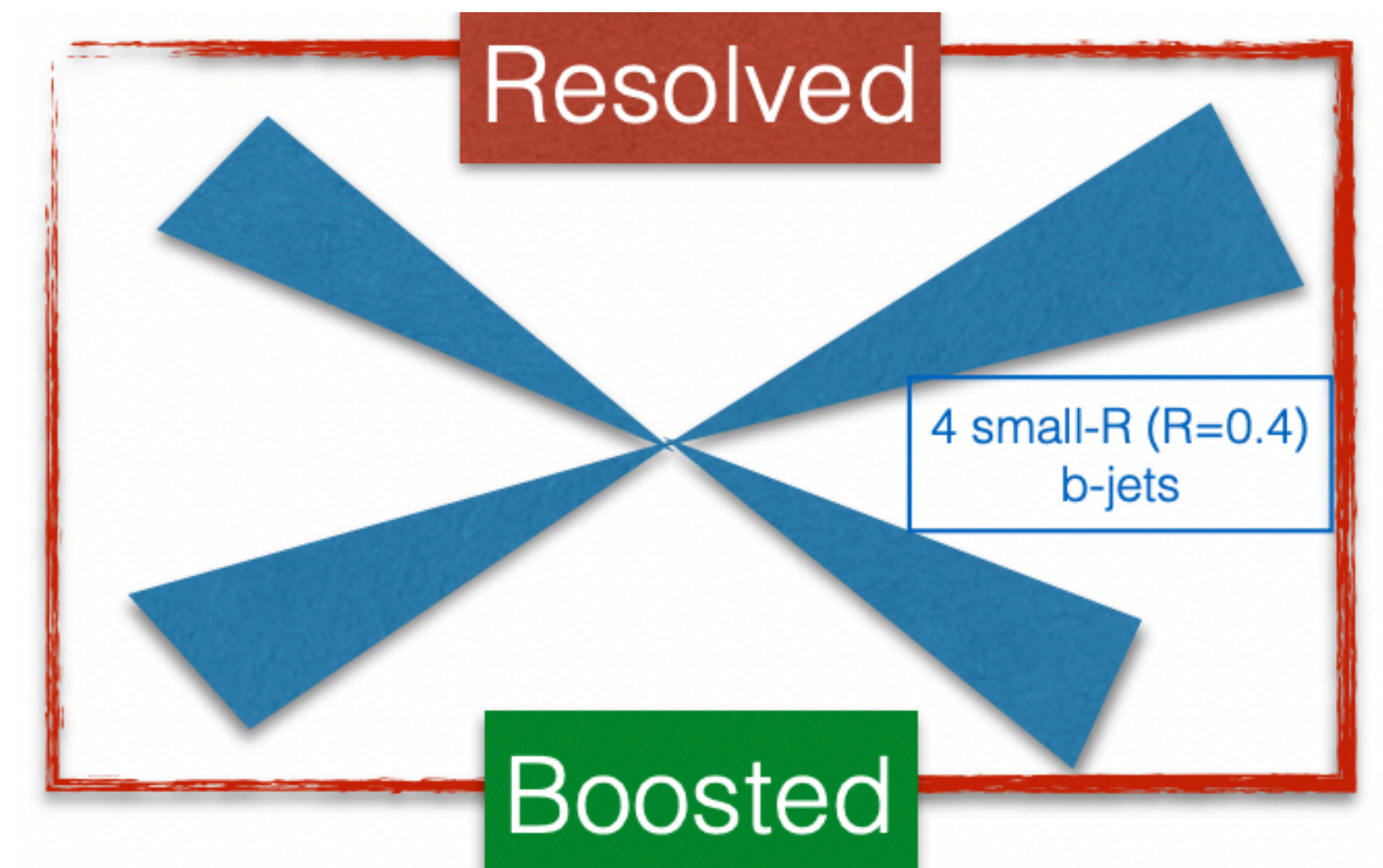
- Search for BSM resonant HH production: resonances with masses between 250 GeV and 3 TeV
- $X \rightarrow HH \rightarrow bbbb$
- Resolved and boosted categories

Resolved category:

- $m_X \in [250, 1500]$ GeV
- At least 4 b-tagged small-radius jets ($\Delta R = 0.4$)
- Boosted Decision Trees used to pair the 4 b-jets to form the 2 Higgs candidates
- Fully data-driven total background estimation (95% QCD multijet, 5% $t\bar{t}$)

Boosted category:

- $m_X \in [900, 5000]$ GeV
- High mass resonance \rightarrow boosted Higgs bosons \rightarrow merged b-jets from the Higgs
- At least two large-radius jets ($\Delta R = 1.0$)
- **2b, 3b and 4b categories**
- Fully data-driven QCD multi-jet background estimation (70%-90%)
- $t\bar{t}$ from Monte Carlo simulations (30-10%)

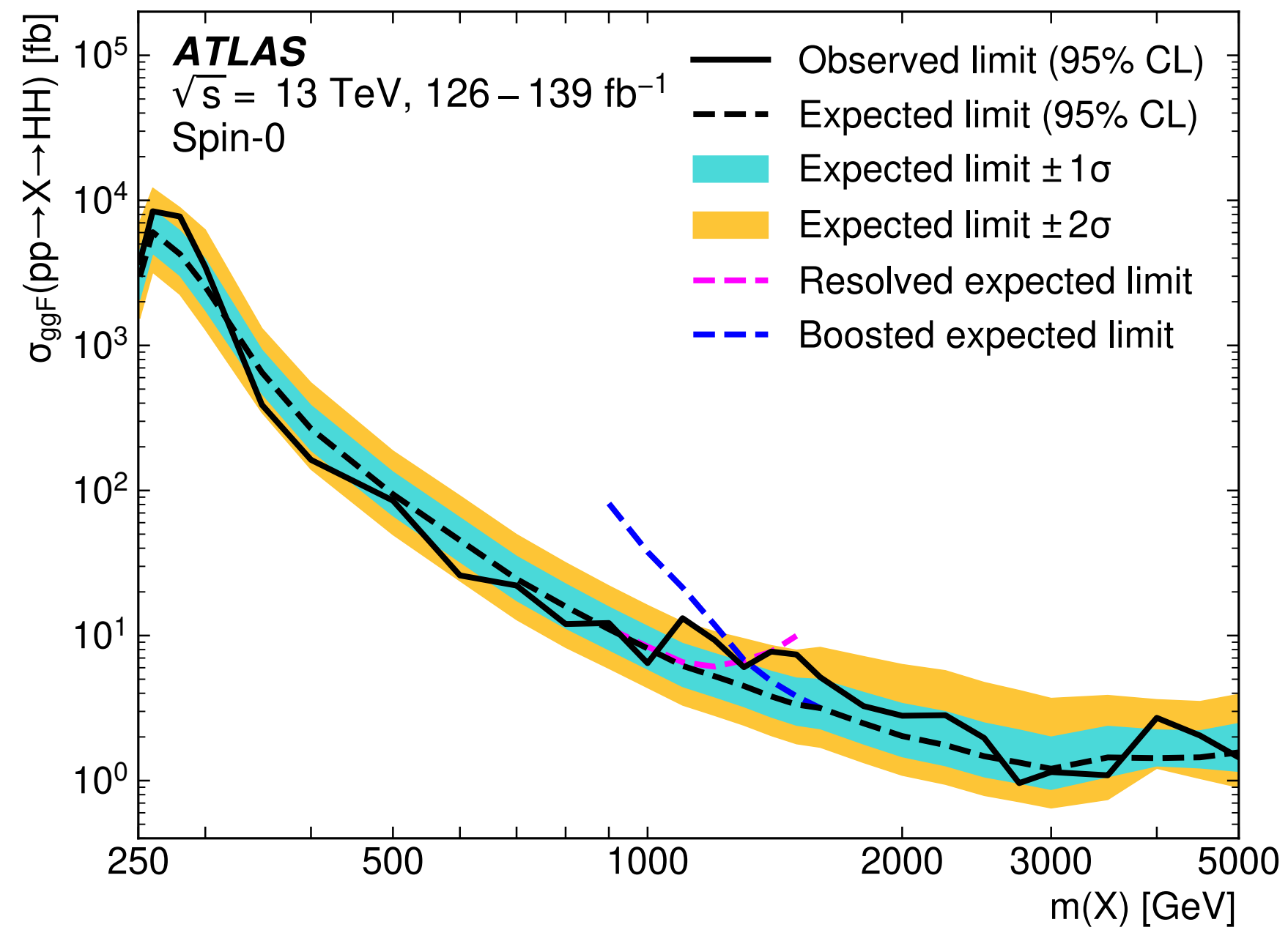


Resonant $HH \rightarrow b\bar{b}b\bar{b}$ with full Run 2 data

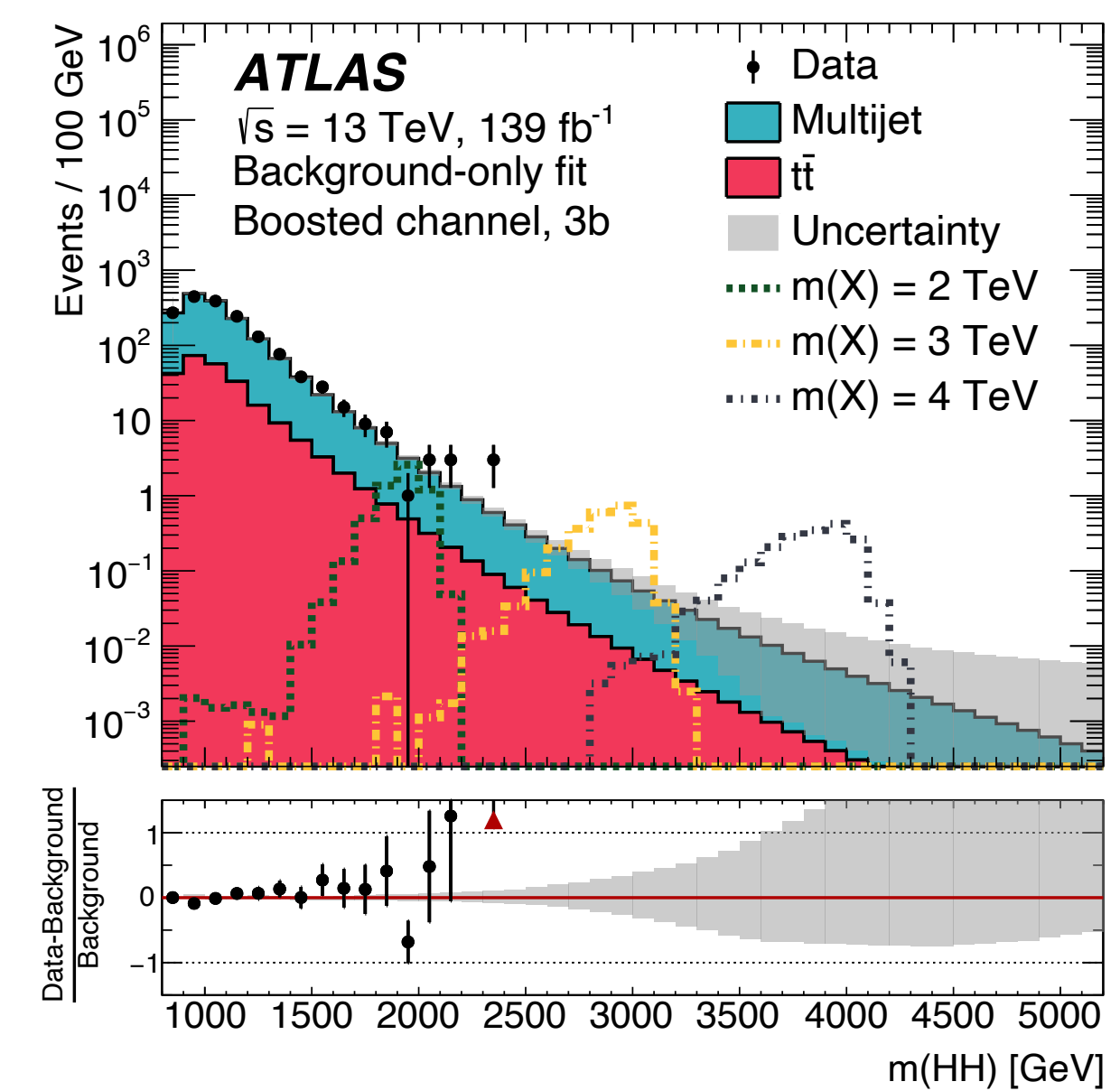
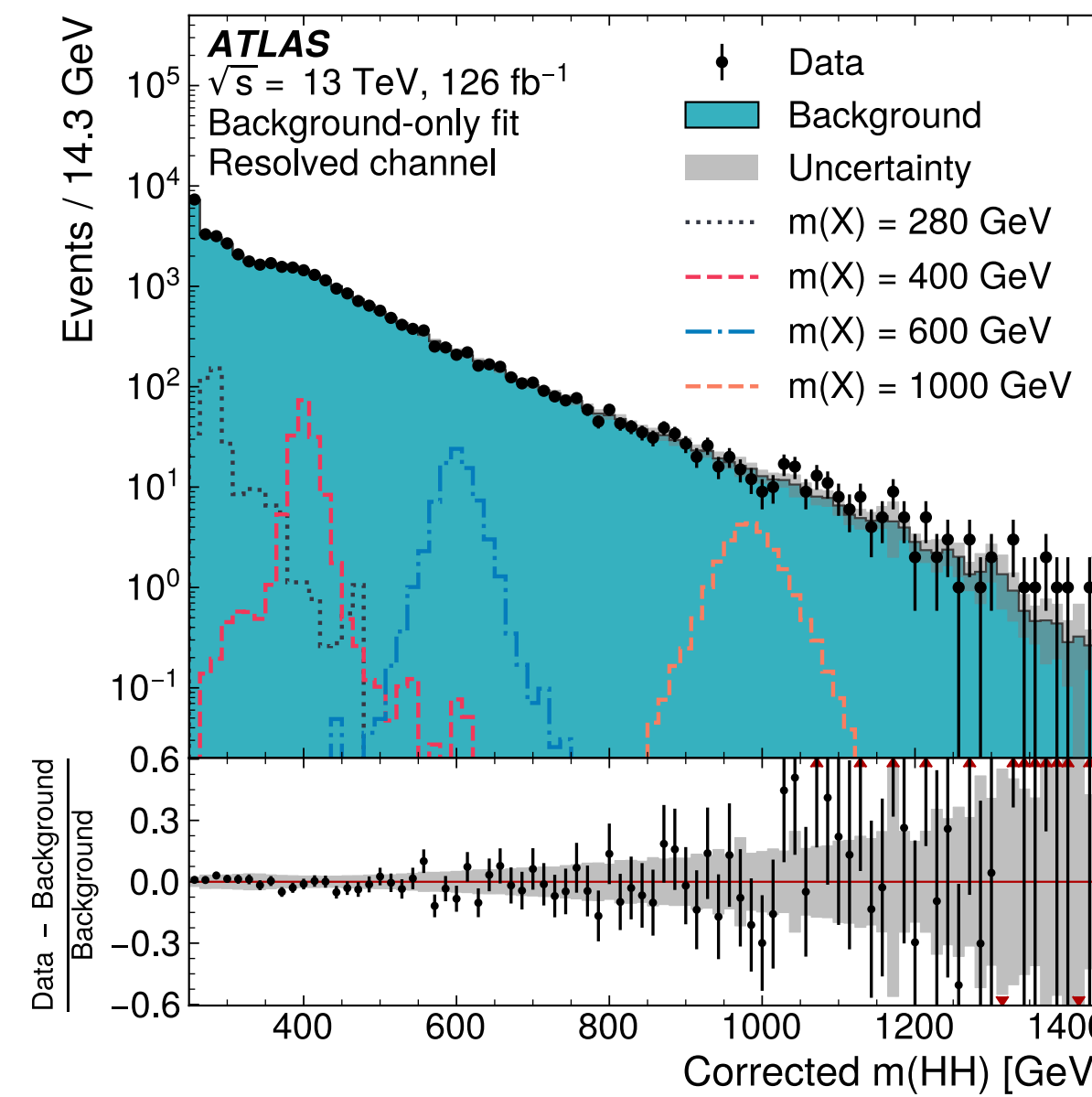
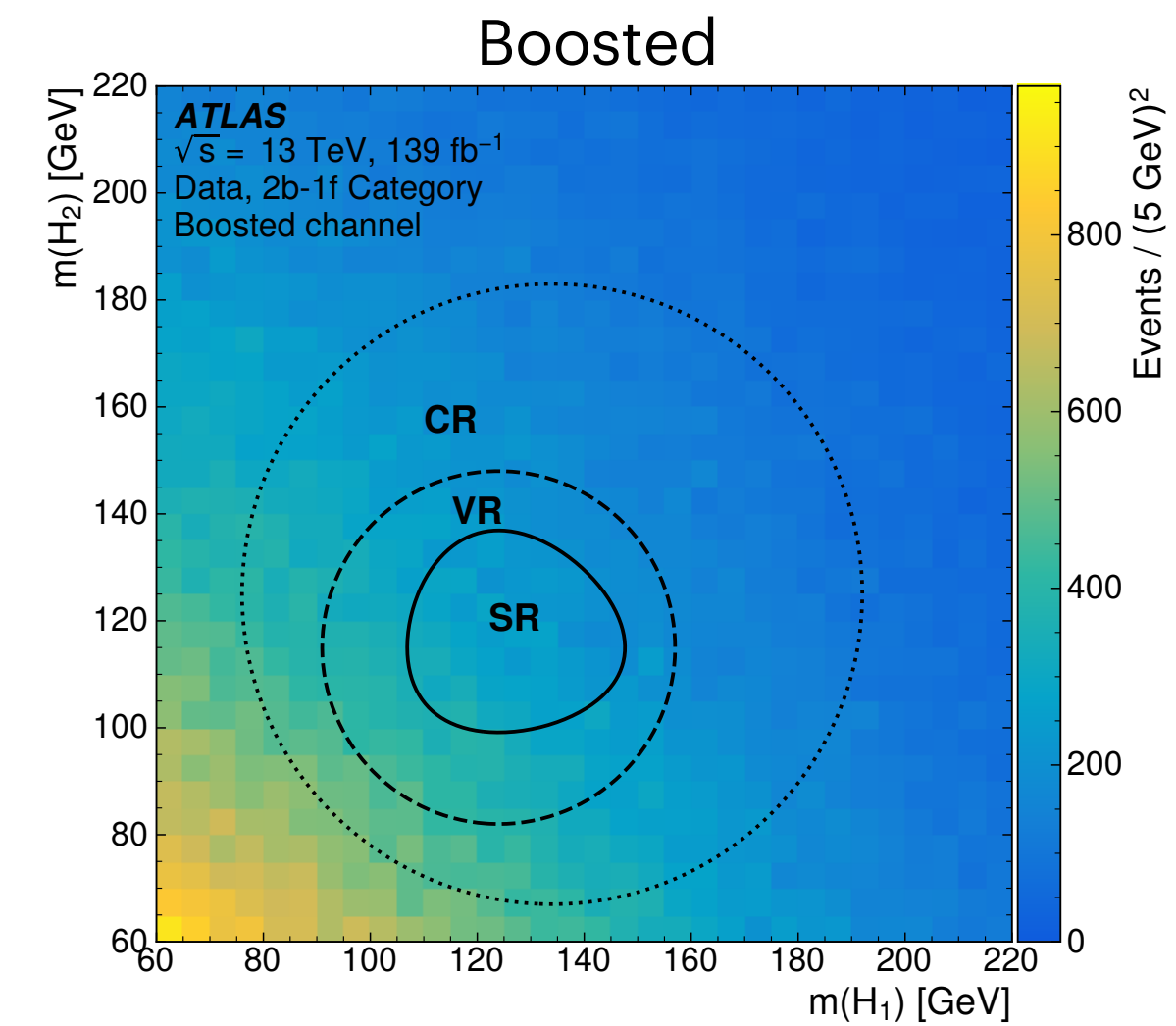
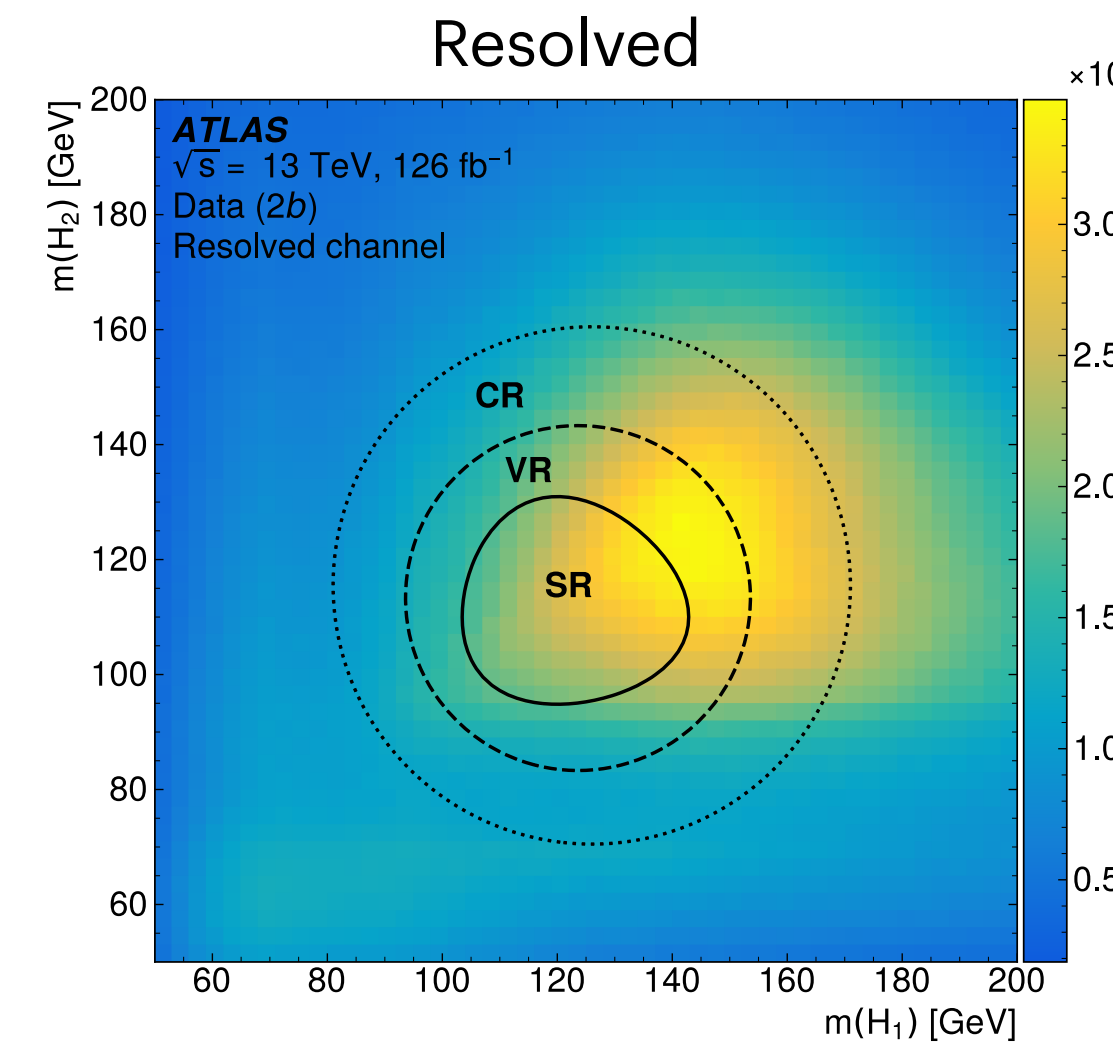
Signal regions defined by selections in the 2D $m_{H1}-m_{H2}$ plane

m_{HH} used as final discriminant variable, searching for a “bump” from the decay of a new BSM resonance

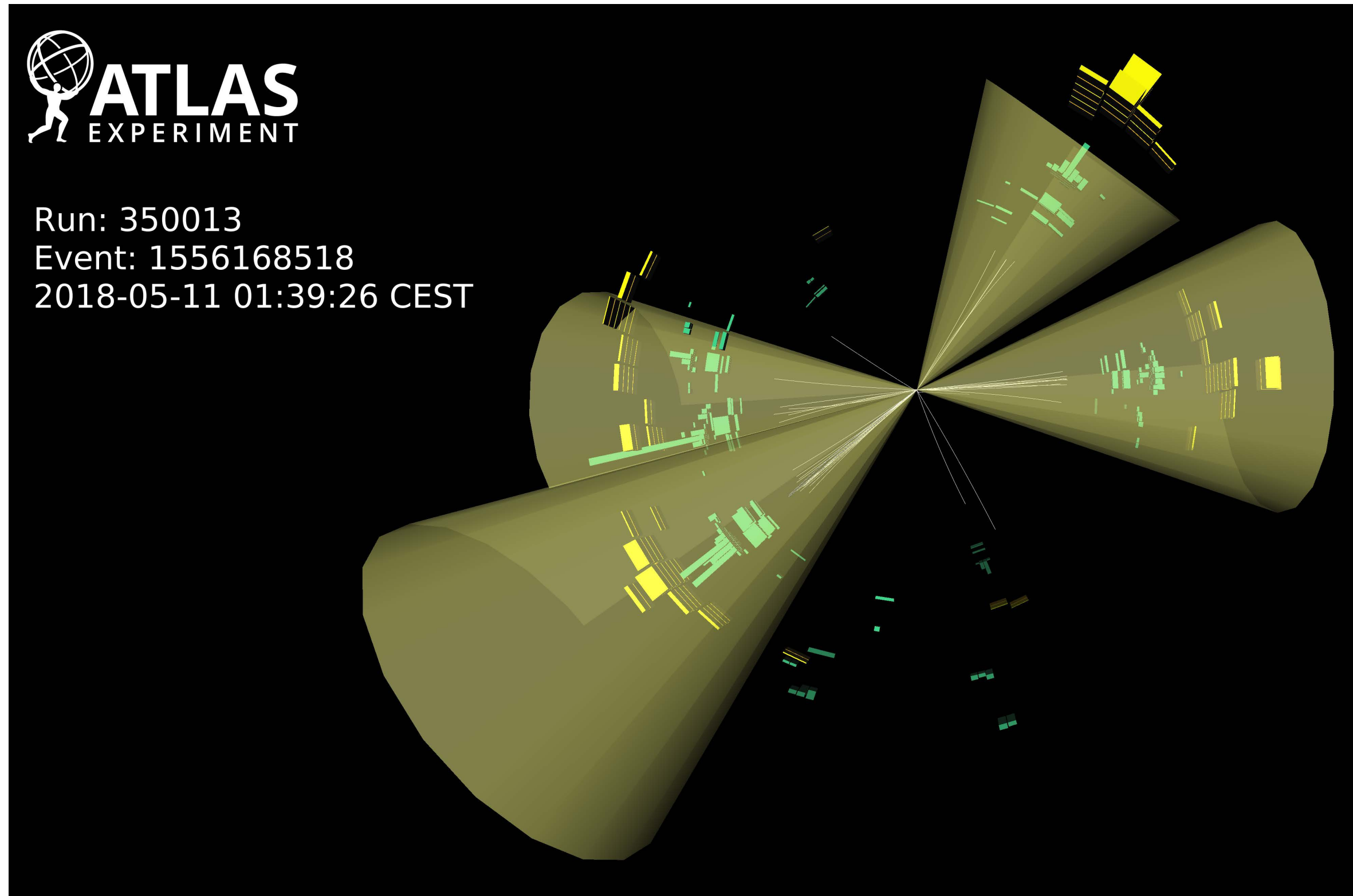
Phys. Rev. D 105, 092002



Small data excess at 1.1 TeV,
 local (global) significance = 2.6σ (1.0σ)

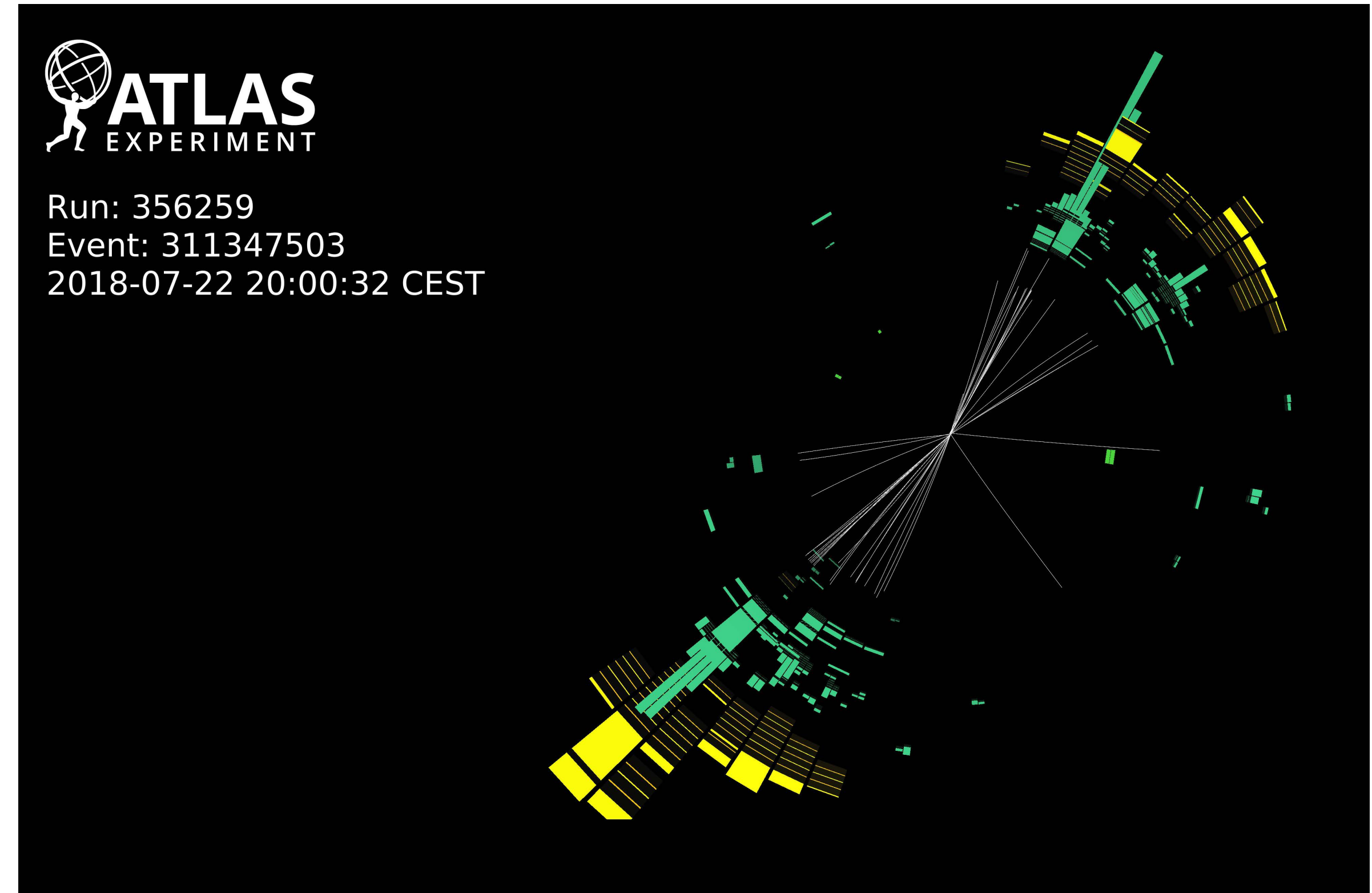


Resonant $HH \rightarrow b\bar{b}b\bar{b}$ with full Run 2 data



Data event passing the resolved signal region event selection

$$m_{HH} = 629 \text{ GeV}, m_{H1} = 111 \text{ GeV} \text{ and } m_{H2} = 116 \text{ GeV}$$

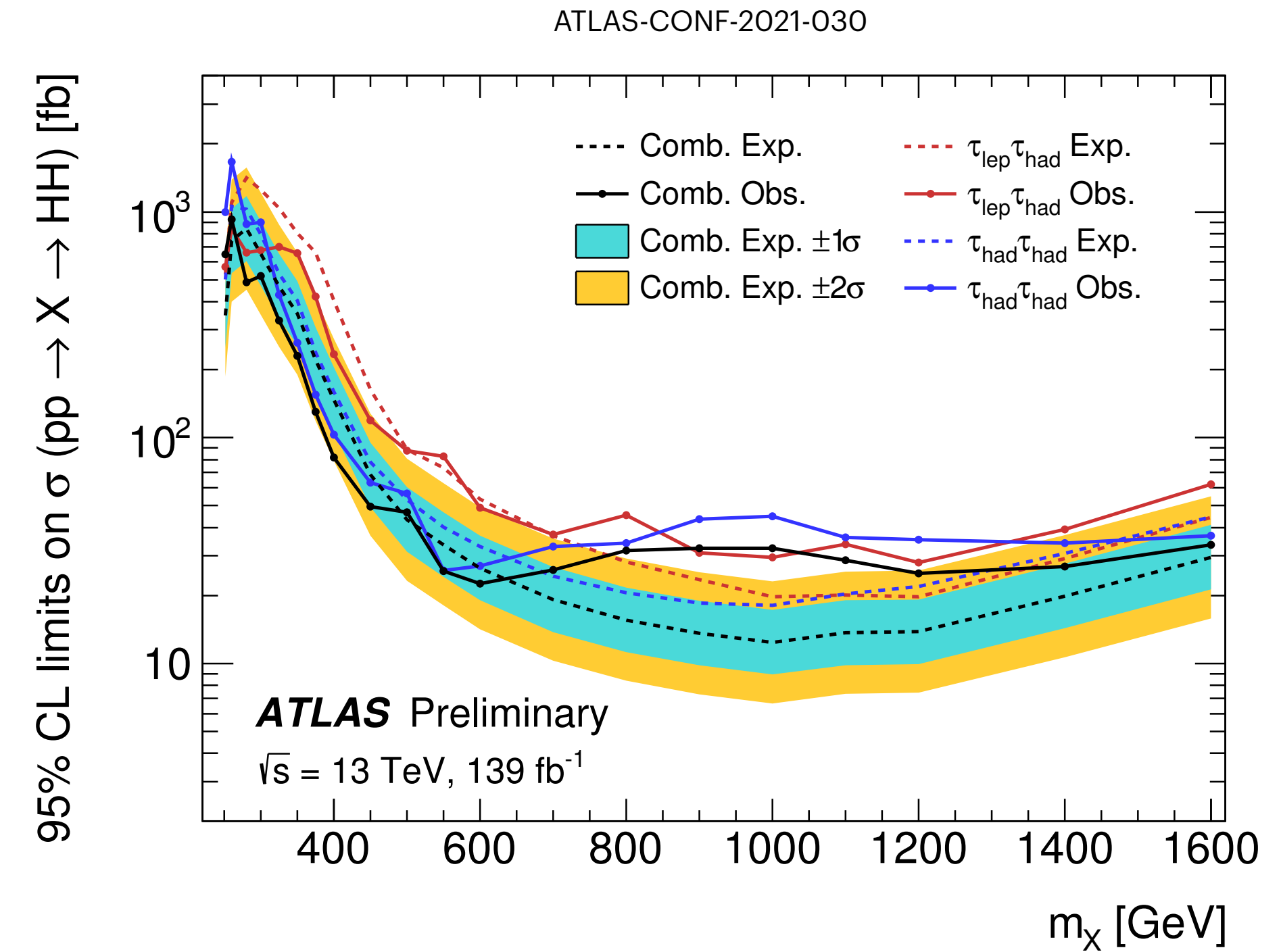
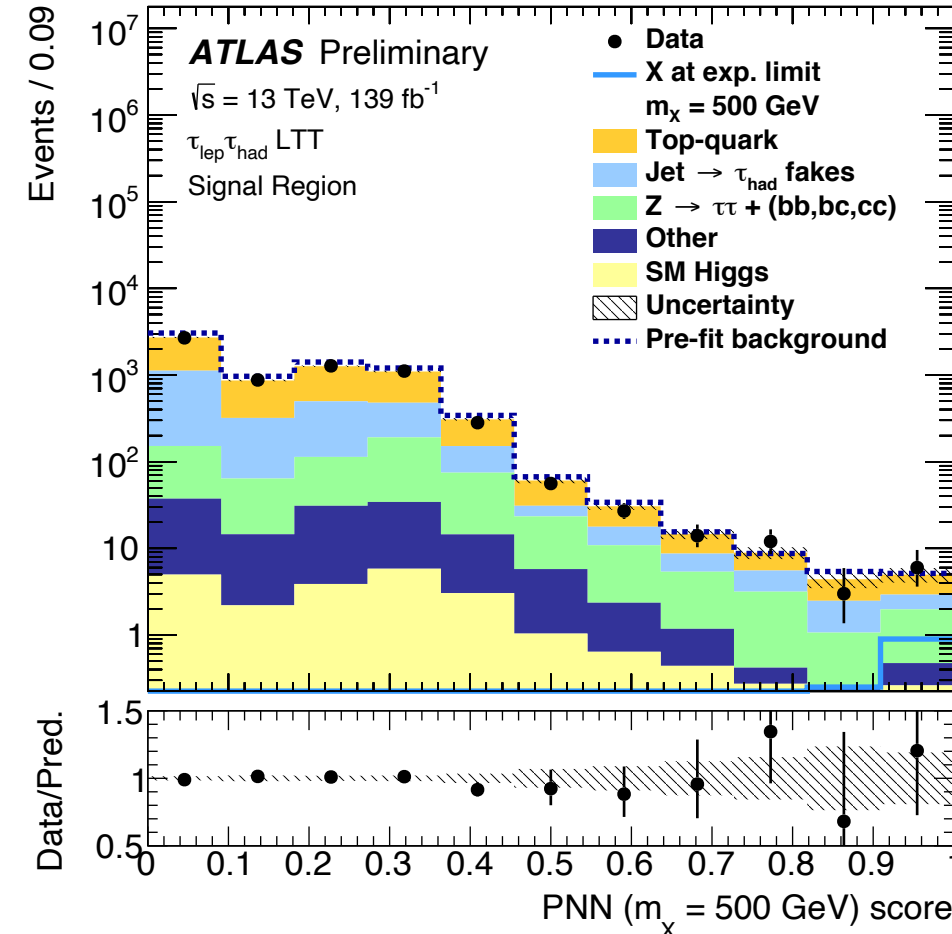
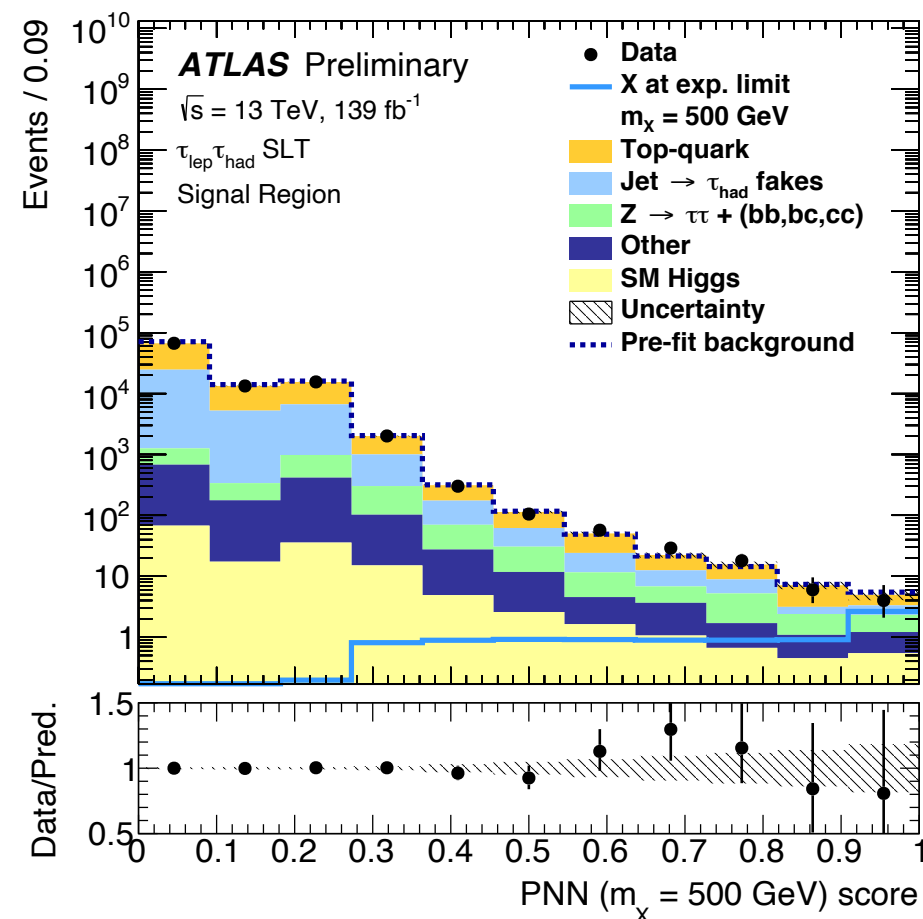
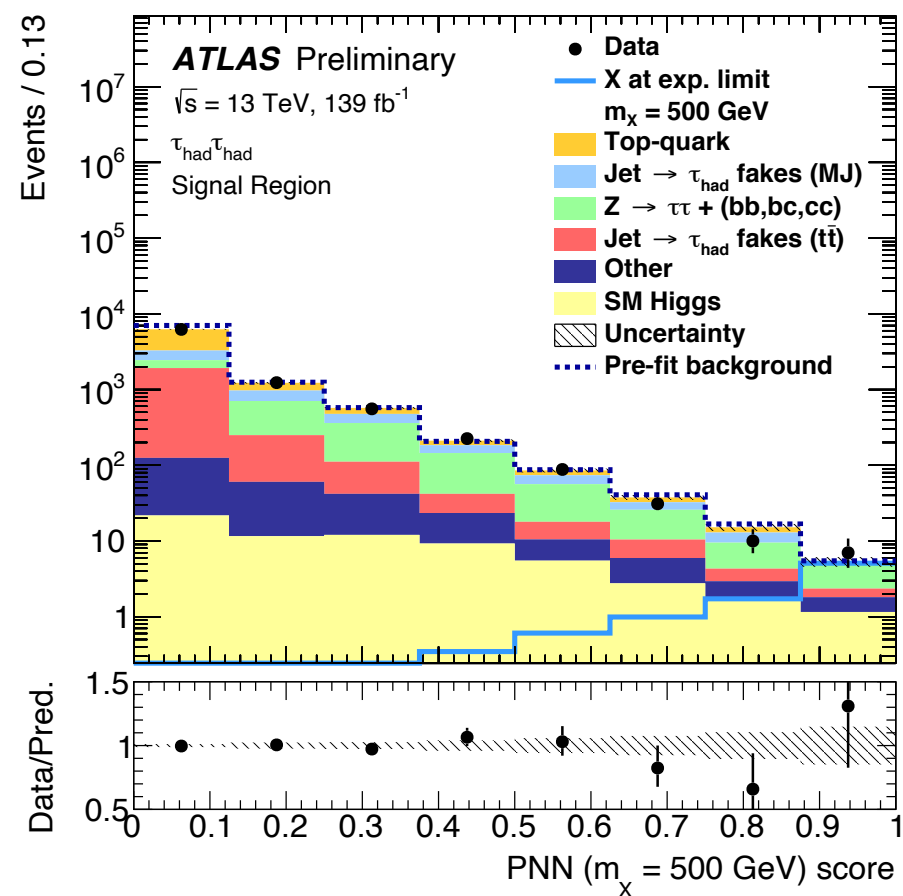


Data event passing the boosted 4b signal region event selection

$$m_{HH} = 1023 \text{ GeV}, m_{H1} = 127 \text{ GeV} \text{ and } m_{H2} = 123 \text{ GeV}$$

Resonant $HH \rightarrow bb\tau\tau$ with full Run 2 data

- Search for BSM resonant HH production: resonances with masses between 250 GeV and 1.6 TeV
- $X \rightarrow HH \rightarrow bb\tau\tau$
- Same 3 signal regions and background estimation as non-resonant search
- Parameterized Neural Network (PNN), with mass of the resonance as parameter, used to separate signals with different mass hypotheses from background
- PNN outputs used as final discriminants searching for an excess of events in the most signal-like bins of the PNNs



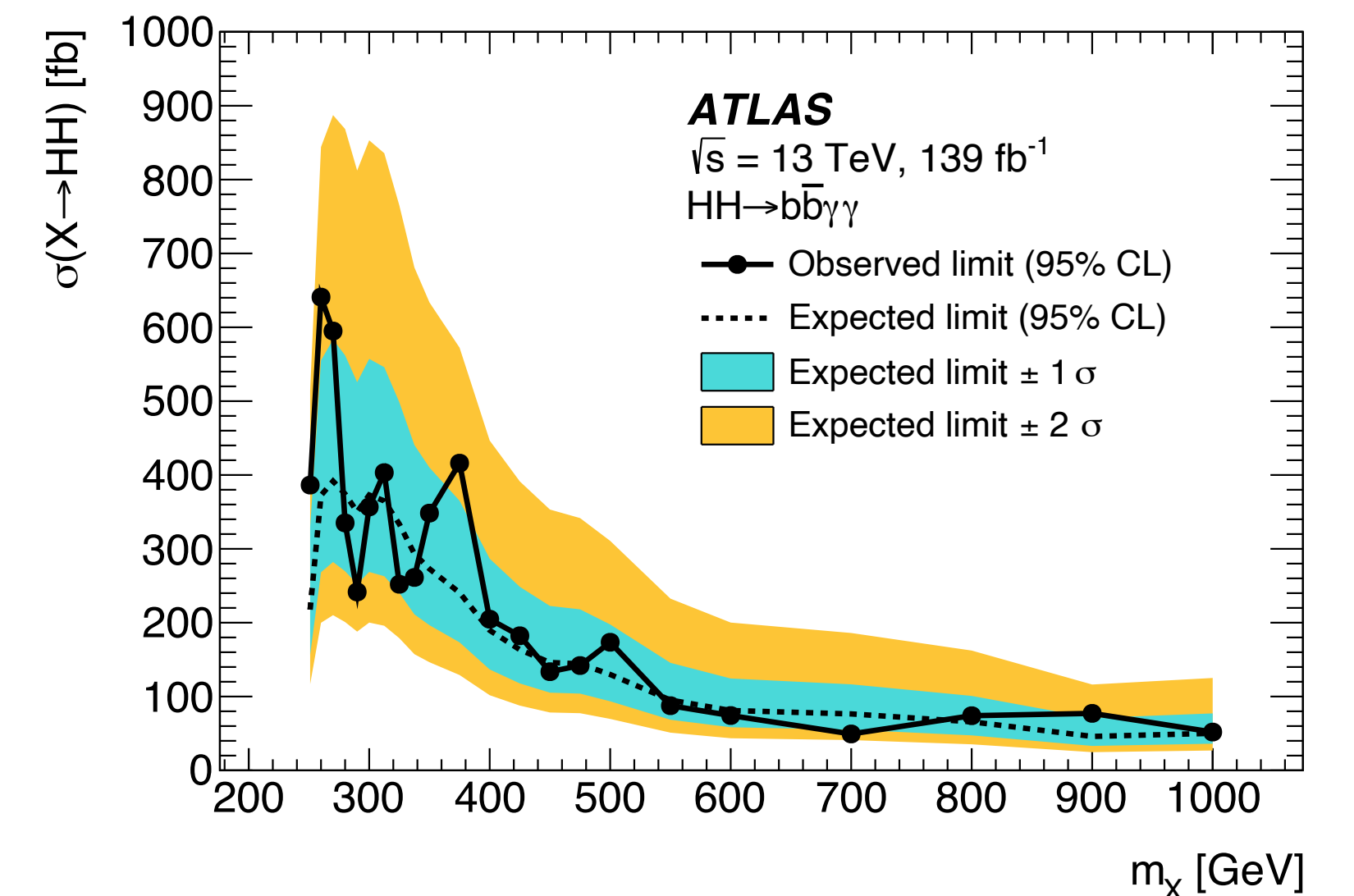
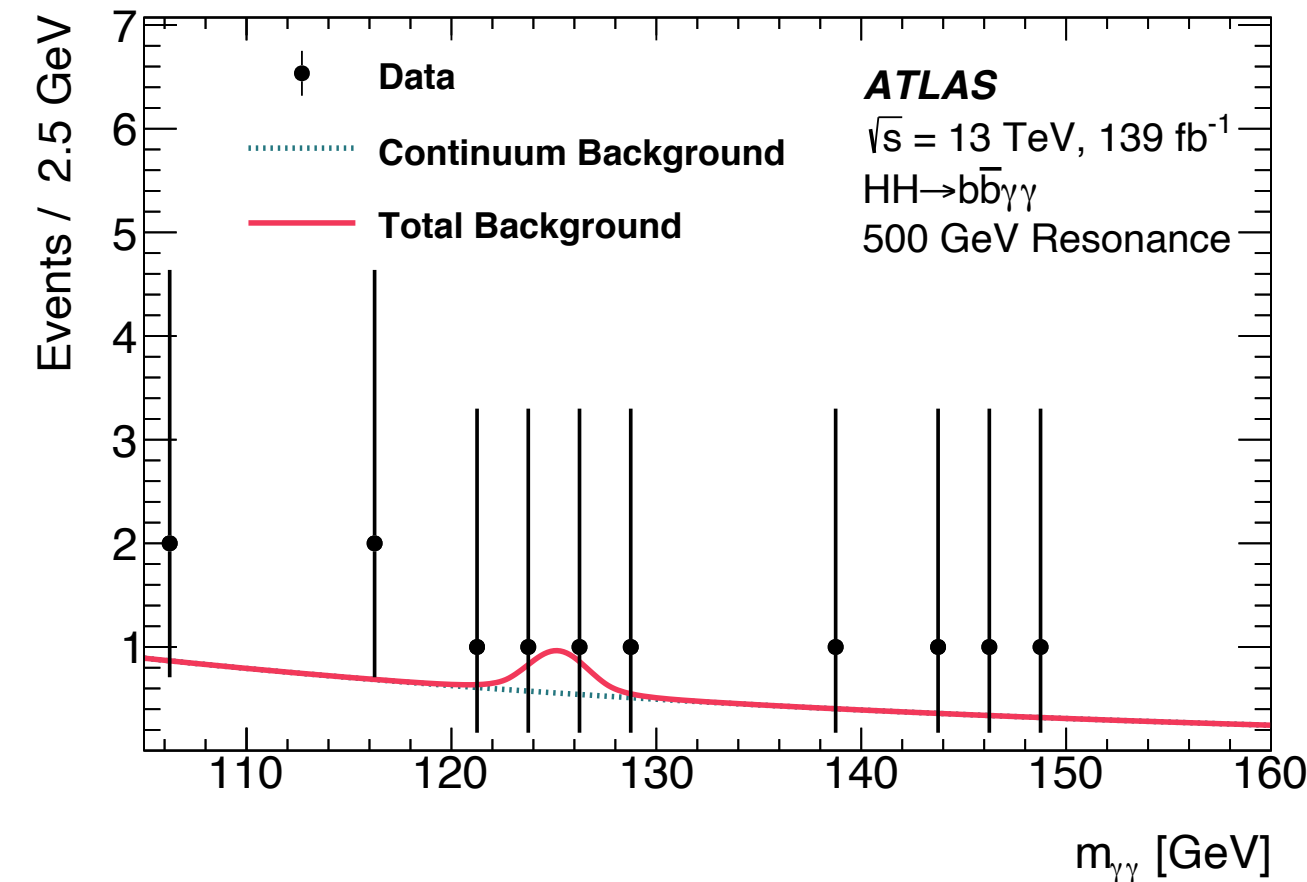
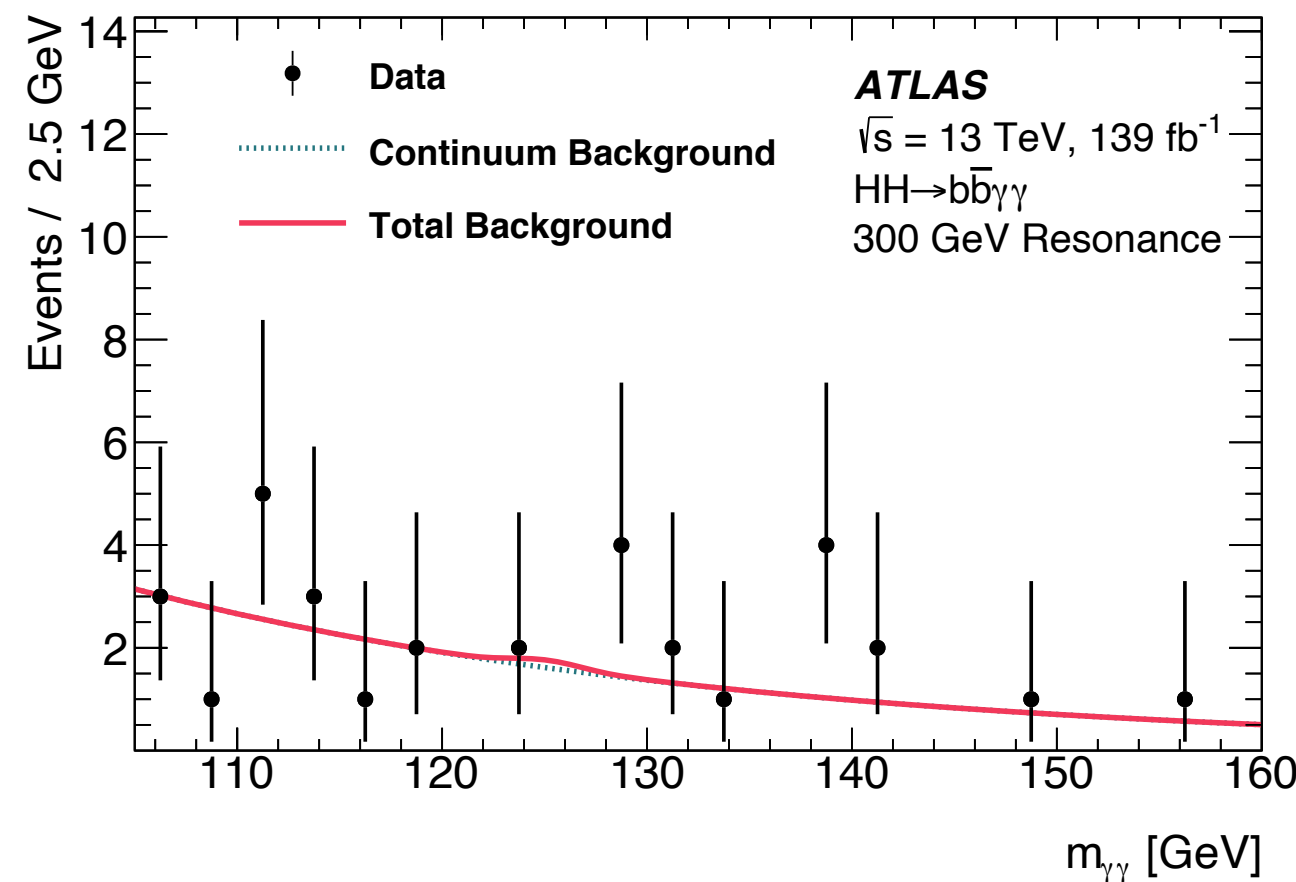
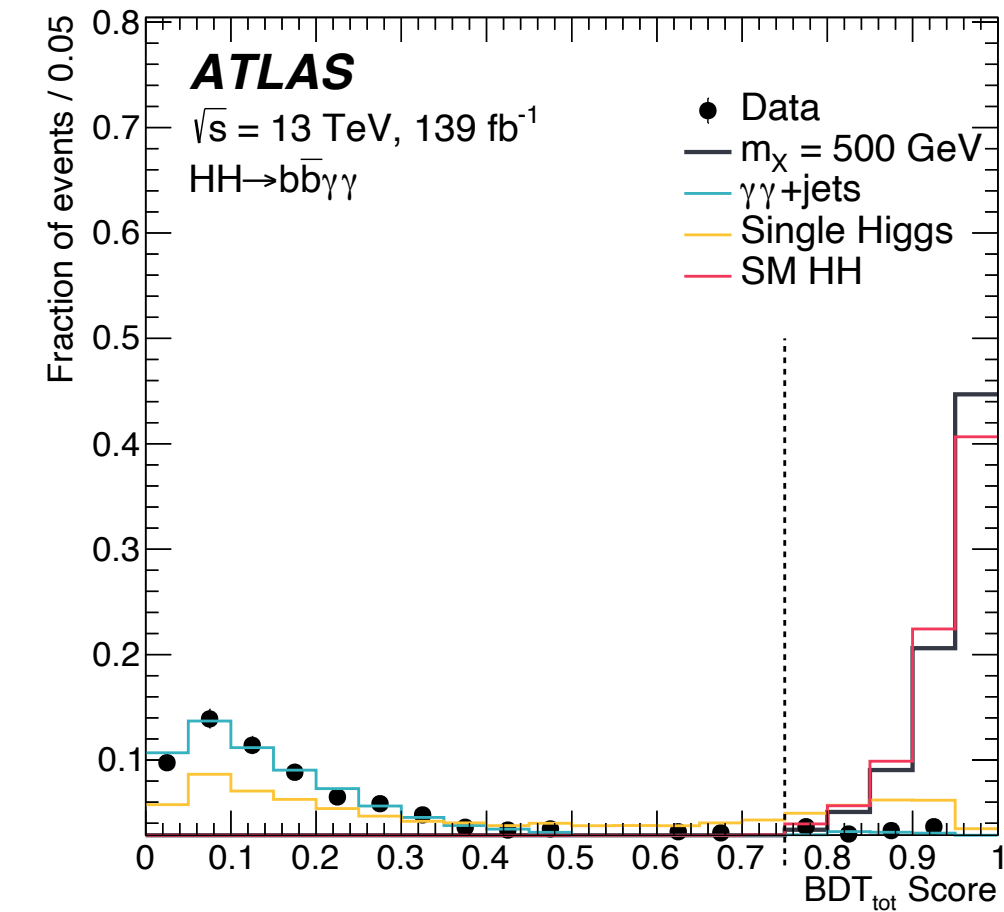
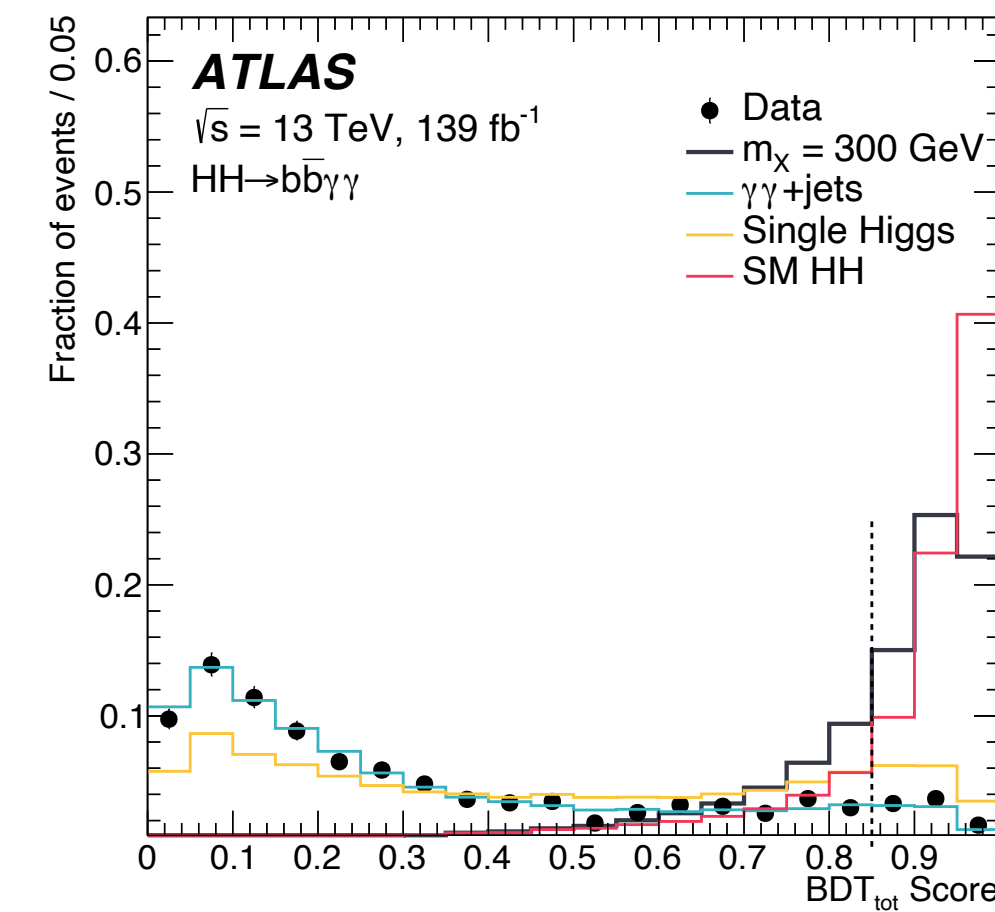
Small data excess between 800 GeV and 1.1 TeV, largest significance at 1 TeV, 3σ (2σ) local (global)

Resonant $HH \rightarrow b\bar{b}\gamma\gamma$ with full Run 2 data

- Search for BSM resonant HH production: resonances with masses between 250 GeV and 1 TeV
- $X \rightarrow HH \rightarrow b\bar{b}\gamma\gamma$
- Baseline event selection and background estimation same as in the non-resonant search

arXiv:2112.11876

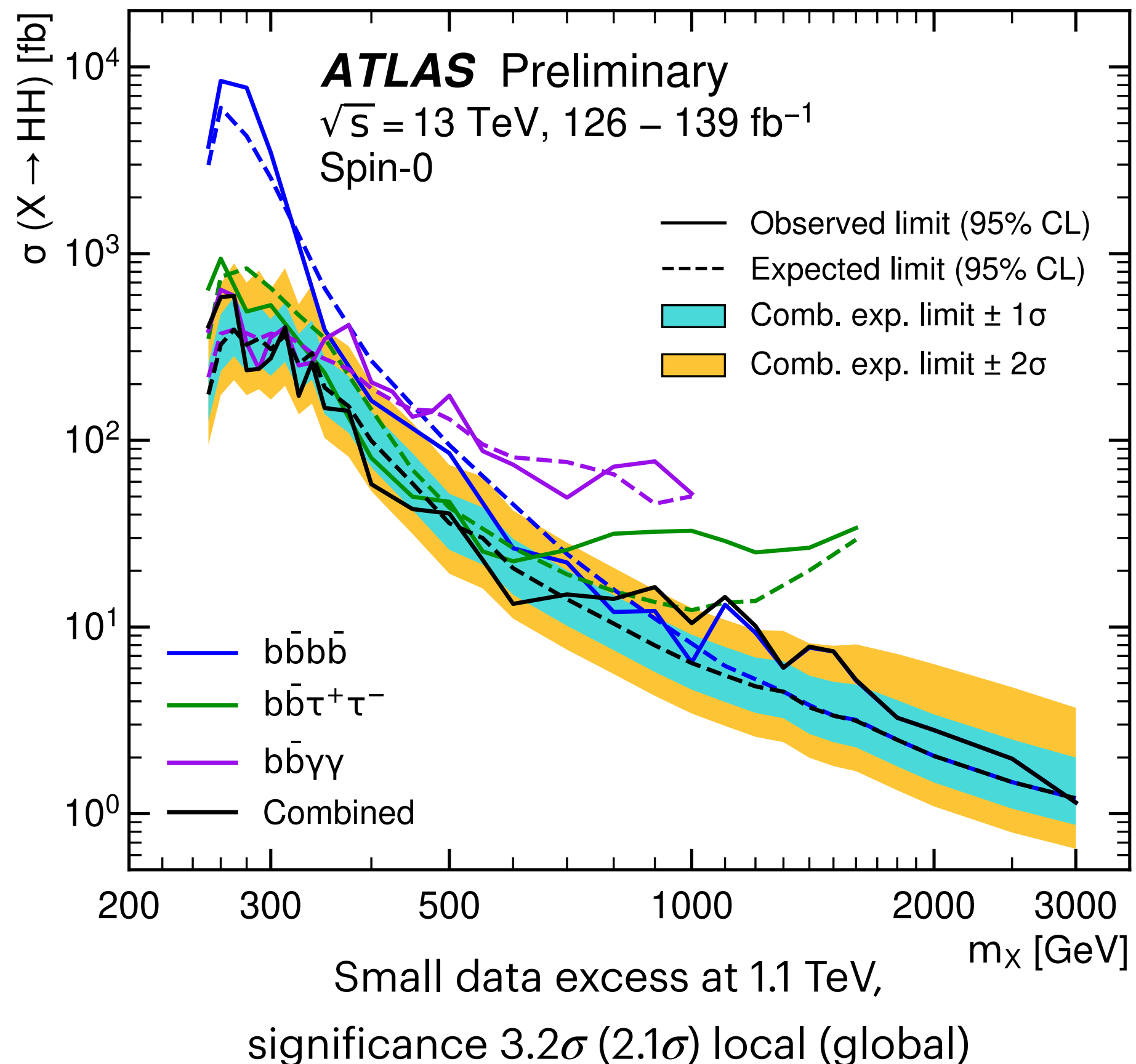
- Boosted Decision Trees used to discriminate signal and background
- Two BDTs trained one against $\gamma\gamma$ +jets and one against single-Higgs backgrounds and combined in one BDT_{tot} variable
- 1 signal region for each mass hypothesis defined by mass-dependent m_{HH} window selection and mass-dependent BDT cut



Resonant HH combination with full Run 2 data

- Searches for BSM resonant HH production: resonances with masses between 250 GeV and 5 TeV
- $X \rightarrow HH \rightarrow bbbb, bb\tau\tau, bb\gamma\gamma$
- Similar baseline event selections and background estimations to the non-resonant searches in the same final states
- Optimised signal region selections and discriminants specifically for the resonant signals

ATLAS-CONF-2021-052



Combination of HH analyses performed in 3 decay channels using full LHC Run 2 data corresponding to 139 fb^{-1} :

- $bb\tau\tau$, $bb\gamma\gamma$ and $bbbb$ channels for the searches for resonant HH production

Complementarity of searches in different decay channels:

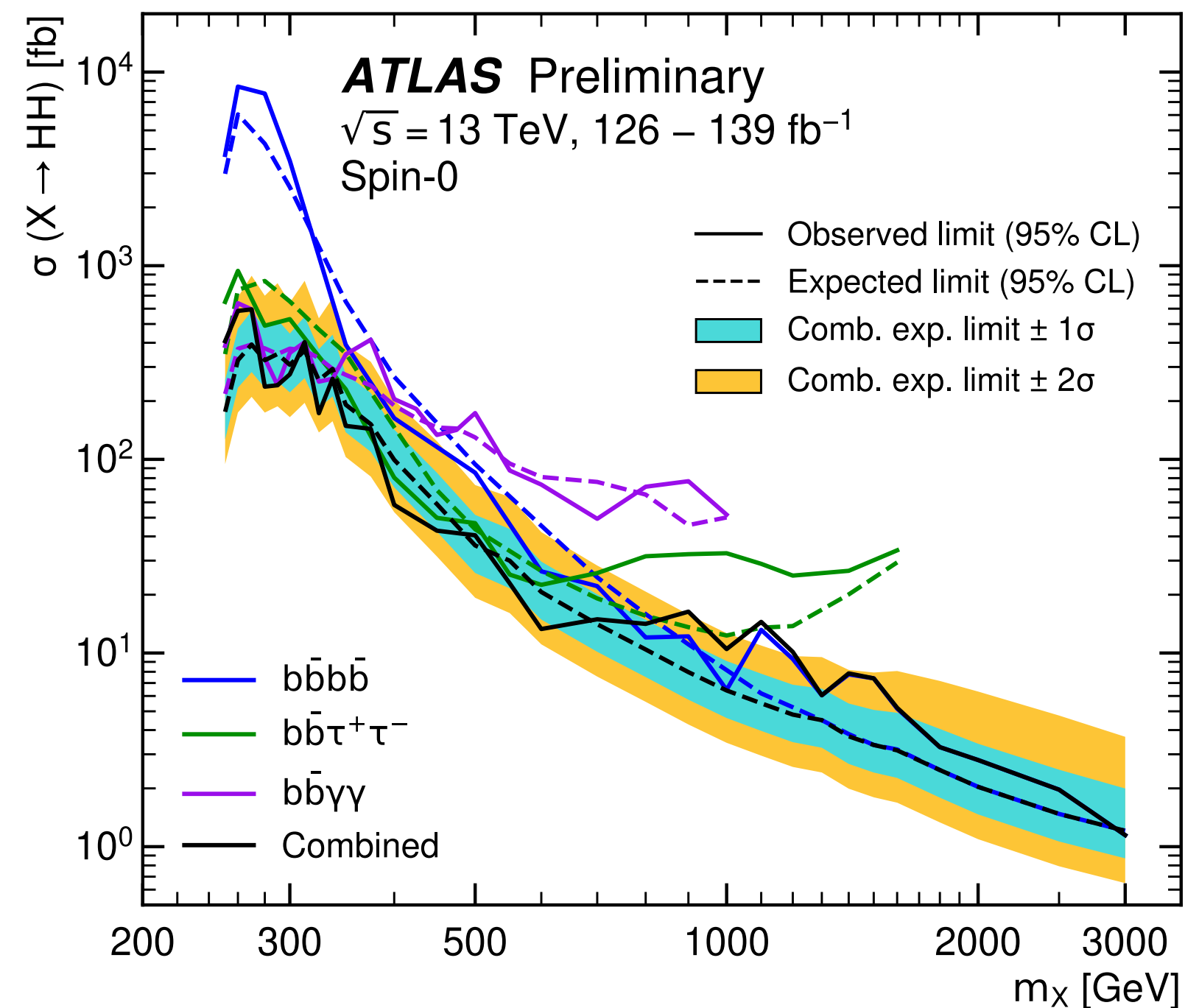
- $bb\gamma\gamma$ best sensitivity at low mass arXiv:2112.11876
- $bb\tau\tau$ best sensitivity in medium mass range ATLAS-CONF-2021-030
- $bbbb$ best sensitivity at high mass Phys. Rev. D 105, 092002

Resonant HH combination with full Run 2 data

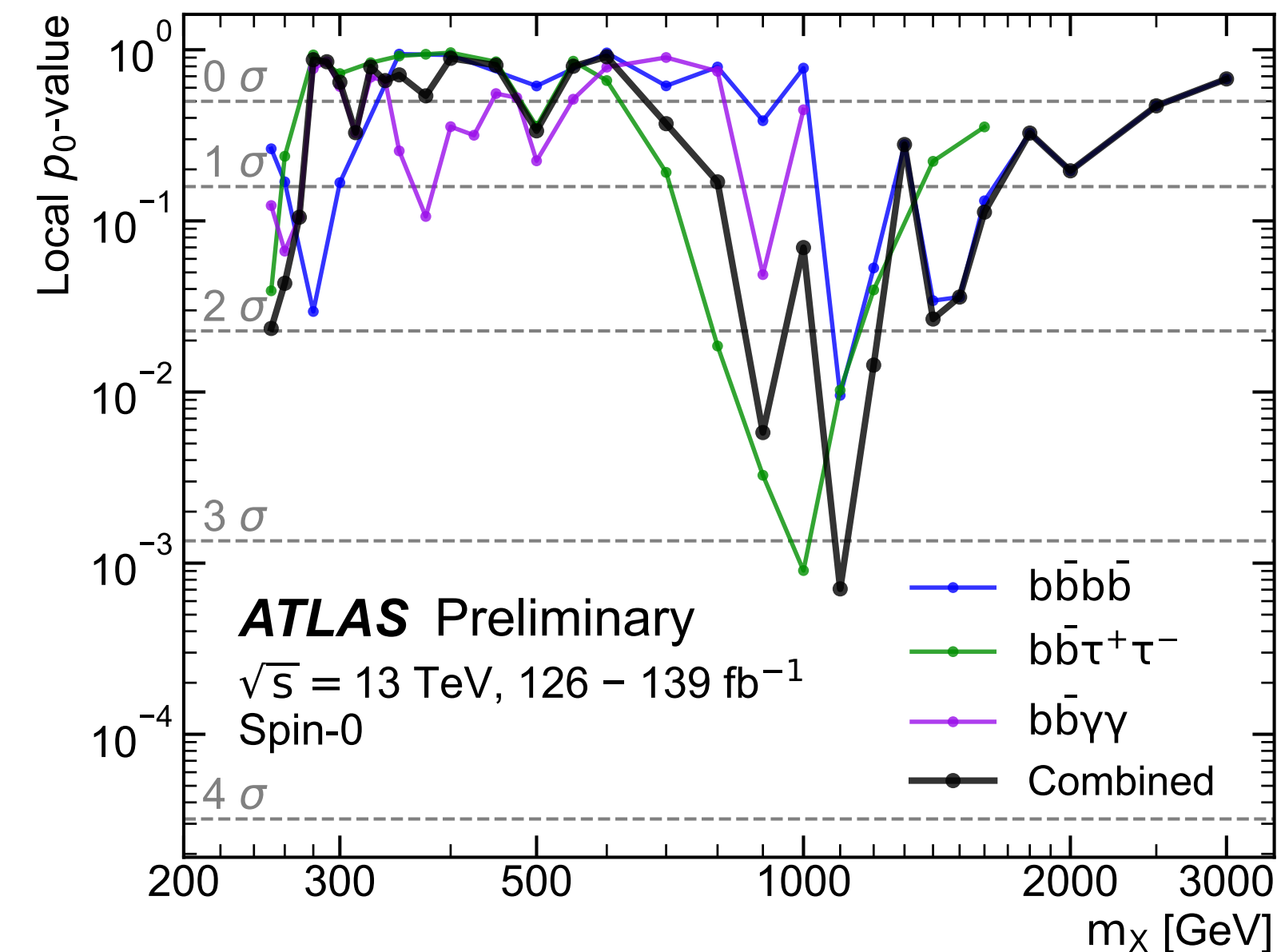
Combination of HH analyses performed in 3 decay channels using full Run 2 LHC data corresponding to 139 fb^{-1} :

- $b\bar{b}\tau\tau$, $b\bar{b}\gamma\gamma$ and $b\bar{b}b\bar{b}$ channels for the searches for resonant HH production

ATLAS-CONF-2021-052



Small data excess at 1.1 TeV,
 significance 3.2σ (2.1σ) local (global)



At 1.1 TeV: Local significance = 3.2σ and Global significance = 2.1σ

$4b$ and $b\bar{b}\tau\tau$ measured signal strengths
 compatible with each other with a p-value of 33%

Non-resonant $HH \rightarrow bbbb$ with full Run 2 data

Event selection

ATLAS-CONF-2022-035

	Data	ggF Signal		VBF Signal	
		SM	$\kappa_\lambda = 10$	SM	$\kappa_{2V} = 0$
Common preselection					
Preselection	5.70×10^8	526.6	7337.7	22.3	626.1
Trigger class	2.49×10^8	381.8	5279.1	16.1	405.2
ggF selection					
Fail VBF selection	2.46×10^8	376.6	5198.0	13.9	334.4
At least 4 b -tagged central jets	1.89×10^6	86.0	1001.7	1.9	65.2
$ \Delta\eta_{HH} < 1.5$	1.03×10^6	71.9	850.6	0.9	46.4
$X_{Wt} > 1.5$	7.51×10^5	60.4	569.0	0.7	43.1
$X_{HH} < 1.6$ (ggF signal region)	1.62×10^4	29.1	182.7	0.2	23.0
VBF selection					
Pass VBF selection	3.30×10^6	5.2	81.1	2.2	70.7
At least 4 b -tagged central jets	2.71×10^4	1.1	15.3	0.7	27.6
$X_{Wt} > 1.5$	2.18×10^4	1.0	11.2	0.7	26.5
$X_{HH} < 1.6$	5.02×10^2	0.5	3.1	0.3	17.3
$m_{HH} > 400$ GeV (VBF signal region)	3.57×10^2	0.4	1.8	0.3	16.4

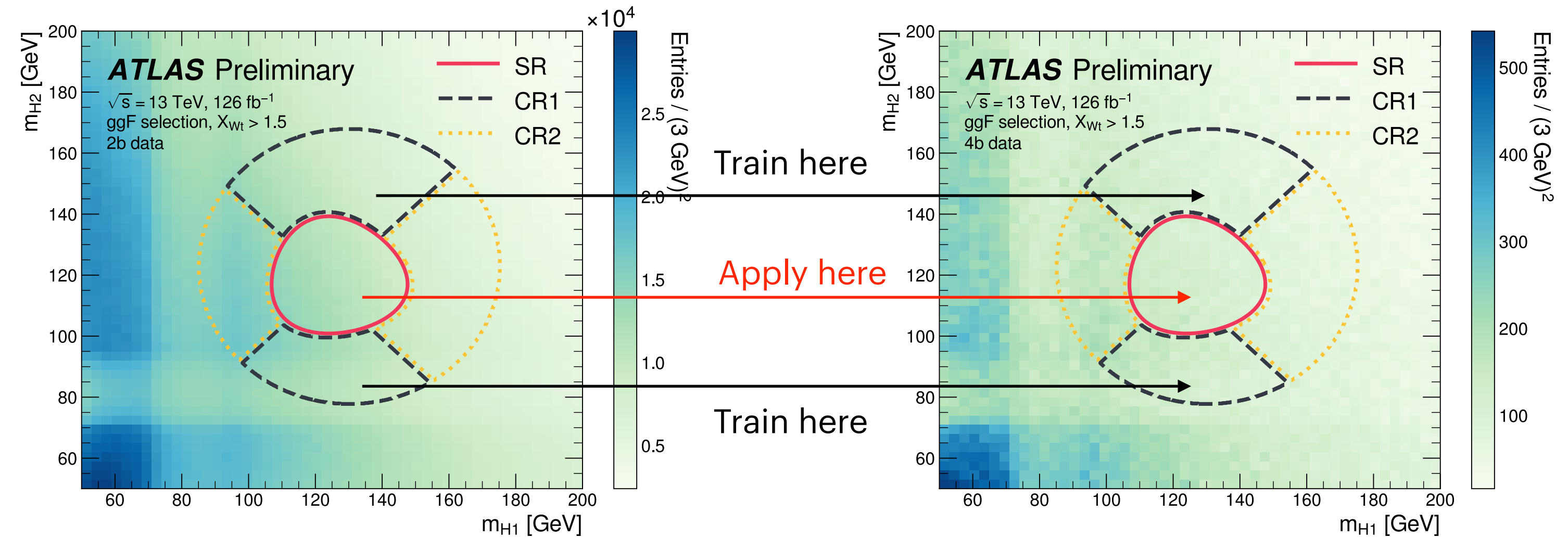
Non-resonant $HH \rightarrow b\bar{b}b\bar{b}$ with full Run 2 data

Main background: QCD multi-jet background

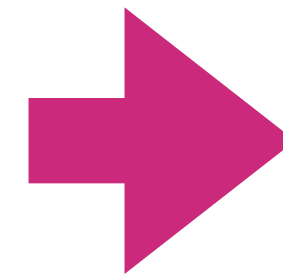
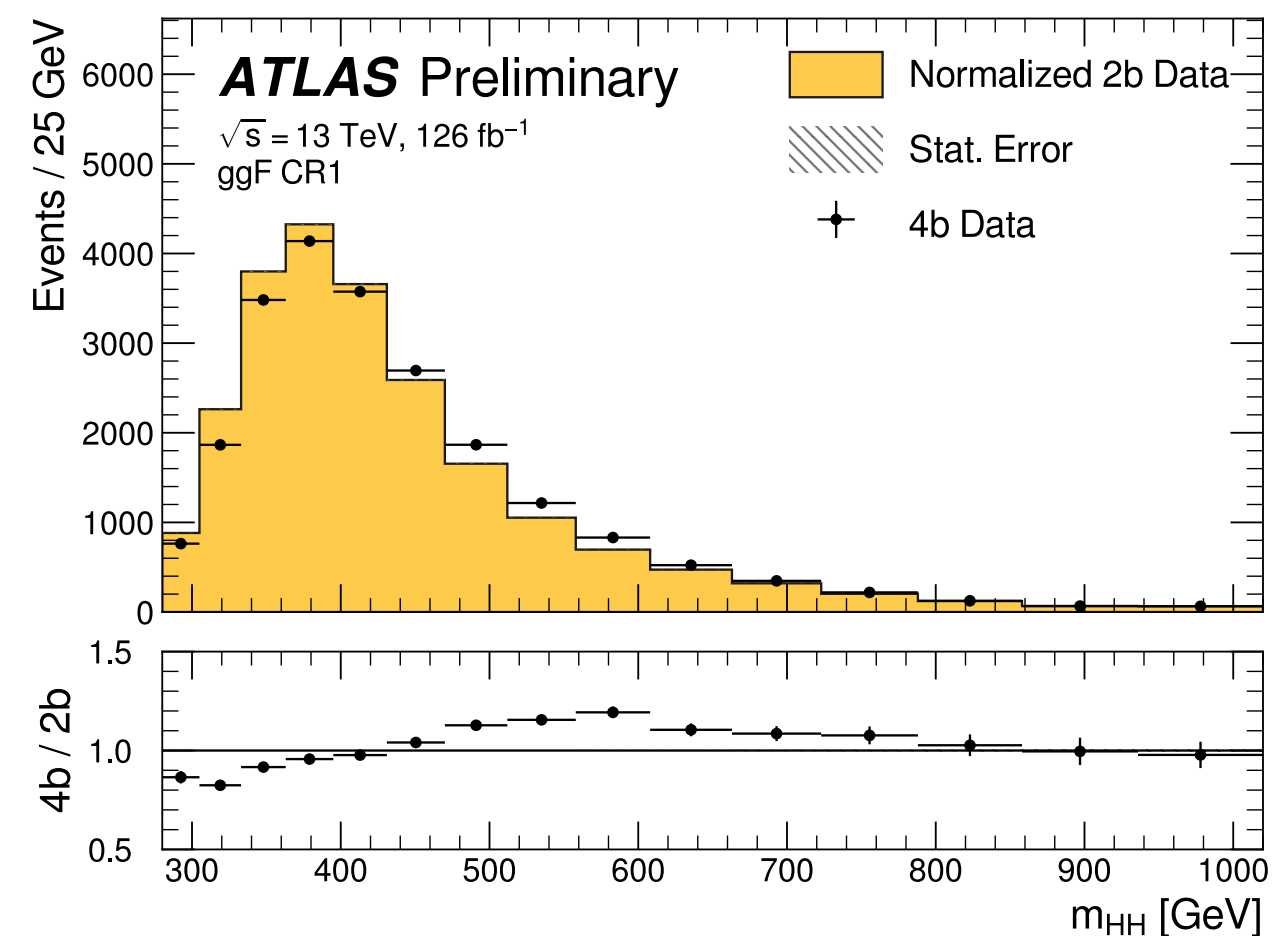
Data-driven estimation for the total background:

using a neural network trained in control regions to reweight 2b data to look like 4b data, then applied to 2b data in the signal region to model 4b data in the signal region

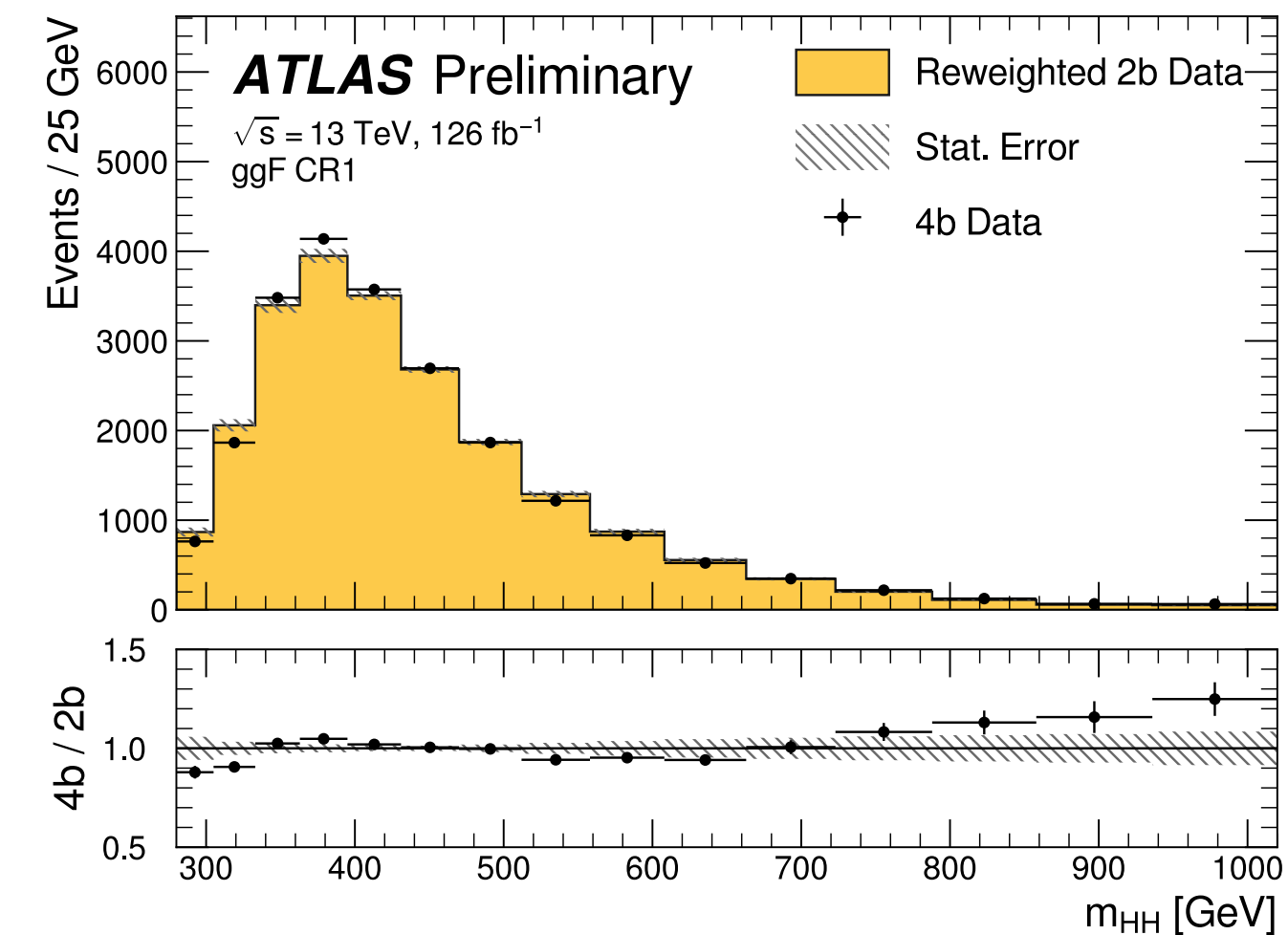
ATLAS-CONF-2022-035



Before re-weighting



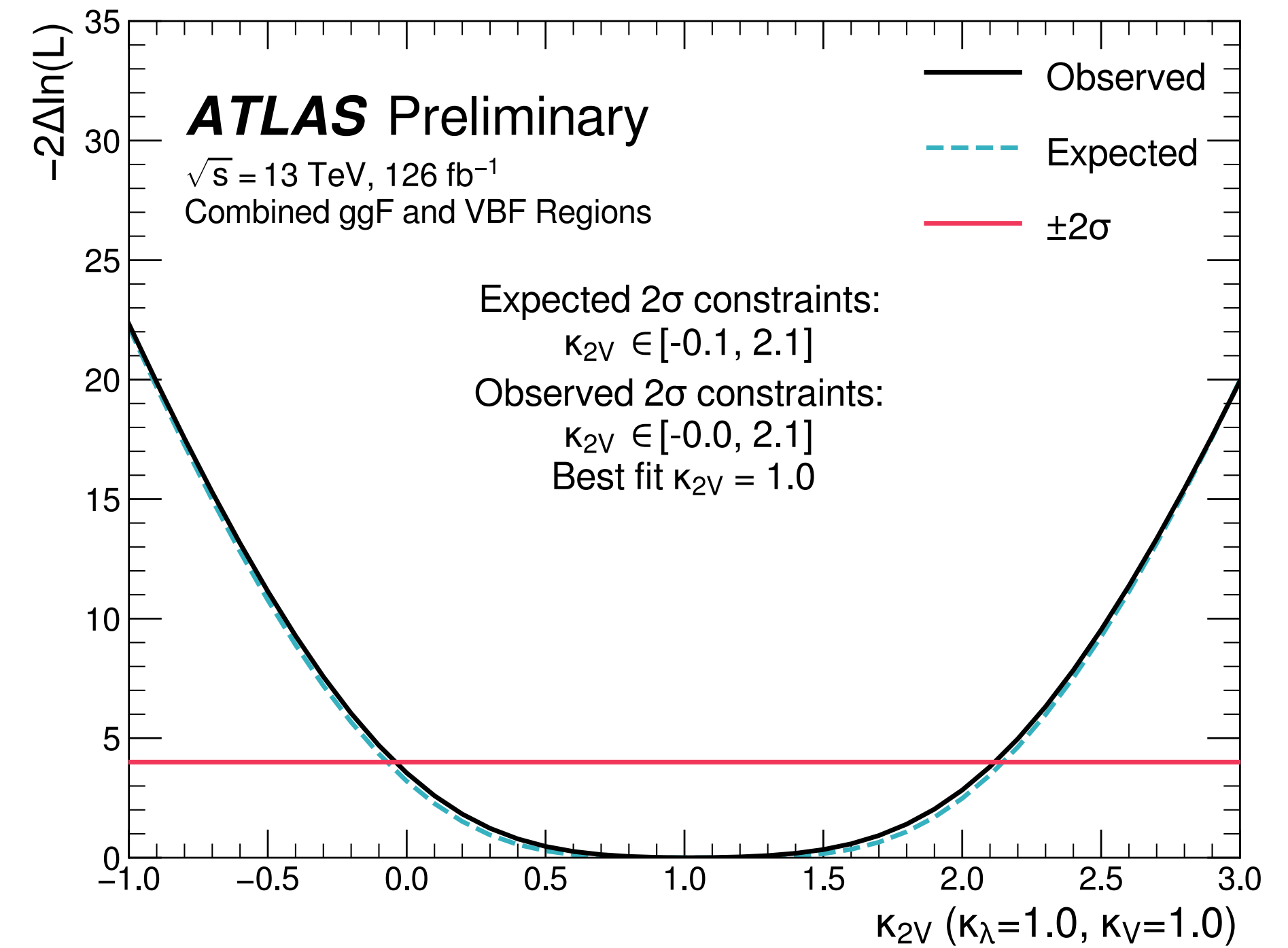
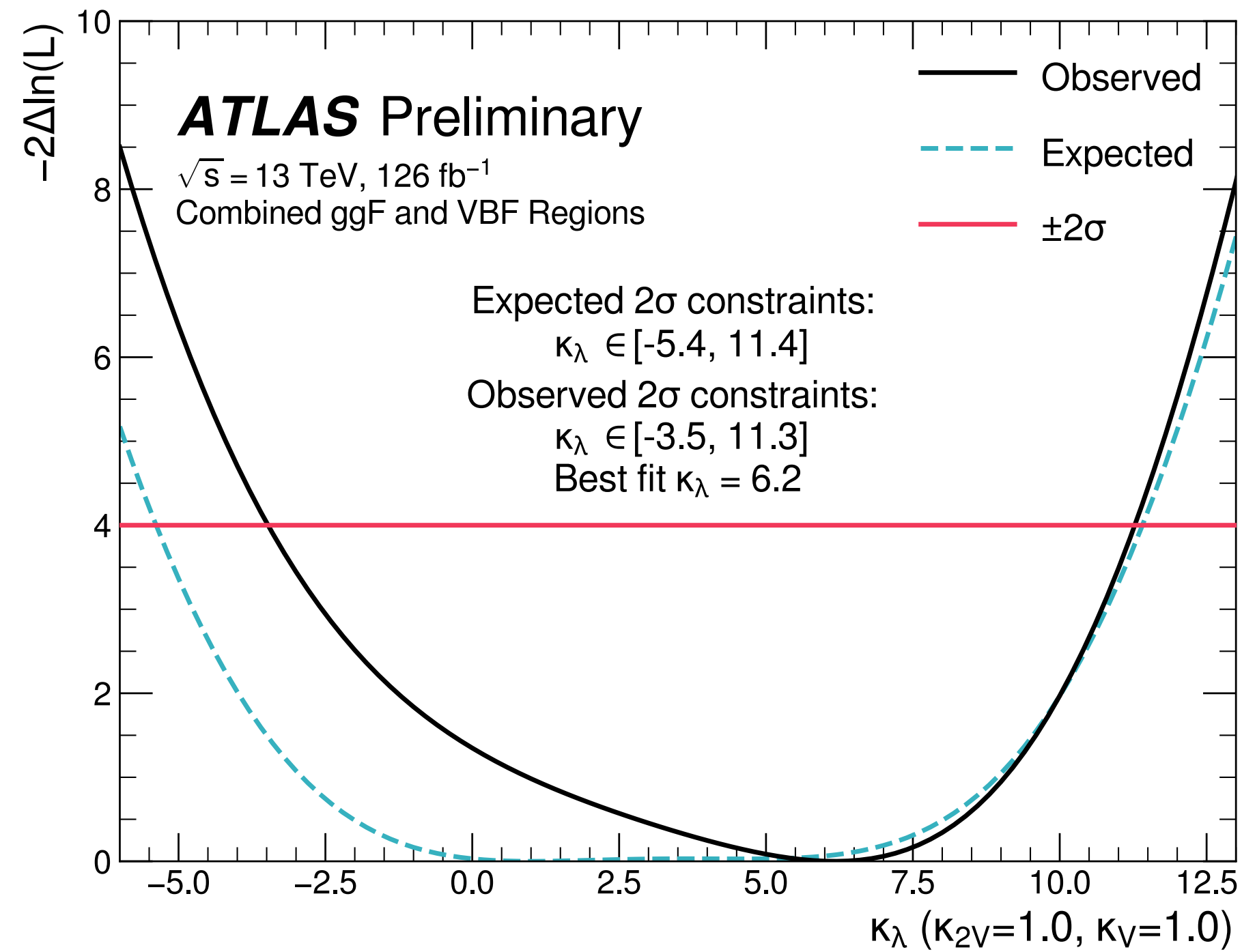
After re-weighting



Non-resonant $HH \rightarrow bbbb$ with full Run 2 data

Likelihood scans

ATLAS-CONF-2022-035



Non-resonant $HH \rightarrow b\bar{b}b\bar{b}$ with full Run 2 data

NN input variables

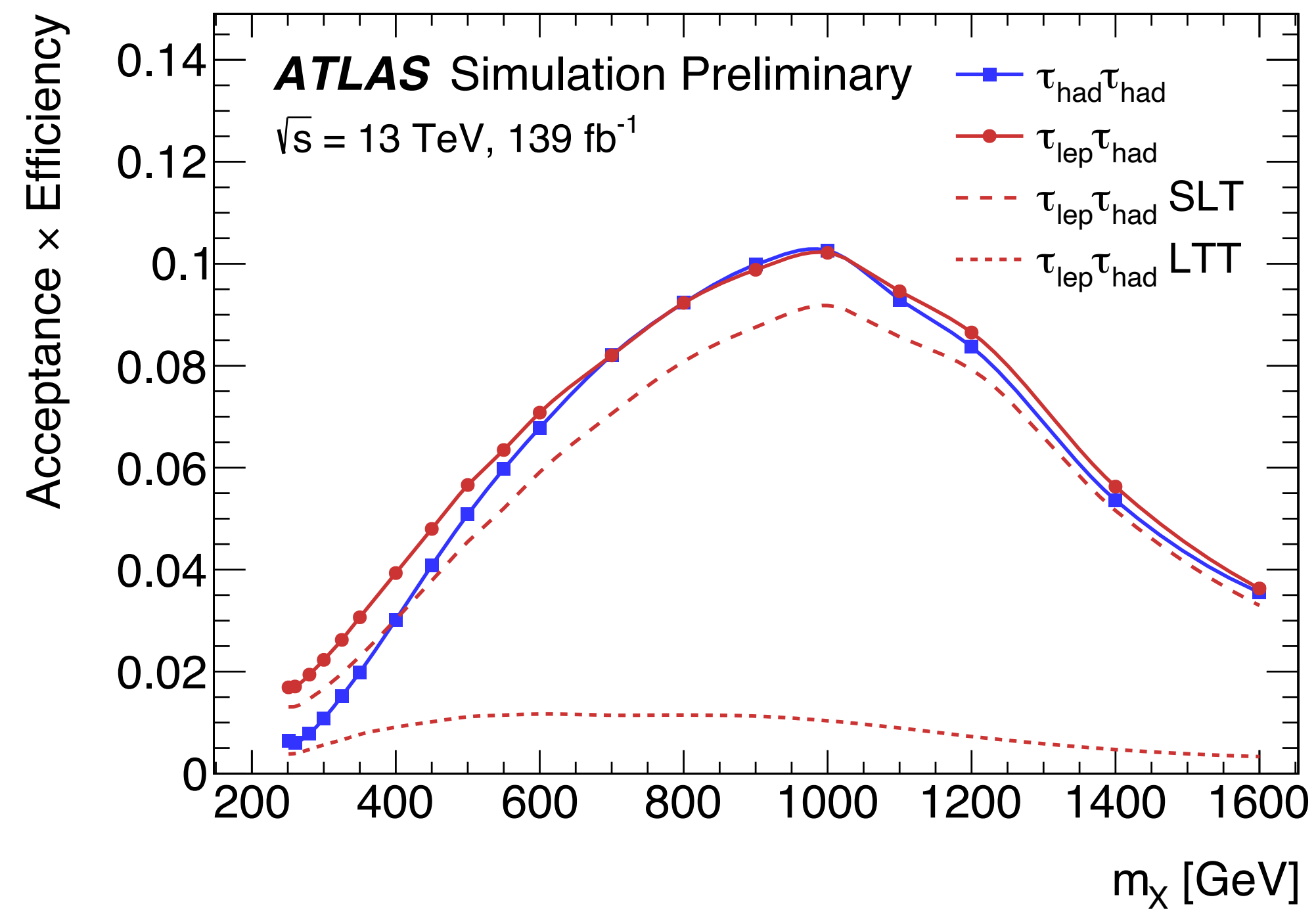
ATLAS-CONF-2022-035

ggF	VBF
1. $\log(p_T)$ of the 2 nd leading Higgs boson candidate jet	1. Maximum di-jet mass out of the possible pairings of the four Higgs boson candidate jets
2. $\log(p_T)$ of the 4 th leading Higgs boson candidate jet	2. Minimum di-jet mass out of the possible pairings of the four Higgs boson candidate jets
3. $\log(\Delta R)$ between the closest two Higgs boson candidate jets	3. Energy of the leading Higgs boson candidate
4. $\log(\Delta R)$ between the other two Higgs boson candidate jets	4. Energy of the subleading Higgs boson candidate
5. Average absolute η value of the Higgs boson candidate jets	5. Second smallest ΔR between the jets in the leading Higgs boson candidate (out of the three possible pairings for the leading Higgs candidate)
6. $\log(p_T)$ of the di-Higgs system	6. Average absolute η value of Higgs boson candidate jets
7. ΔR between the two Higgs boson candidates	7. $\log(X_{Wt})$
8. $\Delta\phi$ between jets in the leading Higgs boson candidate	8. Trigger class index as one-hot encoder
9. $\Delta\phi$ between jets in the subleading Higgs boson candidate	9. Year index as one-hot encoder (for years inclusive training)
10. $\log(X_{Wt})$	
11. Number of jets in the event	
12. Trigger class index as one-hot encoder	

HH \rightarrow bb $\tau\tau$ with full Run 2 data

Acceptance x efficiency

ATLAS-CONF-2021-030



HH → bbττ with full Run 2 data

Different data-driven methods used in the HadHad and LepHad channels to estimate the contribution from events with jets faking hadronically decaying τ-leptons

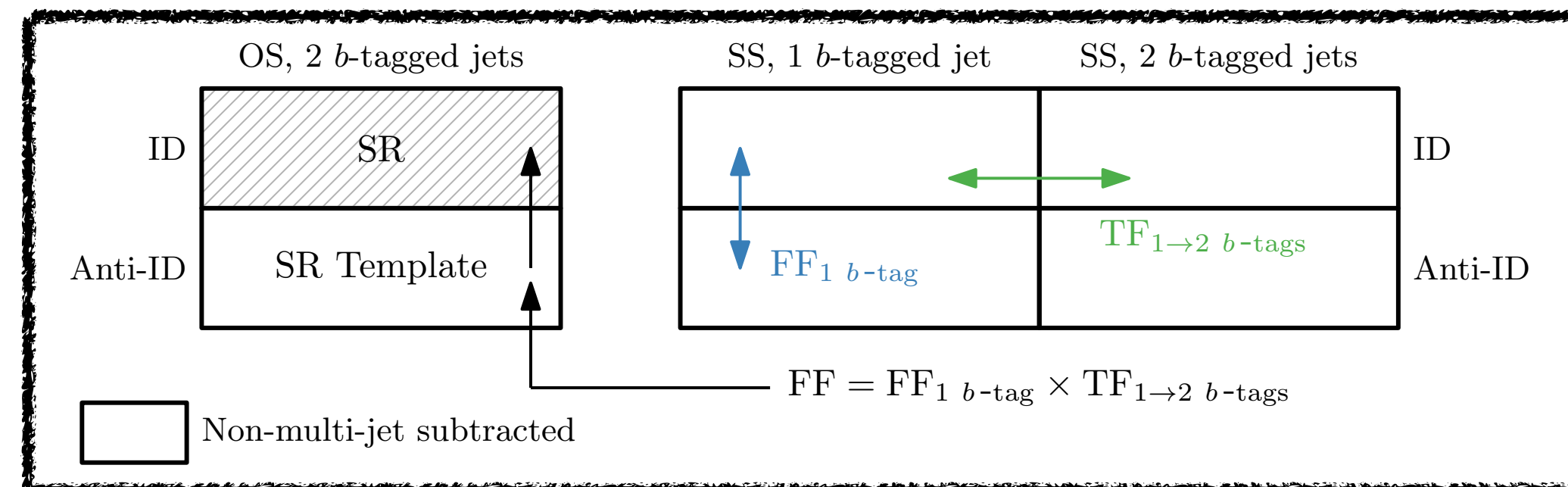
HadHad channel:

- QCD multi-jet: fake-factor method with fake-factors derived from data in 2 control regions and applied to data in a 3rd control region to obtain the signal region template
- ttbar fakes: scale-factor method with scale-factors derived from data in a control region using MC template fits and applied to the MC in the signal region to obtain the corrected template

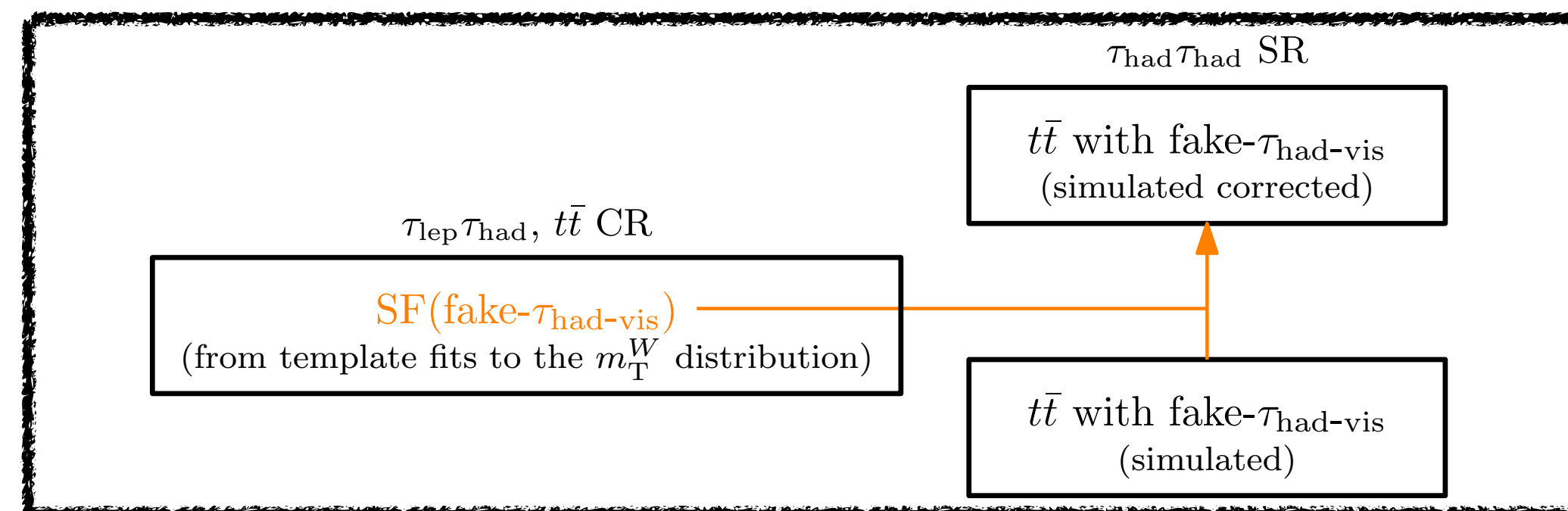
LepHad channel:

- Combined fake-factor method for fakes from QCD and ttbar with separate fake-factors derived in dedicated control regions then combined and applied to data in another control region to obtain the signal region template

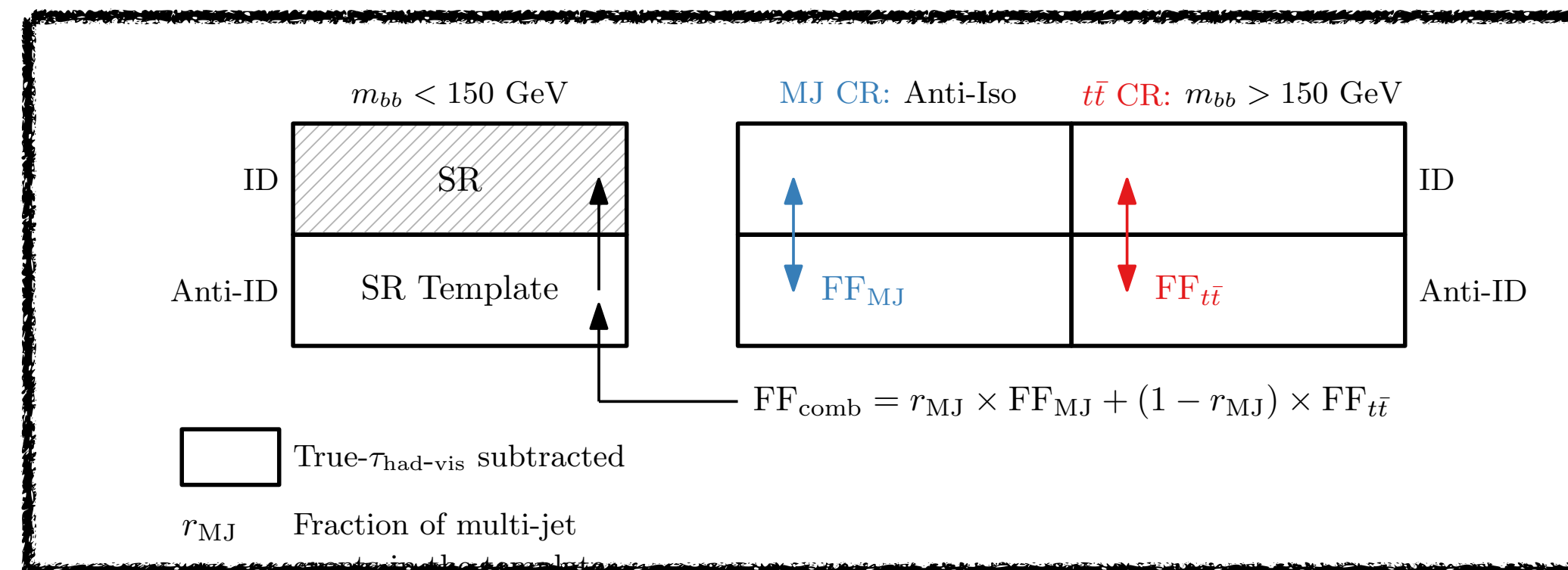
HadHad QCD fake-factors method



HadHad ttbar scale-factor method



LepHad combined fake-factor method



HH → bbττ with full Run 2 data

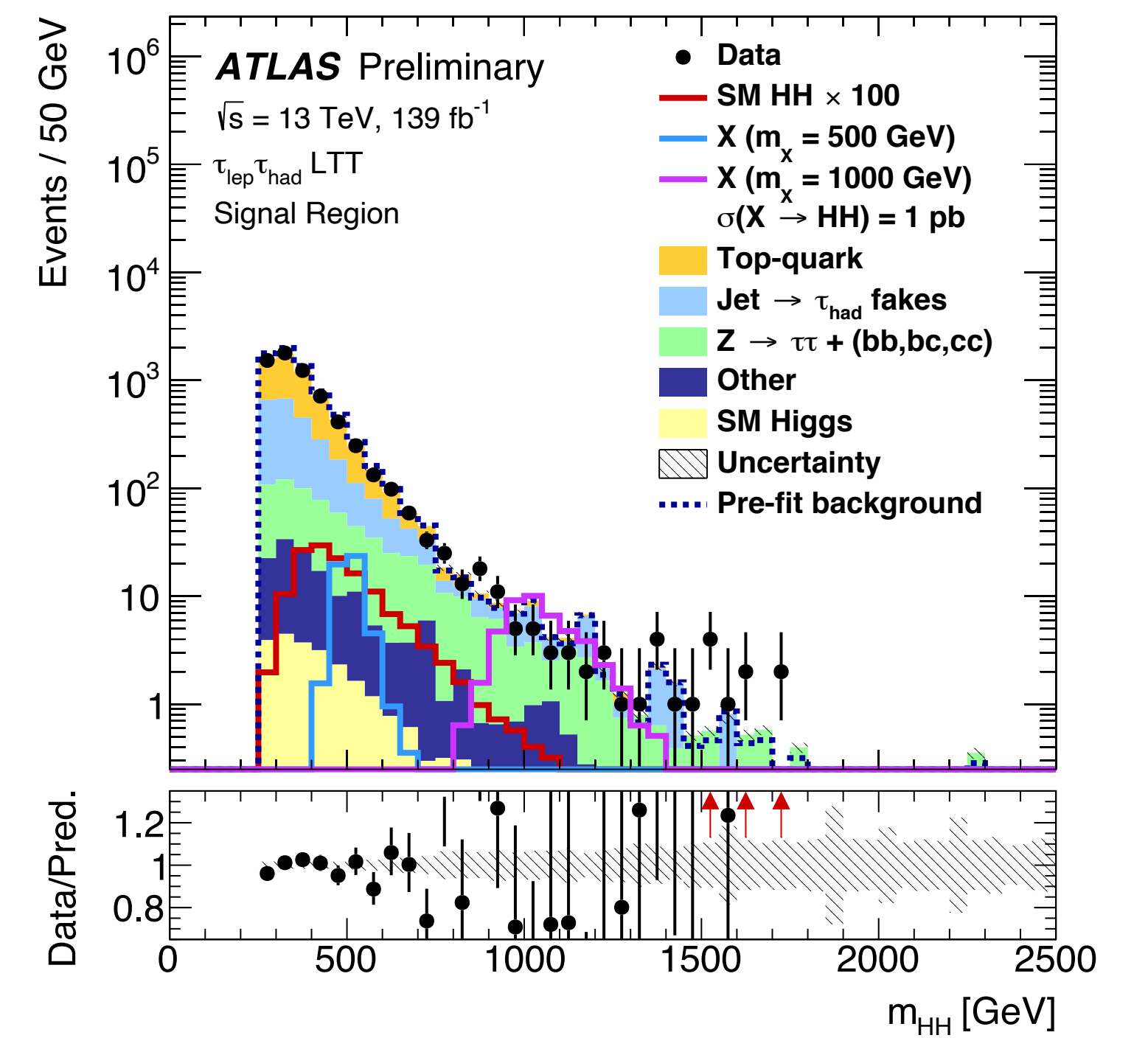
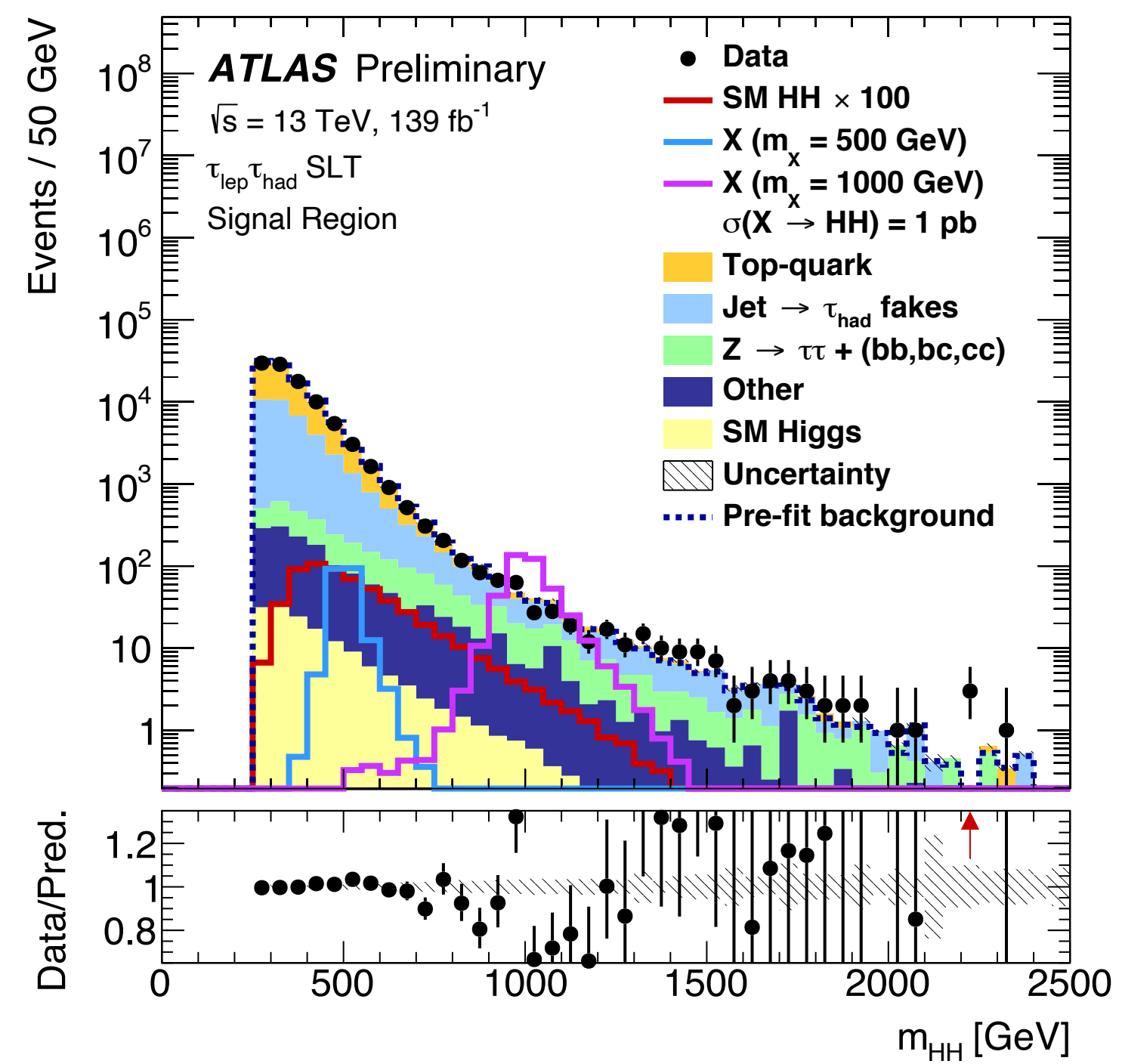
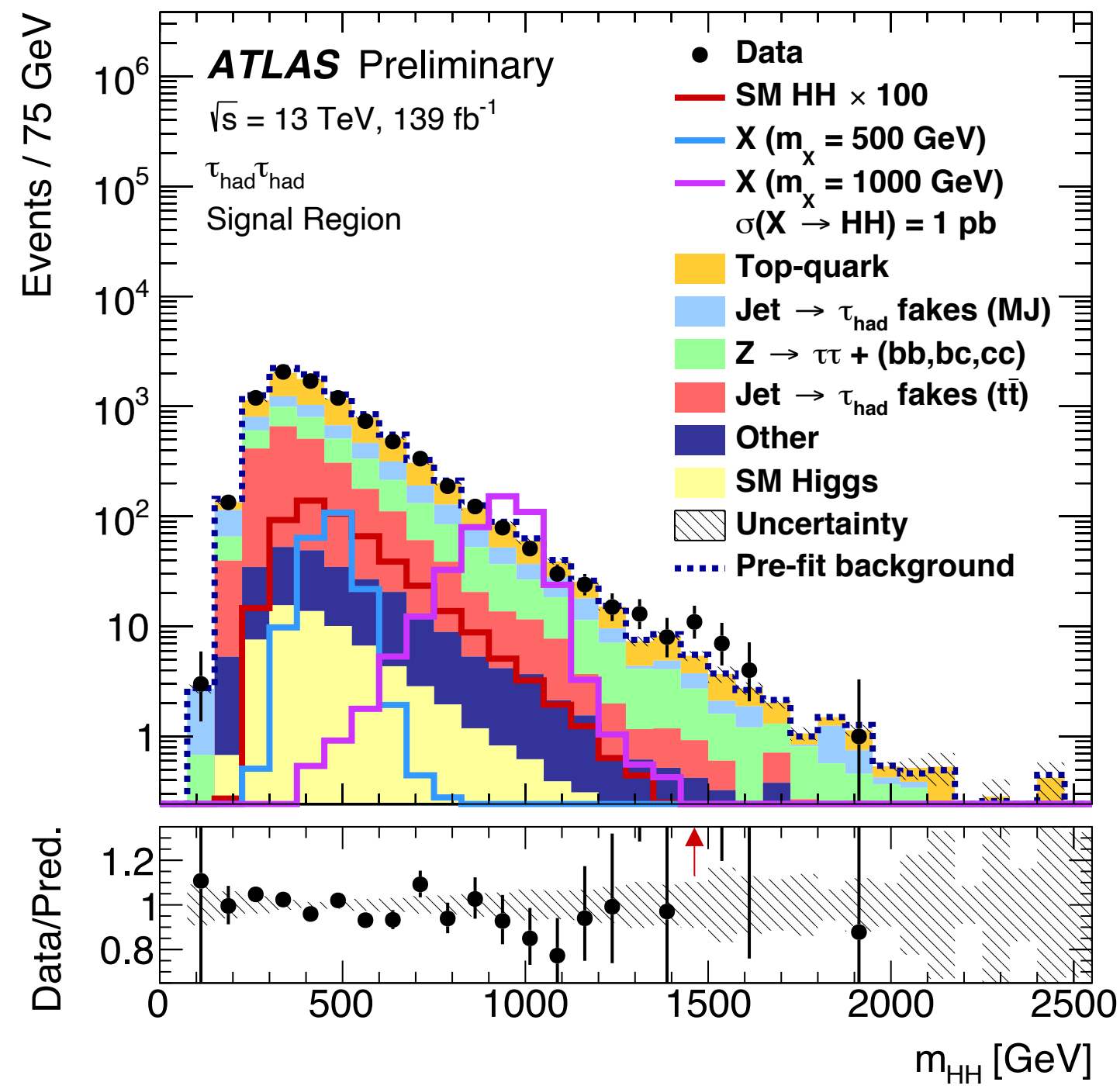
MVA input variables

ATLAS-CONF-2021-030

Variable	$\tau_{\text{had}}\tau_{\text{had}}$	$\tau_{\text{lep}}\tau_{\text{had}}$	SLT	$\tau_{\text{lep}}\tau_{\text{had}}$	LTT
m_{HH}	✓				✓
$m_{\tau\tau}^{\text{MMC}}$	✓				✓
m_{bb}	✓				✓
$\Delta R(\tau, \tau)$	✓				✓
$\Delta R(b, b)$	✓				
$\Delta p_{\text{T}}(\ell, \tau)$				✓	✓
Sub-leading b -tagged jet p_{T}				✓	
m_{T}^{W}				✓	
$E_{\text{T}}^{\text{miss}}$				✓	
$\mathbf{p}_{\text{T}}^{\text{miss}}$ ϕ centrality				✓	
$\Delta\phi(\tau\tau, bb)$				✓	
$\Delta\phi(\ell, \mathbf{p}_{\text{T}}^{\text{miss}})$					✓
$\Delta\phi(\ell\tau, \mathbf{p}_{\text{T}}^{\text{miss}})$					✓
S_{T}					✓

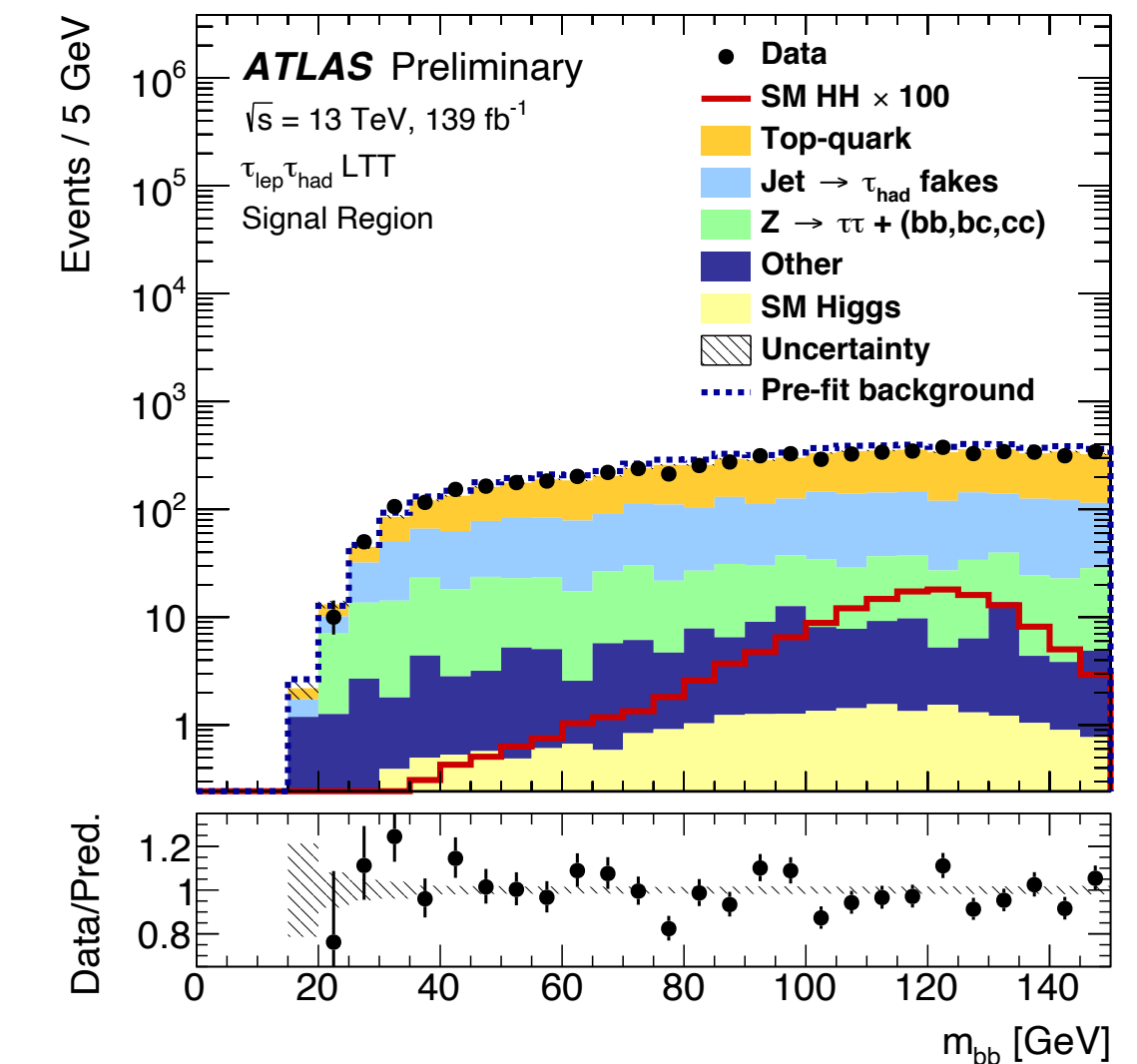
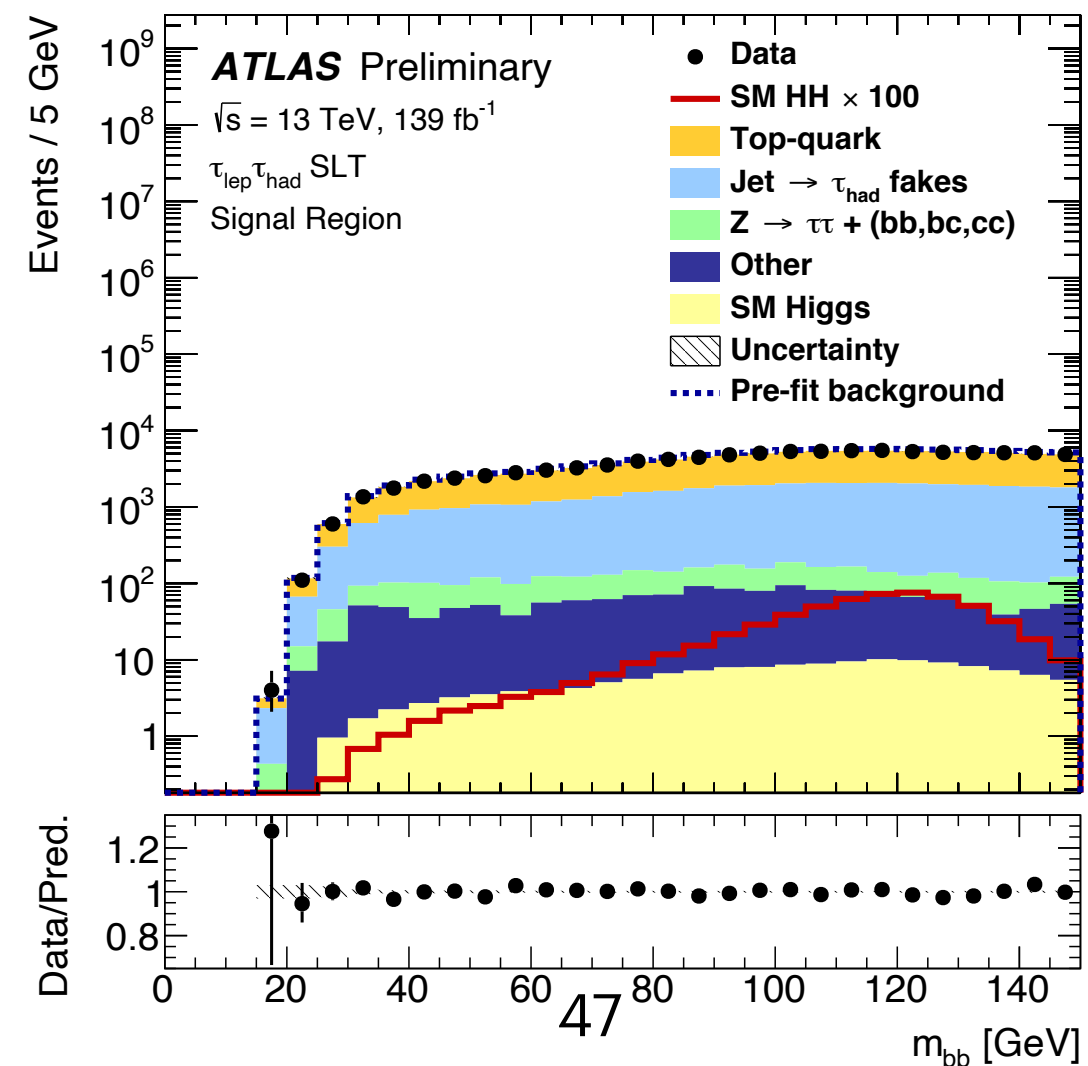
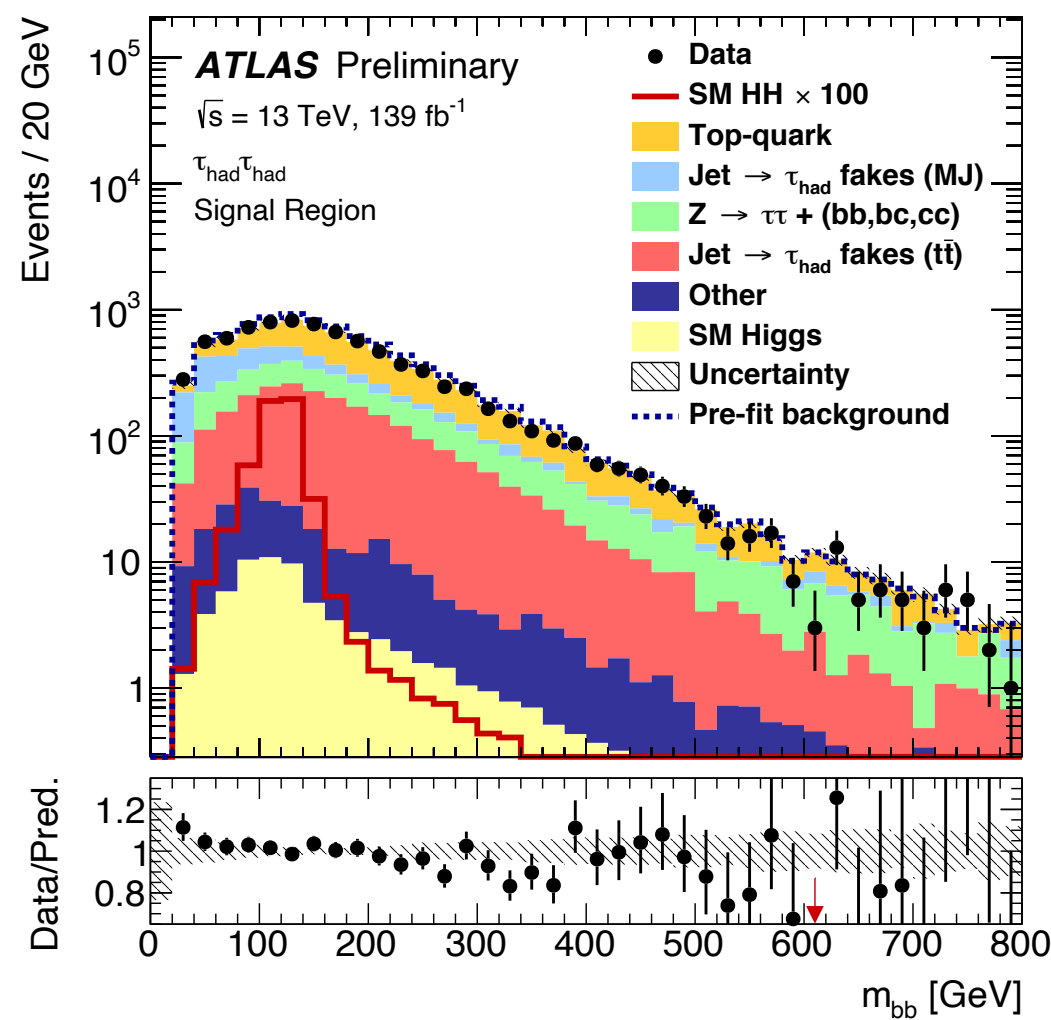
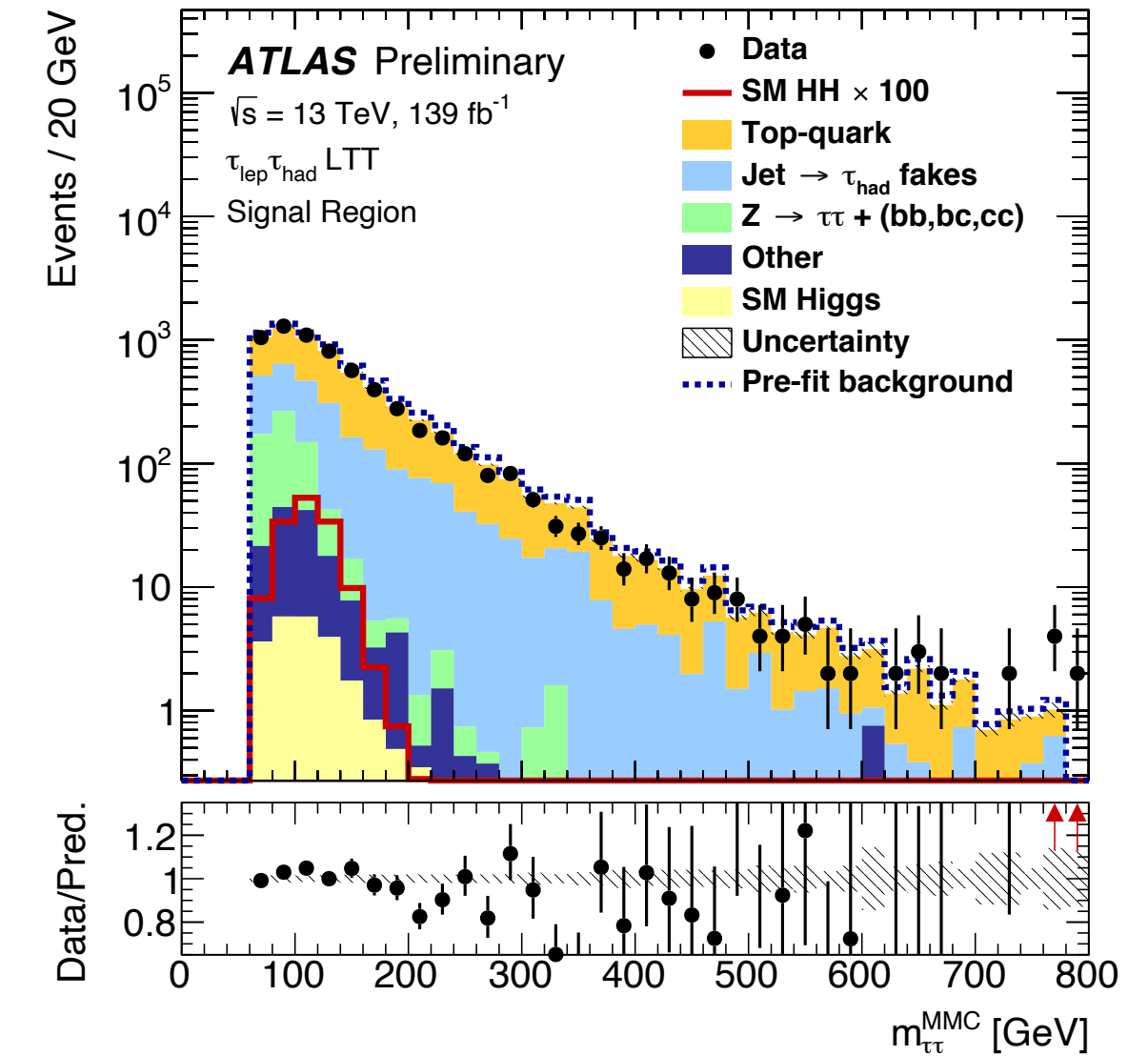
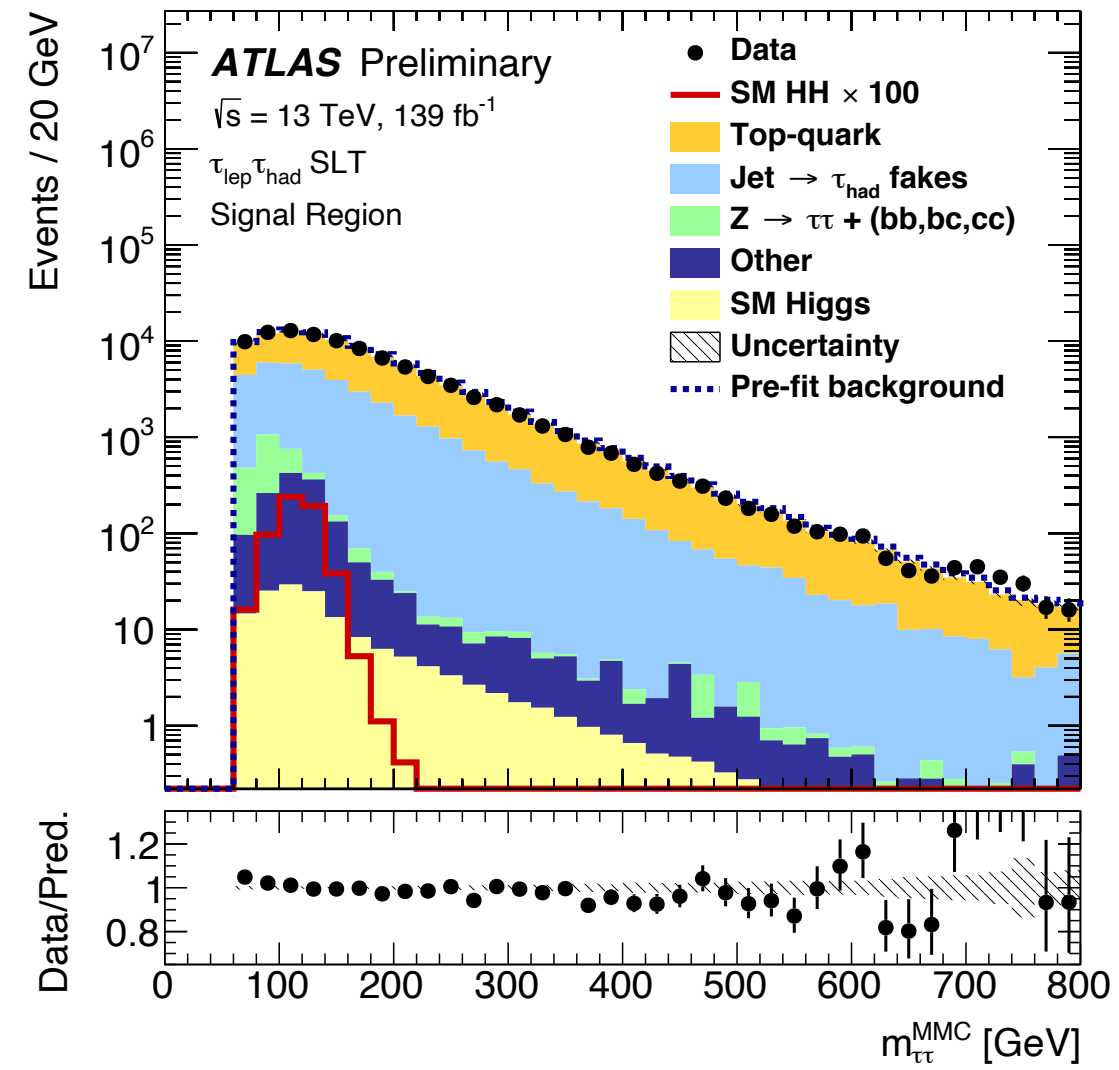
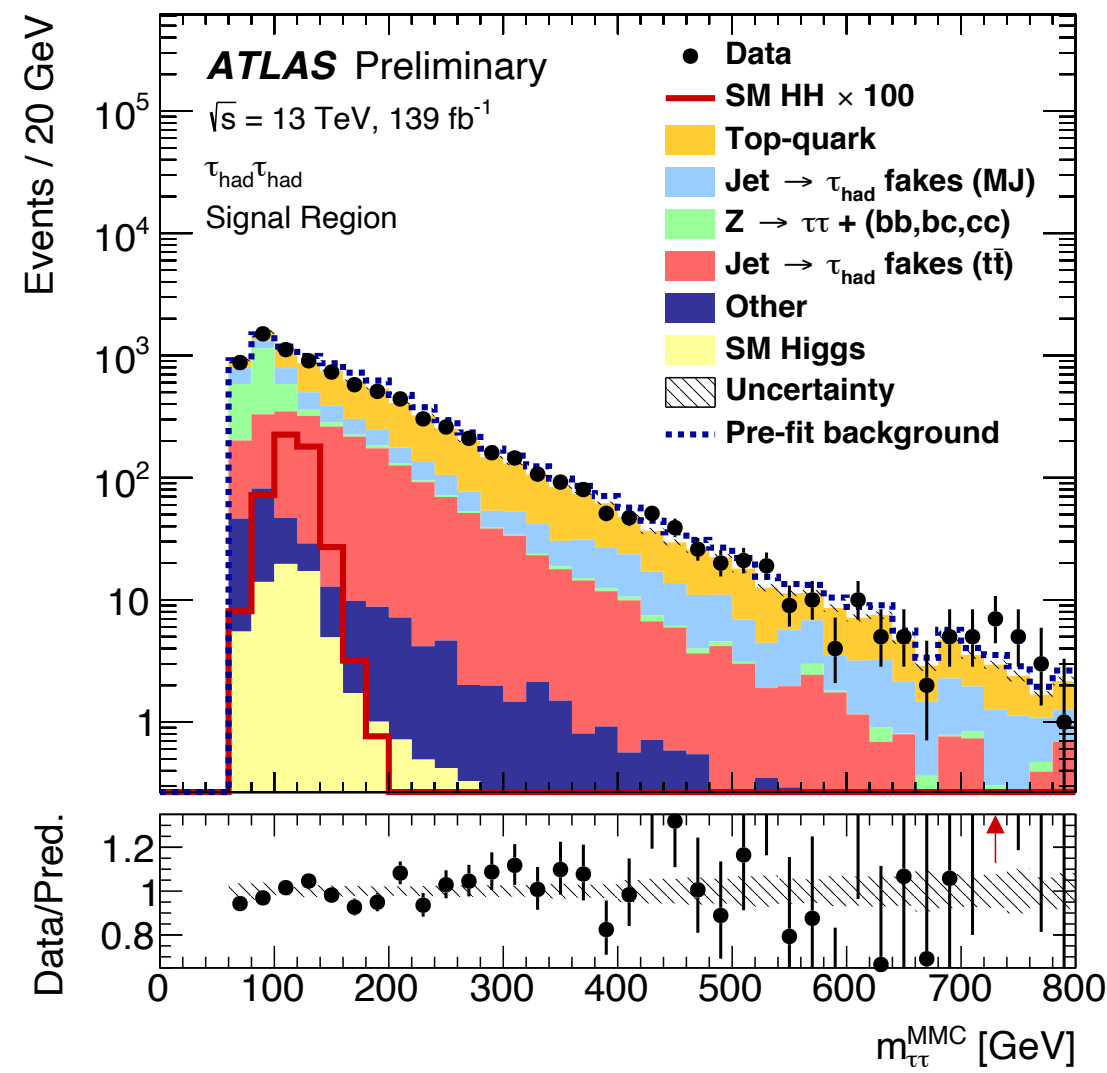
HH \rightarrow bb $\tau\tau$ with full Run 2 data

MVA input variables



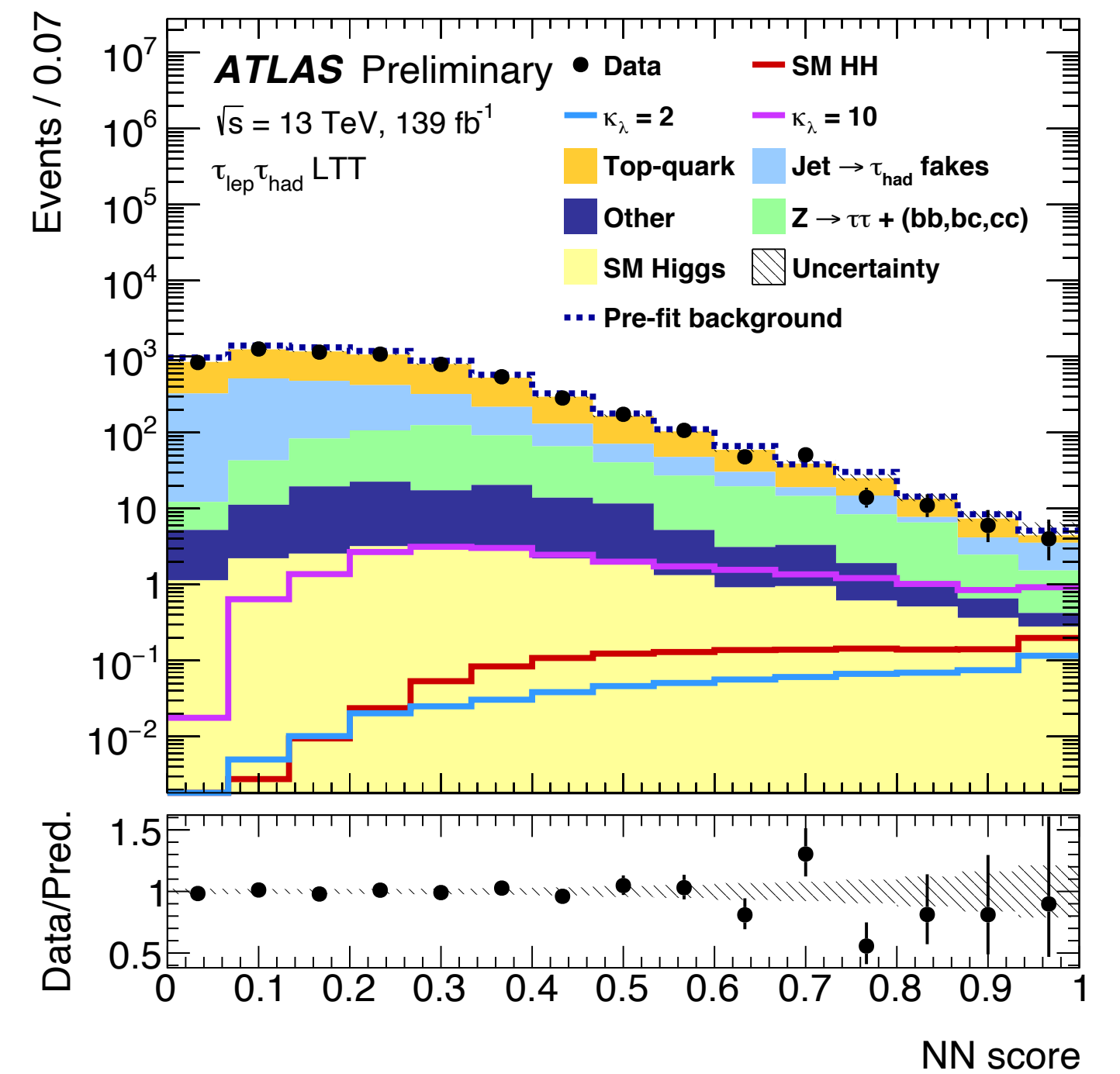
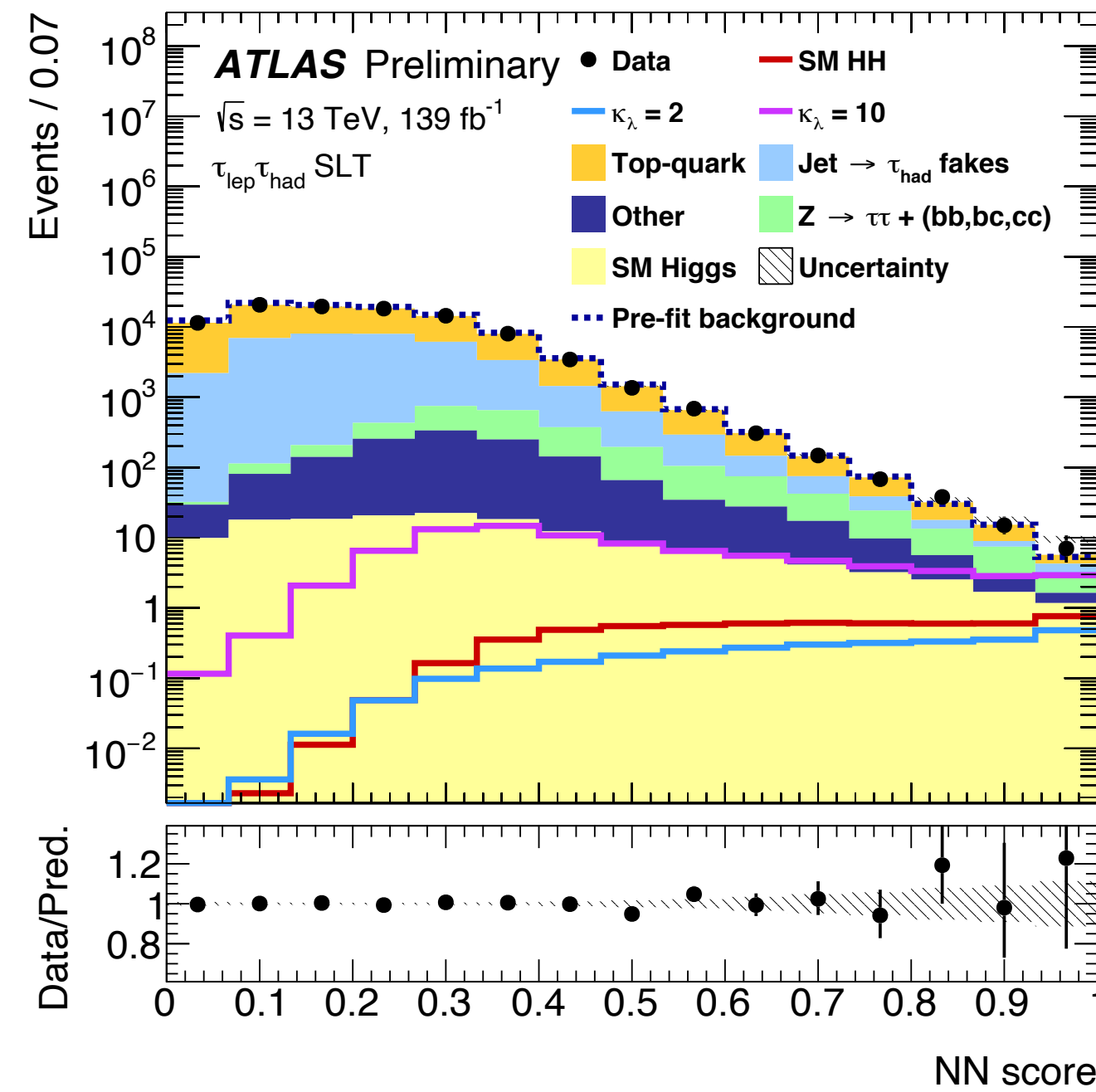
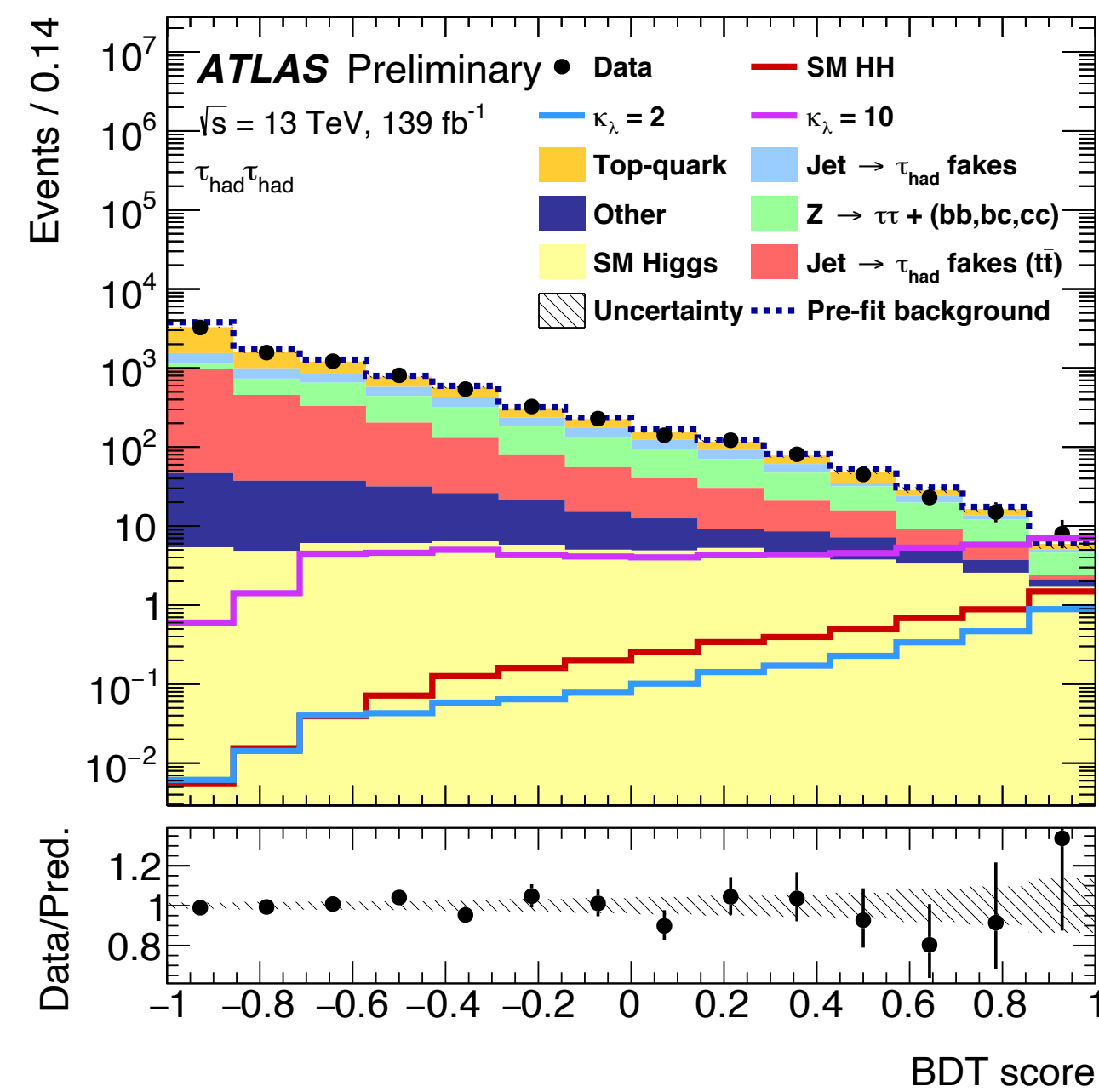
HH \rightarrow bb $\tau\tau$ with full Run 2 data

MVA input variables



HH \rightarrow bb $\tau\tau$ with full Run 2 data

MVA outputs



HH → bbττ with full Run 2 data

Systematic uncertainties

ATLAS-CONF-2021-030

Uncertainty source	Non-resonant HH	Resonant $X \rightarrow HH$		
		300 GeV	500 GeV	1000 GeV
Data statistical	81%	75%	89%	88%
Systematic	59%	66%	46%	48%
$t\bar{t}$ and $Z + \text{HF}$ normalisations	4%	15%	3%	3%
MC statistical	28%	44%	33%	18%
Experimental				
Jet and E_T^{miss}	7%	28%	5%	3%
b -jet tagging	3%	6%	3%	3%
$\tau_{\text{had-vis}}$	5%	13%	3%	7%
Electrons and muons	2%	3%	2%	1%
Luminosity and pileup	3%	2%	2%	5%
Theoretical and modelling				
Fake- $\tau_{\text{had-vis}}$	9%	22%	8%	7%
Top-quark	24%	17%	15%	8%
$Z(\rightarrow \tau\tau) + \text{HF}$	9%	17%	9%	15%
Single Higgs boson	29%	2%	15%	14%
Other backgrounds	3%	2%	5%	3%
Signal	5%	15%	13%	34%

HH \rightarrow bbyy with full Run 2 data

BDT input variables

arXiv:2112.11876

Non-resonant

Variable	Definition
Photon-related kinematic variables	
$p_T/m_{\gamma\gamma}$	Transverse momentum of the two photons scaled by their invariant mass $m_{\gamma\gamma}$
η and ϕ	Pseudo-rapidity and azimuthal angle of the leading and sub-leading photon
Jet-related kinematic variables	
b -tag status	Highest fixed b -tag working point that the jet passes
p_T , η and ϕ	Transverse momentum, pseudo-rapidity and azimuthal angle of the two jets with the highest b -tagging score
$p_T^{b\bar{b}}$, $\eta_{b\bar{b}}$ and $\phi_{b\bar{b}}$	Transverse momentum, pseudo-rapidity and azimuthal angle of b -tagged jets system
$m_{b\bar{b}}$	Invariant mass built with the two jets with the highest b -tagging score
H_T	Scalar sum of the p_T of the jets in the event
Single topness	For the definition, see Eq. (1)
Missing transverse momentum-related variables	
E_T^{miss} and ϕ^{miss}	Missing transverse momentum and its azimuthal angle

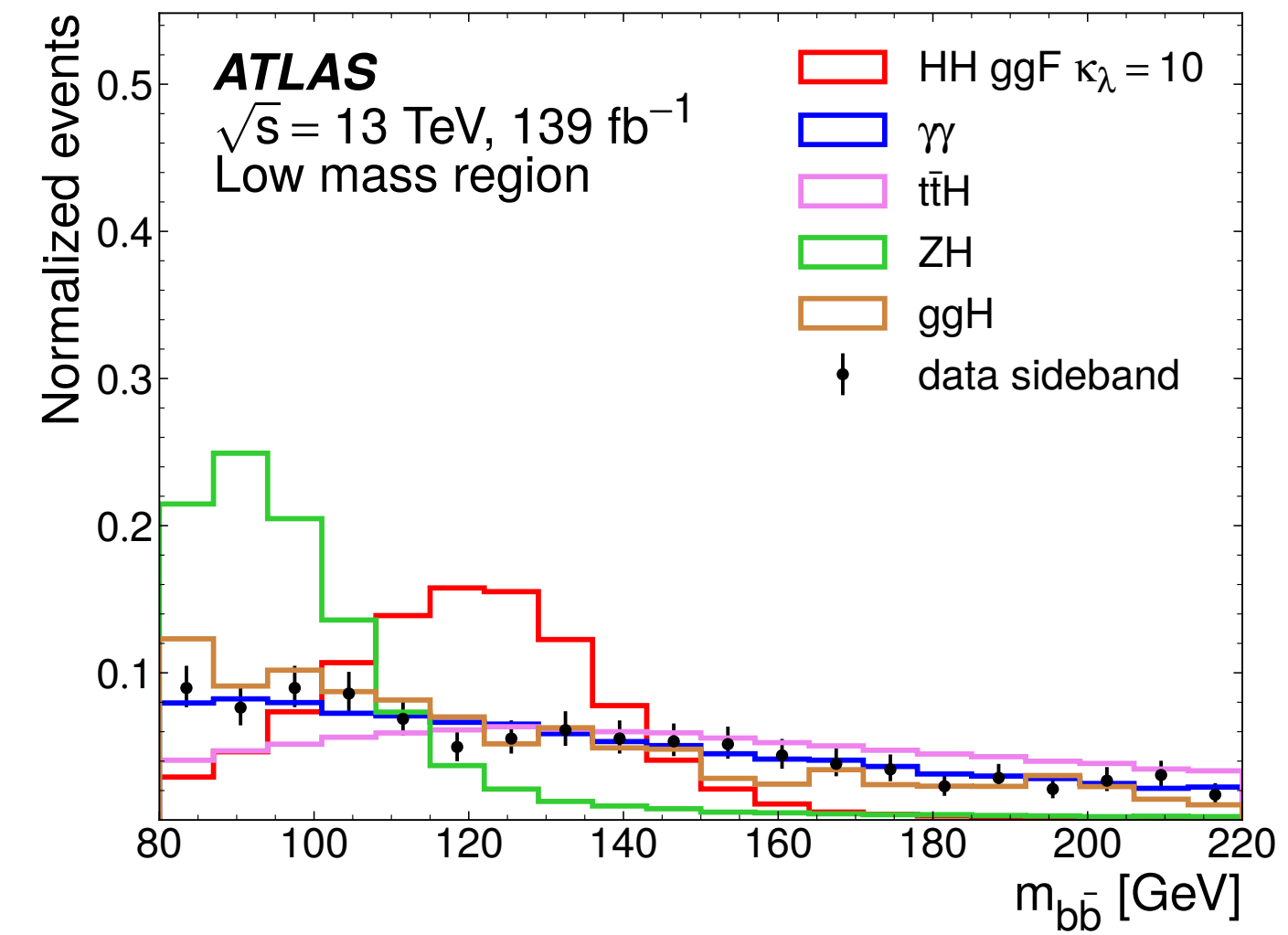
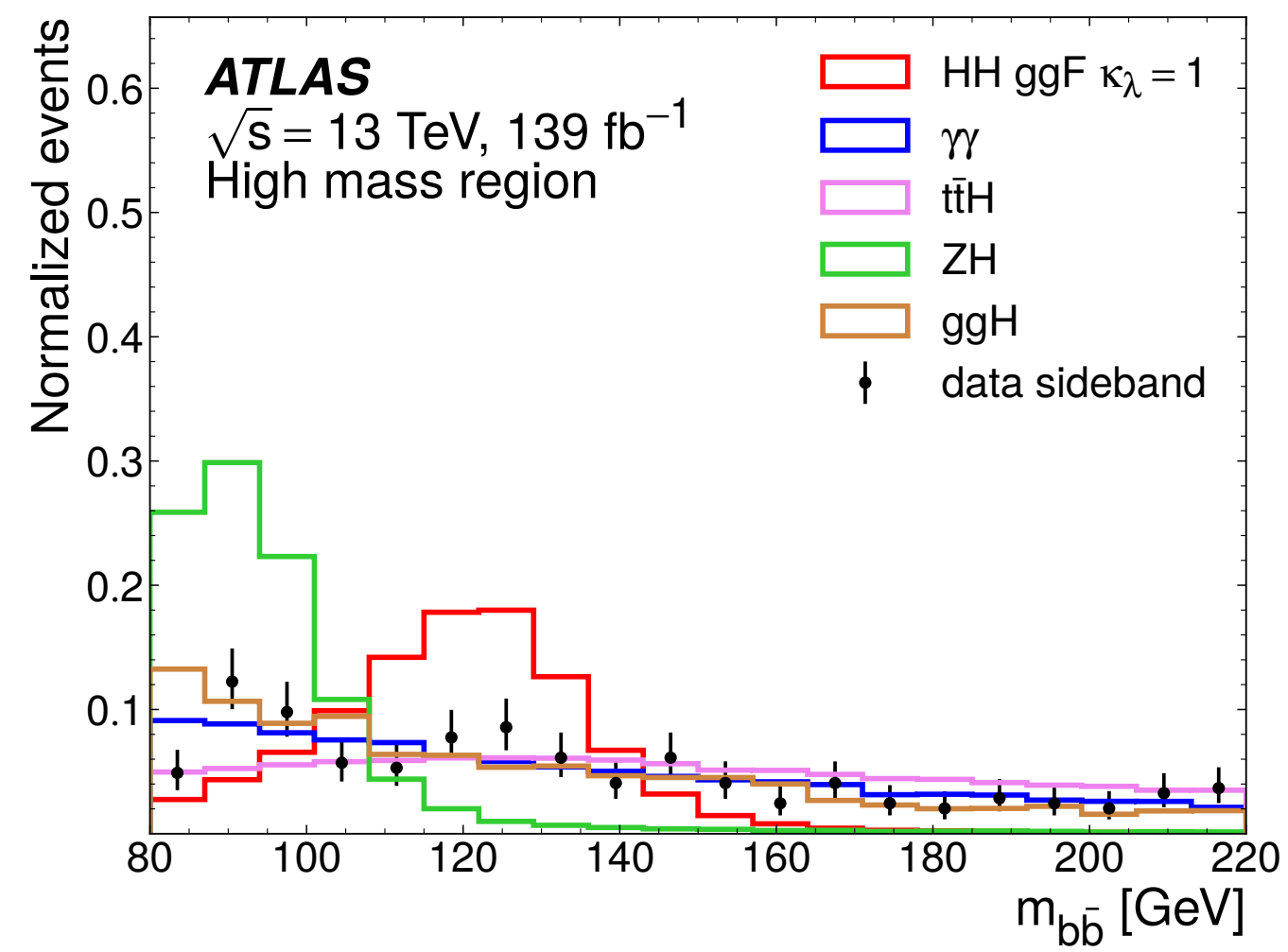
Resonant

Variable	Definition
Photon-related kinematic variables	
$p_T^{\gamma\gamma}$, $y^{\gamma\gamma}$	Transverse momentum and rapidity of the di-photon system
$\Delta\phi_{\gamma\gamma}$ and $\Delta R_{\gamma\gamma}$	Azimuthal angular distance and ΔR between the two photons
Jet-related kinematic variables	
$m_{b\bar{b}}$, $p_T^{b\bar{b}}$ and $y_{b\bar{b}}$	Invariant mass, transverse momentum and rapidity of the b -tagged jets system
$\Delta\phi_{b\bar{b}}$ and $\Delta R_{b\bar{b}}$	Azimuthal angular distance and ΔR between the two b -tagged jets
N_{jets} and $N_{b\text{-jets}}$	Number of jets and number of b -tagged jets
H_T	Scalar sum of the p_T of the jets in the event
Photons and jets-related kinematic variables	
$m_{b\bar{b}\gamma\gamma}$	Invariant mass built with the di-photon and b -tagged jets system
$\Delta y_{\gamma\gamma, b\bar{b}}$, $\Delta\phi_{\gamma\gamma, b\bar{b}}$ and $\Delta R_{\gamma\gamma, b\bar{b}}$	Distance in rapidity, azimuthal angle and ΔR between the di-photon and the b -tagged jets system

HH \rightarrow bby with full Run 2 data

BDT input variables

arXiv:2112.11876



HH \rightarrow bbyy with full Run 2 data

Event selection

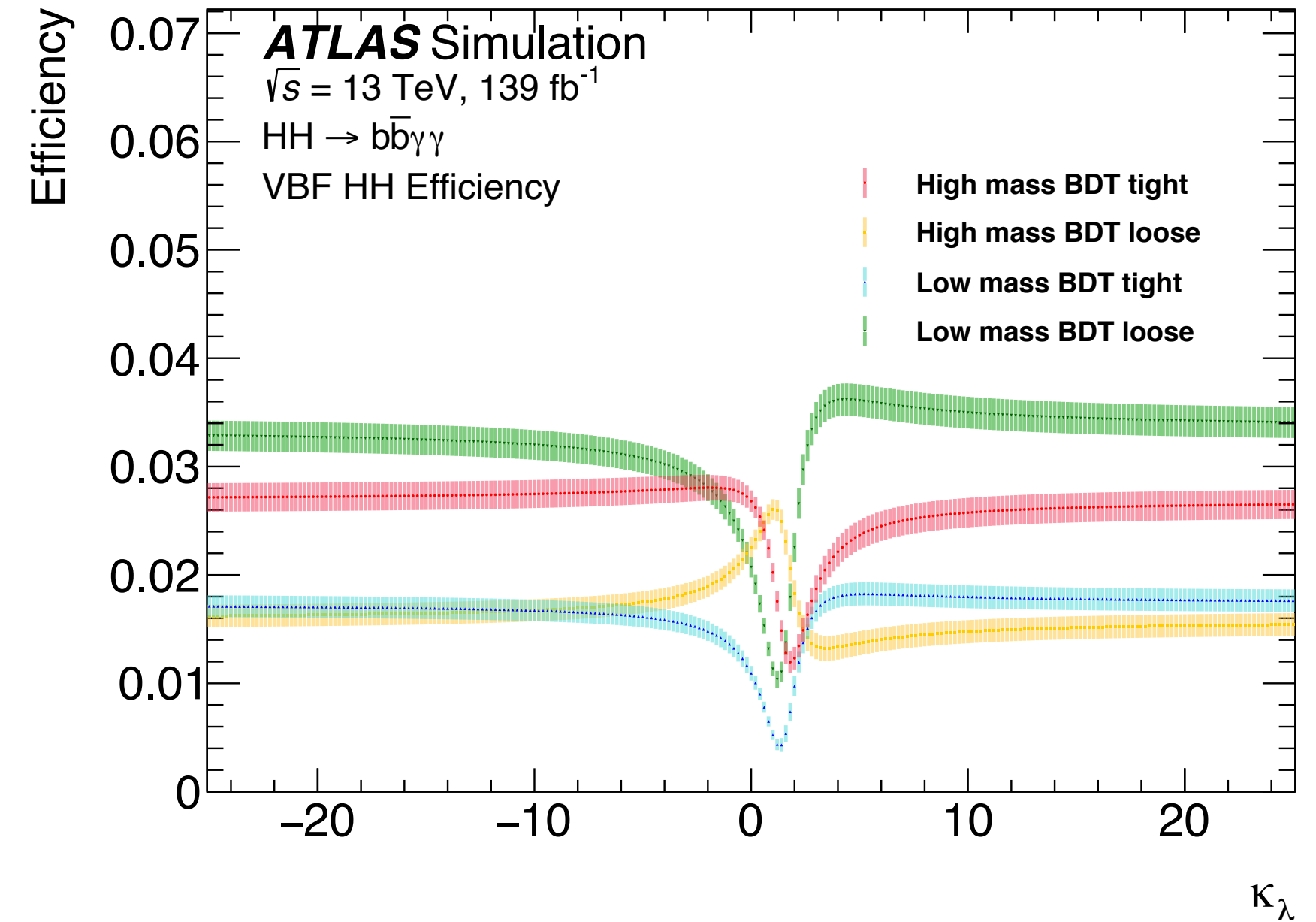
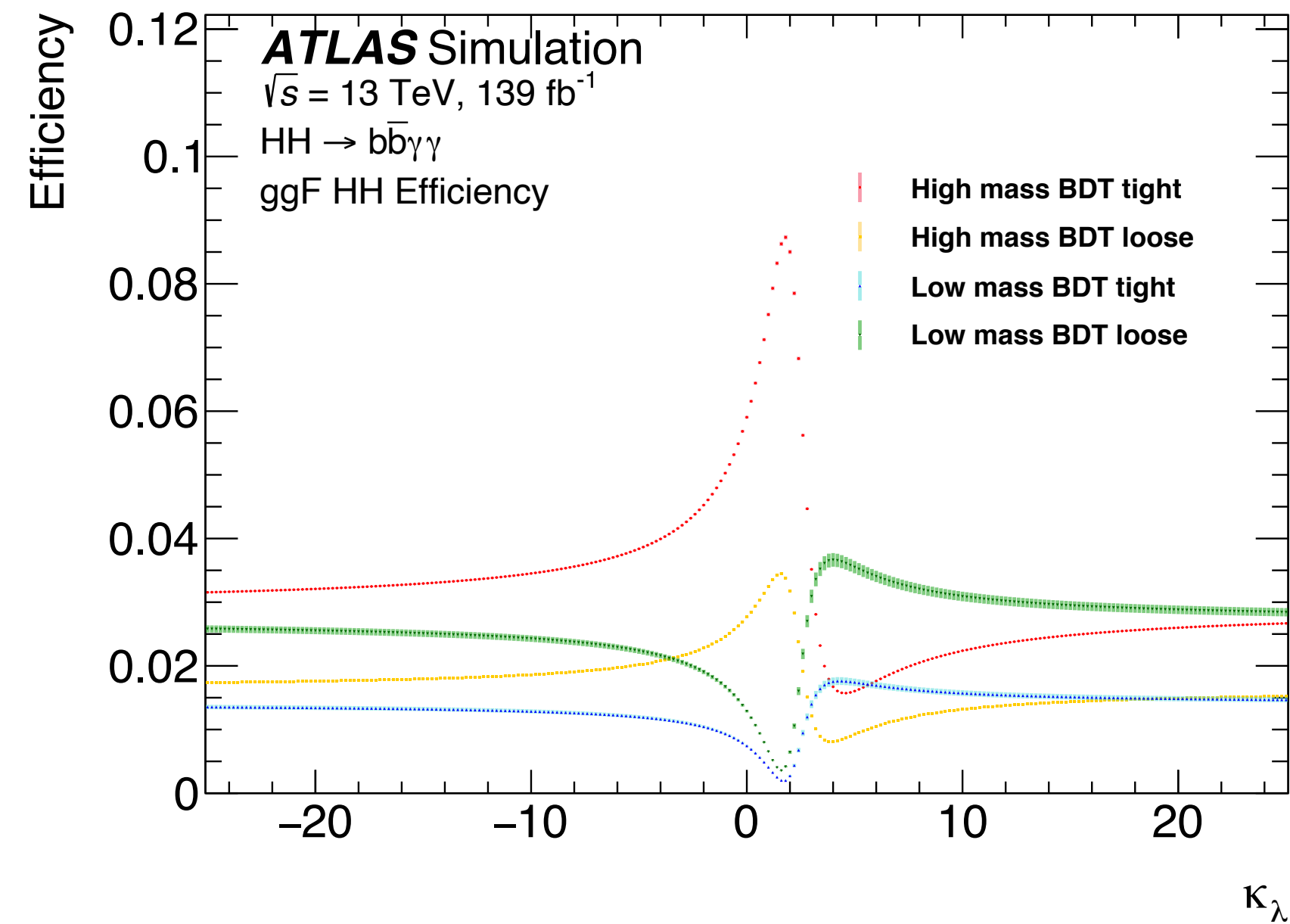
arXiv:2112.11876

Cuts	Yields	Efficiency [%]
All events	12.11	100.00
Pass trigger	9.81	80.97
Has Primary Vertex	9.81	80.97
2 loose photons	7.07	58.42
$e - \gamma$ ambiguity	7.07	58.40
Trigger match	6.71	55.46
Photons tight ID cut	5.89	48.62
Photons isolation cut	5.22	43.13
rel. p_T cuts	4.70	38.78
$m_{\gamma\gamma} \in [105, 160]$ GeV	4.69	38.73
$N_{lep} = 0$	4.67	38.55
$N_j \geq 2$	3.94	32.53
N_j central <6	3.84	31.68
2 b -jets with 77% WP	1.62	13.37
Di-Higgs invariant mass >350 GeV	1.42	11.78
Di-Higgs invariant mass <350 GeV	0.19	1.58

HH \rightarrow bb $\gamma\gamma$ with full Run 2 data

Acceptance x efficiency

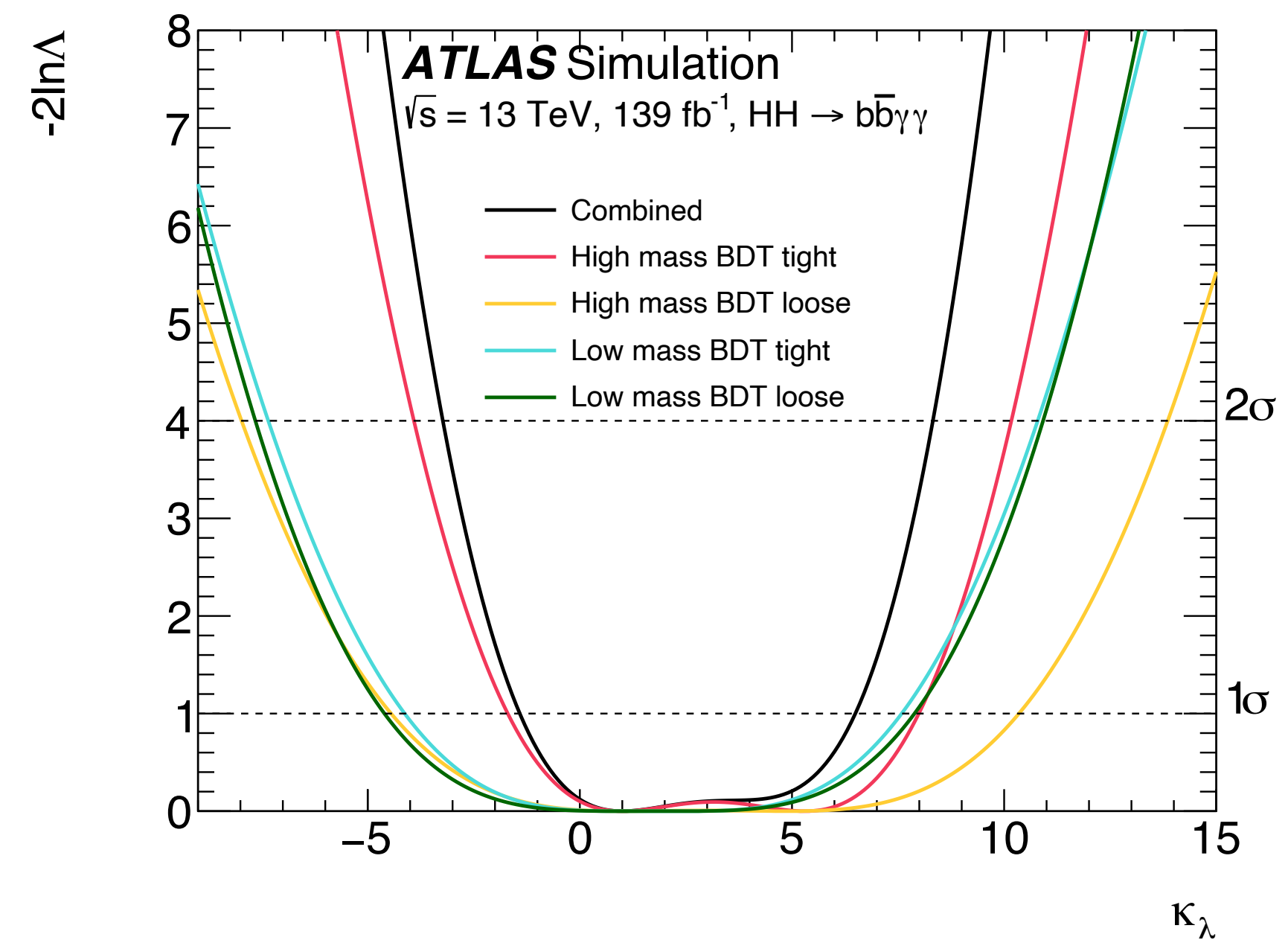
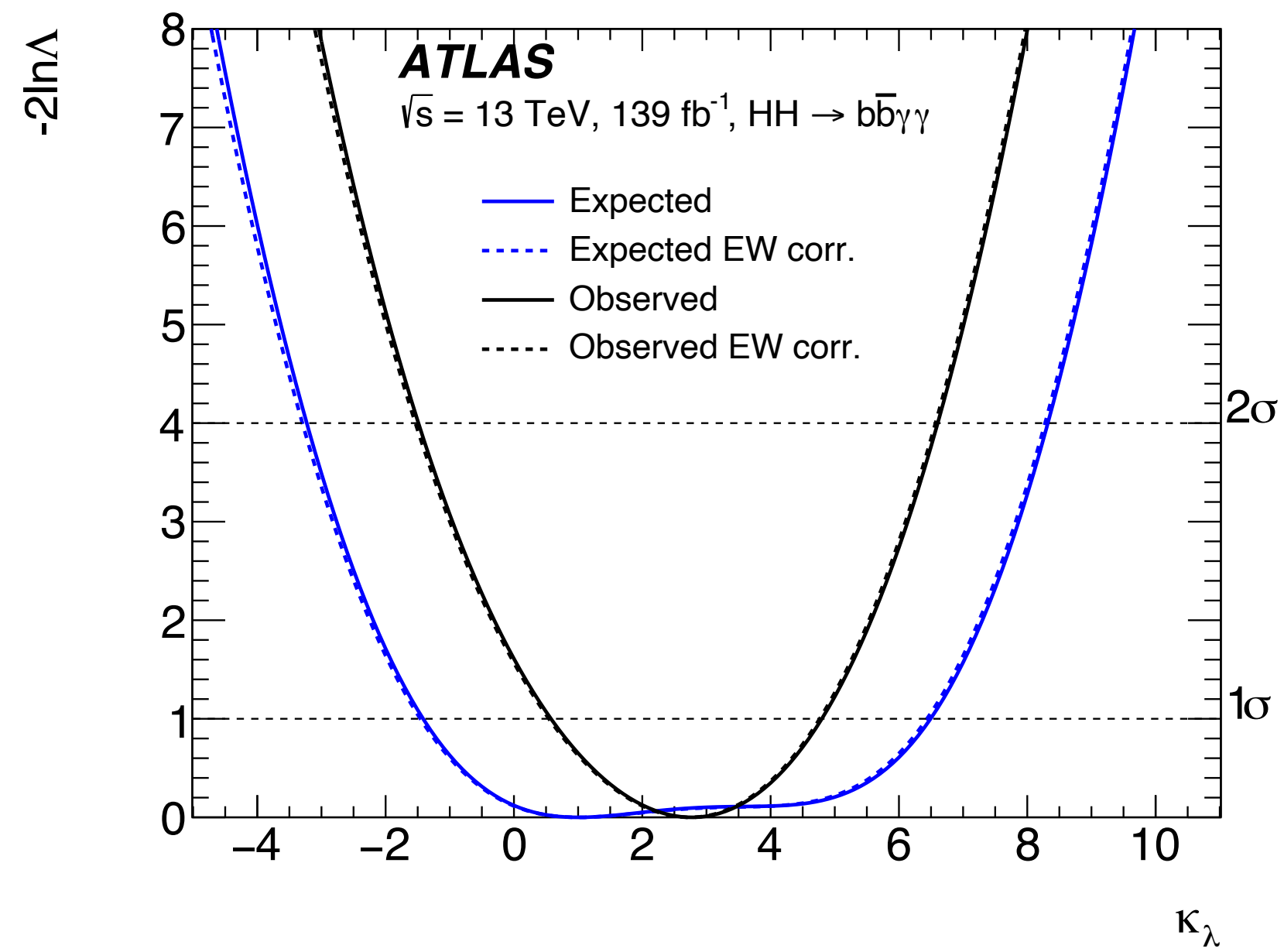
arXiv:2112.11876



HH \rightarrow bb $\gamma\gamma$ with full Run 2 data

Likelihood scans

arXiv:2112.11876



HH \rightarrow bbyy with full Run 2 data

Systematic uncertainties

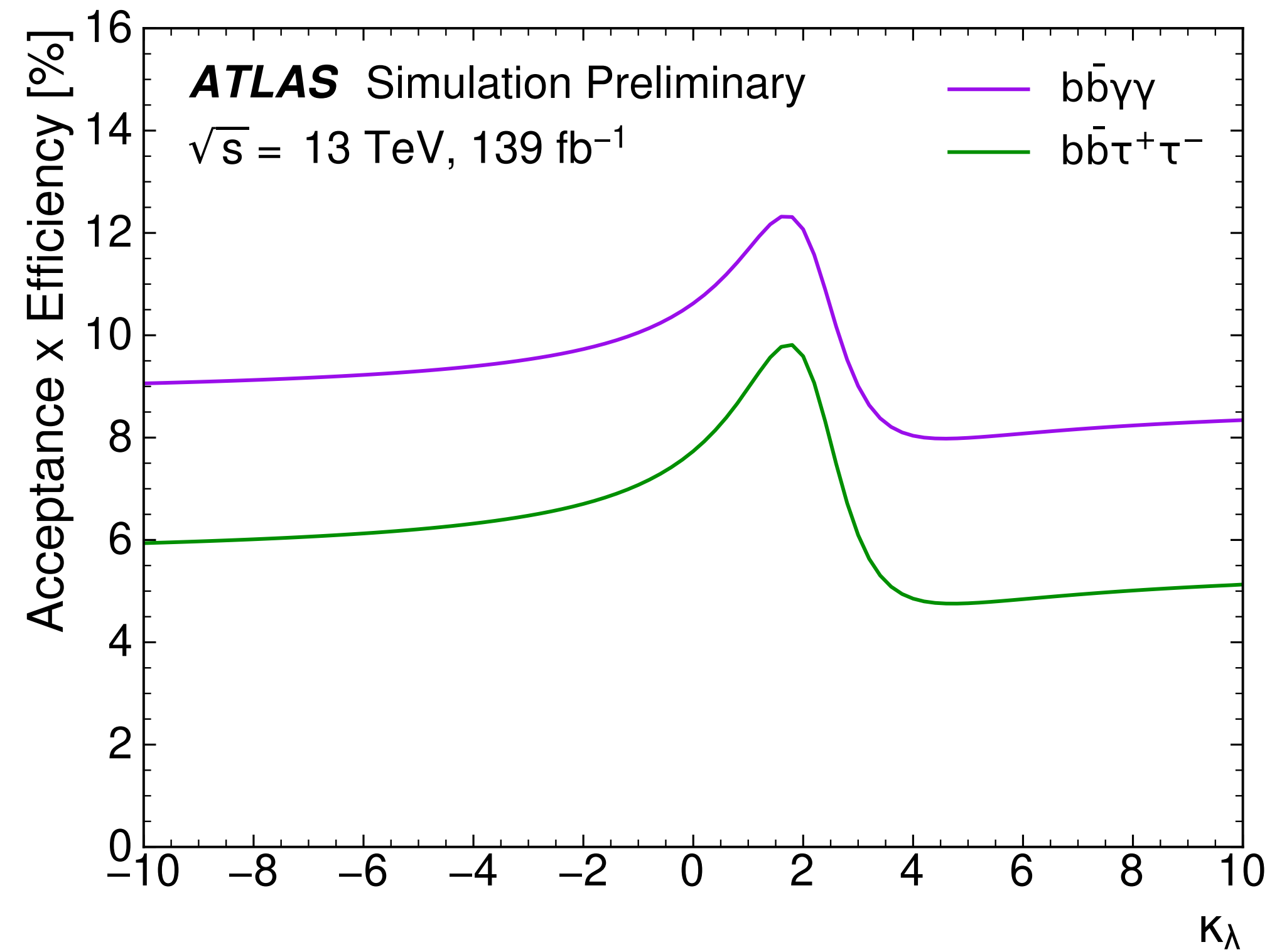
arXiv:2112.11876

Source	Type	Relative impact of the systematic uncertainties [%]	
		Nonresonant analysis HH	Resonant analysis $m_X = 300$ GeV
Experimental			
Photon energy resolution	Norm. + Shape	0.4	0.6
Jet energy scale and resolution	Normalization	< 0.2	0.3
Flavor tagging	Normalization	< 0.2	0.2
Theoretical			
Factorization and renormalization scale	Normalization	0.3	< 0.2
Parton showering model	Norm. + Shape	0.6	2.6
Heavy-flavor content	Normalization	0.3	< 0.2
$\mathcal{B}(H \rightarrow \gamma\gamma, b\bar{b})$	Normalization	0.2	< 0.2
Spurious signal	Normalization	3.0	3.3

HH \rightarrow bb $\tau\tau$ and HH \rightarrow bb $\gamma\gamma$ with full Run 2 data

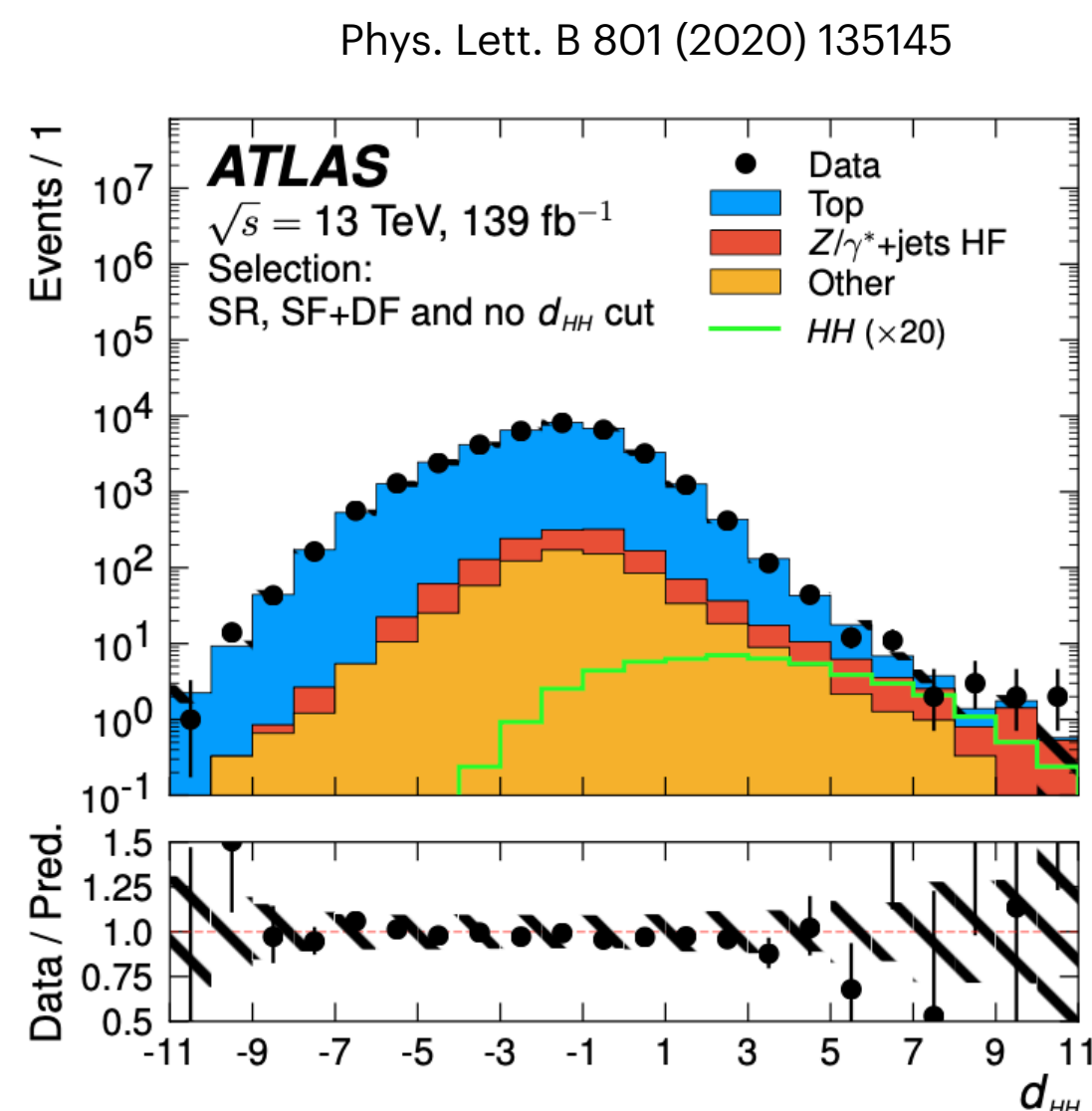
Acceptance x efficiency

ATLAS-CONF-2021-052



Non-resonant $HH \rightarrow bbl$ with full Run 2 data

- Search for SM and BSM non-resonant HH production
- Only ggF HH production
- Looking for the HH decays with one $H \rightarrow bb$ and the other $H \rightarrow WW, ZZ, \tau\tau$ in the 2 leptons final state
- At least two b-tagged jets and exactly two leptons (e/ μ) with opposite charge
- 2 categories: same-flavour (SF) and different-flavour (DF) for the lepton pair
- Signal region defined by: $20 < m_{\ell\ell} < 60$ GeV, $110 < m_{bb} < 140$ GeV and a cut on a discriminant built from the output of a multi-class deep neural network (DNN) classifier ($d_{HH} > 5.45(5.55)$ for SR-SF (SR-DF))
- Event-counting analysis with a simultaneous fit of 2 signal regions: SF and DF



	-2σ	-1σ	Expected	$+1\sigma$	$+2\sigma$	Observed
$\sigma(gg \rightarrow HH)$ [pb]	0.5	0.6	0.9	1.3	1.9	1.2
$\sigma(gg \rightarrow HH) / \sigma^{\text{SM}}(gg \rightarrow HH)$	14	20	29	43	62	40

→ sensitivity not comparable to the other HH searches
 as upper limits are one order of magnitude higher
 (results not included in combinations)

